Journal of the OPTICAL SOCIETY *of* AMERICA

VOLUME 38
No. 7

JULY
1948

Photographic Reciprocity-Law Failure for Radiations of Different Wave-Length . . . . . M. BILTZ AND J. H. WEBB 561

Two-Quanta Hypothesis as a General Explanation for the Behavior of Threshold Values and Visual Acuity for the Several Receptors of the Human Eye . . . . . M. A. BOUMAN AND H. A. VAN DER VELDEN 570

Preparation and Optical Properties of Gold Blacks . . . . . LOUIS HARRIS, ROSEMARY T. MCGINNIES, AND BENJAMIN M. SIEGEL 582

Lens Design and Tolerance Analysis Methods and Results . . . . . PAUL C. FOOTE AND ROBERT A. WOODSON 590

Some Considerations of the Effect of Radiation on the Performance of Liquid Fuel Rockets . . . . . S. S. PENNER AND S. WEINBAUM 599

Aerial Photographic Equipment and Applications to Reconnaissance . . . . AMROM H. KATZ 604

Scattered and Rescattered Sunlight . . . . . A. HAMMAD 611

Improved Jamin Interferometer . . . . . J. B. HAWKES AND R. W. ASTHEIMER 617

Improvement of Savart's Polariscope . . . . . M. RICHARTZ 623

Comparative Study of Five Tests of Color Vision . . . . . ALPHONSE CHAPANIS 626

Erratum: The Relation between Efficiency and Exciting Intensity for Zinc-Sulfide Phosphors . . . . . H. A. KLASENS, W. RAMSDEN, AND CHOW QUANTIE 649

Letters to the Editor:

Applicability of Judd's Color Tolerance formula in the Case of Titanium Pigments . . . . . ARTHUR C. HARDY 650

Ultraviolet Phase Microscopy . . . . A. H. BENNETT, D. L. WOERNLEY, AND A. J. KAVANAGH 650

Visual Performance and the Surround . . . . . PARRY MOON AND DOMINA EBERLE SPENCER 651

Minutes of the Thirty-First Meeting of the Board of Directors of the Optical Society of America, Incorporated 652

Annual Report of the Editor of Publications 652

Annual Report of the Secretary of the Optical Society of America, Inc., for the Calendar Year 1947 653

Annual Report of the Treasurer of the Optical Society of America 655

Proceedings of the Winter Meeting of the Optical Society of America 658

Published monthly
at Prince and Lemon Sts., Lancaster, Pa.
by the
AMERICAN INSTITUTE OF PHYSICS
Incorporated
57 East 55 Street, New York 22, New York
FOR AND UNDER THE EDITORIAL SUPERVISION OF THE
OPTICAL SOCIETY OF AMERICA

THE OPTICAL SOCIETY OF AMERICA

Officers of the Society

RUDOLF KINGSLAKE, *President*
Eastman Kodak Company
Rochester, New York

WILLIAM F. MEGGERS, *Vice President*
National Bureau of Standards
Washington 25, D. C.

ARTHUR C. HARDY, *Secretary*
Massachusetts Institute of Technology
Cambridge 39, Massachusetts

W. W. GRAEPER, *Treasurer*
Bausch & Lomb Optical Company
Rochester 2, New York

The Board of Directors consists of the above officers; the Editor of the Journal; the Past President; and five directors-at-large.

G. R. HARRISON, *Editor and Past President*
Massachusetts Institute of Technology
Cambridge 39, Massachusetts

Directors-at-Large

FRANK BENFORD
General Electric Company
Schenectady, New York

F. M. BISHOP
Eastman Kodak Company
Rochester 4, New York

WALLACE R. BRODE
Ohio State University
Columbus 10, Ohio

A. H. BENNETT
American Optical Company
Buffalo 11, New York

E. H. LAND
Polaroid Corporation
Cambridge, Massachusetts

Local Sections

STANLEY S. BALLARD, *Secretary for the Local Sections*

Rochester Section

JOHN H. MCLEOD, *President*
HARRY D. POLSTER, *Vice President*
JAMES R. BENFORD, *Secretary*
LUVILLE T. STEADMAN, *Treasurer*

Detroit Section

DAVID L. FRY, *Chairman*
KARL W. BEYER, *Vice Chairman*
DANIEL L. HARMON, *Secretary*
W. R. O'NEILL, *Treasurer*

Niagara Frontier Section

GALEN PORTER, *President*
LELAND E. HAVENS, *Secretary*
CLAIR M. BIRDSALL, *Treasurer*

Ohio Valley Section

M. E. MERCHANT, *Chairman*
J. F. WOODRUFF, *Chairman-elect*
C. S. MILLS, *Secretary-Treasurer*

Patrons

AMERICAN OPTICAL COMPANY — BAUSCH & LOMB OPTICAL COMPANY
EASTMAN KODAK COMPANY

Corporation Members

ALLIED CHEMICAL AND DYE CORPORATION, NATIONAL ANILINE DIVISION, Buffalo, New York
AMERICAN CYSTOSCOPE MAKERS, INC., New York, New York
AMERICAN OPTICAL COMPANY, Southbridge, Massachusetts
ARGUS, INCORPORATED, Ann Arbor, Michigan
BAUSCH & LOMB OPTICAL COMPANY, Rochester, New York
BELL & HOWELL COMPANY, Chicago, Illinois
BELL TELEPHONE LABORATORIES, INC., New York, New York
CENTURY LIGHTING, INC., New York, New York
CORNING GLASS WORKS, Corning, New York
R. R. DONNELLEY & SONS COMPANY, Chicago, Illinois
E. I. DUPONT DE NEMOURS & COMPANY, INC., Chemical Department, Experimental Station, Wilmington, Delaware
EASTMAN KODAK COMPANY, Rochester, New York
EDMUND SALVAGE COMPANY, Oaklyn-Audubon, New Jersey
FAIRCHILD AVIATION CORPORATION, Jamaica, New York
FARRAND OPTICAL COMPANY, INC., New York, New York
FISH-SCHURMAN CORPORATION, New York, New York
GAERTNER SCIENTIFIC CORPORATION, Chicago, Illinois
W. & L. E. GURLEY, Troy, New York
INTERCHEMICAL CORPORATION, New York, New York
KEUFFEL & ESSER COMPANY, Hoboken, New Jersey
KOLLSMAN INSTRUMENT DIVISION OF SQUARE D COMPANY, Elmhurst, New York
NATIONAL CARBON COMPANY, Cleveland, Ohio
NATIONAL TECHNICAL LABORATORIES, South Pasadena, California
PERKIN-ELMER CORPORATION, Glenbrook, Connecticut
POLAROID CORPORATION, Cambridge, Massachusetts
PORTMAN MACHINE TOOL COMPANY, New Rochelle, New York
SIMPSON OPTICAL MANUFACTURING COMPANY, Chicago, Illinois
SOCONY-VACUUM LABORATORIES, Paulsboro, New Jersey
ARTHUR H. THOMAS COMPANY, Philadelphia, Pennsylvania
UNIVIS LENS COMPANY, Dayton, Ohio
ZENITH OPTICAL COMPANY, Huntington, West Virginia

THE OPTICAL SOCIETY OF AMERICA was organized in 1916 "*to increase and diffuse the knowledge of optics in all its branches, pure and applied, to promote the mutual interests of investigators of optical problems, of designers, manufacturers and users of optical instruments and apparatus of all kinds and to encourage cooperation among them.*" It aims to serve the interests of all who are engaged in any branch of optics from fundamental research to the manufacture of optical goods.

MEMBERSHIP

Regular Members: "Any person who has contributed materially to the advancement of optics is eligible for regular membership."

Associate Members: "Any person who is interested in optics is eligible for associate membership."

Corporate Members: "Any corporation desirous of encouraging the work of the Society is eligible for corporation membership."

Patrons: The payment, within any one year, of $1000 or more toward the expenses of the Society by any corporation or individual entitles such corporation or individual to the rank of patron.

The Society cordially invites to membership all who are interested in any branch of optics, either in research, in instruction, in optical or illuminating engineering, in the manufacture and distribution of optical goods of all kinds, or in physiological and medical optics.

ANNUAL DUES

Regular members, $8.50; Associate members, $6.00; Corporate members, $50.00. These dues include subscription to the Society's official journal, the *Journal of the Optical Society of America.*

CHANGES OF ADDRESS

All changes of address of members of the Optical Society of America should be communicated to the Secretary, Professor Arthur C. Hardy, Massachusetts Institute of Technology, Cambridge 39, Massachusetts.

Journal of the
OPTICAL SOCIETY
of AMERICA

VOLUME 38, NUMBER 7 JULY, 1948

The Photographic Reciprocity-Law Failure for Radiations of Different Wave-Length*

M. BILTZ AND J. H. WEBB
Kodak Research Laboratories, Rochester, New York

(Received February 16, 1948)

The reciprocity-law failure of a number of dye-sensitized emulsions has been studied for radiations of different wave-length. The curves showing the exposure, It, to give a certain density, d, as a function of the exposure time, t, are found to be essentially, but not always exactly, parallel if curves referring to the same density are compared. This is in agreement with previous experience. For the case of complete parallelism, a relation is derived between the slope, G, of the intensity scale H and D curves obtained with radiations of different wave-length, λ_1 and λ_2, and exposure times, t_1 and t_2:

$$1/G(\lambda_1, t_1) - 1/G(\lambda_2, t_1) = 1/G(\lambda_1, t_2) - 1/G(\lambda_2, t_2).$$

This means that, for a given emulsion, the shapes of spectral-sensitivity curves (log exposure required to obtain a certain density as a function of wave-length) for different exposure times are identical, providing all the exposures within one spectral-sensitivity curve are of the same duration. The above equation is compared with the experimental results and found to hold within rather narrow limits.

The bearing of the experimental results on tone reproduction and on the distribution of the latent image within the silver bromide grains is discussed.

INTRODUCTION

THE work reported in this paper is an attempt to elucidate a few points of the photographic reciprocity-law failure which, so far, have not always been fully understood.

It has been known for a long time[1] that the Schwarzschild exponent,

$$p = \frac{\log I_2 - \log I_1}{\log t_1 - \log t_2},$$

or the slope of the reciprocity-law failure curve,

$$p - 1 = \frac{\log(I_2 t_2) - \log(I_1 t_1)}{\log t_1 - \log t_2},$$

where I_1 is the illumination required to obtain a certain density, d, with the exposure time, t_1; and I_2 is the illumination required to obtain the same density, d, with another exposure time, t_2, is constant only within a limited range of exposure times.

Becker and Werner[2] and Baker[3] have shown that, within this range, the Schwarzschild exponent is nearly independent of the wave-length of the exposing radiation, in other words,

* Communication No. 1181 from the Kodak Research Laboratories.

[1] E. Englisch, "Das Schwärzungsgesetz für Bromsilbergelatine," W. Knapp, Halle a. d. Saale, 1901, p. 14, see S. E. Sheppard and C. E. K. Mees, *Investigations on the theory of the photographic process*, Longmans, Green and Co., London, 1907, pp. 214–224; E. Kron, Publikationen des astrophysikalischen Observatoriums zu Potsdam No. 67, Vol. **22**, Part 5, 1913; E. Kron, Ann. d. Physik (4)**41**, 751–758 (1913).

[2] A. Becker and A. Werner, Zeits. f. wiss. Phot. **5**, 382–391 (1907).

[3] E. A. Baker, Proc. Roy. Soc. Edinburgh **45**, Part II, 166–186 (1925); **47**, Part I, 34–51 (1927).

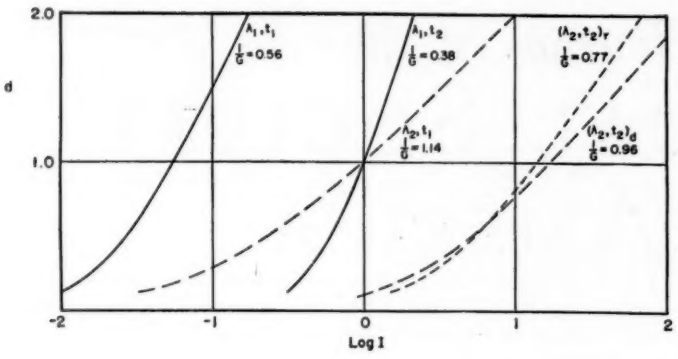

FIG. 1. Intensity-scale H and D curves to illustrate the slope conditions: $1/G$ = reciprocal value of slope between densities, 0.5 and 1.5. Difference slope condition (4) illustrated by curves λ_1, t_1; λ_2, t_1; λ_1, t_2 and $(\lambda_2, t_2)_d$. Condition (1) is fulfilled for any constant density value; ratio slope condition (7) illustrated by curves λ_1, t_1; λ_2, t_1; λ_1, t_2; $(\lambda_2, t_2)_r$. Condition (1) is fulfilled only for the (arbitrary) density, 0.6.

that the reciprocity curves for different colors are nearly parallel. Further investigations of the manner in which the photographic reciprocity-law failure varies for radiations of different wave-length were carried out by Hnatek,[4] by Storer,[5] by Wildt,[6] and by Webb.[7]

Webb found that the reciprocity curves for radiations of different wave-length, plotted so as to show the logarithm of the exposure ($\log It$) to produce unit density as a function of the logarithm of the exposure time ($\log t$), are essentially parallel. This was found to hold not only for the narrow exposure-time range within which the Schwarzschild exponent is constant but over a wide exposure-time range.

THEORETICAL CONSIDERATIONS

From Webb's findings mentioned in the last paragraph,[7] he made a statement (given later) with regard to photographic tone reproduction (p. 319 of Webb's paper[7]). Kienle[8] pointed out that it would follow from this statement, which he thinks is a correct conclusion from Webb's experiments, that the shapes of the intensity scale H and D curves would be identical for all wave-lengths. Because this is, of course, not the case, he doubts the accuracy of Webb's experiments. Although there is actually no reason to doubt the accuracy of his experiments, the statement as it stands is open to misunderstanding. In order to make clear what is meant, it is written down in a slightly different form: "The experimental fact manifested by the parallelism of the reciprocity curves for different wave-length radiations has a bearing upon the subject of tone reproduction of colored objects. For example, let it be assumed that two objects of different color are photographed simultaneously at a particular level of illumination and that the relative brightness of the two objects is such as to produce equal densities on the photographic emulsion. If, now, the level of illumination on both objects is changed to any other value (the relative brightness of the objects remaining the same) *and the exposure time is so adjusted that one of the objects produces the same density as before*, then the other object also produces the same density."**.[9] Now, it will be seen that this statement does not mean that the shape of the H and D curve is independent of the wave-length. What it means is that the shapes of the spectral sensitivity curves ($\log It$ required to obtain a certain density as a function of wave-length) for different exposure times are identical, providing all the exposures within one spectral-sensitivity curve are of the same duration.

From the parallelism of the reciprocity curves,

[4] A. Hnatek, Zeits. f. wiss. Phot. **22**, 177–192 (1923).
[5] N. W. Storer, Lick. Obs. Bull. **14**, 41–57 (1929); H. Kienle, Zeits. f. Astrophys **1**, 332–335 (1930).
[6] R. Wildt, Zeits. f. Astrophys **3**, 386–390 (1931); Phot. Korr. **69**, 81–86 (1933).
[7] J. H. Webb, J. Opt. Soc. Am. **23**, 316–323 (1933).
[8] H. Kienle, Naturwiss. **23**, 762–767 (1935) on p. 764; Zeits. f. wiss. Phot. **37**, 282–283 (1938).

** Narath (see reference 9) remarks that such a general conclusion cannot be drawn from the experimental facts given in Webb's paper, because these experiments refer only to unit density. On the other hand, such a conclusion, as revised above, can be drawn if it is proved that the parallelism of the reciprocity curves ($\log It$ *vs.* $\log t$) for different colors holds not only for unit density but for any density. In fact, at the time Webb's paper was published, his results gave evidence of such a behavior of the curves, although they were not included in the paper. Further evidence will be given in what follows.

[9] A. Narath, Zeits. f. wiss. Phot. **37**, 162–192 (1938) on p. 179; **37**, 283 (1938).

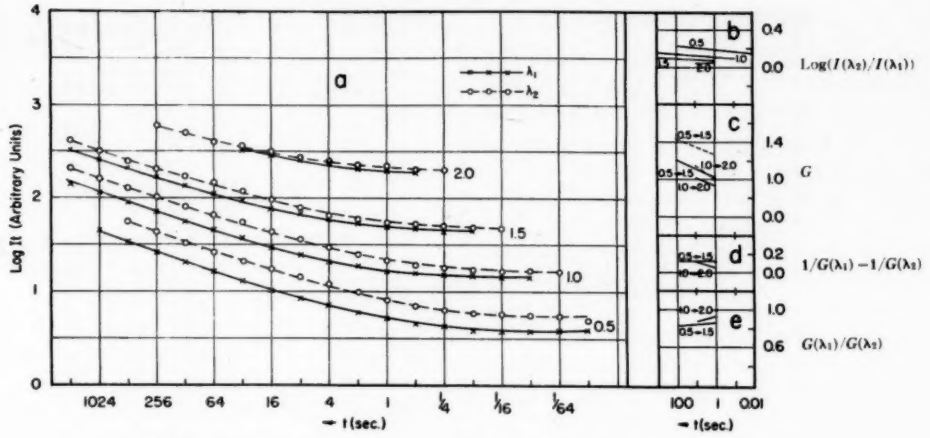

FIG. 2. Medium-contrast orthochromatic emulsion: λ_1 with Wratten filters, 36 and 38; λ_2 with Wratten filter, 23*B*.

Explanation of Figs. 2–7: Curves *a* are reciprocity-law failure curves indicating exposure, *It*, necessary to obtain constant density as function of exposure time, *t*. Density to which each curve refers is written on the curve.

Curves *b* show ratio, $I(\lambda_2)/I(\lambda_1)$, of the illumination required to obtain constant density with light of different color, λ_1 and λ_2, as function of exposure time, *t*. Density to which each curve refers is written on the curve.

Curves *c* show slope, *G*, of intensity-scale *H* and *D* curves as function of exposure time, *t*. Inscriptions, 0.5→1.5 and 1.0→2.0, indicate that curve refers to average slope between densities, 0.5 and 1.5, and 1.0 and 2.0, respectively.

Curves *d* show difference between reciprocal slope values, $G(\lambda_1)$ and $G(\lambda_2)$, of intensity-scale *H* and *D* curves made with light of different color, λ_1 and λ_2, as function of exposure time, *t*. Curves demonstrate validity of "difference slope condition" (4). The inscriptions, 0.5→1.5 and 1.0→2.0, indicate that the curve refers to average slope between densities, 0.5 and 1.5, and 1.0 and 2.0, respectively.

Curves *e* show ratio of slope values, $G(\lambda_1)$ and $G(\lambda_2)$, of intensity-scale *H* and *D* curves made with light of different color, λ_1 and λ_2. Curves demonstrate validity of "ratio slope condition" (7). Inscriptions, 0.5→1.5 and 1.0→2.0, indicate that curves refer to average slope between densities, 0.5 and 1.5, and 1.0 and 2.0, respectively.

the following conclusion with regard to the shape of the characteristic curves for radiations of different wave-length can be drawn: Let $I(d_1, \lambda_1, t_1)$ and $I(d_1, \lambda_2, t_1)$ be the illuminations which give a certain density, d_1, with the exposure time, t_1, at the wave-lengths, λ_1 and λ_2. The corresponding values of illumination for another exposure time are $I(d_1, \lambda_1, t_2)$ and

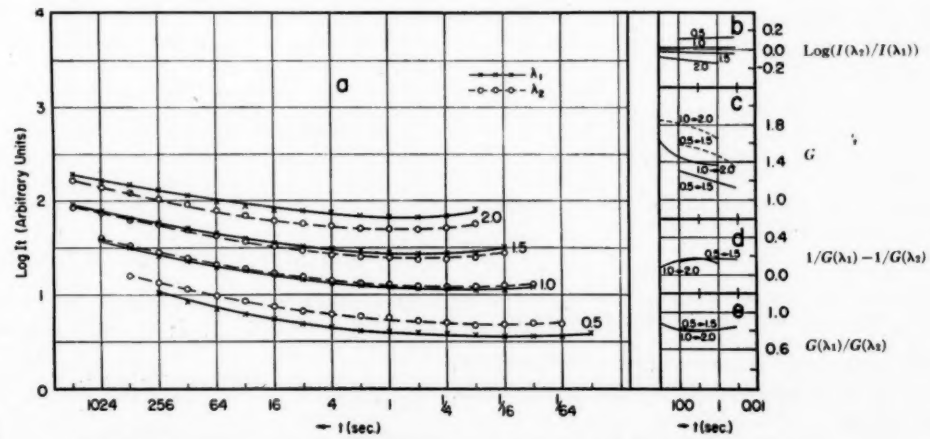

FIG. 3. High-contrast orthochromatic emulsion: λ_1 with Wratten filter, 36; λ_2 with Wratten filter, 22.

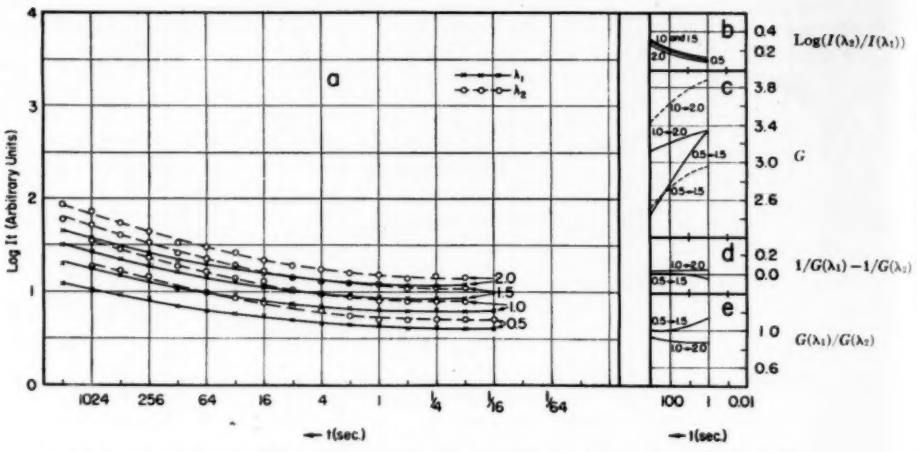

FIG. 4. Very high contrast orthochromatic emulsion: λ_1 with Wratten filter, 36; λ_2 with Wratten filter, 21.

$I(d_1, \lambda_2, t_2)$. For $d_1 = 1$, we obtain, according to Webb's findings,

$$\log I(d_1, \lambda_1, t_1) - \log I(d_1, \lambda_2, t_1) = \log I(d_1, \lambda_1, t_2) - \log I(d_1, \lambda_2, t_2). \quad (1)$$

If this equation is assumed to hold not only for $d_1 = 1$, but for any density, d, then, by subtracting from (1) a corresponding equation for the density, d_2, the following equation is obtained:

$$\log I(d_1, \lambda_1, t_1) - \log I(d_2, \lambda_1, t_1) - [\log I(d_1, \lambda_2, t_1) - \log I(d_2, \lambda_2, t_1)] = \log I(d_1, \lambda_1, t_2) - \log I(d_2, \lambda_1, t_2) - [\log I(d_1, \lambda_2, t_2) - \log I(d_2, \lambda_2, t_2)]. \quad (2)$$

As the reciprocal value of the slope of the characteristic curve between the densities, d_1 and d_2, is

$$\frac{1}{G} = \frac{\log I(d_1) - \log I(d_2)}{d_1 - d_2}, \quad (3)$$

Equation (2) can be written as representing a "difference slope condition":

$$\frac{1}{G(\lambda_1, t_1)} - \frac{1}{G(\lambda_2, t_1)} = \frac{1}{G(\lambda_1, t_2)} - \frac{1}{G(\lambda_2, t_2)}. \quad (4)$$

This is the correct interpretation of Webb's experiments. Parallelism of the characteristic curves for different wave-lengths $[G(\lambda_1, t_1) = G(\lambda_2, t_1)$ and $G(\lambda_1, t_2) = G(\lambda_2, t_2)]$ is a special case which is not frequently met, as was correctly stated by Kienle, but by no means is it a conclusion from Webb's experiments. The statement just given regarding tone values can readily be verified by inspection of the H and D curves of Fig. 1, which follow Condition (1) for any value of density and, therefore, also follow the difference slope condition, (4).

Webb[10] has shown that there is a simple relation between intensity-scale H and D curves made at different wave-lengths but with the same exposure time, t. This relation is expressed by the equation

$$G(\lambda_1, t_1)/G(\lambda_2, t_1) = K_1, \quad (5)$$

where K_1 is a constant independent of density. For another exposure time, t_2, there would be

$$G(\lambda_1, t_2)/G(\lambda_2, t_2) = K_2. \quad (6)$$

One might expect the "stretching constant," K, to be independent of the exposure time ($K_1 = K_2$), in which case the "ratio slope condition" would hold:

$$G(\lambda_1, t_1)/G(\lambda_2, t_1) = G(\lambda_1, t_2)/G(\lambda_2, t_2). \quad (7)$$

But this equation is generally not compatible with Eq. (4) (Fig. 1). It is compatible only if

$$G(\lambda_1, t_1) = G(\lambda_1, t_2) \quad \text{and} \quad G(\lambda_2, t_1) = G(\lambda_2, t_2), \quad (8)$$

[10] J. H. Webb, J. Opt. Soc. Am. **26**, 12–23 (1936).

i.e., if the slope is independent of the exposure time, or if

$$G(\lambda_1, t_1) = G(\lambda_2, t_1)$$
$$\text{and} \qquad (9)$$
$$G(\lambda_1, t_2) = G(\lambda_2, t_2),$$

i.e., if the slope is independent of the wave-length. Figure 1 shows that even when the slope of the H and D curve changes considerably with exposure time and wave-length, the curves calculated from the "difference slope condition" and from the "ratio slope condition" are not far apart. Therefore, although, generally, neither of the two pairs of equations, (8) and (9), are strictly fulfilled over a wide range of exposure times and wave-lengths with modern commercial emulsions, the deviations from either (8) or (9) are so small that it is hardly possible to prove which one of the equations, (4) or (7), they follow more closely. For example, with the panchromatic plate "Guilleminot 2000 H & D Antihalo," Bernanose[11] found no appreciable change in the slope of intensity-scale H and D curves made at the same wave-length, with exposure times ranging from 30 to 600 seconds (i.e., Eq. (8) holds), although different slopes were obtained at different wave-lengths (i.e., Eq. (9) does not hold).

EXPERIMENTAL RESULTS

Some recent experimental data on reciprocity-law failure for radiations of different wave-length will now be given. The results will be used to check the previously derived equations, (1) (parallelism of the reciprocity curves for different wave-lengths), (4) (difference slope condition), and (7) (ratio slope condition).

The experimental procedure is similar to that used in previous work.[7] By means of a sector wheel which makes one revolution during the exposure, time-scale exposures consisting of ten power-of-two steps are made. The instrument with certain improvements was fully described by Jones[12] and by Webb.[13] In order to be able to measure reciprocity curves at various wave-lengths, instead of the mercury-vapor arc lamp used for previous work, tungsten-filament lamps (with filters) were employed at a color temperature of 2500°K. For the high intensity exposure, a 115-volt, 500-watt projection lamp was operated at 3.20 amperes. Its luminous intensity was 172 candles. For the low intensity exposures, a 10-volt, 3.5-ampere photometric lamp, with a single vertical wire, was run at 3.00 amperes. By means of a horizontal slit in front of the lamp its luminous intensity was adjusted to about 2.7 candles (1/64 of the other lamp). An intensity

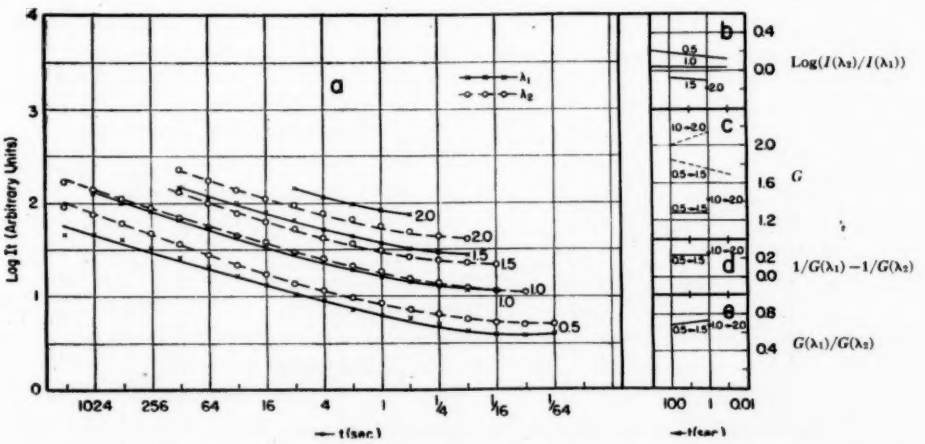

FIG. 5. Experimental panchromatic emulsion showing a large slope difference for light of different wave-lengths: λ_1 with Wratten filters, 36 and 38; λ_2 with Wratten filter, 29.

[11] A. Bernanose, Arch. origin. Docum. CNSR, No. 255; Sci. et ind. phot. (2) **18**, 15–18, 289–294 (1947).
[12] L. A. Jones, J. Opt. Soc. Am. **7**, 305–319 (1923).
[13] J. H. Webb, J. Opt. Soc. Am. **23**, 157–169 (1933).

variation in the ratio 256:1 for the high intensity lamp, and in the ratio 128:1 for the low intensity lamp was attained by changing the distance between the light source and the photographic emulsion by a factor of 16:1 and of 11.3:1, respectively. With both lamps, an intensity ratio of 8192:1 could be covered, the illuminations given by the lamps overlapping by a factor of two at the limits of their ranges. This overlapping was necessary in order to connect the measurements carried out with the two lamps. Two series of time-scale exposures were made, one of them with a blue filter, the other with a filter which transmitted only the longest wave-lengths to which the emulsion in use was sensitive. The filters were arbitrarily chosen so that, with the other experimental conditions unchanged, in every case full time-scales could be obtained. Therefore, for emulsions of low sensitivity, filters transmitting a wider wave-length region were used than for emulsions of high sensitivity.

Great care was taken to keep the luminous flux constant. Voltage regulation was obtained by means of an electronic regulator. The luminous flux was recorded on a recording ammeter by means of a photronic cell and a direct-current amplifier. Throughout one experimental series, the luminous flux remained constant within ± 2 percent, which is well within the limits of the other experimental errors (development, density reading, etc.). On every emulsion tested, thirty-four time-scale curves were made, for which four film sheets, 5×7 inches, were used. On the first sheet, nine exposures were made with blue light from the high-intensity lamp, the intensity varying by a factor of 2 from one exposure to the next. The second sheet received the corresponding exposures for light of longer wave-lengths. On the third and fourth sheets, eight exposures from the low intensity lamp were made with the same variation factor for the intensity and with light of short and of long wave-lengths, respectively.

The four sheets were developed simultaneously in Kodak D-19 Developer for a period of 5 minutes at a temperature of 20°C by means of the developing machine described by Jones, Russell, and Beacham.[14] From the family of time-scale exposure curves obtained for intensity values varying by powers of two, it is possible to derive a family of intensity-scale curves. In this way twenty intensity-scale H and D curves were plotted for exposure times from 1/256 to 2048 seconds, varying with a time factor of 2 from one curve to the next. These curves were used to plot reciprocity-law failure curves, the logarithm of the exposure ($\log It$) required to produce a certain density as a function of the logarithm of the exposure time ($\log t$). As the absolute

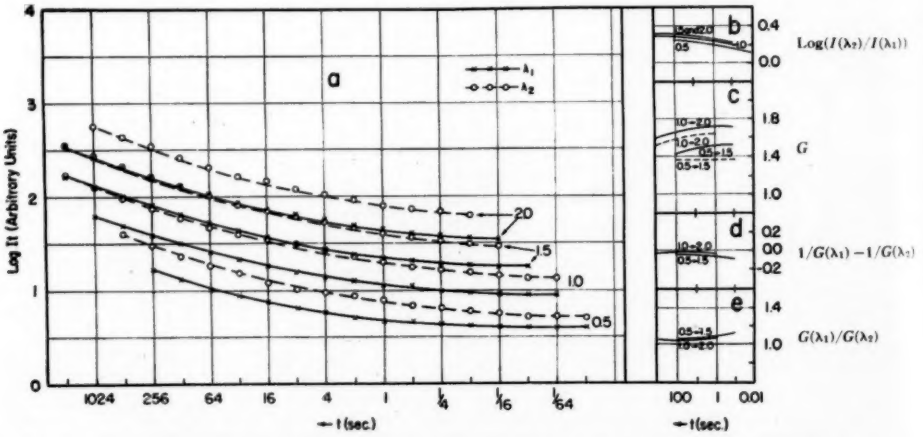

FIG. 6. Panchromatic emulsion: λ_1 with Wratten filters, 38A and 39; λ_2 with Wratten filters, 29 and neutral density 0.6.

[14] L. A. Jones, M. E. Russell, and H. R. Beacham, J. Soc. Mot. Pict. Eng. **28**, 73–94 (1937).

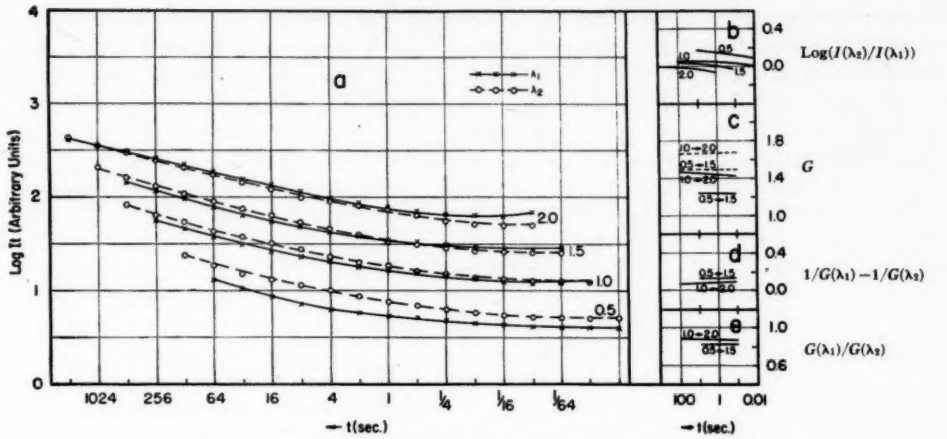

FIG. 7. Panchromatic reversal emulsion: λ_1 with Wratten filters, 38 and 39; λ_2 with Wratten filters, 23 and 33.

values of the illumination have not been measured, the units of the ordinate are arbitrary. Usually, the points for light of short and long wave-lengths (λ_1 and λ_2) at an exposure time of 1/128 second were placed on log *It* values of 0.6 and 0.7, respectively. The positions of all other points are then fully fixed. The curves were plotted for the densities, 0.5, 1.0, 1.5, and 2.0. For testing Eqs. (4) and (7), the slope values are read from the curves. It can easily be seen that the reciprocal value of the average slope between the densities, 0.5 and 1.5 $[1/G(t, \lambda)]$, is the vertical distance of the reciprocity-law failure curves for these two densities.

The experiments were restricted to photographic materials coated with a single emulsion layer. This rigid restriction should be carefully kept in mind, since it prevents generalization of the results to a great many commercial emulsions. This restriction was felt to be necessary, since the present work was undertaken primarily not to give data applicable for scientific or technical problems (celestial photography, spectroscopic analysis, etc.), but to contribute to the theory of the photographic process. Materials coated with two emulsions of different sensitivity and slope do not necessarily give smooth *H* and *D* curves for filtered light and sometimes do not follow Condition (5).

At first sight, the reciprocity curves shown in Figs. 2a to 7a look parallel. A more careful comparison of the pairs of curves referring to the same density but to different wave-lengths shows that in several cases there are small but real deviations from parallelism. The comparison is facilitated by Figs. 2b to 7b, which show the differences between the pairs of curves as a function of the exposure time. If the pairs of curves were exactly parallel (Eq. (1) were fulfilled), then these difference curves would be horizontal. The differences tend to increase with increasing exposure time but, usually, the deviations from parallelism are small. The largest deviations have been found for the very high contrast orthochromatic emulsion (Fig. 4) and for the panchromatic reversal emulsion (Fig. 7). Over an exposure time range of 1:1000 and 1:10,000, respectively, the ordinate values (Figs. 4b and 7b) change by about 0.15 unit. This means that over the exposure range mentioned the ratio of the exposures required to obtain a certain density with light of different wave-lengths $(I(\lambda_1)/I(\lambda_2))$ changes by 40 percent.

Figures 2c to 7c show the slope of the intensity-scale *H* and *D* curves between the densities, 0.5 and 1.5, and those between the densities, 1.0 and 2.0. It is seen that large slope differences for different wave-lengths are compatible with constant exposure ratios, $I(\lambda_1)/I(\lambda_2)$.

For all the materials tested, the "difference slope condition," (4), holds even better than Eq. (1), because the deviations from (1) tend to

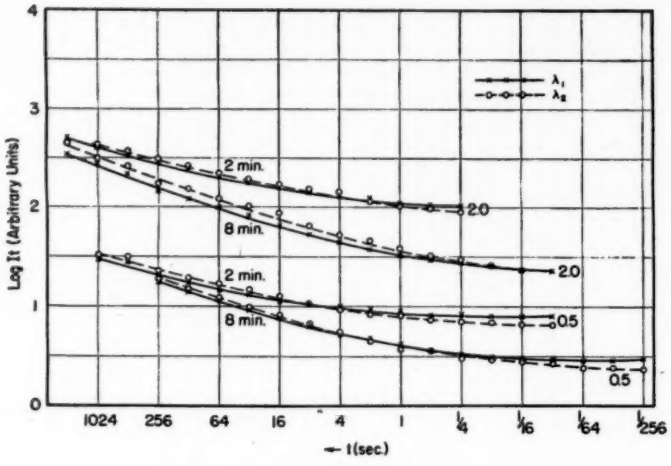

FIG. 8. Reciprocity curves of a panchromatic reversal emulsion for 2 and 8 min. development time. Density to which each curve refers is written on the curve: λ_1 with Wratten filters, 38 and 39; λ_2 with Wratten filters, 23 and 33.

be equal for different densities (the curves of the Figs. 2b to 7b tend to be parallel). This is shown by Figs. 2d to 7d, the curves of which are essentially horizontal. Deviations from Eq. (4) as large as 0.15 unit within a density range of 0.5, as found by Hopwood and Craggs,[15] were never observed. These authors compared the shape of the *H* and *D* curves obtained under different exposure conditions at different wavelengths. An exposure was made first, continuously, with a tungsten-filament lamp, and second, with a hydrogen spark, the duration of one discharge being 1 to 20 microseconds. No exposure times were given. Although, according to former experiments[7] and those presented in this paper, such a large deviation as that found by Hopwood and Craggs would not be expected, there is no doubt that their findings are correct for the particular emulsions and conditions of their experiments.

Finally, Figs. 2e to 7e are plotted to show how well the "ratio slope condition" is fulfilled. In comparing the deviations of these curves from the horizontal with the corresponding deviations of the curves of Figs. 2d to 7d, it should be kept in mind that the deviations should be considered in logarithmic ordinate units rather than in numerical units. It is then evident that Condition (7) holds as well as Condition (4).

Further experiments were made on the dependence of reciprocity-law failure upon development. That the Schwarzschild exponent changes with changing time and temperature of development was observed by Werner.[16] Kron[1] found that the latent image produced with a long exposure time is developed more quickly than that produced with a short exposure time. These results were confirmed and extended by Odencrants,[17] Baker,[3] Jones, Hall and Briggs,[18] Cabannes,[19] Hofmann,[20] Strock,[21] Bäckström and Gordon,[22] Viollet,[23] and De Vaucouleurs and Viollet.[24] They were explained by Lüppo-Cramer,[25] and by Berg, Marriage, and Stevens[26] on the assumption, proved experimentally by the latter authors, that with increasing exposure time the greater part of the latent image is situated near the grain surface. Furthermore, Baker has found (reference 3, p. 177) that, on a panchromatic plate, the Schwarzschild exponent

[15] W. Hopwood and T. D. Craggs, J. Opt. Soc. Am. **37**, 560–565 (1947).

[16] A. Werner, Zeits. f. wiss. Phot. **6**, 25–29 (1908).

[17] A. Odencrants, Zeits. f. wiss. Phot. **18**, 220–226 (1919).

[18] L. A. Jones, V. C. Hall, and R. M. Briggs, J. Opt. Soc. Am. **14**, 223–232 (1927).

[19] J. Cabannes, "La diffusion moléculaire de la lumière," Paris, 1929, p. 83.

[20] P. O. Hofmann, Physikal. Zeits. **36**, 650 (1935).

[21] L. W. Strock, Skrifter utgitt av det Norske Videnskaps-Akademi i Oslo, Mat.-naturv. Klasse, 1938, No. 10.

[22] H. Bäckström and H. Gordon, Ingeniörs Vetenskaps Akademien Handlinger (Proc. Roy. Swedish Inst. for Engineering Research), No. 176 (1944).

[23] R. Viollet, Comptes rendus Ac. Sc. **220**, 396–398 (1945).

[24] G. de Vaucouleurs and R. Viollet, Sci. et ind. phot. (2) **18**, 97–100 (1947).

[25] Lüppo-Cramer, Phot. Korr. **72**, 1–3 (1936).

[26] W. F. Berg, A. Marriage, and G. W. W. Stevens, J. Opt. Soc. Am. **31**, 385–394 (1941). For additional information, see: P. C. Burton and W. F. Berg, Phot. Jour. **86B**, 2–24 (1946); W. F. Berg, Phot. Jour. **86B** 154–158 (1946).

is independent of the wave-length of the exposing radiation for a development time of 1.5 minutes in pyro-soda developer, as well as one of 4 minutes, although the exponents were different for the different development times.

The reciprocity curves of the panchromatic reversal emulsion for radiations of different wave-length and for different development times (Fig. 8) agree with those of the former experiments and extend them beyond the range of a constant Schwarzschild exponent. With the same development time, the reciprocity curves are parallel for radiations of different wave-length within narrow limits, although the curves for different development times are not parallel.

DISCUSSION

The bearing of the experimental results on tone reproduction was discussed earlier in this paper. Another aspect will now be discussed briefly.

The effective light-absorption in a sensitized grain takes place only at the surface where the dye is adsorbed, whereas, in a nonsensitized grain, light is absorbed throughout the grain. As a result, one might expect a different distribution of the latent image in the two cases and, therefore, a different behavior with regard to reciprocity-law failure and development speed. But, from the fact that the reciprocity curves for radiations of different wave-length are essentially parallel, and this holds true for any development time, it follows that the distribution of the latent image within a silver bromide grain is essentially the same in both cases.

This result is in agreement with former experience[27, 28] and was originally explained by Leszynski[27] and Eggert[28] on the assumption that a liberated electron is able to travel over many ion distances in the silver bromide crystal to a distant silver ion.*** This assumption is supported by photoconductivity measurements which show that the mean free path of an electron liberated by light is of the order of the grain dimension.[29] Another explanation[30] is that even in the region of natural sensitivity only bromide ions which are situated near the grain surface participate in the formation of the latent image by releasing electrons. These ions are supposed to be less stable than those in the interior of the grain, because they are situated at irregular spots (cracks, sites of distortion) in the lattice. This explanation necessitates the assumption of a transfer of energy[31] absorbed by the silver bromide in the interior of the grain to the unstable bromide ions which are situated—as is the silver bromide-dye combination—near the surface. So far, there is no conclusive experimental evidence for the occurrence of such an energy transfer within a silver bromide grain.

The small deviations from parallelism of the reciprocity curves for different colors indicate small differences in the distribution of the latent image which, however, do not warrant making any important change in the preceding considerations.

SUMMARY

Using a number of dye-sensitized emulsions, reciprocity-law failure curves (showing the exposure required to give a certain density as a function of the exposure time) are drawn for radiations of different wave-length from measurements of high accuracy. In agreement with previous experiments it is found that the curves referring to different wave-lengths at the same density level are essentially parallel, although small deviations from parallelism are found. This is found to be true for several development times.

From these findings the following relation is derived between the slopes, G, of the intensity-scale H and D curves obtained with different wave-lengths, λ_1 and λ_2, and exposure times, t_1 and t_2:

$$\frac{1}{G(\lambda_1, t_1)} - \frac{1}{G(\lambda_2, t_1)} = \frac{1}{G(\lambda_1, t_2)} - \frac{1}{G(\lambda_2, t_2)}.$$

Furthermore, it can be concluded that the distribution of the latent image within the silver bromide grain is independent of the wave-length of the light by which it is obtained. Possible explanations for this behavior are discussed.

[27] W. Leszynski, Zeits. f. wiss. Phot. **24**, 261–275 (1926).
[28] J. Eggert, Zeits. f. Elektrochemie **32**, 491–501 (1926).
*** According to modern conceptions, the term "silver ion" should be replaced by the term "sensitivity speck."
[29] K. Hecht, Zeits. f. Physik **77**, 235–245 (1932).
[30] J. Eggert and M. Biltz, Trans. Faraday Soc. **34**, 892–901 (1938) on p. 894.
[31] J. Franck and E. Teller, J. Chem. Phys. **6**, 861–872 (1938).

The Two-Quanta Hypothesis as a General Explanation for the Behavior of Threshold Values and Visual Acuity for the Several Receptors of the Human Eye

M. A. BOUMAN AND H. A. VAN DER VELDEN
Physical Institute of the University of Utrecht, Utrecht, Netherlands

(Received January 20, 1948)

With the aid of the three methods for the determination of the number of absorbed quanta necessary for light perception described in previous papers, it is found from extensive threshold measurements with flashes for foveal and peripheral vision that a "red cone" in the periphery probably gives rise to a light impression when two quanta are absorbed in it within a time τ.

For the foveal cone systems a light impression is caused for every wave-length by the absorption of two quanta within a time τ and within an angular distance of 2–4 minutes. The different kinds of receptors proved to be capable of reacting in mutual dependence on each other, and the conclusion is drawn that all receptors send a nerve impulse to the nerve connection when one quantum is absorbed.

A light impression will occur when a second quantum is absorbed after the first absorption within τ sec. within a receptor within a distance D of the first receptor.

Experiments on the visual acuity demonstrate that for all wave-lengths, for foveal as well as for peripheral vision, the dependence of the visual acuity on the intensity agrees with the two-quanta theory.

I. INTRODUCTION

IT has turned out that for the peripheral rod vision the fluctuating results in determining threshold values, the dependence of these values on time and area, and the visual acuity as a function of intensity could all of them be described by the two-quanta explanation of van der Velden[1–3]; two quanta have to be effectively absorbed in the rhodopsin of two rods situated within a distance corresponding with a visual angle D of each other and within a time τ in order to result in a light perception. Each of the absorbed quanta gives rise to a nerve impulse in the rod in which it is absorbed, and these two stimuli will cooperate in producing a light perception only when the conditions just mentioned are satisfied.

These conclusions were drawn from three independent ways of approach for the determination of the number of quanta k necessary for the light perception. For none of these three methods the losses of light by reflection and absorption in the various parts of the eye have to be known. One of them consists in measuring the dependence of the chance of observation of a light flash on the average number of quanta per flash. From the slope of this curve *the upper limit* of the number k can be deduced with the aid of the well-known Poisson formula. When k proved to be not equal to one, the exact determination is not possible with this method as the chance for a light perception will also depend on the casual time between the two absorbed quanta in the flash and the casual distance of the rods in which they are absorbed: When the time between the two absorptions increases the chance for a light perception will not suddenly fall from a constant value to zero, and the same is true with regard to the distance.[3] For these reasons the slope of the curves according to Poisson's formula will become steeper so that the real number of quanta k cannot be deduced from the slope of the experimental curves and only an upper limit for k is obtained. It is evident that the agreement with the theoretical curve for the number k will be closest when the time of the flash as well as the visual angle are as small as possible.

In a previous paper[3] it was shown that the two other methods for the determination of k are free from these complications. The threshold values $\bar{N}_{60\text{ percent}}$ (which we defined as the average number of quanta of the flash for which the chance of observation is 60 percent) as a function of the flash time t for small visual angles for the case $k=2$ is proportional to the root square of t when $t \gg \tau$ and independent of t when $t \leqq \tau$. For the general case $\bar{N}_{60\text{ percent}}$ is proportional to $t^{k-1/k}$ when t is large. From the experiments according to this second method for rod vision

[1] H. A. van der Velden, Physica 11, 179 (1944).
[2] H. A. van der Velden, Opthalmologica 111, 321 (1946).
[3] M. A. Bouman and H. A. van der Velden, J. Opt. Soc. Am. 37, 908 (1947).

7° nasal from the fovea for 5100A, k proved to be 2 and τ about 0.03 sec.

The threshold values $\bar{N}_{60\ \text{percent}}$ for short flashes as a function of the visual angle d is proportional to $d^{2(k-1)/k}$ when $d \gg D$ and almost independent of d when $d < D$. Again $k=2$ was found with this third method and D was about 12′.

The slope of the probability curve yielded by the first method for the smallest visual angles and shortest flash times agreed, moreover, fairly well with $k=2$.

In accordance with these facts the visual acuity has to be proportional to the reciprocal value of the intensity, so long as the details of the figure that must be recognized are greater than the distance within which the stimuli of the absorbed quanta can cooperate to a single light perception. For the threshold of recognition we chose the threshold for which the chance of recognition was again 60 percent. We found that the visual acuity for the peripheral rod vision obeys indeed the two-quanta case.

In this paper we present the experiments about the threshold values and visual acuity for various other wave-lengths for peripheral as well as for foveal vision, both for cones and rods.

II. THE EXPERIMENTAL ARRANGEMENT

In Fig. 1 we give the experimental arrangement. The tungsten ribbon filament lamp L is focused on the slit of a Hilger monochromator with a prism of constant deviation. The second slit is focused by the lens a on the artificial pupil p of 2-mm diameter. The visual angle could be changed by diaphragms b in front of the lens a. The time of observation could be adjusted by a disk c driven by a synchronous motor. The range of wave-lengths let through by the monochromator never exceeded 150A. For the peripheral as well as for the foveal measurements the right eye of M.A.B. was used. This eye was fixed peripherally by means of a red fixation light observed with the fovea of the left eye, in such a way that the spot of the retina with which the flashes were seen was 7° nasal from the fovea of the right eye. For foveal measurements a light source fixed by the left or right eye is of no use as the flashes would then appear on the same place of the visual field as the fixation light. We used for the foveal measurements a ring concentric with the place of the flashes and provided with two arrows, as shown in Fig. 1. This figure was illuminated with white light as weak as possible so that it was just visible to the same eye, with which the measurements were performed. The diameter of the ring was about 7 degrees so that its image activated the peripheral rods. The observer tried to fix as well as possible the center of this figure. In this center the flashes were seen. As regards the foveal measurements the fixation figure and the flashes were seen in this way with the same eye so as to prevent deviations in fixation by the non-parallelism of the two eyes. The intensity of the flashes was varied by means of the current of the tungsten ribbon filament lamp, which was calibrated in the way developed and used by Ornstein.[4] The energy at the pupil p was measured with a thermopile calibrated for absolute value. The eye of the observer was always completely dark-adapted before the experiment was started.

III. THE PERIPHERAL THRESHOLD MEASUREMENTS

In all previous papers the experimental circumstances were such that only the peripheral rods were stimulated. By varying the wave-length from the extreme blue to the extreme red we pass from rod vision to cone vision, so that a region of wave-lengths will exist in which the sensitivity of the two systems is of the same order of magnitude. Outside this region the

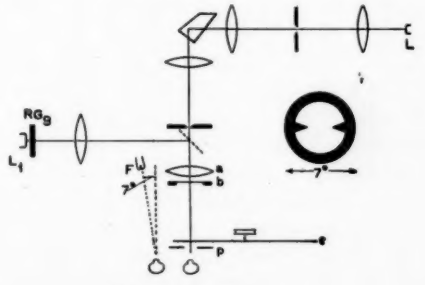

FIG. 1.

[4] L. S. Ornstein, W. J. H. Moll, and H. C. Burger, *Objective Spektral Photometrie Sammlung Vieweg*, Braunschweig, 1932; L. S. Ornstein, J. Opt. Soc. Am. **20**, 573 (1930); L. S. Ornstein, Mlle, J. G. Eymers and M. D. Vermeulen, Revue d'optique **12**, 385 (1933).

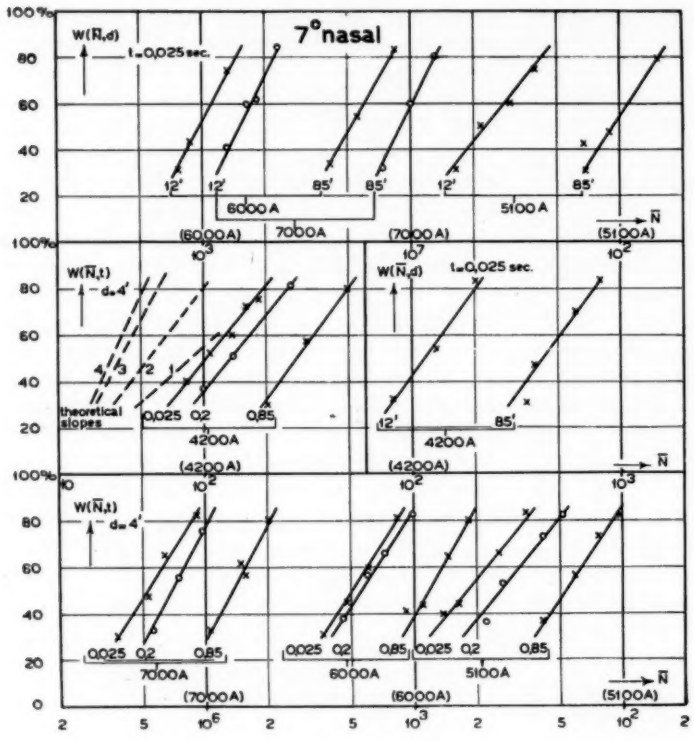

FIG. 2. The chance of observation $W(\bar{N},t,d)$ as a function of $\bar{N}$ for various wave-lengths and for different combinations of d (12′ and 85′) and t (0.025, 0.2, 0.85 seconds). The theoretical slopes for the 1, 2, 3, and 4 quanta cases according to Poisson's law are submitted (dotted lines). The level of energy for each wave-length is indicated along the abscissa.

slope of the probability curve giving the chance of observation as a function of the average number of quanta per flash will on the blue side refer to the rod system and on the red side to the cone system. As already pointed out in the introduction and in reference 3, we can only deduce from this slope the upper limit of the number of quanta k necessary for the two systems. It is possible that the slopes of the probability curves do not agree, even when the two numbers k are equal. Indeed, the time and distance within which the k quanta must be absorbed may differ for the two systems so that the deviations from the theoretical slope according to Poisson may differ for the two systems for reasons mentioned in the introduction.

A question of great importance is whether or not the several systems react independently. In other words, will the absorption of N_1 quanta by the first system and N_2 quanta by the second one result in a light perception or not when both N_1 and N_2 are smaller than the numbers k required by each system separately?

The slope of the probability curve in the region within which the sensitivity of the two systems are of the same order will depend on these curves for the two systems separately. In the case of independence, so that the stimuli of the systems cannot cooperate to produce a light impression in part of this region, the slope of the resulting probability curve will be steeper than those of the two curves of the separate systems. In the case of dependence, so that the stimuli of the two systems can cooperate in producing a light impression, the resulting slope will be intermediate between the slopes of the individual systems.

Figure 2 shows the probability curves for various combinations of flash time and visual area, related to four wave-lengths, the dark-adapted right eye, 7° nasal from the fovea. Besides the slight increase of the slope with increasing time or visual angle which was to be expected,[3] it appears from Fig. 2 that the curves are steeper in the red end of the spectrum.

In one of the graphs of Fig. 2 we plotted also

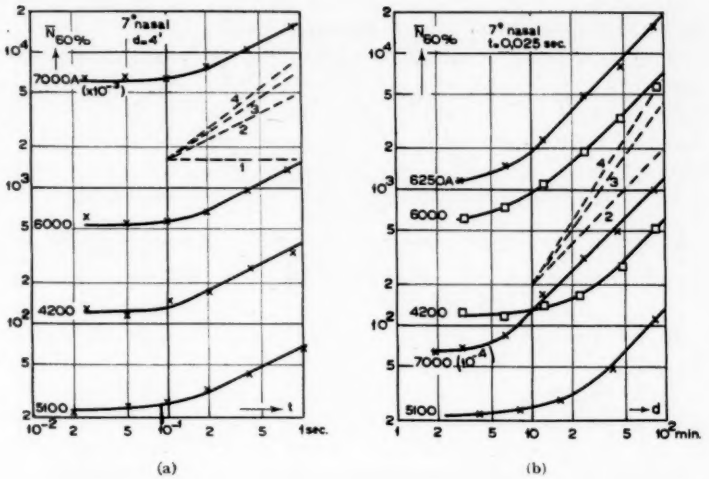

FIGS. 3a and 3b. The average number of quanta, necessary for a chance of observation of 60 percent as a function of t and d, respectively, for various wave-lengths. The theoretical slopes for the 1, 2, 3, and 4 quanta cases are submitted for $d \gg D$ and $t \gg \tau$ (dotted lines).

the theoretical slopes according to Poisson's law. We can deduce along the lines given in the introduction and in reference three that for rod vision the upper limit of the number of effectively absorbed light quanta k necessary for the light perception is 2. From the previous papers we know that k is 2. For cone vision this upper limit is obviously higher, namely, about 3. As we can expect that at about 6000A the rods and cones are almost equally sensitive, the slopes of the curves in this region can give information about the dependence of the different systems. It is noticed that the slopes are not steeper compared with the slopes for 7000A and 5100A. If they were independent, the slope should be steeper compared with the slope for 7000A as well as for 5100A. Although the reliability of the measurements is rather poor for drawing this conclusion, it is likely that the systems are not independent at the threshold of vision.

In Section V we shall use a much more appropriate method by which this conclusion is confirmed.

For the exact determination of k we must make use of the two other methods indicated.[3]

Figure 3 shows the threshold values $\bar{N}_{60\text{ percent}}$ for various combinations of flash time and visual angle. Regarding the curves as a function of time of Fig. 3a we see that the shape is almost the same for all wave-lengths. The slope for t very large agrees for all wave-lengths with $k=2$, as for this case $\bar{N}_{60\text{ percent}}$ has to be proportional to $t^{\frac{1}{2}}$. The slope certainly doesn't agree with $k=3$, as proportionality with t would be required.

The curves of Fig. 3a do not show the existence of the two separate systems because the differences in the time value at which the $\bar{N}_{60\text{ percent}}$ from being independent of t alters into a function of t, proportional to $t^{\frac{1}{2}}$, is very small and might be due to the unavoidably limited accuracy of measurements of this kind.

We can conclude that for the rod and cone system the number k is 2 and these two quanta must be absorbed in a time, which is the same for the two systems, and is equal to about 0.04 sec.[1-3]

The slope of the threshold curves $\bar{N}_{60\text{ percent}}$ as a function of the visual angle d of the flashes of Fig. 3b when d is large agrees again for all wave-lengths with $k=2$, since $\bar{N}_{60\text{ percent}}$ is proportional to d. Using the method of the probability curves (see Fig. 2) we found for 6000A and 7000A an upper limit for k equal to 3 and for smaller wave-lengths 2. This confirms the fact that in the region of the longer wave-lengths another kind of receptor is stimulated than in the green and blue part of the spectrum. This is further confirmed by the appearance of a sensation of color in our threshold measurements in the red region of the spectrum. For all wave-lengths larger than 6000A we experience a reddish sensation, for the other wave-lengths a colorless rod sensation. In the behavior of the threshold curves as

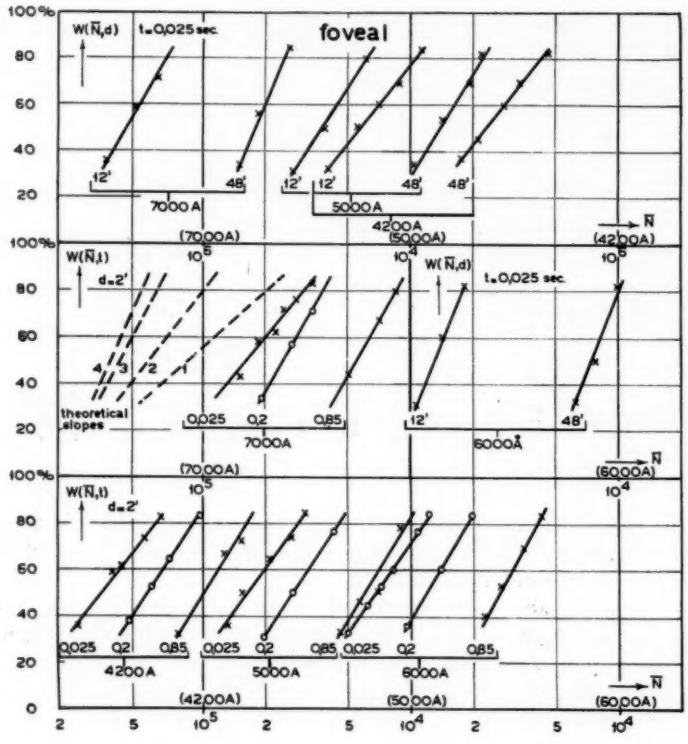

FIG. 4. The chance of observation $W(\bar{N},t,d)$ as a function of $\bar{N}$ for various wave-lengths and for different combinations of d (12′ and 48′) and t (0.025, 0.2, 0.85 seconds). The theoretical slopes for the 1, 2, 3, and 4 quanta case according to Poisson's law are submitted (dotted lines). The level of energy for each wave-length is indicated along the abscissa.

a function of the visual angle we observe a well defined difference between the rod and the cone system. The visual angle value at which $\bar{N}_{60\text{ percent}}$ from being nearly independent of d becomes a quantity proportional to d is almost equal to the distance D within which the two quanta k have to be absorbed in order to result in a light impression.[1-3] It is seen that for the wave-lengths 6000A and 7000A this value becomes about 3 to 4 minutes, whereas for the other wave-lengths D is about 12 minutes. Such a dependence on the wave-length of the distance D within which the two quanta have to be absorbed is only possible when there are more systems than one. In the region of wave-lengths within which the sensitivity of the two systems is of the same order of magnitude the threshold curve as a function of d will change with wave-length from the curve belonging to the rods to the curve of the cones. The way in which the threshold curve is changed from being independent of d to being proportional to d depends not only on this ratio, but also on any possible interaction between the two systems and, moreover, on the facts by which the method of the measuring of the probability curve is not suitable for the exact determination of the number k mentioned in the introduction as these facts can differ for the two systems. For these reasons it cannot be ascertained from the way in which the threshold curve is changed from $D \approx 12'$ to $D \approx 3'$ whether or not the two systems can cooperate, nor can the ratio between their sensitivities as a function of wave-length be determined out of this change.

Accepting the results of Østerberg,[5] there are about 100 rod-like receptors in an area with a visual angle of 10 minutes 7° nasal from the fovea, within which the two quanta must be absorbed. As the chance is negligible that at the threshold for rod vision the two quanta are absorbed in one of this number, a rod reacts on the absorption of one quantum. The rod will send a nerve impulse to its nerve connection. Two impulses of two rods within the distance D

[5] G. Østerberg, Acta Ophthalm. 13 (Supplement) (1935).

mentioned will cooperate and give rise to a light perception.

In a region of 3 to 4 minutes within which the two quanta must be absorbed for cone vision the number of cone-like receptors is very small at 7° nasal from the fovea, namely, about two, according to Østerberg.[5]

So when we identify the rod-like and cone-like receptors of Østerberg with our rod and cone systems, it may be that for the cone system 7° nasal since the wave-length is larger than about 6500A the two quanta have to be absorbed within the self-same receptor. Perhaps by this reason the probability curves of Fig. 2 are steeper in the red compared with the slopes in the blue part of the spectrum, in agreement with the remarks in the introduction. Of course, it might be that the nerve fibers of the separate cones are not long enough to reach the nerve-connection of the next cone as the number of cones is so few in this region of the retina. It is clear that in this case impulses from two cones cannot cooperate. The time within which the two quanta must be absorbed does not differ for the two systems. As for the rod system, each of the two quanta gives rise to a nerve impulse which mutually cooperates in the nerve system; it is very probable that each of the absorbed quanta in a cone for 6500A or larger also causes a nerve impulse and that these two impulses cooperate in a nerve element of the retina similar to the element in which the rod cooperation occurs. If the two quanta absorbed in a cone would give rise to one single nerve impulse, it is rather strange that the time within which the two quanta must be absorbed in the cone agrees with the time mentioned for the rods, which is of nervous origin. From the experiments of Section V it is confirmed that indeed each absorbed quantum arouses a nerve impulse.

IV. THE CENTRAL FOVEAL THRESHOLD MEASUREMENTS

Figure 4 shows probability curves for various combinations of visual angle and flash time for the central fovea of the dark adapted right eye. Neglecting the possibility that for one or more of the chosen wave-lengths the sensitivities of two or more receptor systems are of the same order of magnitude and, moreover, react independently, we can deduce from these curves for the smallest t and d that for all wave-lengths the upper limit of the number k is 3. Most of the curves are steeper than the Poisson formula for $k=2$ requires and less steep than for $k=3$. In paragraph 5 we shall give the experiments as to whether or not an interdependence between various cone systems of the fovea exists according to the method mentioned in the previous paragraph.

For the exact determination of the number k we again used the two other methods. In Fig. 5

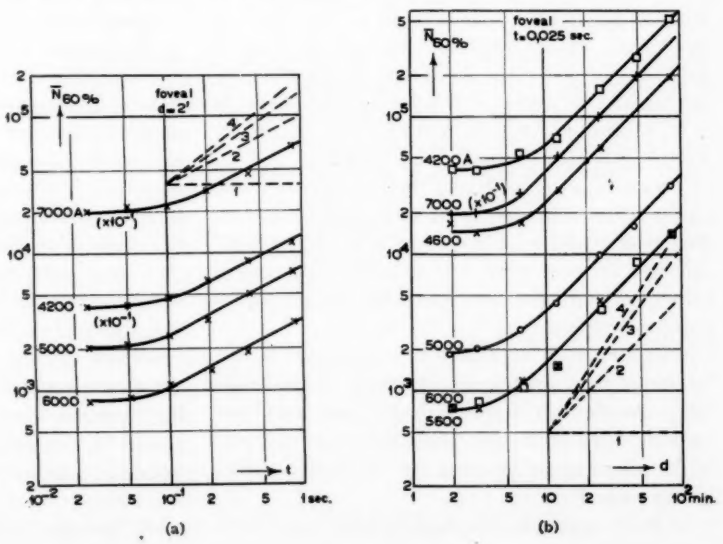

FIGS. 5a and 5b. The average number of quanta, necessary for a chance of observations of 60 percent as a function of t and d, respectively, for various wave-lengths. The theoretical slopes for the 1, 2, 3, and 4 quanta cases are submitted for $d \gg D$ and $t \gg \tau$ (dotted lines).

we give the threshold values $\bar{N}_{60\text{ percent}}$ for various wave-lengths as a function of time and visual angle. The shape of the curves as a function of time is again almost the same for all wave-lengths. The slope with time when t is large agrees with the case $k=2$. From these curves the existence of more systems is not apparent, as here too the difference in the time value, at which the $\bar{N}_{60\text{ percent}}$ shift from being independent of t to the region in which $\bar{N}_{60\text{ percent}}$ is proportional to $t^{\frac{1}{2}}$, is very small.

The slope of the threshold curves $\bar{N}_{60\text{ percent}}$ as a function of the visual angle d of the flashes when d is large agrees again for all wave-lengths with $k=2$. Till now we have from our measurements no evidence that for the foveal vision more than one receptor system exists. The slopes of the probability curves as well as the threshold curves as a function of time or visual angle do not give any clear indication of the actual existence of more than one system. For the measurements of the dependence of $\bar{N}_{60\text{ percent}}$ on the visual angle it is of the greatest importance to apply with the utmost care the necessary corrections for the chromatic aberration of the eye. Without these a great dependence on the wave-length of the region of the visual angle d in which $\bar{N}_{60\text{ percent}}$ is almost independent of d is found, as without a good correction the illuminated area of the retina will not decrease below a definite value, dependent on the wave-length, when the visual angle of the flash is decreased. In our experimental arrangement it was necessary for the right eye of the observer to apply the above correction with a lens of -0.75 diopter for 7000A and with -2.25 for 4200A in front of the artificial pupil.

To summarize, we found that for foveal vision again two quanta must be effectively absorbed within a distance of about 2 to 4 minutes and within a time of about 0.04 sec. This time agrees once more with the time found for the peripheral cone and rod system.

Of course it is necessary to measure this time for more places of the retina, but it seemed that the nerve element in which the cooperation of the two impulses of the two absorbed quanta occurs is for all receptor systems for the whole retina of the same kind.

It is not possible to conclude from our foveal measurements that for foveal vision the two quanta must be absorbed in the same receptor. In a region of about 2 to 4 minutes there are, according to Østerberg, 20 to 90 receptors in the central fovea. The chance that the two quanta are absorbed in two different receptors is not negligible, even down to the smallest areas dealt with. The area of the retina covered by the flash will be enlarged by the size of the Airy diffraction disk. For the experimental arrangement described in Section II we must add to the size of the flashes 2.3 to 1.3 minutes caused by diffraction. In order to test whether this influences the region of d in which $\bar{N}_{60\text{ percent}}$ is almost independent of d, we made an arrangement for which the diffraction was smaller, and only about 0.8 to 0.4 minutes had to be added to the size of the flashes computed purely geometrically. We found no influence on the region of d within which $\bar{N}_{60\text{ percent}}$ is almost independent. When the various kinds of receptors are not evenly distributed over the fovea, as suggested by Hartridge,[6] but form clusters of cones of the same kind, the distance D seemed indeed to be larger. When the area of the retina covered by the flash is smaller than such a cluster, a part of the flashes for a certain wave-length can fall on receptors which are insensitive to the wave-length employed. For this reason for the smallest angles $\bar{N}_{60\text{ percent}}$ would become higher than agrees with a homogeneous distribution.

There might be another reason by which the D of the threshold measurements is influenced, namely, the possibly small involuntary movements of the eye which always occur even when the observer tries to fix his eye as well as possible. By these movements the absorption of two quanta, within a certain area, is impeded and increases the threshold when the visual angle of the flash is of the same order of magnitude as the size of such an area. If we accept the results of Østerberg, for peripheral cone vision in the red region the two quanta must probably be absorbed in one cone. So it might be that in the fovea too this condition must be satisfied for these red wave-lengths. In the previous paragraph we also suggested that each quantum absorbed in a cone in the red region may give rise to

[6] H. Hartridge, Nature **158**, 303 (1946).

a nerve impulse. These two nerve impulses must be transmitted by the nerve connection of this cone within a time of about 0.04 sec. for the light perception. From the electrophysiology of nerve fibers it is known that the impulses can only follow each other with intervals greater than the latency period. These periods are about 10^{-4} second. It would seem, therefore, that with decreasing flash time the $\bar{N}_{60\text{ percent}}$ will increase for t values of 10^{-4} second. As far as we know, such an effect has never been found. In our opinion, this is not an objection to the suggestion that under certain circumstances (for instance, in the red retion of foveal and peripheral vision) two quanta might be necessarily absorbed in one cone for the light perception and that the two quanta each cause a nerve impulse in the nerve connection of the cone. The way in which the absorption of a quantum gives rise to a nerve impulse of the cone is practically unknown. In any case, the time between the absorption of a quantum and the start of the impulse in the nerve connection will not be infinitely small and differ time after time by the inevitable natural fluctuations in the course of the process transmitting the energy of the quantum to the starting of a nerve impulse. If this fluctuation in time is longer than the latency time of the nerve connection, two quanta absorbed at the same moment will give rise to two separate nerve impulses in the nerve fiber.

At the Physiological Conference in Oxford and the International Conference on Colour Vision in July 1947 Hecht dealt with, among other things, his experiments concerning the determination of the number k for the absolute and differential threshold for cone vision. His conclusion that for the absolute, as well as for the differential threshold, the absorption of four quanta in a cone of the test spot is necessary, is found on probability curves obtained by the first method described in Section I. As we pointed out at the time, this method is not suitable for the exact determination of k, moreover, the case $k=4$ can certainly not explain the dependence of the threshold with time or visual angle. As we found $k=2$ for the absolute threshold we also have serious objections to the conclusion as regards the differential threshold (intensity discrimination). It is hard to understand how for all intensity levels of the differential threshold the behavior will be in agreement with $k=4$ except when the surrounding intensity is zero. Our preliminary experiments on the intensity discrimination are in agreement with the suggestion of de Vries,[7] excepting for the lowest intensities.

According to de Vries the intensity-discrimination is proportional to the reciprocal of the square root of the intensity.

TABLE I. Chance of observation of flashes with visual angle of 25′ and time 0.025 second 7° nasal from the fovea for various wave-lengths and combinations of wave-lengths.

$W(\bar{N}_1)$	$W(\bar{N}_2)$	$W(\bar{N}_1,\bar{N}_2)$ experimental	$W(\bar{N}_1\bar{N}_2)$ theoretical independent	$W(\bar{N}_1,\bar{N}_2)$ theoretical dependent
6900A, 27%	5320A, 43%	85%	58%	72%
6900A, 27%	5320A, 30%	80%	49%	62%
6900A, 27%	4800A, 25%	64%	45%	60%
6900A, 27%	4620A, 25%	67%	45%	60%
6900A, 27%	4400A, 25%	67%	45%	60%
6900A, 27%	4200A, 30%	65%	49%	62%
6900A, 27%	4700A, 25%	72%	45%	60%
6900A, 27%	5060A, 27%	75%	47%	72%
6900A, 27%	3900A, 30%	77%	49%	62%
6900A, 27%	4500A, 22%	64%	43%	57%
6900A, 27%	4500A, 40%	80%	56%	70%

V. THE MUTUAL DEPENDENCE OF THE RECEPTORS OF DIFFERENT KINDS IN THE RETINA

Pirenne[8] used a method for investigating any possible mutual influence at the threshold of vision between the two eyes. We used this method in a somewhat different way for investigating whether a mutual dependence exists between the receptors of different kinds in the same eye.

Suppose the chance of observation of a flash presented separately with an average number of quanta $\bar{N}_1$ is $W(\bar{N}_1)$ and of another flash $W(\bar{N}_2)$. When these flashes are presented simultaneously to the observer the resulting chance of ob-

TABLE II. Chance of observation of flashes with visual angle of 25′ and time 0.025 second from foveal measurements for various wave-lengths and combinations of wave-lengths.

$W(\bar{N}_1)$	$W(\bar{N}_2)$	$W(\bar{N}_1,\bar{N}_2)$ experimental	$W(\bar{N}_1\bar{N}_2)$ theoretical independent	$W(\bar{N}_1,\bar{N}_2)$ theoretical dependent
6900A, 32%	4200A, 29%	73%	52%	65%
6900A, 38%	4200A, 25%	71%	54%	66%
6900A, 38%	5250A, 28%	90%	55%	70%
6900A, 45%	4000A, 30%	88%	62%	74%
6900A, 45%	5100A, 30%	85%	62%	74%
6900A, 45%	6000A, 25%	85%	59%	72%

[7] H. de Vries, Physica **10**, 553 (1943).
[8] M. H. Pirenne, Nature **152**, 698 (1943).

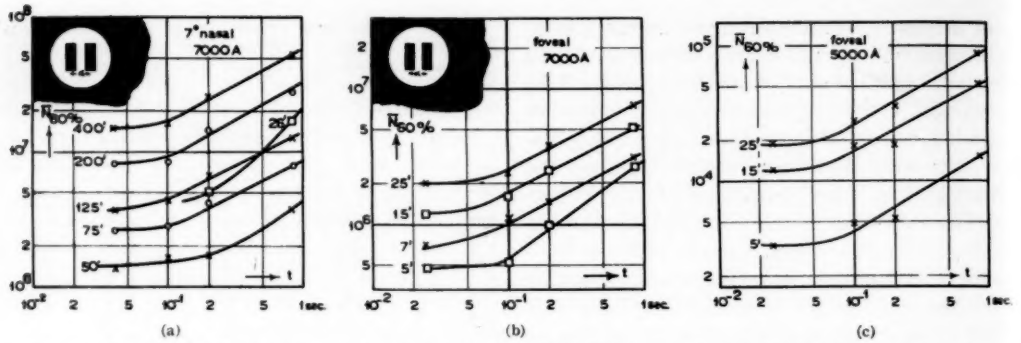

FIGS. 6a, 6b, and 6c. The average number of quanta from the field between the two black stripes as a function of t for different values of the visual angle α for a chance of recognition of 60 percent for some wave-lengths as well for foveal as for peripheral vision.

servation will be $W(\bar{N}_1,\bar{N}_2)=1-[1-W(\bar{N}_1)]\times[1-W(\bar{N}_2)]$ for the case that the receptor system stimulated by the two separate flashes react completely independently. ***As soon as a slight dependence exists, the resulting chance will be greater.***

For the dark adapted eye at 7° nasal from the fovea at the threshold of vision only the cones are stimulated by light of wave-length 7000A and only the rods by quanta from about 6000A downward. In the experimental arrangement of Fig. 1, a glass plate was inserted behind the second slit of the monochromator. By means of this plate the light of a second tungsten ribbon filament lamp L_1 is focused by lens a on the artificial pupil p. The light of L_1 first passed through a Shott RG9 filter so that only quanta of 6900A and greater are used. Now we first determined the current value of L_1 for which the chance of observation of the flash is about 30 percent. The visual angle was always 25′ and the time 0.025 second. We next determined the current values of L for which the chance of observation of flashes of various wave-lengths was again about 30 percent. By the flashes of L_1 only the cones are stimulated. We now expose the eye to the flash of L_1 together with the flashes via the monochromator.

The result is that on the same spot of the retina, and at the same time, quanta of two kinds are absorbed, namely, of 6900A and of another wave-length, depending on the adjustment of the monochromator. In Table I we give the results of these experiments. In the first two columns the chances are given for the components of the mixture separately, in the third the measured resulting chance. From the first and second column the chance is computed for the case of complete independence, and these values are given in column four. In the last column the resulting chances are given for the case where the behavior would have been as of one system and on the assumption that the slope of the probability curve agrees with the Poisson formula for the two quanta case. Table I shows that the resulting chances are always even greater than the chances of the last column. As the experimental resulting chances are greater than the values of a complete independence we can already conclude that there exists mutual dependence. We were forced to choose a rather large visual angle, namely, 25′. It is difficult to check whether for peripheral vision the quanta of the different wave-lengths fall indeed on the same spot of the retina when the flashes are smaller. When for foveal vision the two flashes coincide as regards place, the quanta of the two wave-lengths, if they differ much, are not focused in the same way on the retina when the eye is turned to 7° nasal, as the chromatic deviations of the eye are rather large. In order to make sure that the two flashes coincide, the visual angle of the flashes is chosen rather large and the slopes of the probability curves for the separate flashes will be steeper than agrees with the smallest visual angle (see introduction and reference 3). The slopes will certainly be steeper than the slope of the purely theoretical Poisson curve, so that in the case that there exists mutual dependence of the systems the resulting chances

can even be greater than the chances of the last column. From these considerations we can conclude that the rods and cones react almost completely mutually dependent, as the measured resulting chances are indeed greater than the chances of the last column. The differences of columns 3 and 5 are in fair agreement with the differences between the slopes of the experimental probability curves (see Fig. 2) and the Poisson curve for the two-quanta case.

From the preceding paragraphs and papers it is clear that a rod reacts on the absorption of one quantum and that two rod impulses result in a light perception when the two quanta conditions are satisfied. For peripheral vision in the red region of the spectrum it is probable that two quanta must be absorbed within one cone.

From the interdependence of the rod and cone systems in the periphery we must conclude that if one quantum is absorbed in a cone which is sensitive in the red region of the spectrum and one other quantum is absorbed in a rod situated within a distance D' of the cone a light impression will result.

In Table II we give the results for the foveal measurements. The measured resulting chances show that the receptor system sensitive for a certain wave-length reacts in any case in complete interdependence with the systems sensitive for another wave-length. From what is known concerning the fundamental response curves, reviewed by Wright,[9] the dependence found cannot be explained by a possible overlapping of the sensitivity curves of the three systems. When the two systems are completely independently reacting at the threshold of vision, the resulting chances measured by us should have been smaller for most of the chosen combinations of wave-lengths, even for the curves of Hecht. If our measurements were to be explained by a complete independence, the three response curves must lie closer to each other than Hecht's curves. It turned out to be possible to analyze from foveal threshold measurements the curve representing the sensitivity as a function of wave-length in three components lying very close to the curves of Pitt. We will report on this matter in a later paper. Our components are even somewhat smaller than Pitt's curves. At any rate we must conclude that an almost complete dependence exists between the different cone systems, so that also each absorbed quantum arises a nerve impulse.

We summarize here the information concerning rod and cone vision obtained from our threshold measurements and the investigation about their dependence.

A rod reacts with a nerve impulse in its nerve connection after the effective absorption of one quantum. A light impression is caused by the absorption of a second quantum in a rod within a distance D of the first and within a time τ.

A "red cone" in the periphery gives rise to a light impression when within a time τ two quanta are absorbed in it. The mutual dependence of the peripheral rod and "red cone" sys-

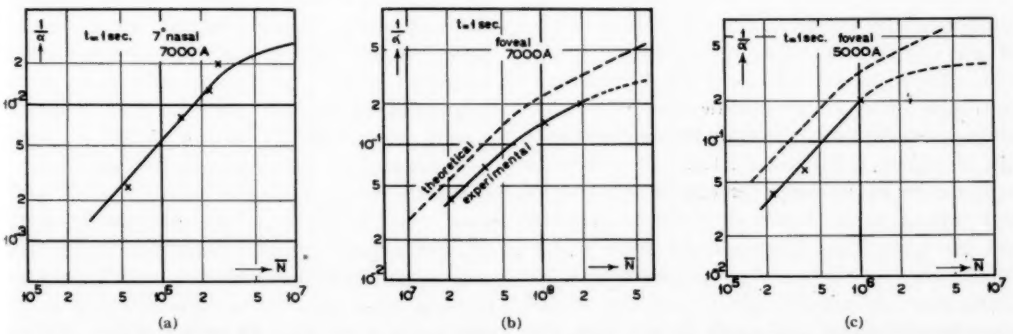

FIGS. 7a, 7b, and 7c. The reciprocal of the visual angle α (visual acuity) as a function of $\bar{N}$, the brightness expressed in the average number of quanta per second per square area (located on the retina) with a visual angle of 10^{-2} radian. The shape of the theoretical curves are given for foveal vision, using the shape of the threshold values as a function of the visual angle from the two-quanta theory.

[9] W. D. Wright, *Researches on Normal and Defective Colour Vision* (Kimpson, London, 1946), p. 371.

tems can only be explained by each absorbed quantum in a cone giving rise to a nerve impulse in the nerve connection of the cone and by one rod stimulus which can cooperate with one cone stimulus to produce a light impression. It is very probable that also for this kind of cooperation the quanta must be absorbed within the time τ and the distance D.

For the foveal cone systems for every wave-length a light impression is caused by the absorption of two quanta within a time τ and a distance D_1 of 2–4 minutes.

The foveal cone systems sensitive for a certain wave-length react at the threshold of vision in complete mutual dependence with the systems sensitive for another wave-length.

A cone of a certain kind reacts with a nerve impulse to its nerve connection after the effective absorption of one quantum. A light impression is caused by the absorption of a second quantum within τ in the same or another cone, which must lie within a rather small distance from the first one. It might be possible that for some wave-lengths the actual distance within which the two quanta must be absorbed are smaller than for other wave-lengths, as the distance D of the measurements ranges from 2 to 4 minutes. For these wave-lengths it is possible that the two quanta must be absorbed within one cone.

A rod stimulus can cooperate with any other second stimulus within a time τ and a distance D to produce a light impression.

It might be possible that the color sensation of a light perception of a "mixed stimulus" can differ definitely from the sensations of the stimuli of the separate systems. In the region within which the sensitivity of two of the systems is of the same order of magnitude and very small areas of the retina are illuminated at the threshold of vision, statistical fluctuations will occur in the color of the light perception as the color will depend on the kinds of receptors in which the two quanta are absorbed. We have started experiments on this subject together with G. ten Doesschate. It seemed likely that for certain wave-lengths short and small flashes can give rise to more than three definitely differing color sensations.[6]

A certain kind of flash, for instance, is sometimes called yellow, sometimes blue or white or green. A further investigation is in the course of being carried out.

VI. THE VISUAL ACUITY

In a previous paper[3] we pointed out that the variation of the visual acuity with the intensity for peripheral rod vision could be described with the two-quanta explanation so long as the details of the figure presented for recognition to the observer are larger than the areas within which the separate stimuli can cooperate. According to this the visual acuity in this region was proportional to the intensity. We investigated this also for a few other wave-lengths for peripheral as well as for foveal vision. The results are shown in Figs. 6 and 7.

For the threshold of recognition of the figure given in Fig. 6 we chose again the average number of quanta $\bar{N}_{60\ \text{percent}}$ of the area situated between the two black stripes for which the chance of recognition was 60 percent. In Fig. 6 the measurements for various flash times are given; Fig. 7 gives the reciprocal values of the distance between the two black stripes as a function of the intensity at the threshold of recognition.

All curves considered as functions of time as well as of intensity agree fairly well with the two-quanta case. For $t>0$, 1 sec. the slopes in Fig. 6 are proportional to the square root of t and for α large, the visual acuity is proportional to the intensity.

As soon as α is increased to values of about 25′, 7° nasal, and to 3′ foveal,[10] deviations from the two-quanta relations occur. In a previous paper[3] it was proved for the rod system that within an area O all stimuli contribute to the brightness impression once a first couple of quanta is absorbed. This area proved to correspond indeed to a visual angle of about 25′.

For the rod system the distance of 25′ is almost twice as large as the distance D within which two quanta must be absorbed for the light perception. Now it turned out that for the peripheral cone system too this distance is 25′, whereas the distance D within which the two quanta for the light perception must be absorbed is very much smaller, namely, about 3

[10] The data for 3′ foveal are similar to those for 26′ of Fig. 6a.

minutes. An area with a visual angle of 25′ acts, therefore, indeed as a recipient unit at 7° nasal from the fovea in the observer's eye. In the fovea this unit is obviously much smaller.

Pirenne[11] also performed some measurements on the visual acuity and determined what the intensity of a very large screen must be so that a round black spot in the middle of it is seen in 50 percent of the cases.

So long as the visual angle of the black spot is large compared with the size of the recipient unit, we must expect that it is "seen" when parts of the surrounding area are seen. It would be stretching the point too much to deduce from the slope of the resulting curve for large visual angle the number k required for the light perception. In the experiments of Pirenne the center of the screen was seen 20° out. The visual angle of the dark spot in the region of large angles ranges from 30° to 3°. It is quite certain that the sensitivity of the retina differs very much over such large angular distances. Moreover, in our opinion, realizing the presence of a black spot in such large surroundings is not very suitable for investigating the number of quanta required for the light perception. For that purpose one must chose the most simple arrangement. Concerning the break in the curve of the visual acuity, we did not find this in our visual acuity measurements, but especially in the region of small visual angles are Pirennes data more complete. In some of our preliminary experiments on brightness discrimination considered as a function of intensity we found a break. It might be possible that the cause for this break and for the sudden bend in the curve of Pirenne are the same. We are collecting further information about this matter. We have some reason to believe that breaks of this kind are partly due to psychological aspects of vision and partly to aspects mentioned by Pirenne in his discussion of the break.

[11] M. H. Pirenne, Proceedings of the Cambridge Philosophical Society **42**, 78 (1946).

The Preparation and Optical Properties of Gold Blacks*†

LOUIS HARRIS AND ROSEMARY T. MCGINNIES**
Massachusetts Institute of Technology, Cambridge, Massachusetts

AND

BENJAMIN M. SIEGEL***
Weizmann Institute of Science, Rehovoth, Palestine

The optical properties of gold smokes deposited on cellulose nitrate films under different experimental conditions have been studied. The conditions of pressure of the inert atmosphere, purity of the gas, rate of evaporation, and the distance between source and deposition surface giving the highest infra-red absorption per unit mass have been found. The thermal mass required for high infra-red absorption is small compared to the thermal masses of other receivers used for infra-red measurements. The gold "blacks" turn yellow and have lower infra-red absorption when heated above 110°C.

Gold "blacks" with very high infra-red transmission (3–15μ) and low transmission at shorter wave-lengths are prepared when oxygen is present in the "inert" atmosphere.

The particle size and particle distribution of the gold smokes deposited under different experimental conditions have been investigated with the electron microscope at high resolution.

INTRODUCTION

THE use of deposits of metallic smokes for thermal receivers was suggested by Pfund[1,2] and by Burger and Van Cittert.[3] Gold "blacks" for absorbing thermal radiation have been reported by several investigators.[4,5] Measurements in this laboratory with a number of metallic smokes indicated that gold "blacks" might have a high ratio of (infra-red absorption/thermal mass). This is an important property for infra-red detectors designed to respond to rapid variations of incident radiation. The quality of the black obtained by evaporating gold in an inert atmosphere depends among other things on the gas pressure, the purity of the gas, the distance between the source and the surface of deposition, the mass of the receiver, the rate of gold evaporation, and the rate of heat conduction from the receiver. We have studied the influence of each of the parameters mentioned upon the quality of the gold "black" and correlated them with measurements of the mass/unit area of the gold deposit.

Absorption properties of the evaporated gold "blacks" were obtained from transmission and reflectance measurements of the smoke deposited on cellulose nitrate films. The transmission to the radiation of a 50°C blackbody, the specular reflection of the 50°C blackbody radiation incident at an angle of 45°, the spectral transmission from 0.4 to 15μ and the diffuse reflection in the visible spectrum, were all measured on deposits made under different conditions.

The fraction of incident radiation absorbed by a blackened film is given by

$$A = 1 - T - S, \tag{1}$$

where T is the fraction transmitted and S is the fraction scattered. By measuring the transmission of the blackened film, only an upper limit to the amount of radiation absorbed is obtained. However, it has been found here that gold "blacks" prepared under certain conditions have a small back scattering and therefore the absorption of such "blacks" can be calculated for comparative measurement from the transmission data alone. The absorption by the cellulose nitrate films used here has been found to be negligible.

* This work has been supported by the Navy Department under Contract NObs 25391.

† Contribution from Department of Chemistry, Massachusetts Institute of Technology, Cambridge, Massachusetts.

** Present address: University of Alabama, Tuscaloosa, Alabama.

*** At the Polytechnic Institute of Brooklyn, New York, by special arrangement.

[1] A. H. Pfund, Rev. Sci. Inst. **1**, 397 (1930).

[2] A. H. Pfund, J. Opt. Soc. Am. **23**, 375 (1933).

[3] Burger and Van Cittert, Zeits. f. Physik **66**, 210 (1930).

[4] L. C. Roess and E. N. Dacus, Rev. Sci. Inst. **16**, 170 (1945).

[5] C. B. Aiken, W. H. Carter, Jr., and F. S. Phillips, Rev. Sci. Inst. **17**, 380 (1946).

Electron microscope studies were made on the gold smoke deposits in order to correlate the observed optical properties with the particle size and distribution of the deposits. They will be reported in detail elsewhere.

EXPERIMENTAL PROCEDURE

The technique employed in producing the gold "blacks" and measuring their properties will be described in detail.

Preparation of Specimens

1. Cellulose nitrate films. The films were made by spreading a solution of thirty-second-viscosity cellulose nitrate, containing plasticizer, on a water surface.

The films weighed $\sim 8\times10^{-6}$ gram/cm^2, corresponding to a thickness of $\sim 5\times10^{-6}$ cm.

The nitrocellulose films were mounted on brass frames 5 cm×5 cm×0.105 cm thick, having a hole 3 cm in diameter, in the center of the frame. A 5-cm square of 0.8-mm thick copper sheet was fastened to the back side of the frame. This copper backing served to dissipate the heat from the cellulose nitrate film during the gold evaporation. The front (film) side of the frame faced the filament from which the gold was evaporated.

2. Evaporation of gold. The "blacks" were prepared in an atmosphere of nitrogen to permit continued use of a tungsten filament. A 5-cm length of 0.5-mm diameter gold wire was wound around the "V" of a 30-mil tungsten filament, 8.7 cm long. The filament was heated in a high vacuum until the gold melted to form a drop at the bottom of the "V," and then the temperature was quickly raised well above that to be used in the preparation of the gold "blacks." The current through the filament was reduced as soon as the "spitting" of impurities ceased. The gold was kept just molten until after the nitrogen was introduced and the pressure adjusted; then the current through the filament was increased to the desired value. A filament can be used twelve to twenty times, if it is not broken while applying the gold wire. It is advisable to examine the filaments carefully under a microscope before inserting them in the electrodes. A crack $\sim 2\times10^{-4}$ cm wide in the "V" of the filament produces a streaked gold "black" deposit.

A shield 1.3 cm from the filament screened the film from most of the tungsten filament.

A solenoid-operated-shutter, between the shield and film, permitted the film to be exposed to the gold-"black" smoke for a desired length of time, and only when the current through the filament was constant.

The apparatus for preparing gold "blacks" is shown in Fig. 1.

In all the experiments, the drop of gold was centered opposite the center of the film; the position of the filament was held fixed at 7 cm from the nearer side of the bell jar, and the position of the film was varied to give the required distance for the given experiment.

Description of Measurements

1. Weighings. The central area of the cellulose nitrate film has a uniform "black" deposit on a circle of diameter of 2.4 cm. A circle of 2-cm diameter was cut from this central area by means of a cork borer.

The circles of cellulose nitrate plus the gold "black" weighed from $\sim 0.05\times10^{-3}$ gram to 0.9×10^{-3} gram. Since a cellulose nitrate film of this area weighed only 0.025×10^{-3} gram, variations of 20 percent in the thickness of the cellulose nitrate films could be tolerated without affecting the required accuracy of the gold weighings. The variations in thickness of cellulose nitrate film were, however, less than 20 percent. The weighings, made with an Ainsworth

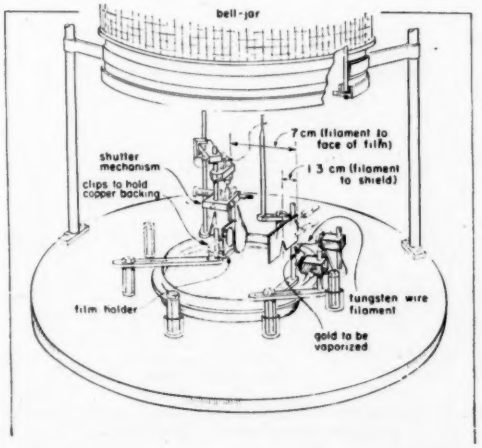

FIG. 1. Apparatus for the preparation of Gold Black.

micro-balance, were reproducable to $\pm 0.002 \times 10^{-3}$ gram. To achieve this accuracy it was necessary to maintain the films in desiccators between operations and measurements. In humid weather, the films were also dried at 60°C for thirty minutes before weighing.

2. Infra-red transmission. A blackbody as described by J. D. Hardy[6] was used as a source of infra-red radiation in the 10μ region. It consisted of a negative cone painted black and immersed in a constant temperature water bath maintained at 50.00±0.05°C. An aluminum mirror was located at 45° to the optical axis and 23.4 cm from a limiting aperture in front of the radiating cone. This mirror was mounted on a rotatable holder so that the mirror could be replaced exactly by one of our experimental films and its function will be described under the reflection measurements. A thermopile connected to a General Motors d.c. Breaker Amplifier was located 2.9 cm from the mirror and adjusted to intercept the radiation reflected at 45°. The amplified response of the thermopile was indicated on a microammeter.

A shutter in which the blackened films were mounted was placed 7 cm from the aluminum mirror so that the film could be placed in the path of the radiation or raised out of the way. A limiting stop was placed in front of the film so that only the central portion of the deposit was irradiated in these measurements. The transmission ratio was the quotient of the meter deflection with the blackened film in the radiation path and the deflection with the film removed.

3. Infra-red reflection. Relative reflections were obtained by mounting blackened films on the opposite side of the rotatable aluminum mirror described above and measuring the deflection of the microammeter when the radiation was reflected from the film and from the aluminum mirror. Thus the angle of incidence for all the infra-red reflectance measurements was 45°. The absolute reflection ratio was somewhat lower than the measured value because the aluminum mirror was not a perfect reflector. Its reflection ratio with respect to a new gold mirror was measured and found to be 0.9. The reflection ratios reported below are corrected to be relative to the reflection from the gold mirror. Black paint and black cardboard had reflection ratios of ~0.025.

A cellulose nitrate film had an infra-red transmission of 99 percent while the infra-red reflection for an angle of incidence of 45° varied between 4 percent and 7 percent. Reflection measured as described here gives a value in excess of the diffuse reflection.

4. Infra-red spectral transmission. The infra-red spectral transmissions were made at the M.I.T. Spectroscopy Laboratory with a Beckman infra-red spectrometer. The measurements extended from 1.0 to 15μ. A Beckman ultraviolet spectrometer was used for the measurements from 0.6μ to 1.0μ.

5. Visible spectral transmission and visible spectral diffuse reflectivity. Spectral diffuse transmissions and reflections in the visible spectrum were made at the M.I.T. Color Measurement Laboratory, using a Hardy colorimeter.

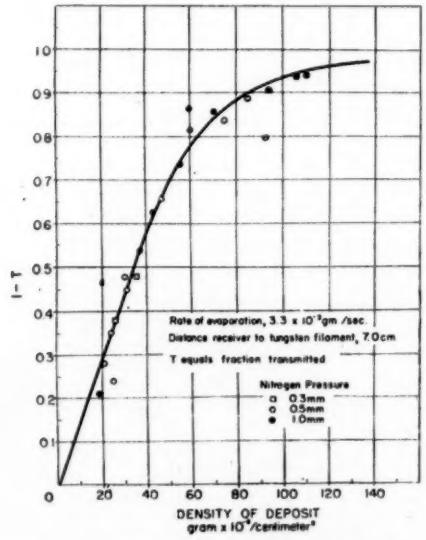

FIG. 2. Absorption of infra-red radiation by gold "blacks" as a function of density of deposit.

OBSERVATIONS AND MEASUREMENTS

1. Infra-red transmission for different thicknesses of gold "black." Figure 2 shows the infra-red transmission of gold "blacks" prepared at the optimum distance, 7 cm, between tungsten

[6] J. D. Hardy, J. Clin. Investigation **13**, 593, 615 (1934).

filament and cellulose nitrate film, and at an intermediate rate of gold evaporation, for this distance, and at different pressures of nitrogen.

2. The effect of distance between filament and film on the nature of the deposit. Gold "blacks" were prepared at different rates of evaporation and at different pressures at distances between tungsten filament and cellulose nitrate film of 3.8 cm, 7.0 cm, and 14 cm.

2a. Deposits prepared at a distance of 3.8 cm. The deposits prepared at a rate of evaporation of 3.3×10^{-3} gram of gold per second and at nitrogen pressures of from 0.5 to 3.0 mm reflected 15 percent of infra-red radiation. The infra-red reflection increased for the deposits prepared at increased rates of evaporation; at the evaporation rate of 16×10^{-3} gram of gold per second, the reflection was 77 percent for a deposit having a transmission of 22 percent. The gold "blacks" prepared at a lower evaporation rate ($\sim1\times10^{-3}$ gram of gold per second) and at a pressure of 2.0 mm gave the best absorption coefficient at this distance (reflection ~8 percent). The absorption "coefficient" was less, however, than that obtained for the 7.0 cm distance.

2b. Deposits prepared at a distance of 7.0 cm. The deposits prepared at a rate of evaporation of 3.3×10^{-3} gram of gold per second showed an infra-red reflection of 15 percent for a pressure of 0.3 mm. The deposits formed at a pressure of 0.3 mm had a yellowish appearance. Of the deposits formed at a pressure of 0.5 mm, the deposits of lower mass reflected 5 percent of the incident radiation; the reflection increased to as much as 15 percent for the heavier deposits. The deposits prepared at a pressure of 1 mm had the lowest reflections. The infra-red reflection increased from less than 1 percent to 4 percent as the evaporation rate increased from 0.5×10^{-3} gram of gold/second to 3.3×10^{-3} gram/second.

Deposits formed at an evaporation rate of $\sim12\times10^{-3}$ gram of gold per second, and at pressures below 1.0 mm, were yellowish. The deposits formed at pressures of 1.0 to 3.0 mm, at this rate, reflected ~11 percent of the incident radiation.

2c. Deposits prepared at a distance of 14 cm. The optimum pressure for the deposition of good infra-red absorbers, at this distance, was also 1 mm. The infra-red absorption per unit mass for the deposits formed at this distance was uniformly lower than for the 7.0-cm distance, except for light deposits.

TABLE I. Infra-red absorption for different rates of gold evaporation.

Filament current (amperes)	Approx. rate of evaporation of gold (gram/sec.)	Time (seconds)	Infra-red (*BB*) transmission, *T* fraction	Infra-red 45° reflection fraction	Weight of gold (gram/cm²)	k^*
21.2	0.5×10^{-3}	300	0.08	<0.01	83×10^{-6}	13,000
23	0.9×10^{-3}	160	0.19	<0.01	58×10^{-6}	12,000
25	1.5×10^{-3}	120	0.21	0.03	56×10^{-6}	12,000
27	2.3×10^{-3}	60	0.21	0.03	57×10^{-6}	12,000
30	3.3×10^{-3}	50	0.225	0.04	55×10^{-6}	12,000

$k^* = (1/\text{gram/cm}^2)\log_{10}1/T$

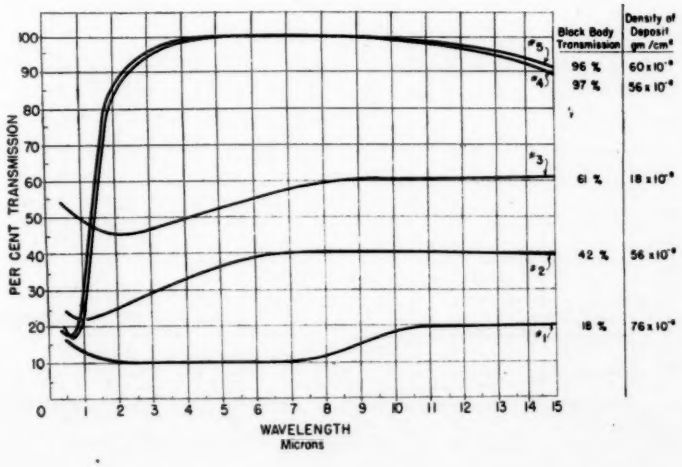

FIG. 3. Infra-red transmission of gold "blacks."

TABLE II. Change in transmission of gold "black" deposits on being heated.

Pressure	Rate of evaporation (g/sec.)	Density of gold "black" (g/cm²)	Before heating			After heating		
			T	R^*	$A=1-(T+R^*)$	T	R^*	$A=1-(T+R^*)$
0.5 mm	3.3×10^{-3}	41×10^{-4}	0.52	0.13	0.35	0.31	0.35	0.34
0.5	10.0×10^{-3}	66×10^{-4}	0.37	0.15	0.48	0.14	0.45	0.41
1.0	3.3×10^{-3}	106×10^{-4}	0.06	0.03	0.91	0.03	0.09	0.88

[a] R^* = infra-red reflectance at 45 degrees.

3. The variation of infra-red absorption with rate of gold evaporation. The data obtained for a pressure of 1 mm and for a distance of 7 cm are given in Table I. There is, thus, very little change in absorption with rate of gold evaporation up to rates as high as 3.3×10^{-3} gram/second; at still higher rates the absorption becomes less. The deposits prepared at the lowest rate have the lowest reflection.

4. Effect of purity of the gas. Gold blacks with the largest k^* (such as those represented in Table I) were made with the purest gas used, nitrogen containing less than 0.3 percent of oxygen, or a partial pressure of 0.003 mm of oxygen. When the nitrogen was enriched in oxygen, the k^* decreased, so that for a gas mixture containing 5.5 percent oxygen the k^* decreased to a value of approximately 1 percent of that for the deposits prepared with the purer nitrogen. For gas mixtures containing between 0.3 percent and 5 percent the k^*'s had values intermediate between that for the purest gas and the low value given.

In order to be certain of obtaining a "black" having a high absorption in the visible and low absorption in the infra-red, the inert gas should contain at least 2 percent oxygen and the rate of gold evaporation should be approximately 0.5×10^{-3} gram/second. (We have obtained deposits having such characteristics with gas mixtures containing even less than 1 percent oxygen, at rates less than 0.5×10^{-3} gram/second.)

5. Spectral transmission in the infra-red. The transmission of radiation of a number of deposits of gold smoke prepared under different conditions is given as a function of wave-length from 0.5μ to 15μ in Fig. 3. The percent transmission of each of these deposits to radiation from the 50°C blackbody is given in the first column on the right and their respective masses in the second column on that side. All the deposits were prepared at a distance of 7.0 cm.

Curves 1 and 3 are given by deposits of different mass produced at 1 mm nitrogen, minimum amount of oxygen, and intermediate rate. The transmission can be seen in both cases to decrease slightly to a minimum just beyond 2μ and then to rise gradually a few percent, remaining constant beyond 8μ to 10μ. Curve 2, obtained from a deposit made in 1.0 mm of nitrogen but at a fast rate of evaporation (approximately 12×10^{-3} g/sec. of gold) has similar characteristics but is a poorer absorber per unit mass.

Curves 4 and 5 show the very interesting characteristics of deposits produced when oxygen present. These curves have a pronounced minimum at 0.8μ and then a sharp rise to 2μ so that

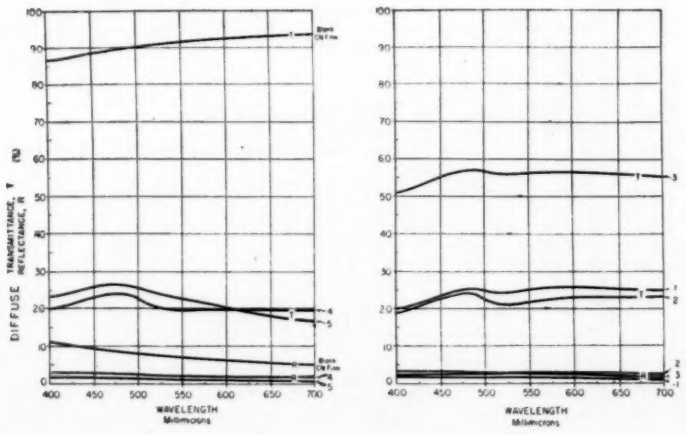

FIG. 4. Visible diffuse transmission and reflection of gold "blacks."

TABLE III. Summary of electron microscope studies of gold smoke deposits.

Rate of gold evaporation	Nitrogen pressure	Size of unit colloid particle limits	average	Number of particles in initial aggregates	Type of aggregation
0.5 to 3.3 $\times 10^{-3}$ gram/sec.	0.5 to 1.0 mm*	10–150A	50A	many	open network
	3.0 mm*		250A	many	open network
3.3×10^{-3} gram/sec.	0.3 mm	15 to 100A	50A	few	uniform
	0.5 mm	25 to 200A	100A	intermediate	sponge-like
	1.0 mm	75 to 250A	150A		sponge-like
10×10^{-3} gram/sec.	0.5 to 1.0 mm	10 to 200A	40A	few	uniform

* One percent oxygen present.

the deposits are almost completely transparent between 3μ and 10μ and falling to approximately 90 percent at 15μ. The deposit for curve 5 was made at a total pressure of 1 mm and at a low rate of gold evaporation. Such a curve is characteristic of deposits made at 1 mm pressure, slow rate, and oxygen partial pressure of 0.02 mm. Curve 4, which has the same optical characteristics as curve 5, was obtained for a deposit made at a total pressure of 3.0 mm and at an intermediate rate. It is characteristic of intermediate rates of deposit if the partial pressure of oxygen is greater than 0.06 mm.

If care is exercised that no oxygen is introduced with the introgen, that the bell jar system is tight, and that there is a minimum of adsorbed oxygen, good quality deposits such as illustrated by curves 1, 2, and 3 and in Table I can be obtained at 1-mm pressure with low rates of evaporation or at 3.0 mm and intermediate rates.

The transmissions indicated in Fig. 3 show that the transmissions obtained with the 50°C blackbody are satisfactory measures of the transmission between 2μ and 15μ.

6. Spectral properties in the visible. The diffuse reflection of visible radiation was measured as a function of wave-length on several deposits to determine whether there is a characteristic scattering in the visible region which might be used as a criterion for the character of the "black" as an absorber of infra-red radiation. These data are shown in Fig. 4.

All the gold "blacks" show low reflection, nearly all show slightly less reflection in the red than the blue.

All the deposits are characterized by a maximum transmission at 480 mμ. *Bright gold* deposits have the maximum transmission at 500 mμ.

The gold "black" deposits with the highest infra-red absorption per unit mass (No. 1 and No. 3) have greater transmission in the red than in the blue, while gold "black" deposits with low infra-red absorption coefficient (No. 5 and No. 4) have nearly the same or slightly lower transmission in the red than in the blue. In a number of cases, deposits prepared under the conditions used for No. 5 and No. 4 appeared blue to the eye by transmitted light (incandescent source).

7. Effects of heating gold deposit. There are several other factors which influence the character of the gold deposit and one of them is the temperature of the receiving surface, or the subsequent heat treatment to which the deposit is subjected. In our study the deposits whose transmission and reflection had been measured, were heated to 120°C for two to three hours and then the changes in transmission and reflection were observed. (The cellulose nitrate film upon which the gold was deposited limited the temperature for heating to a maximum of 120°C.) The "black" deposits took on a yellowish appearance after this heat treatment. Table II lists the observations which were made on such deposits.

It is immediately evident that there is a loss in transmission upon heating and that this loss is caused by increased reflection. There is a tendency for the amount absorbed to decrease and in some cases the reflectivity increased

TABLE IV. Comparison of gold "blacks" and carbon as infra-red absorbers.

	Percent absorption	Mass	Thermal mass
Gold "black"	80	56×10^{-4} g/cm^2	1.7×10^{-4} cal./°C/cm^2
Carbon†	72	180×10^{-4} g/cm^2	36×10^{-4} cal./°C/cm^2

† Clemens Schaefer and F. Matossi, Das Ultrarote Spektrum (Verlag Julius Springer, Berlin, 1930).

considerably above the loss in transmission, indicating that elevated temperatures introduce a definite limitation in gold "black" as an absorber.

At higher temperatures there is apparently a sintering of the metal deposit, and since gold diffuses readily at relatively low temperatures, this sintering effect already occurs to a considerable extent at 120°C. Beeck, Smith, and Wheeler[7] found in studying the sintering of nickel deposited in this manner that the same effects were observed if the original deposit was made on a massive surface heated to a given temperature during deposition or if the metal were deposited on the same surface at room temperature and then heated to the elevated temperature.

8. Effect of backing. The metal backing behind the cellulose nitrate film has been described above and its function pointed out. Without a backing only a very small amount of gold deposits on the cellulose nitrate film and the same effect has been observed in the case of very thin metal foils. The distance between the film and the backing has a pronounced effect on the quality of the gold deposits obtained.

The rate of deposition and the optical properties of the black deposit are determined, in addition, by the nature of the receiving surface. A few observations have been made on surfaces of other materials. For example much lighter gold deposits are formed on thin strips of nickel, having masses of 86×10^{-6} g/cm², than on the cellulose nitrate films having masses of 8×10^{-6} g/cm², as used in our experiments, for the same time and rate of evaporation. It was necessary to bring the metal backing in contact with the nickel strips in order to obtain a good deposit of gold "black." On massive surfaces the gold smoke deposits readily.

9. Electron microscope studies. The gold smokes deposited under varying conditions show pronounced differences in particle size and distribution. We shall only summarize the results of these studies, since they will be treated in detail elsewhere.

The electron micrograph images of thin deposits indicate that the gold deposits in small spheroidal particles, and the broadening of the diffraction rings indicate crystal sizes of about 50A. The unit spheroids observed in the electron microscope could appear to be crystallites.

The electron micrographs clearly show an increase in size of the unit colloidal particle and increasing tendency to cluster with increasing pressure of nitrogen in which the evaporation takes place.

The results of the electron microscope studies are summarized in Table III.

Electron diffraction patterns of all gold deposits show randomly distributed crystallites. The effect of oxygen could not be detected in the electron diffraction patterns; only the lattice spacing of pure gold was apparent.

DISCUSSION OF RESULTS

Gold smoke deposits upon thin cellulose nitrate films have the best properties for the absorption of infra-red radiation when produced under conditions which are in an intermediate range of nitrogen pressure, rate of evaporation, and distance between source and surface of deposition. The partial pressure of oxygen in the gas should be less than 0.003 mm. The optimum range of experimental conditions for gold "blacks" having the highest infra-red absorption per unit mass is: (a), an atmosphere about 1.0-mm pressure of nitrogen; (b), evaporation rate of 0.5×10^{-3} to 3×10^{-3} gram of gold per second; (c), distance of about 7 cm between the source of evaporation and the surface on which the gold is depositing; (d), copper backing 0.1 cm or closer behind the film being deposited.

The "blacks" produced under these conditions have excellent characteristics for infra-red absorbers of low thermal mass. Deposits having a mass of only 45×10^{-6} gram/cm² can be prepared which will absorb 68.4 percent (~90 percent for a double traversal) of the incident radiation to 15μ.

It is of interest to compare the absorption of infra-red radiation (average for 9μ) of the best gold "blacks" with deposits of carbon, as is done in Table IV. Thus, these gold "blacks" have a thermal mass of approximately 1/20th that of carbon.

An important application of the gold "blacks" deposited in an atmosphere of oxygen-enriched nitrogen is as a filter for transmitting infra-red

[7] Otto Beeck, A. E. Smith, and Ahlborn Wheeler, Proc. Roy. Soc. **A177**, 62 (1941).

radiation beyond 2μ. Such deposits have a sharp cut-off at about 1μ and are good absorbers of the shorter wave-lengths. A triple filter of this type will transmit less than 1 percent of the radiation below 1μ and more than 90 percent of the radiation beyond 3μ.

SUMMARY

We have studied the optical properties of gold smokes deposited on cellulose nitrate films under different experimental conditions. The conditions of pressure of the inert atmosphere, the rate of evaporation, and the distance between source and deposition surface, and the backing for the film giving the highest infra-red absorption per unit mass have been found. The particle size and particle distribution of the gold smokes deposited under the different experimental conditions have been investigated with the electron microscope at high resolution.

ACKNOWLEDGMENTS

We are indebted to Miss Beatrice Alexander and to Miss Alice M. Pearson for their excellent technical assistance, to Dr. Charles W. Young for his many helpful discussions and suggestions, and to Mr. David Jeffries for his able assistance with many of the measurements.

Lens Design and Tolerance Analysis Methods and Results*

PAUL C. FOOTE
Bell & Howell Company, Chicago, Illinois
AND
ROBERT A. WOODSON**
Consultant Optical Engineer, Chicago, Illinois

(Received January 27, 1948)

The need for a systematic design and tolerance analysis of optical systems arises from the demand for better optical systems manufactured more economically. Methods are presented for obtaining the optimum design possible with a given type of system using Design Analysis (DA), and for specifying optical and related mechanical tolerances for most economical manufacture using Tolerance Analysis (TA). First-order Design and Tolerance Analysis (D&TA) controls the Gaussian first-order optical dimensions such as EFL, BF, f/number, etc. Third-order D&TA controls the third-order aberrations. A simple extension of the procedure will take care of higher order aberrations.

INTRODUCTION

THE design of most photographic lenses has been more of an art than a science. Lens designers for the most part considered their field too complex for analytical solutions. Hunches based upon empirical information led to most of the present lens designs. When a particularly good lens design was discovered, the task of getting the most out of it was stupendous. In general, the design was investigated enough to find what changes would produce an acceptable lens, and there the designer stopped. When the need arose for a better lens, work would be resumed, perhaps disclosing that a few minor changes in the former design satisfied the new requirements.

The manufacture of most photographic lenses has also been more of an art than a science. Lenses generally have been made by skilled craftsmen who have had years of training as apprentices. Their goal was to make a lens as nearly like the specifications as possible. If manufacturing tolerances were used at all, they were either "guesstimated" or based upon incomplete empirical information. When the guessed tolerances were too liberal, selective assembly was often resorted to. This usually reduced the cost of manufacture, but without a systematic analysis of the tolerances, the savings achieved were relatively small.

Design Analysis (DA) is the systematic analysis by which optimum performance is achieved from the nominal data of the final design, considering all possible small variations of the constructional parameters. The performance of a lens can be measured in terms of image quality, H, which is a composite measure of resolution and contrast. In general H is a function of the relative aperture, $1/(f/\text{number})$, and the semi-field angle, J. Figure 1 shows in graphs (a), (b), and (c) several curved surfaces in three dimensions corresponding to the image quality of several lenses. Graph (a) shows the image quality of a lens that does not completely satisfy the established standard. For small apertures and small field angles, the lens is satisfactory, but it is below standard for higher apertures and larger field angles. The design must obviously be revised to meet the standard. The nominal finished design has the improved image quality shown in graph (b). The use of DA insures that the nominal design has maximum image quality.

Tolerance Analysis (TA) is the systematic analysis for specifying the manufacturing tolerances which result in maximum economy, maintaining acceptable performance. Graph (b) shows the case in which the specified tolerances are too tight and the worst resulting image quality is much better than the established standard. The available margin of H has not been fully used, resulting in excess costs. In case the tolerances are too generous, the tolerance limit of H will be below the standard and, therefore, some of the

* Presented at the 31st meeting of the Optical Society of America in New York, New York, on October 5, 1946.
** Formerly with the Bell & Howell Company.

lenses so made will be rejected. In this case the tolerance limit will resemble the unfinished design in graph (a). The use of TA insures that the tolerance limit is just above the standard as shown in graph (c).

Design Analysis by itself permits the correction of an unfinished design so that it will meet a higher standard of image quality. This results in better lenses. Tolerance Analysis by itself permits the fullest utilization of the margin of image quality between the nominal design and the standard. This results in cheaper lenses. The combination of Design and Tolerance Analysis (D&TA) should be used for maximum economy, even though the existing lens design is above standard. Economy results from liberal tolerances. For a given standard, there are two ways to permit more liberal tolerances. First, raise the nominal H, which DA does to the maximum. Second, lower the tolerance limit H, which TA does to the minimum permitted by the standard. Another source of additional economy is mass production. Those lenses for which there is a large potential demand can be assembled cheaper from interchangeable parts which have been made cheaper in large quantities. TA permits the most economical manufacture of interchangeable parts. Thus, D&TA aids the optical industry to achieve its aims of quality, quantity and economy. Even for lenses for which the required quantity is small, D&TA still yields quality and economy.

The definitions of DA and TA indicate that they are distinct and that either may be used without the other. Even though this is the case, there is a close relation between DA and TA. Both use the same coefficients, G, which specify the partial derivative of a dependent performance variable, h (such as EFL, spherical aberration or chromatism), with respect to an independent constructional parameter, z (such as curvature, separation or refractive index),

$$G = \partial h / \partial z. \tag{1}$$

Because of the relation between DA and TA, their history is a joint one. When progress had been made in the development of one, that gave a boost to the development of the other. This is easily traced in the following brief resume of the development of D&TA at Bell & Howell Company.

Quantitative Design Analysis was started about four years ago when some of the G coefficients were computed for a triplet anastigmat. Shortly afterward changes in equivalent focal length, EFL, and back focus, BF, of a high aperture doublet were found for changes in each constructional parameter equal to its respective tolerance, Δz_j. Later DA was made more effective by plotting a graph of lines through the origin having slopes equal to the corresponding value of G for spherical aberration, SA, and for sine condition, SC, with respect to each parameter, j, thus permitting a quick evaluation of the result on SA and SC of a small change in any z_j. This G-slope type of graph was then used in TA to compute graphically the EFL and BF errors resulting from any tolerance, Δz_j. Finally DA and TA were developed to a standard D&TA procedure which has been in regular use at Bell & Howell for over two years.

This relation between DA and TA has also been observed by others working in this field. Cruickshank[1] developed a systematic DA and predicted that it would permit the estimation of tolerances for use in production. Later, Cruickshank[2] developed a systematic paraxial DA which was shown to specify completely the effect of the variation of all of the constructional parameters of a lens system on its EFL and thus permits tolerances to be established for each parameter to insure production within the specified EFL tolerance. Recently Stark[3] showed how Herzberger's[4] Gaussian Bracket coefficients can be converted into a form adapted for easy computing of manufacturing tolerances based on a paraxial ray trace.

FIRST-ORDER DESIGN AND TOLERANCE ANALYSIS

First-order DA applied to a lens system provides control of first-order Gaussian optical dimensions, h, such as EFL, BF, f/number, magnification, and deviation. The optical performance, H, is a composite of the different h's

[1] F. D. Cruickshank, Proc. Phys. Soc. **57**, 350 (1945).
[2] F. D. Cruickshank, J. Opt. Soc. Am. **36**, 13 (1946).
[3] Stephen W. Stark, J. Opt. Soc. Am. **37**, 990 (1947).
[4] Max Herzberger, J. Opt. Soc. Am. **33**, 651 (1943).

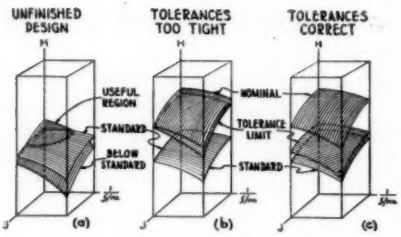

FIG. 1. Image quality standards and tolerances. The image quality, H, is a function of the relative aperture, $1/(f/\text{number})$, and the semifield angle, J. Several conditions of the nominal and the tolerance limit image qualities are shown with respect to the standard image quality.

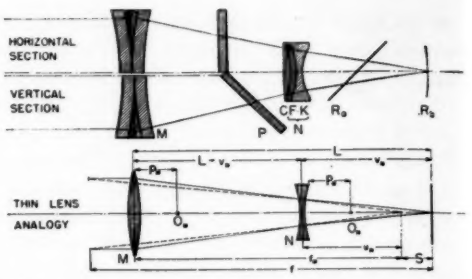

FIG. 2. Catadioptric telephoto system. The parts of this system and its thin lens analogy are shown to facilitate its analysis as a stadiametric ranging sight. The Mangin mirror has been replaced by its optically equivalent lens having a hypothetical element with a negative refractive index.

and is a function of the constructional parameters, z_j. By determining how H varies with each z_j, it is possible to find values of z_j for which H has a maximum value. It may be that the theoretical solution is not practical. If so, it is possible to limit the range of each z_j to practical values in finding the maximum H.

First-order TA (using the same G coefficients as in first-order DA) enables us to set a reasonable tentative tolerance, Δz_j, on each value of z_j. The contribution, Δh_j, of each tentative tolerance, Δz_j, to the resulting variation, Δh, of a first-order dimension is found and compared with other contributions. Tolerances, Δz_j, are then adjusted so that the total contribution fits the tolerance limit as shown in Fig. 1c.

A catadioptric telephoto system will be used to illustrate first-order D&TA. The device shown with its thin lens analogy in Fig. 2 is to be used as a stadiametric ranging sight. The problem to be solved consists of revising the optical design (to eliminate interference) and the establishing of tolerances. In the figure both the horizontal and vertical sections are shown. However, the principles of D&TA will be adequately illustrated by considering only the vertical section. The horizontal section can be analyzed in the same way.

In Fig. 2 the Mangin mirror, M, has been represented by its optically equivalent lens consisting of two unsilvered Mangin mirrors "back to back" with a pair of zero-thickness plano-concave lenses sandwiched in between, one of them having a refractive index, n_m, equal to that of the Mangin mirror, the other having a negative refractive index, $n_n = -n_m$. This hypothetical lens is convenient for both graphical and trigonometrical ray tracing.

The principal image forming parts of the system are the negative doublet, N, made up of a flint element, F, and a crown element, K, and the Mangin mirror, M, which collimate light from the reticle, R_b (curved to fit the curved focal surface of the system). This collimated beam from M is partially reflected by the inclined semireflecting plate, P, thus superimposing the reticle image on the target which is seen directly through the plate, P, along a line perpendicular to the principal optical axis. Divergent light going from N to M is transmitted by the inclined plate, P. The astigmatism thereby produced is minimized by the cylindrical element, C. The front surface mirror, R_a, permits folding the system for compactness.

This sight is focused (during assembly) so that it will project a virtual recticle image of adjustable size onto the target. Knowing the size of the target, its range can be found by "measuring" the angle it subtends. When the reticle size has been adjusted until its image subtends the same angle as the target, a coupled range scale indicates the range directly. The accuracy of the ranging depends upon several factors—the one we are concerned with in this discussion is the EFL of the system. Thus a tolerance on range readings imposes a tolerance on EFL. The sighting function of the instrument is accomplished by pointing it optically at the target. This function requires that eccentricity and other deviation errors be compensated during assembly.

The preliminary optical design is to be revised using first-order DA so that the dependent performance variables meet the mechanical requirements. The essential features of this problem are shown in the thin lens anology of Fig. 2. The over-all length, L, must be altered to fit mounting requirements. The image distance, v_N, must be decreased to eliminate optical interference of the C and N mount with the direct beam from the target. The EFL, f, must be adjusted to fit the existing reticle dimensions. These three dependent quantities are controlled by three independent parameters: the focal length, f_M, of the Mangin mirror, the focal length, f_N, of the negative doublet, and the separation, $(L-v_N)$, between these elements, M and N. The three equations which establish the relations between these variables, L, v_N, f, f_M, f_N, and $(L-v_N)$, reduce to only two equations because not all of the variables are independent. Equation (2) gives the focal length, f, of a combination of two separated thin lenses. Equation (3) is the well-known thin lens equation applied to the negative doublet, N.

$$1/f=(1/f_M)+(1/f_N)-[(L-v_N)/f_Mf_N], \quad (2)$$

$$1/v_N=[1/(f_M+v_N-L)]+[1/f_N]. \quad (3)$$

These two thin lens equations are not adapted for use directly in our thick lens problem, so the corresponding differential forms will be used in the DA.

As was done by McAuley and Cruickshank[5] and independently by us, differential coefficients of the dependent performance variables are found for the independent constructional parameters. The form of the solution is as follows:

$$df_M=(\partial f_M/\partial L)dL+(\partial f_M/\partial v_N)dv_N+(\partial f_M/\partial f)df, \quad (4)$$

$$df_N=(\partial f_N/\partial L)dL+(\partial f_N/\partial v_N)dv_N+(\partial f_N/\partial f)df, \quad (5)$$

$$d(L-v_N)=[\partial(L-v_N)/\partial L]dL+[\partial(L-v_N)/\partial v_N]dv_N+[\partial(L-v_N)/\partial f]df, \quad (6)$$

where the left-hand members of the equations are the required changes needed to correct the dependent variables, L, v_N, f, by the amounts, dL, dv_N, df, respectively. Equation (6) obviously reduces to

$$d(L-v_N)=dL-dv_N, \quad (7)$$

the differential coefficients here being 1, -1, 0, respectively.

There are two alternative methods available for evaluating the differential DA coefficients. The first is to differentiate Eqs. (2) and (3) and solve for the desired DA coefficients. The second method is to apply trial increments to the independent variables, f_M, f_N, $(L-v_N)$, successively and by Eqs. (2) and (3) find the resulting increments of the dependent variables. Six simultaneous equations of the form (4) and (5) result, from which the DA coefficients can be found.

The first method will be used in this case. If h is one of the optical performance dimensions, its dependency upon one of the independent constructional parameters, z, defines the corresponding differential DA coefficient, G.

$$G=\partial h/\partial z. \quad (1)$$

There is a value of G for each combination of an h with a z. Not counting the values of G already determined by Eq. (7), there are six G coefficients to be found. After differentiation of Eqs. (2) and (3) and their solution for the G's, we obtain

$$\partial f_M/\partial L=(C+2ySQ)/C, \quad (8)$$

$$\partial f_M/\partial v_N=BD/C, \quad (9)$$

$$\partial f_M/\partial f=-SE/Cf, \quad (10)$$

$$\partial f_N/\partial L=-2xy/C, \quad (11)$$

$$\partial f_N/\partial v_N=AD/C, \quad (12)$$

$$\partial f_N/\partial f=xE/Cf, \quad (13)$$

where the following substitutions have been made for simplification:

$$S=L-f_M,$$
$$Q=(S^2-4f_NS)^{\frac{1}{2}},$$
$$w=f_M/f,$$
$$x=v_N-f_N,$$
$$y=f_N/f,$$
$$A=2f_N-S+(1-2y)Q,$$
$$B=2[S+(w-1)Q],$$
$$C=AS+Bx,$$
$$D=S-2v_N$$
$$E=S(S-4f_N)-Q(S-2f_N).$$

[5] A. L. McAuley and F. D. Cruickshank, Proc. Phys. Soc. **57**, 302 (1945).

Equations (4), (5), and (6) apply strictly for infinitesimal changes. However, if the G coefficients are not changing too rapidly, finite changes may be made with adequate accuracy. (Note that the G's are constant in Eq. (6) as shown in Eq. (7).) Small finite changes in f_M and f_N can be computed from Eq. (14) using G's obtained in Eq. (8) through (13).

$$\Delta f_M = (\partial f_M/\partial L)\Delta L + (\partial f_M/\partial v_N)\Delta v_N + (\partial f_M/\partial f)\Delta f, \quad (14a)$$

$$\Delta f_N = (\partial f_N/\partial L)\Delta L + (\partial f_N/\partial v_N)\Delta v_N + (\partial f_N/\partial f)\Delta f, \quad (14b)$$

$$\Delta(L - v_N) = \Delta L - \Delta v_N. \quad (14c)$$

This Design Analysis problem then is solved by Eq. (14) since it gives the changes which must be made in the independent constructional parameters, f_M, f_N, and $(L - v_N)$, in order to produce the desired changes in the dependent variables, L, v_N, f. This is confirmed by the successful results obtained on the stadiametric ranging sight.

First-order Tolerance Analysis will now be illustrated using the same catadioptric optical system as the example. TA is the procedure by which tolerances on the constructional parameters, z, are established so that the optical performance variables, h, will fit their established tolerances. In this example there are three first-order optical performance variables. They are focusing adjustment range, EFL tolerance, and aiming adjustment range.

In assembly the Mangin mirror, M, is mounted at a fixed axial distance, p_M, from the reference point, O_M, on the mount as shown in Fig. 2. During assembly the device is focused by adjusting the position, p_N, of the negative doublet, N, measured from its fixed reference point, O_N. Thus a mechanical limitation on the range of adjustment of p_N imposes limitations on the tolerances of the constructional parameters, z.

After the ranging sight is focused, its EFL, f, must be within tolerance. This imposes its own restrictions to the tolerances of the z's.

A lateral adjustment, e_M, is provided for the Mangin mirror, M, so that the sight can be aimed correctly. Mechanical limitations on e_M restrict the eccentricity and deviation tolerances which apply to the constructional parameters, z.

The constructional parameters, z, for the TA can be chosen in many different ways. They are chosen in this case so that they can be used directly in setting the manufacturing tolerances. These z's can be grouped by type into six categories; longitudinal position of mounting surfaces, p; curvatures (measured in "kilorings" = 1000 Newton rings), c; refractive indices, n; thickness of elements, t; eccentricity of elements, e; inclination of elements, i. Note that no separation, s, parameters are used here since the method of mounting the elements requires tolerances on p instead. The curvatures, c, are specified in this TA by the sagitta value corresponding to the full aperture.

The differential TA coefficients have the same form as those for the DA, but in this example the dependent performance variables and, also, the independent constructional parameters were selected differently for the DA and the TA and so are not the same. The TA equivalent of Eqs. (2) and (3) are best represented by Gaussian brackets for the first-order case. Herzberger[4] has described their use in the Gaussian thin lens equations.

The solution of this TA problem has the same form as that of the DA problem given in Eqs. (4), (5), and (6), but the number of constructional parameters is greater, as shown in Eqs. (15), (16), and (17).

$$dp_N = \sum_{j=1}^{28}(\partial p_N/\partial z_j)dz_j = \sum_{j=1}^{7}(\partial p_N/\partial p_j)dp_j + \sum_{j=1}^{11}(\partial p_N/\partial c_j)dc_j + \sum_{j=1}^{5}(\partial p_N/\partial n_j)dn_j + \sum_{j=1}^{5}(\partial p_N/\partial t_j)dt_j, \quad (15)$$

$$df = \sum_{j=1}^{28}(\partial f/\partial z_j)dz_j = \sum_{j=1}^{7}(\partial f/\partial p_j)dp_j + \sum_{j=1}^{11}(\partial f/\partial c_j)dc_j + \sum_{j=1}^{5}(\partial f/\partial n_j)dn_j + \sum_{j=1}^{5}(\partial f/\partial t_j)dt_j, \quad (16)$$

$$de_M=\sum_{j=1}^{11}(\partial e_M/\partial z_j)dz_j=\sum_{j=1}^{7}(\partial e_M/\partial e_j)de_j$$

$$+\sum_{j=1}^{3}(\partial e_M/\partial i_j)di_j+\sum_{j=1}^{1}(\partial e_M/\partial t_j)dt_j. \quad (17)$$

The sixty-seven differential G coefficients above may be determined either from an analytical solution, as in the case of the DA, or by tracing a ray for each of the thirty-nine z_j's, giving a trial increment, Δz_j, to each z_j in turn. If the former method is used, the partial longitudinal and transverse magnifications developed by us and used independently by Cruickshank[6] simplify the problem. If the latter method is used, the paraxial ray tracing of thirty-nine rays through the part of the system that follows the corresponding $z_j+\Delta z_j$ requires about as much time as tracing twenty rays through the complete system, since on the average the trial increment is applied in the middle of the system.

In this case the TA G-coefficients were computed analytically and tentative tolerances, Δz_j, were chosen to fit standard manufacturing practice as well as to limit the total contribution to Δp_N, Δf, and Δe_M. These tolerances are optical, but contain related mechanical tolerances implicitly, such as spacer thickness and diameter. A convenient method of evaluating the results of these tentative tolerances is to plot a graph of the coefficients *vs.* parameter tolerances as shown in Fig. 3. A separate graph is drawn for each dependent variable, h. The tolerances, Δz_j, are plotted horizontally in the order in which they occur in the optical system as labeled. Positive G's are plotted above the axis, negative below. The area of each black rectangle is a measure of the contribution, Δh_j, made by the tolerance, Δz_j. The shaded area is the sum of the absolute values of the black areas in each graph. The height of the shaded area is the weighted average of the G's. The length of the shaded area is the sum of the tolerances, $\sum\Delta z$. Thus the shaded area is the maximum resulting error, $\sum\Delta h$, when the signs of the parameter errors are such that all contributions have the same sign and when each parameter error is at the tolerance limit. This is the worst possible case, and the optical quality distribution curve will show many units with much smaller values of $\sum\Delta h$ due to partial compensation.

In the chosen example of first-order TA, the tentative tolerances satisfy all the requirements, so they are adopted. If they had resulted in too large or too small values of $\sum\Delta h$, the tolerances, Δz, would be adjusted accordingly. The graphs of Fig. 3 show which parameters are the worst offenders and which are the least offenders. This greatly simplifies the adjustment of tentative tolerances.

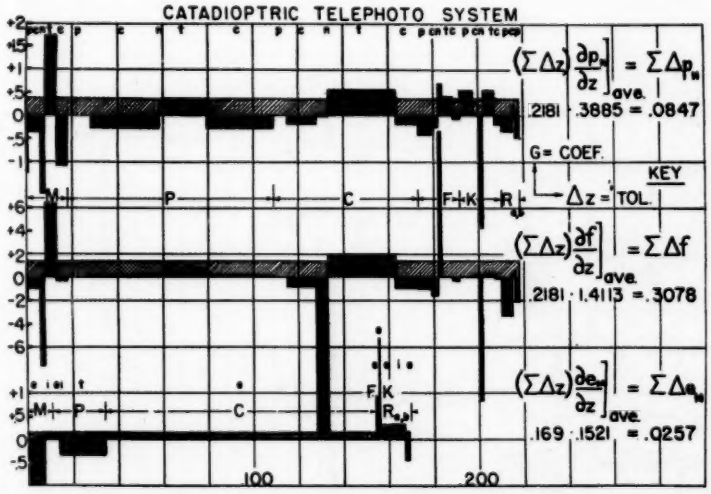

FIG. 3. First-order Tolerance Analysis. Tolerance Analysis graphs are shown for the catadioptric telephoto system in which the magnitude, sign, and contribution of each G coefficient are given for each independent constructional parameter. Each component of the system is identified by its corresponding capital letter, and within each component the individual parameters are indicated by the corresponding lower case letters.

[6] F. D. Cruickshank, J. Opt. Soc. Am. **36**, 103 (1946).

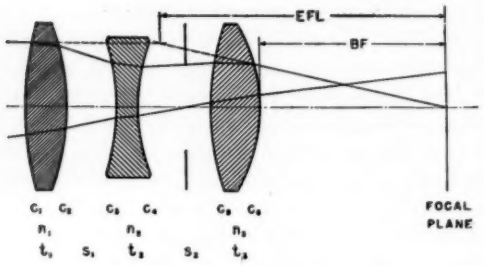

FIG. 4. Triplet anastigmat system. The fourteen constructional parameters are identified and the two first-order performance variables (EFL and BF) are indicated.

THIRD-ORDER DESIGN AND TOLERANCE ANALYSIS

Third-order DA extends the control of Design Analysis to the third-order aberrations of an optical system. The basic concepts and methods of first-order DA are applied now to other optical performance dimensions. Referring again to Fig. 1, the image quality, H, is to be raised to its maximum by DA. This means that third-order DA must minimize the aberrations, h, in such a way that H is a maximum.

Third-order TA similarly extends the control of Tolerance Analysis to the constructional parameters, z_j, so that the aberrations are held within the specified limits, Δh. As shown in graph (c) of Fig. 1, the result of third-order TA is that the tolerance limit is just above the standard.

A triplet anastigmat photo objective will be used to illustrate third-order D&TA. This lens system is shown in Fig. 4. The independent variables are the fourteen constructional parameters—six curvatures, c, three refractive indices, n, three thicknesses, t, and two separations, s. The dependent variables are two first-order optical performance dimensions, EFL and BF, and fourteen third-order aberration dimensions identified in Fig. 5. These aberration performance variables are: Spherical aberration at the $\sqrt{2}/2$ zone, SA_z, and at the edge, SA_e; sine condition aberration at the $\sqrt{2}/2$ zone, SC_z, and at the edge, SC_e; coma for the upper ray at the intermediate field angle, CA_i, and at the corner of the field, CA_c; coma for the lower ray at the intermediate field angle, CB_i, and at the corner of the field, CB_c; curvature of the tangential image at the intermediate angle, T_i, and at the corner, T_c; curvature of the radial image at the intermediate angle, R_i, and at the corner, R_c; and distortion at the intermediate angle, D_i, and at the corner D_c. Chromatic aberrations have been omitted in this example, but as Cruickshank[6] shows, they can be included.

In this example the same independent and dependent variables are used in both the Design Analysis and the Tolerance Analysis. This results in identically the same G coefficients for DA and TA. These differential coefficients can be

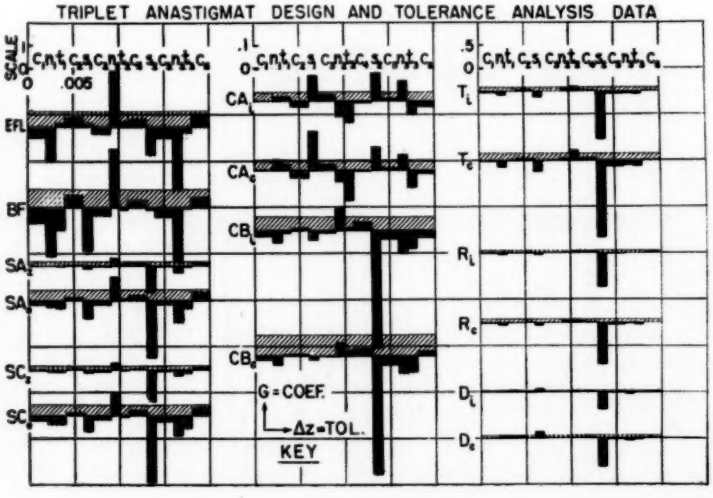

FIG. 5. Performance coefficients and tentative tolerances. The first- and third-order G coefficients are plotted for the triplet anastigmat lens. Note that the one constructional parameter having the greatest G values is s_2. Note also that the three thicknesses, t_1, t_2, and t_3, have very small G values for most of the performance variables.

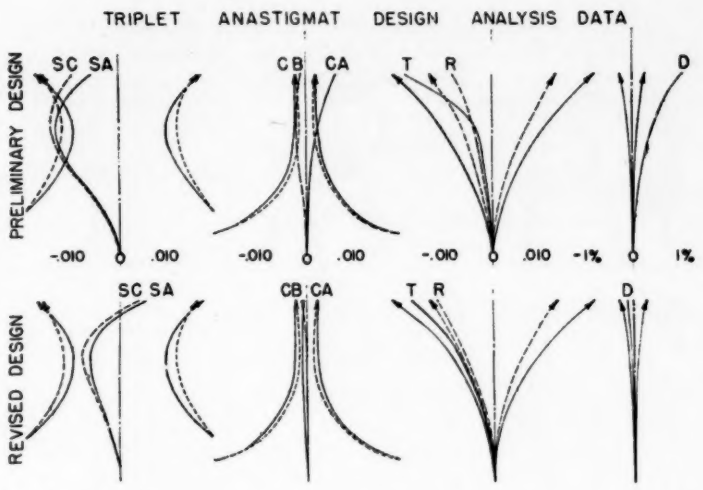

FIG. 6. Third-order performance curves. Aberration curves are shown for the preliminary design and the revised design of the triplet anastigmat lens. Performance tolerance limit curves based upon circle of confusion and contrast criteria are drawn on the graph with arrows for identification. Note that the preliminary design trespasses the performance tolerances, whereas the final design revised by DA is well within tolerances.

found by McAuley and Cruickshank's[1,2,5–8] methods in which a few nominal rays are traced and the data obtained is used algebraically to compute the coefficients. In this example, however, the other alternative method is used; namely, tracing fourteen additional rays for each of the nine nominal rays (paraxial, zonal, edge, principal intermediate, principal corner, upper intermediate, upper corner, lower intermediate, lower corner), giving a trial increment, Δz_j, to a different parameter, z_j, for each of the fourteen rays. The contribution, Δh_j, to each performance variable, h_j, by each Δz_j is found, thus enabling us to compute G by Eq. (18) with sufficient accuracy if the Δz_j is not too large.

$$G \doteq \Delta h / \Delta z. \tag{18}$$

Whichever method is used for finding the G coefficients, they may be plotted as shown in Fig. 5 (as was done in Fig. 3 for the first-order TA) with the performance tendencies of each parameter given for each dependent variable. This forms a ready reference chart for both DA and TA.

Figure 6 shows the third-order performance curves for both the preliminary design and the final design which was revised with the use of DA. Performance tolerance limit curves, based upon circle of confusion and contrast criteria, are drawn on the graph with arrows for identification. Note that the preliminary design trespasses the performance tolerances. Thus if the lens were made to the nominal data, it would be unsatisfactory as shown in graph (a) of Fig. 1. The direction and magnitude of changes in the parameters which improve the nominal design are found in Fig. 5. If the required changes are small, analytical methods will yield just those changes which raise the nominal performance to the maximum, using any desired criterion of performance. Moreover, if the required changes are small, the G coefficients will not be altered appreciably by the changes. This means that the graph of Fig. 5 is still valid after the preliminary design has been revised and so may be used for the TA.

The third-order TA will make the best possible use of the tolerance margins of the revised design shown in Fig. 6. The same methods used for the DA will yield tolerances as well as parameter increments. These tolerances, Δz, and their contributions are shown graphically in Fig. 7. It is readily seen from Fig. 5 that the second separation, s_2, has a large G coefficient for most of the aberrations, so its tolerance has been made small to keep its contribution down. On the other hand, the thicknesses, t_1, t_2, and t_3, all have rather small G coefficients for most of the aberrations, so their tolerances have been made liberal. The final result of the third-order D&TA

[5] F. D. Cruickshank, Proc. Phys. Soc. **57**, 362 (1945).
[6] F. D. Cruickshank, J. Opt. Soc. Am. **36**, 296 (May, 1946).

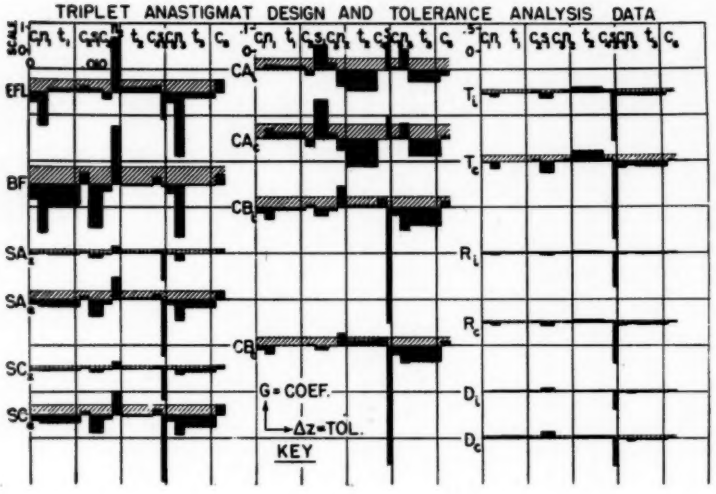

FIG. 7. Performance coefficients and revised tolerances. The first- and third-order G coefficients and the revised tolerances are plotted for the triplet anastigmat lens. Note that for s_2 the large G value is compensated by specifying a tight tolerance. Note also that the tolerances have been increased on the three thicknesses, t_1, t_2, and t_3, taking advantage of the small G values involved. Compare with Fig. 5.

is shown in Fig. 8, the shaded areas representing the range in which the performance curves will lie as a result of the tolerances on the parameters shown in Fig. 7. Note that these shaded areas take full advantage of the performance limits. Figure 8 shows that we have achieved for each aberration the best nominal design and the largest permissible tolerances, and so the lens satisfies the ideal condition of Fig. 1c.

CONCLUSION

Design and Tolerance Analysis has proved over several years to be economically valuable at Bell & Howell Company. Since the criterion for setting tolerances takes into account the relative cost of the operation involved, the extra time spent on TA is well repaid by reduced manufacturing costs. The handy form in which the G coefficients are shown in Fig. 7 permits a rapid adjustment of tolerances from parameter to parameter when a change occurs in the manufacturing process, accompanied by a change in the relative cost of the different operations.

The G coefficients also indicate which manufacturing operations should be made more precise in order to relax the tolerances on other param-

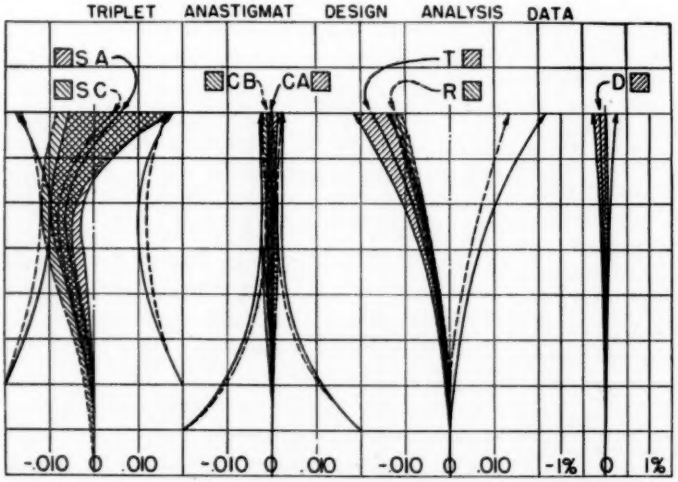

FIG. 8. Revised tolerances and performance curves. This shows the final result of third-order Design and Tolerance Analysis on the triplet anastigmat lens. The shaded areas represent the range in which the performance curves will lie as a result of the tolerances on the parameters shown in Fig. 7. Note that these shaded areas will take full advantage of the performance limits.

eters and reduce the cost still more. An example of this is the second separation, s_2, which is very critical. By improving the mount design or by changing the manufacturing process to more economically hold a tighter tolerance on s_2, it would be possible to readjust the tolerances for more economical production.

Another economical advantage of D&TA is that it can be performed by less experienced lens designers, thus releasing the senior lens designer for more difficult problems than trimming up a preliminary design to its maximum performance and the setting of tolerances. Note that after D&TA has been completed on a certain type of design intended for a definite use, no further improvement can be made in the design without using "large" changes in the constructional parameters. It is on these "large" design changes that the senior lens designer can be of most value.

D&TA procedure, in brief, consists of selecting the optical performance dimensions and the constructional parameters to be analyzed. Theoretically there should be an equal number of each, but practically either may outnumber the other with valuable results. The parameters are weighted from a manufacturing economy standpoint, taking advantage of statistical analysis of past experience. The aberration limit standards are set to suit the image quality standard. This is empirical, but is subject to analysis. The G coefficients are found for the preliminary design and are used to obtain the revised design by DA. If the revised design is considerably different from the preliminary design, the G coefficients should be redetermined (and if sufficiently different, should be used to obtain a new revised design). The TA then uses the G coefficients for establishing the optical and related mechanical tolerances.

The standard practice of using Design and Tolerance Analysis at Bell & Howell has benefitted both the company and the customer by improving the products, improving production, and reducing costs.

JOURNAL OF THE OPTICAL SOCIETY OF AMERICA VOLUME 38, NUMBER 7 JULY, 1948

Some Considerations of the Effect of Radiation on the Performance of Liquid Fuel Rockets

S. S. PENNER AND S. WEINBAUM
Jet Propulsion Laboratory, California Institute of Technology, Pasadena, California
(Received January 13, 1948)

Equations have been developed for estimating the temperature rise, caused by the absorption of radiant energy, of a small volume element of cool gas or of a liquid droplet moving along the axis of a cylindrical chamber. The absorbing material was assumed to move with constant velocity and to be surrounded at all times by hot radiating gases distributed uniformly throughout the cylindrical chamber. A sample calculation has been carried out for an absorbing volume element of gas moving with a linear velocity of 1.15×10^4 cm/sec. through a cylindrical chamber (30 cm in length and 14 cm in diameter) filled uniformly with graybody emitters at 3000°K and 20 atmos. pressure. The mass emissivity of the radiating gases was chosen to be 40 sq. cm/g. The upper limit for the temperature rise of the moving gases, caused by the absorption of radiant energy, was found to be about 100°K for the chosen conditions.

I. INTRODUCTION

IN connection with the performance of liquid fuel rockets, it is of interest to ascertain the energy transfer by radiation to moving gases and liquids. An increase in the temperature of the chemical reactants at each step of the liquid or gas phase reactions results in a more rapid rate of reaction. The present analysis may be applied to estimate an upper limit for the radiation temperature rise of moving gases and liquid droplets.

Significant changes in the mechanism and the rate of chemical reactions may be associated with photo-chemical activation. A discussion of

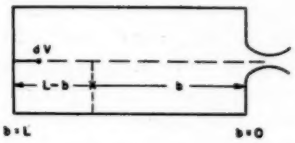

FIG. 1. Rocket chamber of length L with volume element dV moving along its axis.

processes of this type falls outside the scope of the present study.

The influence of radiation on the performance of solid fuel rocket motors has been discussed.[1,2] The treatment for the radiant energy transfer to moving gases and liquid droplets employed in the present calculations is similar, in principle, to that used for the studies on solid fuel rockets.

II. FORMULATION OF PROBLEM

When a receiver of radiant energy is exposed to a volume filled continuously with emitters of radiant energy, then the radiant energy incident on 1 sq. cm of receiver per second may be expressed by the relation[1]

$$\int_\lambda I_\lambda' d\lambda = \int_\lambda I_\lambda^0 (1-\exp[-k_\lambda \rho l])d\lambda, \qquad (1)$$

where I_λ^0 represents the energy (in cal./sec.) which is emitted by 1 sq. cm of a blackbody at the temperature of the radiating gases in the wave-length region between λ and $\lambda+d\lambda$, I_λ' is the corresponding energy received per second by 1 sq. cm of receiver, k_λ is the average mass absorption coefficient for the indicated wave-length region, ρ is the gas density, and l is the radiation path length (in cm), that is the linear distance throughout which emitters are distributed and can be "seen" by the receiver. In a closed container, uniformly filled with emitters throughout the path length l, the radiant energy $\int_\lambda I_\lambda d\lambda$ incident on a small volume element of receiver from a given direction is equal to the sum of $\int_\lambda I_\lambda' d\lambda$ and of the radiant energy reflected from the wall and transmitted through the length l. The reflected energy may be neglected for approximate calculations.[3]

Equation (1) is materially simplified if the emitters of radiant energy are treated as gray-body emitters. In this case Eq. (1) becomes

$$I = I^0(1-e^{-k\rho l}), \qquad (2)$$

where I represents the total radiant energy incident on 1 sq. cm of receiver per second and I^0 is the total radiant energy emitted by a blackbody radiator per square centimeter of surface per second.

It is desired to calculate the maximum possible temperature rise caused by the absorption of radiant energy when a volume element dV moves with uniform velocity along the axis of a cylindrical rocket chamber (see Fig. 1). As dV moves through the chamber and out through the rocket nozzle, it is exposed to different radiation intensities. A fraction of the radiant energy incident on dV is absorbed; thus the temperature of dV is raised continuously as it moves through the motor chamber. Instead of computing the time-dependent temperature changes and calculating their sum in order to obtain the total temperature rise, it was found preferable to determine the total radiant energy incident on dV during its residence time in the chamber. The total temperature rise may then be computed by allowing the entire radiant energy passing through dV during its travel time through the chamber to be incident on dV at one time.

The formulation of the problem outlined here implies a number of approximations. In particular, the neglect of the loss of energy by radiation from dV will have the effect of maximizing the calculated temperature rise associated with the absorption of radiant energy. Furthermore, the present treatment gives too large values for the temperature rise since the absorbing gases and liquid droplets in an actual rocket chamber are not surrounded by hot radiating gases on all sides.

[1] W. H. Avery, OSRD Report No. 3880, 1944; Paper 24 presented before the Symposium on Kinetics of Explosives at the 112th Meeting of the American Chemical Society, New York City.

[2] J. Beek, Jr., W. H. Avery, M. J. Dresher, F. T. McClure, and S. S. Penner, OSRD Report No. 5817, June, 1946. See also S. S. Penner, J. App. Phys. 19, 392 (1948).

[3] The reflection coefficient of the oxidized steel wall is of the order of 0.2. Neglect of the reflected energy will introduce an error of about 10 percent.

III. THE RADIANT ENERGY INCIDENT ON A SMALL VOLUME OF GAS DURING ITS RESIDENCE TIME IN THE MOTOR CHAMBER

The element dV is located initially on the axis of the cylinder at the position $b=L$ in Fig. 1. It is assumed that dV moves with constant velocity v along the axis. In order to evaluate the temperature rise, it is necessary to calculate first the energy of radiation I_T incident on dV during its travel time.

The volume element dV at any point of its path is at a distance $L-b$ from its starting point. A quadrant of the cylinder with dV located on the axis is shown in Fig. 2.

From Fig. 2 it can be seen that $l_1=(a^2+b^2)^{\frac{1}{2}}$, $l_2=(a'^2+(L-b)^2)^{\frac{1}{2}}$, and $l_3=(a^2+y^2)^{\frac{1}{2}}$. The radiant energy incident on the volume element dV when it is at a distance b from the chamber exit is given by the relation

$$I_\lambda'(b)=I_\lambda^0\langle(1-\exp[-k_\lambda\rho l])\rangle$$

$$=(I_\lambda^0/A)\int_A(1-\exp[-k_\lambda\rho l])dA,$$

where the quantity in angular brackets denotes an average value and dA is an element of surface of the chamber walls. Therefore,

$$I_\lambda'(b)=4I_\lambda^0/(2\pi a^2+2\pi aL)\int_0^{\pi/2}d\theta$$

$$\times\Big[\int_0^a(1-\exp[-k_\lambda\rho(a^2+b^2)^{\frac{1}{2}}])ada$$

$$+\int_0^a(1-\exp[-k_\lambda\rho(a'^2+(L-b)^2)^{\frac{1}{2}}])a'da'$$

$$+\int_0^b(1-\exp[-k_\lambda\rho(a^2+y^2)^{\frac{1}{2}}])ady$$

$$+\int_0^{L-b}(1-\exp[-k_\lambda\rho(a^2+y^2)^{\frac{1}{2}}])ady\Big]. \quad (3)$$

The radiant energy received over all wavelengths at a fixed position is given by

$$I'(b)=\int_\lambda I_\lambda'(b)d\lambda.$$

As the volume element dV moves along the axis of the cylinder, b assumes all values between $b=L$ and $b=0$.

Since dV moves with uniform velocity v, it follows that

$$\left.\begin{aligned}&b=L \text{ when } t=0,\\&b=0 \text{ when } t=L/v \text{ and, at any time,}\\&b=L-vt.\end{aligned}\right\} \quad (4)$$

Therefore, the sum of the energies I_T incident on the receiver during its residence time in the chamber is

$$I_T=\int_0^{L/v}I'(b)dt. \quad (5)$$

After combining Eqs. (3)–(5) it is found that

$$I_T=\int_0^{L/v}I'(L-vt)dt$$

$$=\frac{2}{\pi a(a+L)}\int_\lambda I^0d\lambda\int_0^{\pi/2}d\theta\int_0^{L/v}dt$$

$$\times\Big[\int_0^a(1-\exp[-k_\lambda\rho(a^2+(L-vt)^2)^{\frac{1}{2}}])ada$$

$$+\int_0^a(1-\exp[-k_\lambda\rho(a^2+(vt)^2)^{\frac{1}{2}}])ada$$

$$+\int_0^{L-vt}(1-\exp[-k_\lambda\rho(a^2+y^2)^{\frac{1}{2}}])ady$$

$$+\int_0^{vt}(1-\exp[-k_\lambda\rho(a^2+y^2)^{\frac{1}{2}}])ady\Big]. \quad (6)$$

Symmetry considerations make it possible to rewrite Eq. (6), after integration with respect to

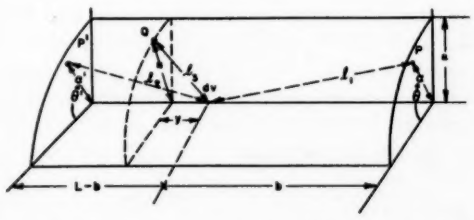

FIG. 2. Quadrant of a cylindrical combustion chamber with a volume element dV moving along its axis.

θ, as follows:

$$I_T=[2/a(a+L)]\int_\lambda I_\lambda^0 d\lambda\int_0^{L/v}dt \times\left[\int_0^a(1-\exp[-k_\lambda\rho(a^2+(L-vt)^2)^{\frac{1}{2}}])ada + \int_0^{L-vt}(1-\exp[-k_\lambda\rho(a^2+y^2)^{\frac{1}{2}}])ady\right]. \quad (7)$$

Since $(L/v)\int_\lambda I_\lambda^0 d\lambda$ represents the radiant energy incident on dV in a blackbody environment during the residence time L/v, it is necessary that

$$\lim_{l \text{ or } k_\lambda\to\infty} I_T=(L/v)\int_\lambda I_\lambda^0 d\lambda.$$

Reference to Eq. (7) shows that I_T fulfills this requirement.

IV. THE MAXIMUM TEMPERATURE RISE OF A SMALL VOLUME OF GAS AS THE RESULT OF THE ABSORPTION OF RADIANT ENERGY

An approximate value for the temperature rise can be calculated by assuming that all of the energy I_T is incident on dV at the same time. If dV is sufficiently small, the radiant energy may be assumed to be incident on dV in a direction normal to the surface of dV. The calculations may be simplified by choosing dV to be a sphere.[4]

If the sphere has a radius δ, the energy absorbed during the residence time in the chamber is

$$E_a=\int_\lambda I_{T\lambda}(1-e^{-2K_\lambda\delta})\cdot 4\pi\delta^2 d\lambda, \quad (8)$$

where $I_{T\lambda}$ is the radiant energy in the wave-length region between λ and $\lambda+d\lambda$ incident on the receiver during its residence time, and K_λ is the absorption coefficient of the receiver of radiant energy. Reflection of radiant energy from the absorbing volume element has been neglected in Eq. (8). If an average value is used for K_λ, Eq. (8) becomes

$$E_a=(1-e^{-2K\delta})\cdot 4\pi\delta^2 I_T. \quad (8a)$$

[4] A cube or a cylinder with diameter equal to its length may also be used. The final temperature rise is independent of the shape of the volume element dV.

The temperature rise of the volume element $(4/3)\pi\delta^3$ caused by the absorption of E_a cal. is

$$\Delta T=E_a/(4/3)\pi\rho_a C\delta^3, \quad (9)$$

where ρ_a is the density of the receiver and C represents the heat capacity of the receiver (in cal./g/degree).

Combining Eqs. (8a) and (9) leads to the result

$$\Delta T=3I_T(1-e^{-2K\delta})/\rho_a C\delta, \quad (10)$$

and if δ is sufficiently small,

$$\Delta T=6I_T K/C\rho_a. \quad (11)$$

For the special case where the receiver of radiant energy consists of gases at a lower temperature than the emitters of radiation, an approximate value may be obtained for ΔT by setting $K=k\rho_a$. For this special case, Eq. (11) becomes

$$\Delta T=6kI_T/C. \quad (12)$$

If the wave-length dependence of K_λ is considered, then Eq. (11) should be replaced by

$$\Delta T=(6/\rho_a C)\int_\lambda K_\lambda I_{T\lambda} d\lambda. \quad (13)$$

Temperature rises of the volume element dV computed by use of Eq. (11) or (13) are only approximately correct because of the many assumptions made in the derivation of these relations. However, the calculated results should be of the correct order of magnitude.

V. TEMPERATURE RISE CAUSED BY ABSORPTION OF RADIANT ENERGY FOR GASES COMPOSED OF GRAYBODY EMITTERS

The actual temperature rise can be computed only if the total incident radiant energy is known. Calculation requires data concerning the wave-length dependence of the mass absorptivity k_λ and of the absorption coefficient K_λ. In the absence of information concerning the variation of k_λ with wave-length, calculations may be carried out by assuming graybody emission, i.e., by choosing for k_λ a constant value independent of wave-length. Similarly, it may be necessary to use an average absorption coefficient K.

A representative calculation has been carried through for the special case where Eq. (12) gives

a correct upper limit for the temperature rise. The following numerical values, which are believed to be approximately valid for the WAC Corporal sounding rocket operating at a temperature of 3000°K and a pressure of 20 atmos., were employed for the calculations: $k=40$ sq. cm/g, assumed to be independent of wave-length, $I_0=115$ cal./sq. cm/degree, $v=1.15\times10^4$ cm/sec., $L=30$ cm, $\rho=2\times10^{-3}$ g/cc, $a=7$ cm, $C=0.437$ cal./g/degree.

Numerical integration of Eq. (7) leads to the result $I_T=0.191$ cal./sq. cm during the residence time of 2.61×10^{-3} second. The calculated upper limit for the radiation temperature rise of the cool gases is therefore found to be about 100°K. The actual temperature rise caused by the absorption of radiant energy may be only a small fraction of the calculated upper limit.

VI. RADIANT ENERGY TRANSFER TO LIQUID DROPLETS

Injection of liquid droplets into a chamber filled with hot radiating gases occurs in Diesel engines as well as in liquid fuel rockets. Vaporization of these droplets is dependent on the rate of heat transfer to the liquid droplets by conduction, convection, and radiation.[5] The present treatment permits approximate calculation of the radiant heat transfer to liquid droplets in a combustion chamber.

If the life of the liquid droplets is such that they move a distance $L-b$ from their point of entry into the motor chamber, then the total radiant energy incident on a droplet located on the axis of the cylinder, during its lifetime $t=(L-b)/v$, is given by Eq. (7) with L/v replaced by $(L-b)/v$ as the upper limit of the integral with respect to time; i.e.,

$$I_T=[2/a(a+L)]\int_\lambda I_\lambda{}^0 d\lambda\int_0^{(L-b)/v} dt$$

$$\times\left[\int_0^a (1-\exp[-k_\lambda\rho(a^2+(L-vt)^2)^{\frac{1}{2}}])ada\right.$$

$$\left.+\int_0^{L-vt}(1-\exp[-k_\lambda\rho(a^2+y^2)^{\frac{1}{2}}])ady\right]. \quad (14)$$

The temperature rise resulting from the absorption of radiant energy by a liquid droplet of radius r is then approximately given by the relation

$$\Delta T=(3/C\rho_a r)\int_\lambda I_{T\lambda}d\lambda(1-e^{-2K_\lambda r}), \quad (15)$$

where K_λ denotes the average absorption coefficient of the liquid for radiation in the wave-length interval between λ and $\lambda+d\lambda$. Equation (15) is based on the assumption that the radiant energy is incident in a direction normal to the surface of the droplet. Allowance will have to be made for the variation of the absorption coefficient of the liquid with wave-length in the same manner as was previously done for double-base solid propellants.[1,2]

[5] W. Wentzel, Forsch. Geb. Ing. 6, 105 (1935).

Aerial Photographic Equipment and Applications to Reconnaissance*

AMROM H. KATZ
Photographic Laboratory, Engineering Division, Air Materiel Command, Wright Field, Dayton, Ohio
(Received February 2, 1948)

This paper covers briefly some of the photographic equipment and applications in use by the U. S. Air Force, with emphasis on reconnaissance photography. Three main divisions of effort are defined: reconnaissance, mapping, and the dual field of photographic instrumentation and instrumentation photography. A heuristic equation is given to demonstrate the usefulness of long focus lenses, and the development of the long focus lenses, shutters, and performance tests is described.

Minimal altitude or "dicing" photography is described, its peculiar requirements noted, and several outstanding examples of its wartime employment cited. High speed shutters are not usable, under low illumination or poor weather conditions. Shutterless strip cameras and moving film magazines are now in use, utilizing image motion compensation. Remarkable photographs have been made under extreme ground speed and low illumination conditions.

New developments in mounts, lenses, cameras, and shutter are described, including the 100-inch f:10 figure 4 camera, the 48-inch f:6.3 camera featuring a novel high speed louvre shutter, and two extremely wide-angle spherical focal plane cameras.

The function of night photographic reconnaissance is discussed, and two night photographic systems described. The first and older system employs flash-bomb illuminants; shutter synchronization is accomplished through a photocell system. The Edgerton flash principle has been used in the second system; units weighing up to 3500 pounds, having a capacitor bank of 7200 microfarads, have been successfully employed up to 10,000-foot altitude.

INTRODUCTION

THE development of aerial photographic equipment and its applications, like that of other tools needed and useful in war, has been marked by much progress in the past few years. This paper will cover briefly some of the equipment and applications in use by the U. S. Air Force, with emphasis on reconnaissance photography; summaries of some of the research work and results obtained will be given, leaving the detailed accounts for future separate papers.

As principal user and pioneer in the development of aerial photography, the Air Force, through its Photographic Laboratory at Wright Field, has conducted much basic research, sponsored university and industrial research, designed equipment, and developed, through many operational missions and test flights, optimum techniques for the use of photographic equipment.

The two main functions of aerial photography are:

(1) The securing and rapid recording of large quantities of detailed information; and

(2) The summarizing and transmission of this recorded information in permanent and easily distributable form.

These two functions are accomplished within three main divisions of photographic effort. The first two of these three divisions, reconnaissance and mapping, are concerned primarily with aerial photography of the ground and activities thereon; an outstanding exception to this is the type of reconnaissance or intelligence-gathering photography performed by combat-recording motion picture cameras, which in many cases yielded otherwise unobtainable information about enemy aircraft and tactics. The third field of effort is the dual field of instrumentation photography and photographic instrumentation.

Instrumentation photography is the employment of photographic techniques and equipment to record the changing readings on meters, gauges, counters, radar scopes, television receivers, and similar instruments. Photographic instrumentation, however, implies direct recording of the phenomena in a manner suitable for subsequent detailed analysis. An example is the high speed photography of the Bikini atomic bomb tests.

This new field of Air Force photographic activity, and new developments in mapping photography, merit full and separate discussion, which will not be attempted here.

WARTIME RESEARCH

At the beginning of the war just past, aerial photography was virtually an unknown military

* Invited paper presented at Annual Meeting, Optical Society of America, Cincinnati, Ohio, October 23rd, 1947.

factor. Prewar photographic planning, however, foresaw correctly the conditions which would obtain: Photographic reconnaissance would be conducted only at the low and high altitude boundary conditions of operational flying. Long-focus lenses—40-inch and greater—were required for the anticipated 30,000-foot altitudes, high speed shutters or their equivalent for low altitude operation.

The size, weight, and mechanical complexity of even the early 40-inch cameras prompted many earnest photographers and military personnel, with an amateur photographic background, to suggest that photographs made with small cameras could be enlarged to the scale of a photograph taken with a longer lens and yield the same definition obtainable with the greater focal length camera. In 1941 the number and rate of such suggestions prompted the author to attempt a quasi-theoretical explanation of the fact that such enlargements could never equal the definition obtainable by longer lenses.

A simple equation relating the separate resolving powers of the lens and film to resolution obtainable on the lens-film combination was proposed; this equation is admittedly of heuristic value only, but served to dispose of the enlargement fallacy for the time being. Where R_F, R_L, and R_{F+L} are the resolution in lines/mm of the film, the lens, and the film-lens combination, respectively, this formula states:

$$1/R_{F+L}=1/R_F+1/R_L.$$

Even on the unnecessarily stringent and generally untrue assumption that angular resolving power of a series of lenses—say, 6-inch, 12-inch, and 24-inch focal length—is constant, it can be easily shown that the enlarged photographs made with the shorter lenses yield far less resolution than obtained with the longest lens. Of course, ample experimental evidence confirming this conclusion has been secured. This particular effect was commented on in detail by Kingslake in March, 1942;[1] by an odd coincidence, the numerical values in the hypothetical examples cited by Kingslake exactly fit the rough equation given above.

Early attempts to use long focus telephoto lenses at high altitudes invariably yielded photographs, the poor quality of which could not be satisfactorily explained. The first aerial resolution tests known to have been conducted in this country commenced in the spring of 1941 at Wright Field—the targets being staked-out patterns formed of black and white blotting paper. The great apparent discrepancy between aerial and bench performance was immediately confirmed, and permanent targets, to permit extensive aerial test work, were painted on the Wright Field runways. A theoretical analysis by the author of the effects of the variation in index of refraction of glass, from sea-level to 30,000 feet, the temperature effects on the lens, lens-barrel, and lens cone, indicated that laboratory focused 40-inch telephoto lenses could be out of focus by as much as 2 millimeters when taken to 30,000 feet. An extensive experimental investigation by Woodford and Nierenberg followed and was reported in 1945.[2] Further comments on this effect were made by Kingslake in January, 1947.[3]

The long focus lens program got under way in 1941, with the formulation by Colonel G. W. Goddard and Dr. J. G. Baker of a plan which called for design and use of a 40-inch f:5.0, a 60-inch f:6.3, and a 100-inch f:10 lens. The entire wartime lens program is discussed in detail by Kingslake[3] and will be referred to again in connection with camera problems.

There existed at the start of the war no satisfactory method of investigating or measuring shutter characteristics, nor had there been formulated any general theory relating shutters to the optics of the camera, and to the integrated performance of the particular photographic system. A complete investigation was begun by the author in January, 1941, and culminated in the development of shutter test methods and definitions which are now American Standards. The relationship of shutter performance to resolution in the final photograph was investigated, and fundamental advances in shutter design and performance were achieved. A detailed account of this work was recently presented by the author in an as yet unpublished paper at the Boston University Optical Research Laboratory symposium on Resolving Power and Shutters; there-

[1] R. Kingslake, J. Opt. Soc. Am. **32**, 129 (1942).

[2] Woodford and Nierenberg, J. Opt. Soc. Am. **35**, 619 (1945).

[3] R. Kingslake, J. Opt. Soc. Am. **37**, 1 (1947).

fore, nothing further will be added here on this subject.

Because of the great time lag between initial research, development, production, and operational use, not as many improved or new cameras reached the service during the war as we in the development end would have liked. Photographic reconnaissance was accomplished in the main from the F-5, which was the photographic version of the P-38 aircraft, although B-17's, B-24's, P-51's, and B-29's were also used, with the F-13 or photographic version of the B-29 especially prominent in photography of Japan. The basic installation in these aircraft was similar, and consisted of three 6-inch focal length K-17 cameras, with plate size 9×9 inches, mounted so as to photograph from horizon to horizon across the line of flight, one vertical K-18 camera with a 24-inch focal length lens and a plate size 9×18 inches, and two "split vertical" 9×9-inch plate size 40-inch K-22 cameras, mounted at a slightly oblique angle, so as to effectively double the width of ground area covered by these long lenses. This type of multi-purpose installation could be modified for special missions.

The great bulk of aerial film used in the war and today is 9½ inches wide, and is available in rolls up to 400 feet in length. The film used in daytime reconnaissance has an ASA speed index of 100, and approximates Super-XX in characteristics.

The use of aerial color film, began during the war, is increasing. Its unique advantages for photo-interpretation work, permitting identification by color of industrial smokes, wastes, and other technical features, insure eventual widespread use.

It has been estimated that as much as 80 percent of the information obtained during the war about the enemy and his activities was secured by aerial photography. An examination of the type of activity and targets furnishes conclusive proof that no single camera or photographic system can be used to encompass the entire range of operational problems.

LOW ALTITUDE PHOTOGRAPHY

Minimal altitude or "dicing" photography is generally accomplished at altitudes of from 50 feet to 200 feet. Details of gun emplacements, radar installations, beach defenses, troop movements, ships, photography of low level bomb or rocket attacks—these are the subject matter of "dicing" photography.

Under operational conditions which rule out low altitude flying, or when greater areas must be covered, maximum altitude reconnaissance with long focus lenses comes into its own. The standard performance test for 30,000-foot photography has been the resolution of individual railroad ties. An impossible accomplishment at the start of the war, the achievement of such resolution is now routine.

Low altitude photography with conventional cameras requires a high speed shutter to reduce the blur caused by image motion. Mr. George Mitchell of the Mitchell Camera Corporation, by a simple modification of the shutter of the 6-inch focal length K-17 camera, doubled the top actual shutter speed, increasing this speed from 1/250th second to 1/500th second. Two such modified cameras were turned over to Colonel Karl Polifka for dicing work in Italy. The following extract from a letter by Colonel Polifka to the author tells, more clearly than any possible theoretical explanation, of the value of such photography:

> "I thought you would be interested to know, and to have as a matter of record, the history and operational performance of your Mitchell high-speed shutters, installed in two 6-inch K-17 cameras.
>
> "The first operation of these two pieces of equipment was performed on November 25 and 26, 1943, and on these two days, low altitude oblique coverage was made of the proposed assault area surrounding Mt. Maggiorre and Mt. Camina which are located between Caserta and Cassino in South Italy. These features had held up the advance of the 5th Army for 29 days as of 26 November. The assault had been repeatedly postponed because it was estimated that 15,000 casualties would result. The preparation was performed by running 7 low altitude strips working from the summit of the mountains in parallel lines down to the base. With the information thereby gained, the 5th Army advanced on November 28 by an infiltration method and took Mt. Maggiorre and Mt. Camina with a total assault casualty of one. Unfortunately, however, one battalion was caught by enemy artillery for 437 casualties. During the two days of this first operation, initial dicing preparations were made for the future assault of Cassino, Valleratonda and the amphibious action on the Anzio beach head. . . ."

It must be noted that low altitude photography with high speed shutters requires good

light and weather conditions. The restrictions imposed by these conditions, plus the necessity of accomplishing low altitude photography at definite times and places independent of weather, severely limit the use of conventional cameras with high speed shutters.

THE STRIP CAMERA AND IMAGE MOTION COMPENSATION

The S-7 shutterless continuous strip camera, developed by Colonel Goddard and built by the Chicago Aerial Survey Company, moves the film past a narrow slit in the focal plane at a speed equal to the forward image speed arising from forward aircraft motion. Exposure time, a function of slit width and synchronous film speed, is regulated by adjusting the slit, and exposure is further regulated by adjusting the lens diaphragm.

Excellent photographs have been made with this camera at low altitudes and high aircraft speeds with effective exposure times as long as 1/10th second. A test photograph was made last year of two soldiers playing cards on the ground. The value of each hand was easily assessed. Two lenses may be mounted on this camera, the stereoscopic photographs resulting being of considerable value to photo-interpreters and photogrammetrists when examined in a stereo-viewer.

During the pre-invasion preparations for the Okinawa campaign, measurements were made from stereo-strip films of the sea-wall at the invasion beach. The estimated height of about 6 feet differed from the post-invasion measurement by but 2 inches. Using color film in the vertically mounted stereo-strip camera, water depths on beaches may be estimated within 10 percent. Special projectors, using crossed polaroid projection and polaroid viewing, have great potential value for briefing purposes, proposed target evaluation, and damage assessment. The need for expensive sand-table models is thus largely eliminated. For a long time the strip camera principle was believed to be inapplicable to side oblique photography because of non-uniform image motion across the focal plane of a camera obliquely mounted. A recently developed technique employing narrow slits canted at a slight angle to the direction of film motion has yielded oblique stereoscopic photographs of excellent quality throughout the image field. This is possible because deviations of foreground and background image speed from the film speed cannot cause perceptible blurring in the short effective exposure times used. These exposure times are of the order of 1/200th second. Nearly complete oblique stereoscopic documentation, in color, of bomb damage in both Germany and Japan has been obtained employing this technique.

An automatic film speed control for the S-7 camera has been perfected and eliminates the dual necessity of manual calculation of image speed and the setting of the film speed control. The scanning unit of this automatic control consists of two gratings separated by several inches and composed of alternate transparent and opaque bands oriented perpendicular to the flight path; a pair of photo-cells is mounted above the top grating. With the unit mounted vertically, and the aircraft in motion over a random set of light and dark ground areas, a pulsating light output will be transmitted to the photo-cells through the grating, the frequency being dependent on both ground speed and altitude of the aircraft. This frequency is compared with a frequency generated as a function of the film speed, and appropriate directional correction to the film speed is applied through a servo system.

There is no apparent limitation because of air speed to the use of the strip camera principle. Several days ago a photograph of a P-80 aircraft flying north at 500 m.p.h. was taken with a strip camera mounted in another P-80 flying south at 500 m.p.h. and several hundred feet above the first aircraft. There was no perceptible blur in the resulting photograph, made, of course, at a relative speed of camera and target of 1000 m.p.h.

The extension of this principle to conventional shutter cameras was immediate. The moving film magazines, A-9A and A-14, move the film at synchronous image speed during the exposure, which is made through a conventional shutter. If need be, the shutter may be held open and a slit mounted in the flat focal plane, any standard camera thereby being converted into a continuous strip camera.

The extension of the photographic day to

include pre-dawn and post-sunset photography with no auxiliary illumination was demonstrated about a month ago. With a quarter-inch wide slit, and flying under conditions which required film motion of about 1 inch/sec., thus yielding about ¼-second exposure time, excellent photography, showing full ground detail, was accomplished at 40 minutes past sunset time. A rough calculation indicated that average ground brightness under these conditions was of the order of 0.01 candle/ft.[2]

HIGH ALTITUDE RECONNAISSANCE

High altitude reconnaissance must utilize long focus lenses, as noted previously. Minus-blue filters are usually employed to reduce haze effects. The resolution requirements for successful high altitude photography are greater than the resolution requirements for successful "dicing" photography by a factor of at least two to four times. The reason for this lies in consideration of the image size of the ground detail necessary for adequate interpretation. Photographs made at minimal altitudes exhibit so much detail that a false evaluation is easily made of the resolution present in the photographs.

Precise performance indices of the resolution obtained during the war are impossible to construct on the basis of the non-random samples usually seen, but relative performance figures may be worth consideration. At the start of the war, average resolution obtained in the service was of the order of 8 lines per mm. Better lenses and cameras, and greater experience, combined to raise this figure to perhaps 12 lines per mm by the end of the war. A goal almost within reach now is performance of 30 lines per mm. These figures apply only to high altitude photography, and the last figure has occasionally been exceeded in test flights.

The goal of reconnaissance photography is to photograph, in sufficient detail, everything in the view of the camera. There are, unfortunately, numerous deteriorative effects which stand in the way of reaching laboratory performance with an airborne camera. Image motion caused by the several angular motions of the aircraft, image motion caused by vibration, and that caused by forward aircraft motion—all these tend to reduce resolution on the photographic negative. Camera stabilization by means of a new electro-optical gyro system now under development and test seems at this time to offer much promise.

Much work on antivibration camera mounts was done during the war by an Eastman Kodak group under N.D.R.C. contract; the mount resulting from this research embodying a helical spring support to reduce the natural frequency of the system, and utilizing dry-friction damping, is still under study.

The most dramatic and immediately observable results have been obtained on the problem of eliminating image motion caused by forward aircraft motion, and have been previously discussed.

RECENT DEVELOPMENTS

A complete listing of the standard cameras used during the war, with lens complement and plate size, is given in the 1947 Kingslake report.[3] Of considerably greater immediate interest and application are the developments now available to the using service.

The Baker 40-inch distortionless telephoto lens, covering a 9×9-inch plate area, is completely corrected for temperature and pressure effects. Electrically heated, and thermostatically controlled, it automatically corrects for focus variations with altitude, and remains in focus down to 2000 feet. The rear element of this seven-element lens is adjusted by a system of pressure-sensitive sylphon bellows. This lens is unsurpassed in performance by any domestic or foreign lens of similar type. Completed and ready for production are 36-inch f:8 and 48-inch f:6.3 telephoto lenses covering 9×18-inch plate areas. The latter lens, manufactured by Eastman Kodak Company, has provision for temperature and pressure compensation, although this is not automatic as in the case of the 40-inch f:5.0. The K-22A camera features a very high performance high speed focal plane shutter incorporating the knowledge learned earlier about focal plane shutters and is intended for use either with the 40-inch f:5.0 lens at high altitudes or with short lenses at very low altitudes.

The K-34 camera is a 9×18-inch high speed focal plane shutter camera of high performance and efficiency and is the forerunner of a long range strategic reconnaissance camera which will

mount 12-, 24-, 36-, 48-, 60-, or 96-inch focal length lenses; it will be noted that no attempt to build the extremely large between-lens shutters required for the long focus lenses is being made. The mechanical difficulties encountered in building large aperture shutters—say 5-inch diameter and larger—have never been completely overcome, and exceed by many times the difficulties encountered with focal plane shutters. An interesting camera type now under development at this time by the Air Force and the Fairchild Camera and Instrument Corporation is the P-1 strike-attack camera, which, using 70 mm film and a 2¼-inch square format, will take photographs of low altitude bomber or fighter strikes, at rates up to 5/sec., and with accompanying shutter speeds up to 1/2500 second.

Several experimental cameras of considerable interest may be mentioned. The 100-inch f:10 Baker lens is mounted in a figure 4 camera designed and constructed by Mr. James Nichols of the Mount Wilson Observatory. This camera utilizes a 9×18-inch focal plane shutter of unique design. Suspended in the bomb-bay of an F-13 aircraft, this camera has consistently yielded outstanding photographs. A 50-inch f:6.3 Petzval type lens, using a field flattener, was designed and built by Dr. Irvine C. Gardner of the National Bureau of Standards, and yielded 9×9-inch photographs of quality equal to the best secured by any lens, including the previously cited 40-inch f:5.0 lens.

The first 9×18-inch photographs with the Eastman Kodak 48-inch f:6.3 telephoto referred to previously were made with a camera designed and constructed by Mr. William Mungall of the Photographic Laboratory at Wright Field. The outstanding feature of this camera is a louvre shutter of unique design and performance. Of greater aperture than any previously successful louvre-type shutter, this shutter has a top actual speed of 1/500 second. This speed is almost twice as great as that of a comparable smaller shutter used extensively in German telephoto cameras during the war. The camera was the largest camera used to photograph the atomic bomb tests at Bikini in 1946, and it is interesting to note that the designer and builder was also the aerial photographer using the camera.

Wide-angle lenses utilizing a flat focal plane are necessarily slow—usually about f:6.3—and there is serious fall-off in illumination at the edge of the field caused both by vignetting and the $\cos^4$ law. A bold and successful attempt to overcome these difficulties was made by Dr. J. G. Baker, who designed and constructed two spherically symmetrical lenses which utilize a spherical focal plane.

The first lens constructed was a 4-inch focal length f:2.8 lens covering 120 degrees. Utilizing a section of the lens, and rotating it across the spherical focal plane, there is insured both uniform definition and illumination over the entire field. The plates used are hemispherical glass shells, emulsion-coated on the inside surface. The second lens constructed is a 6-inch focal length f:3.5 lens, and covers 125 degrees. This lens is now mounted in a camera constructed by the Boston University Optical Research Laboratory, and exhibits uniform visual resolution of 350 lines/mm over the entire field.

This latter camera at an altitude of 40,000 feet will photograph a circular area 29 miles in diameter and covering 660 square miles. A special optical projection system is used to produce flat enlargements from the hemispherical negatives. This wide-angle system is of great potential value; investigation and tests are proceeding, and may point the way to a new technique of wide-angle reconnaissance.

NIGHT PHOTOGRAPHY

Night photography is necessary to secure information about activities conducted under assumed cover of darkness. By the very nature of the targets, night photography is concerned with fine detail such as tanks, small boats, pontoon bridges, truck convoys, and personnel. Two entirely different systems are in current use. The first and older system employs flash-bomb illuminants; the second is the Edgerton-flash system. The standard flash-bomb is the M-46. Weighing 52 pounds, of which about 25 pounds is flash powder, this bomb is dropped from the aircraft and is detonated by a pre-set time fuze. It reaches a peak candlepower of about 500 million in times which vary from 13 to 25 milliseconds. Total duration is about 0.1 second. This time to peak is dependent on the composition of the flash powder; bombs containing

potassium perchlorate reach peak illumination in about 13 milliseconds, while those containing barium nitrate peak in about 25 milliseconds.

The T-9 flash-bomb, under development for the Air Force by the Wesleyan University Ordnance Research Laboratory, will have a peak candlepower of about 1 billion, with a total light output approximately 2½ times that of the M-46. The standard night camera is the K-19B or K-19C, which utilizes a 12-inch f:2.5 Eastman Ektar covering a 9×9-inch plate. Synchronization of shutter action to the bomb detonation is achieved by a photo-cell system which sends a tripping impulse to the between-lens shutter release mechanisms. It is clear that the illumination received by the ground is independent of the altitude of the camera, being dependent only on the location of the illuminant.

Good quality photographs can be made with the K-19 camera at altitudes of 20,000 feet, with the bomb being detonated at about 8000 feet. Unfortunately, at such altitudes the small scale of the photograph makes identification of the small night targets very difficult. Under current development are a 9×18-inch plate size camera utilizing a 24-inch f:3.5 lens, and a 9×9-inch plate size camera utilizing the 40-inch f:5.0 telephoto lens.

Adaptation of the moving-film magazine to night photography has eliminated the loss in resolution previously resulting from use of the necessarily slow shutter speeds.

Another recent development of the Wesleyan Laboratory and the Picatinny Arsenal is the T-12 flash cartridge. Eight (8) inches long and 1½ inches in diameter, this cartridge contains but 5 ounces of powder, yet reaches a peak of about 45 million candlepower. Excellent photographs using the T-12 illuminant have been made from altitudes of several thousand feet.

The Edgerton-flash principle has been successfully adapted to the problem of night photography. Discharge of the energy stored in a bank of capacitors through a xenon-filled tube results in a brilliant flash of short duration. Synchronization of shutter action to the flash is far simpler in this case than in the photo-cell system previously discussed. The shutter is tripped, and when it is in full open position, triggers the flash tube through an auxiliary contact. All of the flash units utilize capacitors charged to 4000 volts from the 28-volt aircraft power supply. The D-1 flash unit is the smallest airborne flash unit. Weighing 125 pounds, it employs a capacitor bank of 75 mf, and can deliver 2 flashes/sec. Its maximum useful altitude is 300 feet, and it requires a continuous charging current of 100 amperes. The D-2 unit weighs 460 pounds, utilizes a 600-mf capacitor bank, and has an operational limit of 2500 feet. The largest of all the units is the D-3 which weighs 3500 pounds, uses 2 lamps, and has a capacitor bank of 7200 mf. This unit is useful up to 10,000 feet altitude and requires a continuous charging current of 600 amperes.

Both the flash-bomb and flash-lamp systems saw extensive use in the war, yielding otherwise unobtainable information of great value.

CONCLUSION

In summary, it may be stated that much progress has been made in understanding and evaluating the factors involved in aerial photography; even more progress has been made in design of aerial photographic equipment and development of techniques. The new problems coming up in the use of jet planes and uninhabited aircraft, coupled with increased severity of operational conditions, will continue to demand the application of the best in scientific thought, research, and practice to these problems.

Those of us who realize the value of aerial photography as a weapon of war know that it can be as successfully applied in keeping the peace. These applications too await our immediate attention.

Scattered and Rescattered Sunlight

A. HAMMAD
Department of Applied Mathematics, Faculty of Science, Cairo, Egypt
(Received March 1, 1948)

In this paper, simple approximate formulas are derived for the intensity of secondary scattered (rescattered) sunlight, in a plane-stratified atmosphere of uniform composition, for high solar altitudes and weakly attenuated radiations. The formulas obtained are compared with those given by L. Silberstein in an earlier investigation and found to be simpler and less elaborate to evaluate. Numerical calculations are made for the functions involved and for the rescattered sunlight received at the ground from different directions, for the case when the sun is overhead and for a wave-length corresponding to weakly attenuated radiations. These calculations show that our approximate formulas are really adequate, giving numerical values in closer agreement with the exact values than those of Silberstein.

For other wave-lengths and other altitudes of the sun, simple approximate expressions have been given elsewhere.

I. INTRODUCTION

IN an earlier paper[1] (here referred to as Paper I), exact formulas were given for the primary and secondary scattered sunlight of any wave-length λ, emitted and received in any direction, at any point in a plane-stratified[2] atmosphere of uniform composition, extending to infinity in all horizontal directions. This paper was supplemented by two other ones,[3] discussing the general features of primary and secondary scattering and indicating the relative magnitudes of the different orders of scattering.

The formulas for the reception of primary scattered light are quite simple and easy to evaluate, but those for secondary are so complicated and elaborate to evaluate that the need was urged for much simpler expressions whose numerical values agree fairly well with those of the exact formulas. Such simpler expressions are of value in the numerical discussion of secondary scattered light itself, and still more because they facilitate the calculation of the scattered light of higher orders.

In a more recent paper,[4] L. Silberstein made an attempt towards that end, but considered a very special case, namely, the case when the sun is overhead and the radiation is weakly attenuated. His formulas, however, are not simple enough. In the present paper we have derived, for this special case, simpler approximate expressions which are more readily evaluated and which give numerical values in closer agreement with the exact values than those of Silberstein. For other wave-lengths and other directions of incidence of the solar beam, simple approximate expressions have been given elsewhere.[5]

II. NOTATION

As in Paper I, the zenith angle of the sun will be denoted by z. Relative to the vertical and the vertical half-plane through the sun, other directions are specified by their polar angles (θ, φ). Light traveling in the direction of the unit vector $\mathbf{k}$ and that traveling in the opposite direction $-\mathbf{k}$ will, however, be denoted by the same angles (θ, φ), so that $\sec\theta \geq 1$. When it is required to distinguish between upgoing and downgoing light, we attach to our symbols a suffix "u" or "d," respectively.

The fraction of the total mass of the atmosphere that lies below the horizontal plane through the point P is denoted, as in Paper I, by m; the remaining fraction above that plane is $1-m$, also denoted by $\bar{m}$. We refer to m as the level, $\bar{m}$ as the depth of the point P in the atmosphere.

The absorption and scattering coefficients of

[1] A. Hammad and S. Chapman, Phil. Mag. **28**, Ser. 7, 99 (1939).
[2] On this account the formulas need correction for low solar altitudes or low altitudes of emission or reception of light, in order to be applicable to an atmosphere resting on a curved earth.
[3] A. Hammad, Phil. Mag. **36**, Ser. 7, 434 (1945), and **38**, 515 (1947).
[4] L. Silberstein, J. Opt. Soc. Am. **33**, No. 9, 526 (1943).
[5] A. Hammad, Phil. Mag., in the press.

TABLE I.

$\bar{m}$	$\bar{m}\log\bar{m}$ $+m\log m$	$-3m\bar{m}$	$\bar{m}^2\log\bar{m}$ $-m^2\log m$	$-0.8m\bar{m}$ $\times(2\bar{m}-1)$
0.0	0.00	0.00	0.000	0.000
0.2	−0.50	−0.48	0.078	0.077
0.3	−0.61	−0.63	0.067	0.067
0.4	−0.67	−0.72	0.037	0.038
0.5	−0.69	−0.75	0.000	0.000

the air, per unit mass, for the wave-length λ, are denoted by $\alpha(\lambda)$ and $\sigma(\lambda)$, or, more briefly, by α and σ; we define a, s, c by

$$a/\alpha = s/\sigma = \mathrm{M}, \quad c = a+s,$$

where M denotes the total mass of air in a vertical column of unit cross section (1 sq. cm) extending from the ground throughout the atmosphere. We shall also write

$$\mathrm{Z} = c\sec z, \quad \Theta = c\sec\theta.$$

III. EMISSION AND RECEPTION OF SECONDARY SCATTERED SUNLIGHT

The exact expression for the intensity of emission E_2 of secondary scattered sunlight, per unit mass of air at any level m, is given in §13 of Paper I. This is:

$$\mathrm{E}_2(\lambda,m,z,\mathbf{k}) = (9s\sigma/256\pi)\mathrm{I}_\infty \times\{\mathrm{A}_0\mathrm{L}_1(c,z,m)+\mathrm{A}_1\mathrm{L}_3(c,z,m)+\mathrm{A}_2\mathrm{L}_5(c,z,m\},$$

where I_∞ is the intensity of the direct sunlight (of any wave-length) outside the atmosphere, and the A's and the L's are functions specified and discussed in §§13 and 17 of Paper I.

The functions L_n are given by

$$\mathrm{L}_n(c,z,\bar{m}) = \int_0^1 \exp(-\mathrm{Z}\bar{m}')\mathrm{E}j_n(c\bar{m}\sim c\bar{m}')d\bar{m}',$$

where

$$\mathrm{E}j_n(t) = \int_1^\infty \exp(-tx)x^{-n}dx.$$

From this definition of L_n, it may be readily seen that it decreases as either n, z, or c increases; its variation with m, however, is not monotonic, and it has a maximum at a level higher than $m=\frac{1}{2}$ (cf., §17, Paper I).

The exact expression for the intensity of reception of R_2 of secondary scattered light is given in §14 of Paper I. For downgoing light this is

$$\mathrm{R}d_2(\lambda,\bar{m},z,\mathbf{k}) = (9s^2/256\pi)\mathrm{I}_\infty\sec\theta \times\{\mathrm{A}_0\mathrm{L}d_1(c,z,\bar{m},\theta)+\mathrm{A}_1\mathrm{L}d_3(c,z,\bar{m},\theta) +\mathrm{A}_2\mathrm{L}d_5(c,z,\bar{m},\theta)\},$$

where

$$\mathrm{L}d_n(c,z,\bar{m},\theta) = \exp(-\Theta\bar{m}) \times\int_0^{\bar{m}}\exp(\Theta\bar{m}')\mathrm{L}_n(c,z,\bar{m}')d\bar{m}'.$$

For upgoing light the intensity is

$$\mathrm{R}u_2(\lambda,m,z,\mathbf{k}) = (9s^2/256\pi)\mathrm{I}_\infty\sec\theta \times\{\mathrm{A}_0\mathrm{L}u_1(c,z,m,\theta)+\mathrm{A}_1\mathrm{L}u_3(c,z,m,\theta) +\mathrm{A}_2\mathrm{L}u_5(c,z,m,\theta)\},$$

where

$$\mathrm{L}u_n(c,z,m,\theta) = \exp(-\Theta m) \times\int_0^{m}\exp(\Theta m')\mathrm{L}_n(c,z,m')dm'.$$

The integrals $\mathrm{L}d_n$ and $\mathrm{L}u_n$ are evaluated in terms of known functions in §18 of Paper I, but the expressions for them are so lengthy and elaborate as practically to preclude their numerical evaluation and discussion. Our object in this paper is to give simple approximate expressions for these integrals, for the case when Z is small.

TABLE II.

Values of $\mathrm{L}_1(\bar{m})$ for $c=0.2$, sec $s=1$.

$\bar{m}$		= 0.0	0.2	0.4	0.6	0.8	1.0
$\mathrm{L}_1(\bar{m})$	Exact =	1.97	2.40	2.51	2.48	2.31	1.89
	Approx. =	*1.98*	*2.38*	*2.55*	*2.51*	*2.28*	*1.86*
	Approx. =	(2.03)	(2.53)	(2.71)	(2.71)	(2.53)	(2.03)

IV. APPROXIMATE FORMS FOR L_n FOR SMALL Z

A. The integrated form for the function L_1 is given in §17 of Paper I. This is:

$$\mathrm{Z}e^{\mathrm{Z}\bar{m}}\mathrm{L}_1(c,z,m) = \log\{(\mathrm{Z}+c)/(\mathrm{Z}-c)\} +\mathrm{E}i\{(\mathrm{Z}-c)\bar{m}\}-\mathrm{E}i\{-(\mathrm{Z}+c)m\} +e^{\mathrm{Z}\bar{m}}\mathrm{E}j_1(c\bar{m})-e^{-\mathrm{Z}m}\mathrm{E}j_1(cm),$$

$\mathrm{E}i(x)$ and $\mathrm{E}i(-x)$ being the well-known exponential integrals.

Consider the right-hand side of the above expression for L_1, and let Z be so small that Z^2 (and, therefore, c^3) and higher powers may be neglected. Using the well-known expansions for

the exponential integrals and retaining the necessary terms, we get

$$\begin{aligned}
Ei\{(Z-c)\bar{m}\} &= \log\{(Z-c)\bar{m}\} \\
&\quad +(Z-c)\bar{m}+(Z-c)^2\bar{m}^2/4+\gamma, \\
Ei\{-(Z+c)m\} &= \log\{(Z+c)m\} \\
&\quad -(Z+c)m+(Z+c)^2m^2/4+\gamma, \\
e^{Z\bar{m}}Ej_1(c\bar{m}) &= (1+Z\bar{m}+Z^2\bar{m}^2/2) \\
&\quad \times\{-\gamma-\log(c\bar{m})+c\bar{m}-c^2\bar{m}^2/4\} \\
e^{-Zm}Ej_1(cm) &= (1-Zm+Z^2m^2/2) \\
&\quad \times\{-\gamma-\log(cm)+cm-c^2m^2/4\},
\end{aligned}$$

where γ is Euler's constant $=0.57722\cdots$.

Thus,

$$\begin{aligned}
&\log\{(Z+c)/(Z-c)\}+Ei\{(Z-c)\bar{m}\} \\
&\quad -Ei\{-(Z+c)m\} = \log(\bar{m}/m)+(Z-c)\bar{m} \\
&\qquad +(Z+c)m+(Z-c)^2\bar{m}^2/4-(Z+c)^2m^2/4
\end{aligned}$$

and

$$\begin{aligned}
&e^{Z\bar{m}}Ej_1(c\bar{m})-e^{-Zm}Ej_1(cm) = -\log(\bar{m}/m)-c \\
&\quad +\tfrac{1}{4}c^2+2\bar{m}(c-\tfrac{1}{4}c^2)+Z\{2c(\bar{m}-1)\bar{m}-(\bar{m}\log\bar{m} \\
&\quad +m\log m)-\gamma-\log c+c\}+\tfrac{1}{2}Z^2\{m^2\log m \\
&\qquad -\bar{m}^2\log\bar{m}-2\bar{m}(\gamma+\log c)+\gamma+\log c\}.
\end{aligned}$$

Hence:

$$\begin{aligned}
&Ze^{Z\bar{m}}L_1 = Z(1-\gamma-\log c)+\tfrac{1}{2}Z^2(\gamma+\log c-\tfrac{1}{2}) \\
&\quad +\tfrac{1}{2}cZ+\bar{m}\{-cZ-Z^2(\gamma+\log c-\tfrac{1}{2})\} \\
&\quad +cZ\bar{m}^2-Z(\bar{m}\log\bar{m}+m\log m) \\
&\qquad -\tfrac{1}{2}Z^2(\bar{m}^2\log\bar{m}-m^2\log m). \qquad (1)
\end{aligned}$$

We shall now replace the function $\bar{m}\log\bar{m}+m\log m$ in the interval $0\leqslant m\leqslant 1$ by an approximate expression of the form $Cm\bar{m}$. This polynomial has the same zeros as the original function, and the constant C will be chosen so that

$$\int_0^1(\bar{m}\log\bar{m}+m\log m)d\bar{m}=\int_0^1 Cm\bar{m}d\bar{m}.$$

This gives $C=-3$.

Similarly we shall put

$$\bar{m}^2\log\bar{m}-m^2\log m = Dm\bar{m}(2\bar{m}-1).$$

Again the zeros of both sides are the same and the constant D is determined as before from the equation,

$$\int_0^{\frac{1}{2}}(\bar{m}^2\log\bar{m}-m^2\log m)d\bar{m}=\int_0^{\frac{1}{2}}Dm\bar{m}(2\bar{m}-1)d\bar{m},$$

which gives $D=-0.818$ or -0.8, approximately.

That these approximations are reasonably satisfactory is born out by Table I.

It is clear that the first two functions are symmetrical about $\bar{m}=\frac{1}{2}$, while the last two are antisymmetrical about the same point, so that it is enough to stop at $\bar{m}=\frac{1}{2}$.

Introducing these approximations in (1) we get:

$$L_1(c,z,\bar{m}) = e^{-Z\bar{m}}\{a_1+b_1\bar{m}+c_1\bar{m}^2+d_1\bar{m}^3\}, \quad (2)$$

where

$$\begin{aligned}
a_1 &= 1-g+\tfrac{1}{2}c-\tfrac{1}{2}Z(\tfrac{1}{2}-g), \\
b_1 &= 3-c-Z(g-0.1), \\
c_1 &= -3+c+1.2Z, \\
d_1 &= -0.8Z,
\end{aligned}$$

and

$$g=\gamma+\log c.$$

We give now the exact values[6] of $L_1(\bar{m})$ for different values of $\bar{m}$, for the case $c=0.2$, $\sec z=1$, together with the approximate values (*in italics*) which are obtained from Eq. (2) (Table II). The values that would be obtained from Silberstein's formula[7] are also given, inside brackets, for the sake of comparison.

Table II shows that our approximation is adequate and gives numerical values in closer agreement with the exact values than those of Silberstein. Calculations carried out for other small values of c and z support the same conclusion.

B. We shall now derive an important recurrence relation, by means of which the functions L_3 and L_5 can be obtained from the function L_1 by simple integration.

TABLE III.

Values of $L_3(c,z,\bar{m})$ for $c=0.2$, $\sec z=1$.

$\bar{m}$		0.0	0.2	0.4	0.6	0.8	1.0
$L_3(\bar{m})$	Exact	0.382	0.403	0.413	0.411	0.400	0.378
	Approx.	*0.389*	*0.473*	*0.495*	*0.489*	*0.455*	*0.372*
	Approx.	(0.5)	(0.5)	(0.5)	(0.5)	(0.5)	(0.5)

TABLE IV.

Values of $L_5(c,z,\bar{m})$ for $c=0.2$, $\sec z=1$.

$\bar{m}$		0.0	0.2	0.4	0.6	0.8	1.0
$L_5(\bar{m})$	Exact	0.200	0.208	0.212	0.211	0.207	0.198
	Approx.	*0.204*	*0.248*	*0.260*	*0.256*	*0.239*	*0.195*
	Approx.	(0.25)	(0.25)	(0.25)	(0.25)	(0.25)	(0.25)

[6] For the exact values, see A. Hammad, Phil. Mag. **38**, Ser. 7, 520 (1947).

[7] L. Silberstein, J. Opt. Soc. Am. **33**, 530 (1943).

TABLE V. Exact and approximate values of $e^{\Theta}Ld_n(c,z,\bar{m}=1,\theta)$ for $c=0.2$, sec $z=1$ (*to three significant figures*).

	$e^{\Theta}Ld_1$			$e^{\Theta}Ld_3$			$e^{\Theta}Ld_5$		
sec θ	Exact	Approx.	Approx.	Exact	Approx.	Approx.	Exact	Approx.	Approx.
1	2.60	*2.60*	(2.79)	0.445	*0.513*	(0.553)	0.230	*0.269*	(0.276)
2	2.89	*2.88*	(3.11)	0.494	*0.569*	(0.615)	0.256	*0.298*	(0.307)
4	3.59	*3.58*	(3.87)	0.616	*0.707*	(0.766)	0.318	*0.370*	(0.383)
6	4.51	*4.50*	(4.88)	0.776	*0.889*	(0.967)	0.401	*0.466*	(0.483)

TABLE VI.

Values of $(A_0Ld_1+A_1Ld_3+A_2Ld_5)$.

secθ	= 1	2	4	6
Exact value	= 7.44	9.12	11.6	14.6
Approx. value	= *7.79*	*9.27*	*11.7*	*14.8*
Approx. value	= (8.34)	(10.0)	(12.7)	(16.1)

As mentioned in §111 above, the function L_n is defined by

$$L_n(c,z,\bar{m}) = \int_0^1 \exp(-Z\bar{m}')Ej_n(c\bar{m}\sim c\bar{m}')d\bar{m}'.$$

Differentiating with respect to $\bar{m}$, we get

$$\begin{aligned}(\partial L_n/\partial\bar{m}) &= \exp(-Z\bar{m})/(n-1) \\ &\quad -c\int_0^{\bar{m}} \exp(-Z\bar{m}')Ej_{n-1}(c\bar{m}-c\bar{m}')d\bar{m}' \\ &\quad -\exp(-Z\bar{m})/(n-1) \\ &\quad +c\int_{\bar{m}}^1 \exp(-Z\bar{m}')Ej_{n-1}(c\bar{m}'-c\bar{m})d\bar{m}' \\ &= -c\int_0^{\bar{m}} \exp(-Z\bar{m}')Ej_{n-1}(c\bar{m}-c\bar{m}')d\bar{m}' \\ &\quad +c\int_{\bar{m}}^1 \exp(-Z\bar{m}')Ej_{n-1}(c\bar{m}'-c\bar{m})d\bar{m}'.\end{aligned}$$

Differentiating once more, we get

$$\begin{aligned}(\partial^2 L_n/\partial\bar{m}^2) &= \{-2c/(n-2)\}\exp(-Z\bar{m}) \\ &\quad +c^2\int_0^{\bar{m}} \exp(-Z\bar{m}')Ej_{n-2}(c\bar{m}-c\bar{m}')d\bar{m}' \\ &\quad +c^2\int_{\bar{m}}^1 \exp(-Z\bar{m}')Ej_{n-2}(c\bar{m}'-c\bar{m})d\bar{m}' \\ &= \{-2c/(n-2)\}\exp(-Z\bar{m})+c^2L_{n-2}, \qquad (3)\end{aligned}$$

considering

$$[dEj_n(t)/d(t)] = -Ej_{n-1}(t), \quad n>1,$$

a relation which has been established in §15 of Paper I.

Putting $n=3$ in (3), we get

$$(\partial^2 L_3/\partial\bar{m}^2) = c^2L_1 - 2c\exp(-Z\bar{m}). \qquad (4)$$

Similarly, for $n=5$, we have

$$(\partial^2 L_5/\partial\bar{m}^2) = c^2L_3 - (\tfrac{2}{3})c\exp(-Z\bar{m}). \qquad (5)$$

Substituting for L_1 from (2) in (4) and integrating twice, we get an approximate expression for L_3. In a similar way we can get an approximate expression for L_5.

C. However, in view of the fact that L_3 and L_5 are much smaller than L_1 and since the coefficient of L_1, in the expression of secondary scattered light, is in most cases much larger than the coefficients of L_3 and L_5, it is hardly necessary to consider the approximate evaluation of L_3 and L_5 in great detail and accuracy. It is sufficient for our purpose to have simple approximate expressions for L_3 and L_5 whose numerical values are not necessarily in very close agreement with the exact values; no serious error is introduced thereby. The following consideration leads to such expressions.

As mentioned above, the function L_n is given by:

$$L_n = \int_0^1 \exp(-Z\bar{m}')Ej_n(x)d\bar{m}',$$

where x stands for $c\bar{m}\sim c\bar{m}'$. Since $0\leqslant\bar{m}'\leqslant 1$ and $0\leqslant\bar{m}\leqslant 1$, x will vary between 0 and c. Hence, the mean value $\bar{E}j_n$ of $Ej_n(x)$, in the interval $0\leqslant x\leqslant c$, is

$$\begin{aligned}\bar{E}j_n &= (1/c)\int_0^c Ej_n(x)dx \\ &= (1/c)\{(1/n)-Ej_{n+1}(c)\}. \qquad (6)\end{aligned}$$

Let us write

$$\begin{aligned}\bar{L}_n &= \int_0^1 \exp(-Z\bar{m}')\bar{E}j_n d\bar{m}' \\ &= \bar{E}j_n\int_0^1 \exp(-Z\bar{m}')d\bar{m}'.\end{aligned}$$

We shall now assume that

$$L_n/L_r=\bar{L}_n/\bar{L}_r=\{(1/n)-Ej_{n+1}(c)\}/\times\{(1/r)-Ej_{r+1}(c)\}.$$

On this assumption

$$\left.\begin{aligned}L_3(c,z,\bar{m})&=\{(\tfrac{1}{3})-Ej_4(c)\}/\times\{1-Ej_2(c)\}\cdot L_1(c,z,\bar{m})\\L_5(c,z,\bar{m})&=\{(\tfrac{1}{5})-Ej_6(c)\}/\times\{1-Ej_2(c)\}\cdot L_1(c,z,\bar{m}).\end{aligned}\right\}\quad(7)$$

That these approximations are reasonably satisfactory is borne out by Tables III and IV, where the exact values[8] of L_3, L_5 are given for the case $c=0.2$, $\sec z=1$, and are compared with their approximate values (given in *italics*) obtained from (7). Their values according to Silberstein are also included (inside brackets). It may be noted that Silberstein[9] gives

$$L_3=\tfrac{1}{2},\quad L_5=\tfrac{1}{4}.$$

V. APPROXIMATE FORMS FOR Ld_n, Lu_n

We shall now apply the approximations given in the previous article to get approximate forms for the functions Ld_n, which occur in the expression of Rd_2 (cf., §III above). A similar procedure would be followed for Lu_n in Ru_2.

As mentioned in §III above, the function Ld_n is defined by:

$$e^{\Theta\bar{m}}Ld_n(c,z,\bar{m},\theta)=\int_0^{\bar{m}}e^{\Theta\bar{m}'}L_n(c,z,\bar{m}')d\bar{m}'.$$

Thus

$$e^{\Theta\bar{m}}Ld_1(c,z,\bar{m},\theta)=\int_0^{\bar{m}}e^{\Theta\bar{m}'}L_1(c,z,\bar{m}')d\bar{m}'.$$

Replacing L_1 by the approximate expression given in (2) of §IVA, we get the following approximate form for Ld_1:

$$\begin{aligned}e^{\Theta\bar{m}}Ld_1(c,z,\bar{m},\theta)&=(e^{Q\bar{m}}/Q)\{a_1+b_1\bar{m}\\&+c_1\bar{m}^2+d_1\bar{m}^3-(1/Q)(b_1+2c_1\bar{m}+3d\bar{m}^2)\\&+(2/Q^2)(c_1+3d_1\bar{m})-(6d_1/Q^3)\}\\&-(a_1/Q)+(b_1/Q^2)-(2c_1/Q^3)+(6d_1/Q^4),\end{aligned}$$

where $Q=(\Theta-Z)$.

This gives Ld_1 at any level. At the ground, i.e., for $\bar{m}=1$ (which is the case considered by Silberstein), this reduces to

$$\begin{aligned}e^{\Theta}Ld_1(\bar{m}=1)&=(e^Q/Q)\{a_1+b_1+c_1+d_1\\&-(1/Q)(b_1+2c_1+3d_1)+(2/Q^2)(c_1+3d_1)\\&-(6d_1/Q^3)\}-(a_1/Q)+(b_1/Q^2)\\&-(2c_1/Q^3)+(6d_1/Q^4).\end{aligned}$$

A glance at page 531 of Silberstein's paper suffices to show that the above approximate expression for Ld_1 is simpler and less elaborate to evaluate than that given by Silberstein.

Similarly, on replacing L_3 and L_5 by the approximate expressions given in (7) of §IVC we get the following approximate forms for Ld_3 and Ld_5, which are obtained from Ld_1 through the multiplication by two factors independent of z, $\bar{m}$, or θ.

$$\begin{aligned}Ld_3(c,z,\bar{m},\theta)&=\{(\tfrac{1}{3})-Ej_4(c)\}/\times\{1-Ej_2(c)\}\cdot Ld_1(c,z,\bar{m},\theta),\\Ld_5(c,z,\bar{m},\theta)&=\{(\tfrac{1}{5})-Ej_6(c)\}/\times\{1-Ej_2(c)\}\cdot Ld_1(c,z,\bar{m},\theta).\end{aligned}$$

It may be noted here that Silberstein gives:

$$Ld_3=e^{-\Theta\bar{m}}\int_0^{\bar{m}}e^{\Theta\bar{m}'}\tfrac{1}{2}d\bar{m}'=(1-e^{-\Theta\bar{m}})/2\Theta,$$

and

$$Ld_5=(1-e^{-\Theta\bar{m}})/4\Theta.$$

In Table V we have given the exact values[10] of

$$e^{\Theta\bar{m}}(Ld_1,\ Ld_3,\ Ld_5)$$

at ground level, for the case $c=0.2$, $\sec z=1$, $\sec\theta=1$, 2, 4, 6, together with the approximate values according to the formulas of this article (given in *italics*); the values that would be obtained from Silberstein's formulas are also included, inside brackets, for the sake of comparison.

It appears from Table V that our approximation gives numerical values in closer agreement with the exact values than those of Silberstein.

To form an idea about the effect of such approximations on the intensity of secondary scattered light received at the ground from different directions, we give in Table VI the exact and approximate values of

$$(A_0Ld_1+A_1Ld_3+A_2Ld_5),$$

[8] For the exact values, see A. Hammad, Phil. Mag. **38**, Ser. 7, 521 (1947).

[9] L. Silberstein, J. Opt. Soc. Am. **33**, 530 (1943).

[10] For the exact values, see A. Hammad, Phil. Mag. **38**, Ser. 7, 527 (1947).

for the case $c=0.2$, $\sec z=1$, $\bar{m}=1$. In this table, the approximate values according to Silberstein's formulae are given inside brackets, and those according to our formulas are given in *italics*.

It is interesting to note that, except for the case $\sec\theta=1$, the error in our estimation ranges between 1 and 2 percent of the exact value; in the case $\sec\theta=1$, however, the error is higher, being equal to five percent of the exact value. The reason for this is that in the case $\sec\theta=1$, $\sec z=1$, the coefficients A_1, A_2 are as large as A_0 (in fact, $A_1>A_0$ in this case), so that the inaccuracies in Ld_3, Ld_5, arising from the inaccuracies in L_3, L_5 (cf. §IVC), will have an appreciable effect on the values of $(A_0Ld_1+A_1Ld_3+A_2Ld_5)$. For $\sec\theta>1$ (or $\sec z>1$), on the other hand, A_0 is larger than both A_1 and A_2, so that the inaccuracies in Ld_3, Ld_5 will not give rise to large error in the final result. In the case of Silberstein's formulas, this table indicates that the error ranges between 9 and 12 percent of the exact values.

VI. CONCLUSION

In the preceding investigation, simple approximate expressions are derived for the functions L_n when c and z are small, corresponding to weak attenuation of radiation and high solar altitudes. With the help of these expressions, the intensity of secondary scattered light received at any level can be easily evaluated within close limits. The expressions given in this paper are compared with those given by Silberstein and are found to be more adequate.

The question of the relative magnitudes of the different orders of scattering has been discussed elsewhere.[11] The results obtained indicate that the contribution of secondary scattering, compared to that of the primary, increases as c increases, being negligibly small for small values of c, especially when the sun is high. For large values of c, the contribution of secondary scattering is comparable to that of the primary, particularly when the sun is low. For these latter cases, simple approximate expressions for the intensity of secondary scattered light are really very desirable. In a forthcoming paper, we shall show that for all wave-lengths and all directions of incidence of the solar beam the elaborate exact expressions of the functions L_n can be replaced by simple approximate ones of the form:

$$A_ne^{p_n\bar{m}}+B_ne^{-p_n\bar{m}}+C_ne^{-z\bar{m}},$$

where p_n, C_n are derived analytically, and A_n, B_n are determined by numerical methods. Such forms for L_n facilitate the evaluation of secondary scattered light and render the estimation of tertiary scattered light possible.

ACKNOWLEDGMENT

I wish to express my gratitude to Mr. M. S. El Mohandis, Astronomy Department, Faculty of Science, Cairo, for the help I have received from him in the preparation of the numerical part of this work.

[11] A. Hammad, Phil. Mag. **38**, Ser. 7, 515 (1947).

An Improved Jamin Interferometer

J. B. HAWKES AND R. W. ASTHEIMER
Stevens Institute of Technology, Hoboken, New Jersey

(Received January 26, 1948)

For the purpose of studying anomalies in the index-temperature relation of transparent liquids, a Jamin interferometer has been developed using special control equipment for accurate constant-rate temperature variation. Simultaneous recording of optical and thermal changes are made on a constant speed paper tape. An estimated precision of 0.7×10^{-6} index units per °C is to be compared with an actual reproducibility of 1 to 2×10^{-6} index units per °C.

INTRODUCTION

IN general, small anomalies in a function are more obvious in the first derivative than they are in the function itself. Thus if the refractive index, n, of a material is a function of temperature, T, the slope, dn/dT, will be more affected by irregular behavior than will the index n. For the direct measurement of dn/dT, the Jamin interferometer[1] is well adapted. It has been used several times in the past for the direct measurement of dn/dT, and, hence indirectly for n as a function of T, once by Jamin himself[1] and somewhat later by Lorenz.[2] With modern methods, the control of temperature can be greatly improved over that in the earlier investigations, and the precision of the method thereby significantly increased. The apparatus to be described was designed for the study of refractive index in transparent liquids, over the range −70°C to +50°C, limits which can easily be extended.

THE OPTICAL SYSTEM

The Jamin interferometer employs two parallel mirrors, M and M', Fig. 1, at about 45° with the axis of the test specimen. Parallel light from a sodium arc, condensed on a pin hole, and then made parallel by a positive lens, falls on the first mirror, M, at A.

The surface, AC, is partially silvered while the back surface, B, is fully silvered. Front and back reflections are formed which travel through equal distances to the second mirror M' (identical with M), where several front and back reflections take place. Only the reflections shown are useful, all others being stopped out and discarded. At C' the desired beams are recombined so that a set of interference fringes appear in the telescope.

If two identical optical specimens are placed in the two paths, as shown (Fig. 1), the fringe pattern will not be affected. However, a continuous change in the index of the "test" specimen (with the other specimen unchanged) will produce a corresponding steady drift of fringes across the field of the telescope. The number of fringes passing is equal to the change of the number of waves of sodium light in the test path. Other effects not being present, this is proportional to the change in index of the "test" material.

In the present instrument, the mirrors are 1" thick by 2" square. The glass has a refractive index 1.50. The mirror faces are plane-parallel to within two wave-lengths of sodium light. The front surface is aluminized for approximately 35 percent reflection, the back surface for full reflection. For adjustment the mirrors may be rotated independently about a vertical and about a horizontal axis, each in the plane of the mirror.

CELL CONSTRUCTION

The cells in the two paths, are each 20 cm long. The specimen space is about 3 mm in diameter and surrounded for its full length by a jacket space, 3 mm in radial thickness. The longitudinal section through a cell is shown in Fig. 2. The ends of the specimen space are closed by windows of thin microscope-cover-glass, attached with sealing wax. It is expected that other methods of attachment will have to be used, because of the possibility of the sealing wax's contaminating the test liquid. (So far, water has shown no evidence of such contamination.) The jacket is filled with rapidly flowing liquid of known, con-

[1] J. Jamin, Comptes Rendus **43**, 1193 (1856).
[2] L. Lorenz, Kgl. Danske Vid. Silskab **5**, No. 8, 220 (1869).

trolled, temperature. The comparison cell jacket contains water of fixed temperature; the test cell jacket contains methanol at a known temperature. This temperature can be varied at a predetermined steady rate. The axial flow of the jacket liquid is at such a velocity that the axial thermal gradient in the specimen is negligible.

CELL SUPPORTS

The cell windows may be cemented to the ends of the cells in approximately parallel planes without undue difficulty. On the other hand, it is unlikely that the windows can be attached normal to the axis of the cell with adequate precision. It is necessary, therefore, to locate and orient the cells in the interferometer by means of adjustable mounts. Highly precise micrometer adjustments are unnecessary for this purpose, the adjustable Vee shown in Fig. 3 being quite adequate. The cell is raised by narrowing the Vee; its lateral position is changed by horizontal motion of the Vee. Two such adjustable saddles are provided for the test cell —one near each end of the cell. One adjustable saddle and one fixed saddle are provided for the comparison cell (Fig. 4).

In practice the comparison cell is first aligned (mirror M' removed) with the beam AA' (Fig. 1) by means of the single adjustable saddle and the adjustment of mirror M. Next the test cell is aligned with beam CC', after which the two beams are merged by successive alternate adjustments of the test cell and of the mirror M'. The final adjustment to procure fringes is usually made by small angular adjustments of mirror M' about its vertical axis, until weak fringes are found. Thereafter the fringe contrast is improved, and the fringes broadened by small successive adjustments of M' about the horizontal and the vertical axes.

THE CIRCULATING SYSTEM

The function of the comparison cell is that of "compensator," so that as long as the refractive index of the contained liquid is constant, the precise value is unimportant. Contamination is consequently not a vital element, and the cell is therefore made of brass, soft soldered at the joints. It is important that the refractive index does not change appreciably during a run and the cell is therefore filled with distilled water kept at a constant temperature (± 0.1°C) between 0.5°C and 1°C, by means of jacket water, cooled by a mechanical refrigerating system (a modified drinking fountain) and circulated by a small rotary gear pump. The temperature of the cooling water is indicated by a mercury thermometer in a well on the inlet side of the comparison cell; the temperature is held constant (± 0.1°C) by adjusting the expansion valve on the refrigerator to a setting giving the proper temperature for the working conditions at the time. Since the thermal coefficient of index for water is small at 0°C, this insures substantially constant index in the comparison cell liquid, and sensitive thermostating is therefore not required. Evaporation of water and absorption of CO_2 from the air is reduced to a minimum by filling the cell to the tops of the filler tubes with freshly distilled water and sealing the tubes.

The test cell, on the other hand, requires much more careful treatment. It is of laboratory Pyrex, of the same form and dimensions as the comparison cell, but cooled with methanol circulated by a small centrifugal pump immersed in a wide-mouthed gallon thermos jug. The methanol is circulated at the rate of about two gallons per minute, which gives a flow velocity of something like 200 cm/sec. through the cell jacket. This high velocity and consequent short time of

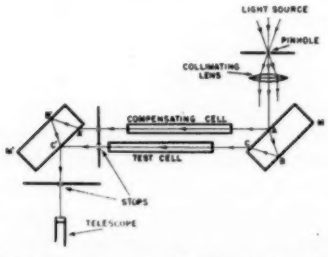

FIG. 1. Diabrammatic sketch of Jamin interferometer.

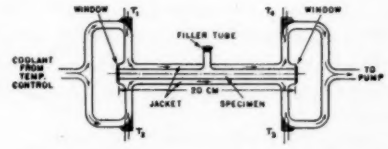

FIG. 2. Section through specimen cell.

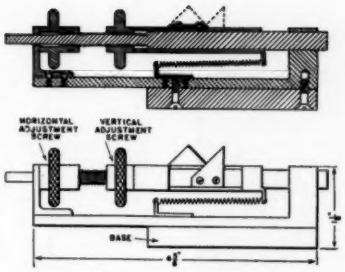

FIG. 3. Assembly drawing of adjustable Vee mount.

passage through the jacket reduces the axial temperature difference in the cell to a small figure. The true jacket temperature can safely be considered as the average of inlet and outlet temperatures.

This average jacket temperature is read directly as the total thermal voltage of four copper-constantan thermocouples in series, arranged as T_1, T_2, T_3, and T_4 in Fig. 2 and Fig. 4. The corresponding four cold junctions are in an ice bath in a wide-mouthed pint thermos jug, as shown in Figs. 4 and 5. Electrolytic voltages and other spurious effects at the cold junctions are eliminated by placing each junction in a thin-walled closed glass tube in which a drop of glycerine has been placed to give good thermal contact.

The thermocouples are connected to a Leeds and Northrup Type *K* potentiometer, for measurement of the thermal voltages. The schematic diagram is shown in Fig. 4. The reversing switch is used in case cell temperatures above and below 0°C are to be used in the same run. For example, water in the test cell might be studied under super-cooled conditions.

TEMPERATURE CONTROL OF TEST CELL

The test-cell temperature is controlled by a pair of photo-cells, 15 ft. away from the Leeds and Northrup Type *R* galvanometer. The reflected light-spot from the galvanometer mirror operates the photo-cells, which in turn drive a locking-relay circuit through a balanced amplifier as shown in Fig. 6a. The locking feature insures proper control of heating current in case a sudden disturbance causes the galvanometer spot to swing completely off the photo-cells.

The drum of the potentiometer can be driven

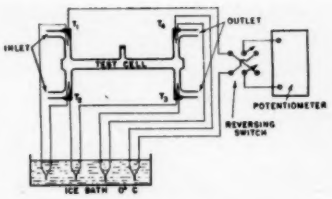

FIG. 4. Thermo couple circuit.

at a constant speed by a motor, thus changing at a uniform rate the cell temperature required to balance the potentiometer circuit. The photo-cell, through the thermostat circuit, controls the heating current so as to keep the potentiometer balanced; the test-cell temperature thus follows the potentiometer setting. The potentiometer drum is driven by a continuously adjustable variable-speed friction drive (see Fig. 7) capable of a maximum speed of ± 4 revolutions per hour (Figs. 6 and 7). The temperature of the test cell may thus be changed at any desired rate between -28°C and $+28$°C per hour.

The photo-cell relays (Fig. 6b) control an incremental heating current superimposed on a steady background current adjusted to be a trifle less than enough to counterbalance the cooling from the cooling coils and mixing valve. The amount of cooling is controlled by a manually adjusted mixing valve; the "background" heating current is controlled by means of a Variac. The "incremental" heating current is adjusted by a variable resistor shunting the contact of the power relay. The Variac, mixing valve, and heating coil (in well), are shown in Fig. 5.

The cooling coils are immersed in a wide-mouthed gallon thermos jug, shown in Fig. 5. The mixing valve, which is also indicated in the same view, is driven through a flexible shaft from a dial on the same panel as the Variac. The mixing valve is a pair of needle valves geared together, so that the opening of a shunt path *across* the cooling coils is accompanied by a simultaneous closing of the path through the cooling coils. This is shown diagrammatically in Fig. 8.

VESTIBULES

Condensation of moisture on cell windows (when operating below the dew point) destroys

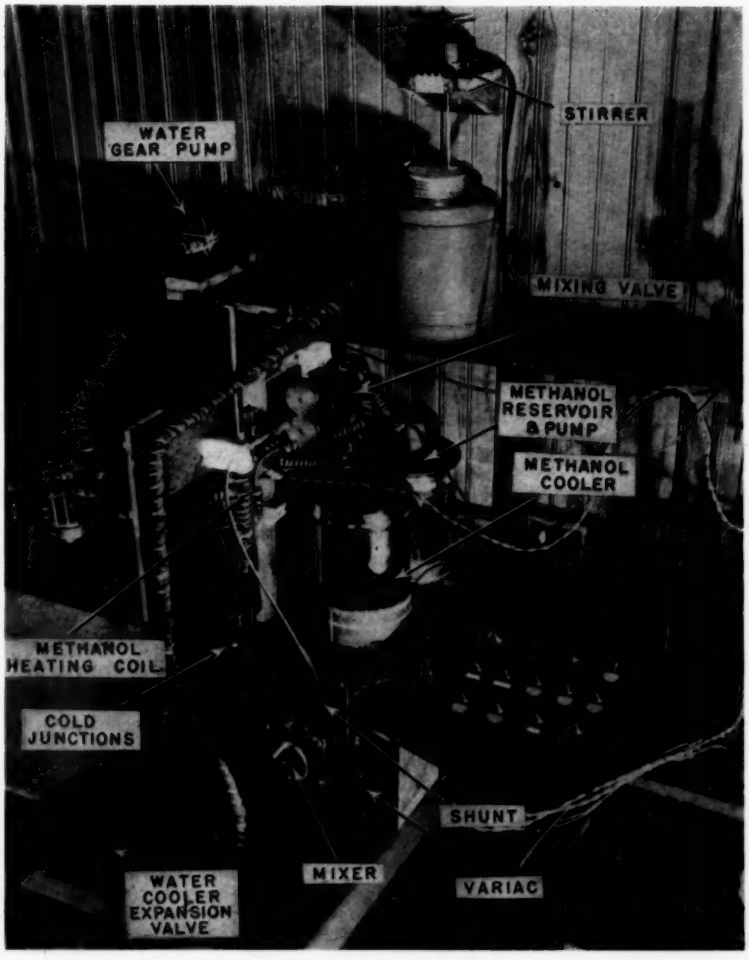

FIG. 5. General view of temperature control apparatus.

the fringe pattern. Such condensation is avoided by the provision before each window of a vestibule fed with dried air or other gas.[3] The vestibule has an opening (for the light beam and for the escape of dry gas) opposite the glass window of the cell. Sufficient flow of dry gas (in the present case CO_2 from dry ice in a small thermos bottle) is provided to sweep away all moisture from before the windows. No correction need be made for the refractive effect of CO_2 replacing air in the vestibules. Since the technique is used in both cells, the effects cancel. Erratic disturbances caused by puffs of CO_2 are not noticeable provided the cold dry-ice vapor is warmed to room temperature before reaching the vestibules and the flow rate is kept as low as possible, but still greater than the diffusion rate of water vapor toward the window.

[3] J. B. Hawkes, Phys. Rev. **53**, 84 (1938).

TAPE RECORDER

To get a continuous set of values of dn/dT at all temperatures in the course of a run, a continuous simultaneous record should be made of temperature, fringe shift, and, if possible, time. This is done by means of a constant-speed paper tape on which are recorded each 50 microvolts of thermocouple voltage change, and each fringe passing under the cross hairs of the telescope.

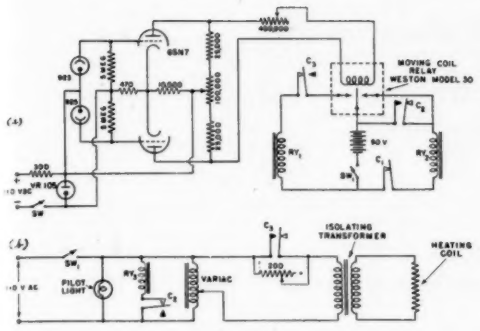

FIG. 6. (a) Photo-cells balanced amplifier, and micro relay; (b) heating control circuit.

The paper is driven by an a.c. clock motor at a linear speed of 3 inches per minute. Time is indicated on the paper tape by punch-marks made every half-minute by projecting pins on the driving drum. The recorder is at the right in Fig. 7.

The changes in thermocouple voltage are recorded as pips on an ink line drawn by a stylus attached to the clapper-arm of an electric door-bell movement. The potentiometer observer taps a key every 50 microvolts (or other suitable interval), thus producing a jog or pip in the microvolt trace. A similar key and stylus on the same paper tape is used by the fringe observer. Ordinarily one pip is given per fringe passing, although other intervals may be better at very high or very low rates of fringe travel. A sample tape record is shown in Fig. 9.

It is found that the on-off cycle of the heating thermostat introduces small fluctuations in the rate of fringe travel. These fluctuations are periodic and not cumulative, so that by taking the fringes per microvolt over a sufficiently large increment in microvolts, this periodic disturbance can be eliminated. The period of the thermostat is about 10 to 15 seconds. Since at the fastest rate of temperature change, a change of 100 μv requires 90 seconds, about 5 or more thermostat cycles are averaged if "fringes/100 μv" are taken as the standard reading for determination of dn/dT.

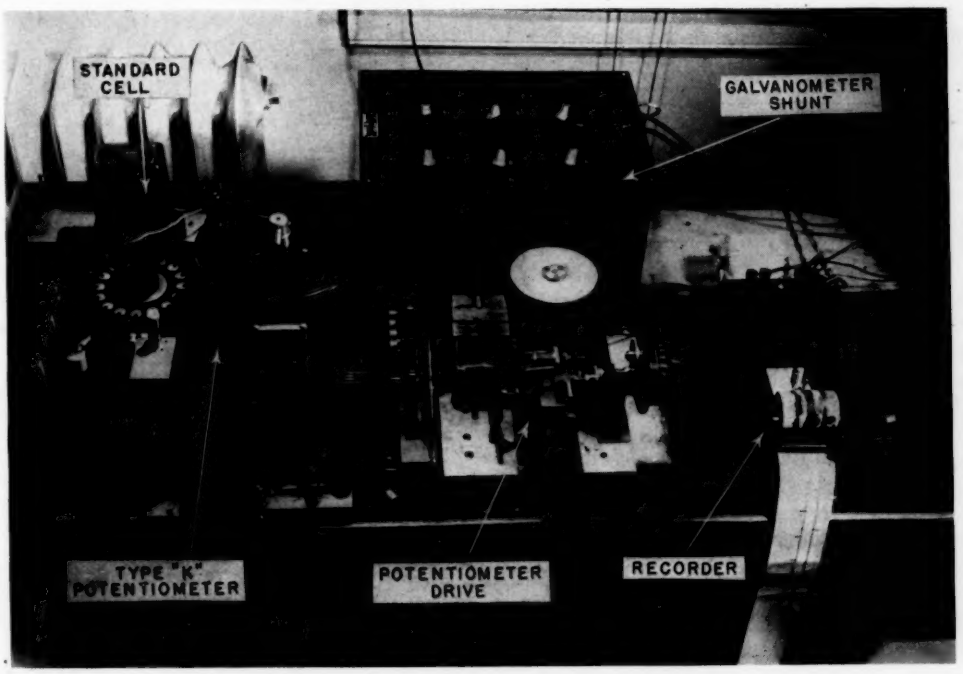

FIG. 7. Potentiometer with friction drive. Tape recorder at right.

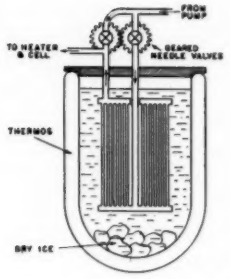

FIG. 8. Sectional view of muthanoe cooler and mixing valves.

PRECISION

The fundamental relation for the number, N, of waves of light in length L of the test path, containing a cell of length, l, in which is a liquid of index n_l, is:

$$N=\frac{ln_l}{\lambda_0}+\frac{(L-l)n_a}{\lambda_0}, \tag{1}$$

where n_a is the index for air, and λ_0 is the vacuum wave-length of the light employed. The number of fringes passing the cross hairs per degree temperature change in the test cell is:

$$\frac{dN}{dT}=\frac{n_l}{\lambda_0}\frac{dl}{dT}+\frac{l}{\lambda_0}\frac{dn_l}{dT}+\frac{n_a}{\lambda_0}\frac{dL}{dT}-\frac{n_a}{\lambda_0}\frac{dl}{dT},$$

or

$$\frac{dN}{dT}=\frac{n_l-n_a}{\lambda_0}\frac{dl}{dT}+\frac{n_a}{\lambda_0}\frac{dL}{dT}+\frac{l}{\lambda_0}\frac{dn_l}{dT}. \tag{2}$$

The term $[(n_l-n_a/\lambda_0)(dl/dT)]$ is due to the thermal expansion of the cell itself. The second term on the right, $[(n_a/\lambda_0)(dL/dT)]$, is due to relative change in distance between mirrors M and M', caused by warping of the interferometer. This term has been investigated and found too small to measure over the range from 0°C to 28°C. The last term on the right, $[(l/\lambda_0)\times(dn_l/dT)]$, contains the quantity under investigation. Solving (2) for dn_l/dT:

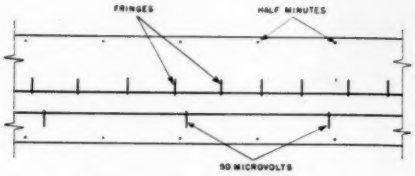

FIG. 9. Typical appearance of recorder tape.

$$\frac{dn_l}{dT}=\frac{\lambda_0}{l}\frac{dN}{dT}-\frac{1}{l}\frac{dl}{dT}(n_l-n_a), \tag{3}$$

where $(1/l)(dl/dT)=\alpha$, the thermal coefficient of linear expansion of the cell. A direct measurement of α on the Pyrex cell was made under working conditions by interferometer methods; a value of $(3.5\pm0.1)\times10^{-6}$ per °C was found.

The wave-length, λ_0, is 5893×10^{-8} cm with negligible error; l is (20 ± 0.01) cm; dN/dT at room temperature is about $(20\pm0.2)fr/$°C, and is negative. From these values dn_l/dT would be

$$\begin{aligned}dn_l/dT&=-5893\times10^{-8}-(3.5\times10^{-6})(0.333)\\&=-58.93\times10^{-6}-1.17\times10^{-6}\\&=-60.10\times10^{-6}\pm1.1\text{ percent},\end{aligned}$$

or

$$dn_l/dT=-(60.1\pm0.7)\times10^{-6}(\text{index units/°C}).$$

This is to be compared with an observed reproducibility of results of $\pm1\times10^{-6}$ per °C in the 0°C to 15°C range, and of $\pm2\times10^{-6}$ per °C in the 15°C to 30°C range.

The best comparable figures for the errors in *direct* measurements from other observers[4] who have used a liquid prism, are of the order of $\pm1\times10^{-5}$ index units per °C.

This work has been supported in part by the Office of Naval Research under contract N6onr-247 Task Order I, Project NR, 032-102.

[4] Tilton and Taylor, J. Research Nat. Bur. Stand. 20, 419 (1938).

An Improvement of Savart's Polariscope

M. RICHARTZ
Fu-Jen University, Peiping, China
(Received May 23, 1946)

INTRODUCTION

THE manifold use of Savart's polariscope in different branches of Natural Sciences (physics, chemistry, meteorology, astronomy) could lead to the assumption that Savart's apparatus had already reached the point of perfection. That, however, appears not to be the case; for so far as I am acquainted with publications already made on the subject, there still is room for betterment. In the following I propose to show a method of improving the Savart polariscope.

USE OF SAVART'S PLATE

Savart's polariscope is a combination of the so-called Savart's plate with an analyzer. The plate consists of two thin plates of Iceland spar (or quartz), cut at an angle of about 45° to the optic axis, and cemented together face to face so that their principal sections are at right angles (Fig. 1). It is attached to an analyzing Nicol in such a manner that the bisector of the angle between the principal sections of its two halves is parallel to that of the analyzer. This arrangement serves to detect small amounts of polarization as well as to determine the direction of vibration of polarized light.

In both cases the principal procedure is as follows: let a parallel (or slightly convergent) beam of monochromatic, polarized light traverse the Savart plate first, and then the analyzer. The field of view then, in general, is crossed by a series of parallel interference fringes. As the polariscope rotates, the fringes disappear in the center of the field of view when the direction of vibration of the incident light is parallel to the principal section of either half of the Savart plate. During one rotation four such positions occur, called "zero positions." On the other hand, when the direction of the incident polarized vibration is perpendicular (or parallel) to that of the analyzer, the fringes appear distinct. When white polarized light is incident, the field of view shows a central dark (or bright) fringe; the other fringes are colored. Thus by measuring the zero positions one can determine the plane of polarization of a polarized light beam.

For this purpose Savart's polariscope has been employed in polarimetry (Wild's polarimeter) as well as in measurements of scattering (especially of skylight: determination of the plane of polarization and of the positions of the neutral points). Satisfactory results depend upon the accuracy of determining the above-mentioned zero positions.

Two methods for finding these positions are generally in use. The first method observes the disappearance of the fringes in the central part of the field of view, when the polariscope rotates. If, however, the amount of polarized light present in the beam under consideration is very small, the fringes are weak and the background is relatively bright. In this case it is rather difficult to observe the disappearance of the fringes, and the first method is not very satisfactory.

The second method observes the change of the fringes from dark to bright, and vice versa, during rotation. It needs some fixed point or line in the field of view in order to mark the central fringe and to observe easily this change. Figure 2 gives the arrangement of this method. The polariscope mounting contains not only the

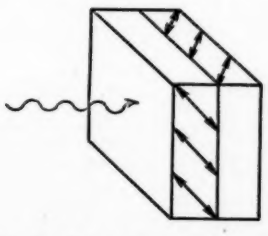

FIG. 1. Double headed arrow—direction of optic axis; curved arrow—direction of incident light.

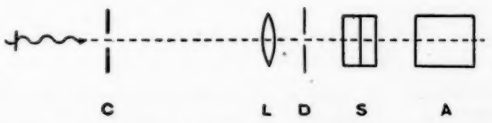

FIG. 2. Improved arrangement.

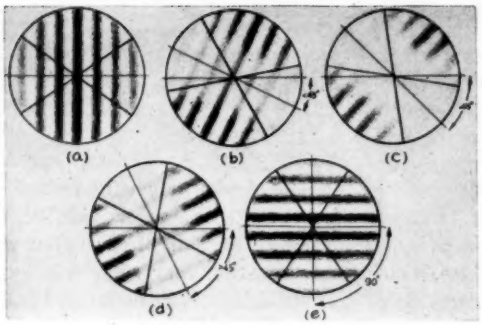

FIG. 3. Field of view (Method A).

analyzer A and the Savart plate S, but also a diaphragm D, a converging lens L, and cross-wires C. The cross-wires are placed at such a distance from the lens that they appear distinct in the field of view.

Figure 3 shows the field of view during a quarter rotation. Starting from the position where the fringes are distinct and the central fringe is dark (Fig. 3 (a)), the polariscope is rotated, say to the right, less than 45°. During this rotation the fringes in the central part become fainter than at the boundary; at the same time they shift to one side (Fig. 3 (b)). When the rotation reaches the angle of 45°, the fringes in the central part disappear (Fig. 3 (c)); but the remaining fringes seem to jump to the other side. During further rotation the fringes reappear, whereas the central fringe now is bright (Fig. 3 (d)). When the rotation reaches 90°, the bright fringe is back in the center of the field of view (Fig. 3 (e)).

IMPROVEMENT

Two reasons must be mentioned why also the second arrangement is not quite satisfactory. When cross-wires are used to mark the central fringe, the crucial point being far away from the fringe in the zero position (see Fig. 3 (c)), a motion of the fringe with respect to this point cannot be well observed. That may be avoided by using a fixed line which bisects the field of view. But there is still another reason for seeking a more suitable device. The Savart fringes are, according to theory, curves of constant phase difference which are parts of equilateral hyperbolae. The center of these hyperbolae, however, does not coincide with that of the field of view. Therefore the central fringe cannot be kept in the center during rotation. New adjustments are always needed, or, what is better, the central fringe should be placed so that during rotation its position is kept with respect to the center. In the latter case the fixed line should be shifted until it coincides with the central fringe.

To avoid these difficulties the cross-wires (or the line) have been replaced by a crystalline plate with a rectangular opening in the center. The boundaries of the long side of the opening, which are arranged perpendicular to the fringes, should be as sharp as possible. Therefore a simple sheet of Cellophane is suitable, because it can be easily cut. The cut should be made so that in the zero positions the fringes within the Cellophane plate remain distinct while the opening is free of fringes. That is, in general, the case when a principal direction of vibration of the plate is parallel to the long sides of the rectangle. Then the incident polarized light having traversed the plate is elliptically polarized in the zero positions. When monochromatic light is incident, as for instance in determining rotatory power, a quarter-wave plate of the wave-length used is most favorable, because the light then becomes circularly polarized and the fringes within the plate have almost the same intensity during rotation.

With this new device the Savart polariscope shows a field of view as drawn in Fig. 4 (a) to (e). The positions of the apparatus correspond to those due to Fig. 3 (a) to (e). The fringes in Fig. 4 (a) and (e) appear as if there were no

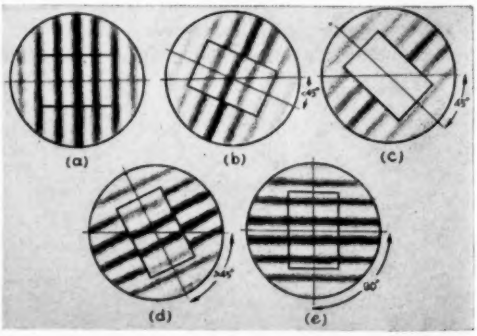

FIG. 4. Field of view (Method B).

TABLE I. Readings of the zero positions with the ordinary polariscope.

R	11° 35′	101° 26′	191° 34′	281° 31′
	38	32	35	32
	37	34	30	36
	39	35	39	36
	31	37	39	28
L	11° 30′	101° 20′	191° 29′	281° 20′
	25	19	20	25
	21	21	23	23
	24	22	28	27
	30	26	25	21
Mean:	11° 31′	101° 27′.2	191° 30′.2	281° 27′.9

TABLE II. Readings of the zero positions with the new device.

R	11° 32′	101° 32′	191° 34′	281° 29′
	39	28	37	33
	36	33	37	30
	36	29	33	32
	31	29	35	29
L	11° 28′	101° 27′	191° 31′	281° 22′
	30	24	29	26
	31	27	30	28
	28	27	29	27
	29	24	30	26
Mean:	11° 32′	101° 28′	191° 32′.5	281° 28′.2

crystalline plate; this is because the plate does not influence the state of polarization when a principal direction of vibration within the plate coincides with that of the incident polarized light. In Fig. 4 (b) and (d) the fringes have been moved, these within the opening to one side, those within the plate to the other. In the position of 45° no fringes are within the central part of the opening; near the boundaries weak fringes (not drawn in Fig. 4 (c)) jump back to the other side. This turning moment can be very well observed. It gives the zero position, the reading of which is to be determined.

ACCURACY

The measurements made by means of this new device were carried out under wartime conditions.[1] Thus the results are not very accurate, but are much better than those obtained with the simple polariscope. The probable error, in general, was less than 1′, while in using the simple arrangement it was about 1.5′ under the same conditions (observer, graduated circle for readings, amount of partially polarized light). This may be seen from Tables I and II which give a series of measurements, namely, the readings during ten rotations, I without the new device (field of view as Fig. 3), II with it (field of view as Fig. 4). The plane of polarization of skylight was determined by taking the readings of the zero positions. During the first five rotations the apparatus was rotated to the right (*R*), while the other five rotations were made to the left (*L*).

This new arrangement, therefore, is obviously an improvement of Savart's polariscope. When applied in measurements of the polarization of skylight, it can serve to determine more accurately the plane of polarization and the positions of the neutral points. Moreover, it seems to me that the improvement will be an advantage to Wild's polarimeter.

[1] This method was applied for the thesis: "Determination of the plane of polarization of skylight" by Mr. Chang Li-chung, May 1943.

JOURNAL OF THE OPTICAL SOCIETY OF AMERICA VOLUME 38, NUMBER 7 JULY, 1948

A Comparative Study of Five Tests of Color Vision

ALPHONSE CHAPANIS*
*Department of Psychology, The Johns Hopkins University, Baltimore, Maryland***
(Received February 3, 1948)

One hundred and twenty men were tested with 5 pseudo-isochromatic tests of color vision, the American Optical Company, Ishihara, Meyrowitz, Boström, and Boström-Kugelberg tests, and with the Royal Canadian Navy color vision test lantern. The results obtained on the lantern were used to classify the subjects into two groups: color normal (86 men) and color deficient (34 men). The criterion of color deficiency used in this study, i.e., one or more errors on the RCN lantern, was found to correlate highly with the total number of plates read correctly on the five pseudo-isochromatic tests.

Each of the pseudo-isochromatic tests was evaluated as a whole, and plate-by-plate, in terms of its efficiency for separating the color normal from the color deficient. It was found that the Boström-Kugelberg test is by far the best all-around test of color deficiency evaluated in this experiment. The Ishihara test is next best. Although the AO test differentiates clearly between the color normal and color deficient, many of the plates are individually non-diagnostic. The Boström and Meyrowitz plates are, in general, unsatisfactory.

Incidental findings show that neither visual acuity nor age is related to performance on the tests used in this experiment.

I. INTRODUCTION

BECAUSE of their simplicity and great convenience, pseudo-isochromatic tests for the detection of color vision defects have been, and probably will continue to be, used extensively. They are compact, can be administered rapidly, and require little apparatus or training of examiners. That tests of this sort contain serious defects, however, has been amply demonstrated by the experience of testers in the armed services who administered them to many thousands of individuals during the war. This awareness has led to a series of research programs aimed at the evaluation of color vision tests in terms of their efficiency for detecting color vision defects. Three large programs of this sort have been carried out recently: by Sloan at the Army Air Forces School of Aviation Medicine (32), by Hardy, Rand, and Rittler at the Institute of Ophthalmology, College of Physicians and Surgeons of Columbia University (13 to 17), and by several investigators in Naval laboratories (7, 29, 30, 33). Individual studies have also been reported recently by Foster (8), Gallagher *et al.* (9), Neubert (26), Philip (27), and Thomas (35).

The present paper reports another experiment in this general area. It compares the following five pseudo-isochromatic tests of color vision:

1. *Pseudo-Isochromatic Plates for Testing Color Perception.* Engraved and printed by the Beck Engraving Company, Inc., New York, 1940. Distributed by the American Optical Company, Southbridge, Massachusetts.
2. S. Ishihara: *Tests for Colour-Blindness* (9th Edition). Printed by Kanehara and Company, Tokyo, 1940. Distributed by the C. H. Stoelting Company, Chicago, Illinois.
3. *Pseudo-Isochromatic Plates for Testing Color Perception* (American Edition). Published by the E. B. Meyrowitz Surgical Instruments Company, Inc., New York, 1940.
4. C. G. Boström: *Tabulae Pseudo-Isochromaticae: Tavlor för Utrönande av Rubbningar i Färgsinnet.* Printed by Kifa, Stockholm, 1935. Distributed by the Nordiska Bokhandeln, Stockholm.
5. C. G. Boström and I. Kugelberg: *Tabulae Pseudo-Isochromaticae: Tavlor för Färgsinnesprövning.* Printed by Kifa, Stockholm, 1944. Distributed by the Nordiska Bokhandeln, Stockholm.

Two of these tests, the American Optical Company (AO) and Ishihara, have already been subjected to critical scrutiny in a number of experiments (7, 8, 9, 13, 14, 16, 17, 26, 27, 29, 30, 32, 33, and 35). Three of them, the Meyrowitz, Boström, and Boström-Kugelberg tests, have apparently never been evaluated.

The subjects in this experiment were also tested with the Royal Canadian Navy color vision test lantern (hereafter referred to as the RCN lantern). This lantern requires the examinee to identify pairs of colored lights similar to those used for signaling purposes. Since a common objection to pseudo-isochromatic tests is that they measure no realistic aspect of color vision, the results obtained on this lantern con-

* The writer is indebted to Mrs. Mary Hall, engineering aide, for her invaluable assistance in this study.
** The data of this study were collected while the author was Captain, Air Corps, in the Aero Medical Laboratory, Air Materiel Command, Wright Field, Dayton, Ohio.

stitute one of the criteria against which the efficiency of the chart tests is assayed in this experiment.

II. SUBJECTS, TESTS, APPARATUS, AND GENERAL PROCEDURES

Subjects

The subjects of this experiment were 120 men selected from civilian and military personnel at Wright Field. Of these, 86 were color normal and 34 color deficient according to criteria to be discussed later. This proportion of color deficient to color normal men is obviously not the result of random selection, since an effort was made to secure a large number of color deficient men for this experiment. The color normal men ranged from 19 to 40 years in age, with an average age of 27.3 years. The color deficient ranged from 18 to 35 years in age, with an average age of 26.5 years.

Visual acuity for all subjects was tested with the American Optical Company Project-o-chart at a distance of twenty feet. Measurements were made for each eye singly and for both eyes together, both with and without correction for those individuals who wore glasses. For the latter group of subjects, the amount and type of correction was measured. Twenty-two (26 percent) of the color normal and nine (26 percent) of the color deficient wore glasses. Binocular visual acuities ranged from 20/10 to 20/50 (corrected visual acuity is meant here in the case of those subjects who wore correction). There were no significant correlations between corrected visual acuity and performance on the color vision tests in this experiment. This finding will be discussed in greater detail in a later section.

Those color deficient subjects whose defect might possibly have been due to injury or disease were eliminated from this experiment. Only subjects whose previous medical history suggested a congenital type of color defect were used.

The Tests

The AO, Ishihara, and Meyrowitz Tests

Very little originality has been shown in the development of pseudo-isochromatic tests in the last twenty years. Most of them depend on principles which were used in the early Stilling and Ishihara tests and, in some cases, plates have been borrowed from these early tests. Table I shows the plates which are common to the AO, Ishihara, Meyrowitz, and 19th edition of the Stilling*** tests. Even though these appear to be

TABLE I. Equivalent plates in the American Optical Company, Ishihara, Meyrowitz, and Stilling tests of color vision.

AO plates	Ishihara plates	Meyrowitz plates	Stilling plates**
1			20
2		8	16
3			18
5	2		
6	3		
8			12
9			14
11	4		
12	5		
13		4	8
15			7
16		1	1
17			15
18		3	19
19	6		
20	7		
22			17
25	1		
26		2	
27			13
28		5	11
31		7	
33	20		
34	21		
35	26		
36	29		
41	8		
42	9		
44		6	
45	30		
46	32		
		9	3
		13	9
		15	5
		16	6
		19	21
		20	23
		21	24
		22	22
		*23	25
		*24	26
		*25	27
		*26	28
		*27	29
		*28	30
		32	31
		33	33
		34	32
		35	34

* These charts were not used in this study.
** This test was not used in this study.

*** E. Hertel, *Stillings Pseudo-Isochromatische Tafeln zur Prüfung des Farbensinnes* (Georg Thieme, Verlag, Leipzig, 1936), nineteenth edition.

equivalent plates—equivalent in the sense that the patterns are the same and that the colors are roughly so—the plates are by no means identical. Variations in the colors of the charts due to differences in printing are quite marked among them. It will be assumed that the reader is familiar with the general nature of these pseudo-isochromatic tests. Excellent descriptions of them are contained in articles by Murray (24, 25) and Hardy *et al.* (13). These articles also trace the historical development of tests of this sort and indicate how the various editions derive from each other.

The Boström Test

The other two tests used in this experiment, the Boström and Boström-Kugelberg, appear to be completely original. The Boström test contains 12 plates with digits and 4 blank "simulation" plates for detecting color defective individuals who may try to fake their results. The test is supposed to measure both the amount and kind of color defect. According to the instructions, plates 1 and 2 are read by all individuals with reasonably normal visual acuity. Plates 3 through 12 are failed by individuals with a "serious color defect;" plates 9 through 12 are failed, and plates 3 through 8 passed, by individuals with a milder defect; individuals who fail only plates 11 and 12 have a questionable color defect, i.e., they are presumably color normal individuals with low color discrimination. In addition, plates 5 and 6 are failed by protanopes and protanomalous with a severe defect; plates 3, 4, 7, and 8 are failed by deuteranopes and deuteranomalous with a serious defect. The digits in this test are made up of spots of fairly saturated pigments, the backgrounds of less saturated spots which are nearly the same hue as those in the figures. There are, at most, two different brightnesses of dots used in the background or figures; in several plates only one brightness is used for the spots making up the digits.

The Boström-Kugelberg Test

This test is considerably different from most pseudo-isochromatic plates. The dots in the plates are all of the same size and are arranged in a symmetrical geometrical pattern. Three or four brightnesses of dots are used in each plate, and the brightnesses of the dots are varied systematically. This regularity of pattern should make the plates virtually unmemorizable on the basis of pattern or brightness, a defect which is characteristic of the AO plates (7, 30, 33) and probably of many others. A single, large, block digit appears on 15 of the plates; two plates contain a winding path for testing illiterates, and the remaining 3 plates are blank "simulation" plates. A single hue is used for the digit and another hue for the background of each plate. The saturations of the hues tend to be fairly low. According to the authors (2), the hues are stable when exposed to daylight or ultraviolet—another difficulty with present tests. This is a simple dichotomous test. According to the instructions, individuals who miss two or more plates are color defective.

Apparatus and General Procedures

Each of the subjects was examined individually in a dark room according to the following schedule: (1) short medical history and interview; (2) visual acuity measurements; (3) test with the Bausch and Lomb visual spectrophotometer to determine the limit of visibility in the red end of the spectrum; (4) examination with the pseudo-isochromatic tests; (5) examination with the RCN lantern.

The chart tests were placed on a table with a black felt background and were viewed at a distance of about 2½ feet. Illumination on the charts and table came from a MacBeth zenith sunlight (Type BX826 skylight) directly above the table. This light furnished 30 footcandles of illumination (of about 5500°K) incident on the test. The tests were tilted slightly to eliminate reflections from the light source. During this part of the examination, all other sources of illumination in the room were extinguished.

Because of the duplication of plates which appears on three of the five tests in this study (cf. Table I), the order of presentation of the tests was randomized. There are 120 different permutations possible with these five tests, and each subject was tested with a different order. No attempt was made to randomize the order of

presentation of individual plates within the tests. The subjects were allowed unlimited time and all responses to each of the charts were noted. In no case, however, did the examiner supply any cue as to whether the response was correct. When a subject gave two or more responses to a chart, he was forced to state which one of the responses seemed to be more clear or "better" to him. This "best choice" response is the one which is scored and tabulated in the following data.

Following the examination with the charts, the room lights were extinguished and the subject was prepared for the examination with the RCN lantern. Details of the lantern test are contained in Section III.

The spectrophotometer test was used to separate the color deficient subjects into two groups: (1) those who had normal sensitivity to long wave-length radiation (deuteranopes and deuteranomalous), and (2) those who had impaired sensitivity to long wave-length radiation (protanopes and protanomalous). The methods and results obtained with this test will be described in a later paper.

III. RESULTS WITH THE ROYAL CANADIAN NAVY COLOR VISION TEST LANTERN

Description of the Lantern

The Royal Canadian Navy (RCN) color vision test lantern exhibits two lights simultaneously. The lights are spaced one inch apart horizontally, and a moveable diaphragm makes it possible to use lights which are either 0.2 or 0.02 inches in diameter. Any one of nine color pairs can be shown: green-white, green-green, red-green, white-red, white-white, red-white, red-red, green-red, and white-green. The filters are polished Pyrex glass. The green filter is a standard signal green (Corning No. 440). The red filter (Corning No. 241) is a deeper red than standard signal red because its recognition, according to the test manual, is supposed to be more difficult for those with any degree of color vision defect. A colorless polished Pyrex (Corning 774) is used for the white. With the exception of the white-white combination, all of the pairs of lights are adjusted, by the use of neutral filters, to appear of approximately the same intensity. In the white-white combination, one of the white lights

TABLE II. Tabulation of responses made to each colored light in the Royal Canadian Navy color vision test lantern by 86 color normal and 34 color deficient subjects, of whom 12 were classified protano and 19 deuterano. (The entries are percentages; entries in parentheses are actual frequencies. Each subject was presented with each test color 12 times.)

			Small apertures				Large apertures			
Test color	Subject's responses		Color normal	All color deficient	Protano's	Deuterano's	Color normal	All color deficient	Protano's	Deuterano's
G	Green	(G)	96.8 (999)	65.2 (266)	49.3 (71)	75.4 (172)	93.8 (968)	68.6 (280)	56.2 (81)	75.9 (173)
	Greenish-blue	(GB)	0.0 (0)	0.0 (0)	0.0 (0)	0.0 (0)	0.0 (0)	0.2 (1)	0.0 (0)	0.4 (1)
	Bluish-green	(BG)	0.3 (3)	0.7 (3)	0.0 (0)	1.3 (3)	0.6 (6)	1.7 (7)	1.4 (2)	2.2 (5)
	Blue	(B)	2.9 (30)	1.7 (7)	2.8 (4)	1.3 (3)	5.6 (58)	6.4 (26)	0.0 (0)	11.4 (26)
	White	(W)		15.7 (64)	16.0 (23)	14.0 (32)		22.3 (91)	41.0 (59)	9.6 (22)
	Yellow	(Y)		8.1 (33)	20.1 (29)	1.8 (4)		0.5 (2)	1.4 (2)	0.0 (0)
	Amber	(A)		0.2 (1)	0.0 (0)	0.4 (1)		0.2 (1)	0.0 (0)	0.4 (1)
	Reddish-yellow	(RY)		0.2 (1)	0.7 (1)	0.0 (0)		0.0 (0)	0.0 (0)	0.0 (0)
	Red	(R)		8.1 (33)	11.1 (16)	5.7 (13)		0.0 (0)	0.0 (0)	0.0 (0)
R	Red	(R)	100.0 (1032)	97.8 (399)	97.2 (140)	98.7 (225)	100.0 (1032)	98.5 (402)	100.0 (144)	97.4 (222)
	Yellow	(Y)		0.5 (2)	0.0 (0)	0.9 (2)		1.0 (4)	0.0 (0)	1.8 (4)
	White	(W)		0.2 (1)	0.0 (0)	0.4 (1)		0.0 (0)	0.0 (0)	0.0 (0)
	Green	(G)		0.5 (2)	0.0 (0)	0.0 (0)		0.2 (1)	0.0 (0)	0.4 (1)
	Blue	(B)		0.7 (3)	2.1 (3)	0.0 (0)		0.2 (1)	0.0 (0)	0.4 (1)
	Nothing	(—)		0.2 (1)	0.7 (1)	0.0 (0)		0.0 (0)	0.0 (0)	0.0 (0)
W	White	(W)	48.5 (501)	23.8 (97)	20.8 (30)	24.6 (56)	56.5 (583)	27.7 (113)	25.0 (36)	27.2 (62)
	Whitish-yellow	(WY)	0.3 (3)	0.0 (0)	0.0 (0)	0.0 (0)	0.0 (0)	0.0 (0)	0.0 (0)	0.0 (0)
	Yellowish-white	(YW)	0.2 (2)	0.0 (0)	0.0 (0)	0.0 (0)	0.6 (6)	0.0 (0)	0.0 (0)	0.0 (0)
	Yellow	(Y)	39.4 (407)	16.4 (67)	26.4 (38)	12.3 (28)	34.8 (359)	17.9 (73)	25.0 (36)	14.9 (34)
	Orange-yellow	(OY)	0.1 (1)	0.0 (0)	0.0 (0)	0.0 (0)	0.0 (0)	0.0 (0)	0.0 (0)	0.0 (0)
	Yellow-orange	(YO)	0.7 (7)	0.0 (0)	0.0 (0)	0.0 (0)	0.1 (1)	0.0 (0)	0.0 (0)	0.0 (0)
	Orange	(O)	4.4 (45)	3.2 (13)	0.7 (1)	5.3 (12)	2.5 (26)	4.9 (20)	0.7 (1)	7.0 (16)
	Amber	(A)	6.4 (66)	3.4 (14)	0.0 (0)	6.1 (14)	5.5 (57)	4.2 (17)	0.0 (0)	7.5 (17)
	Reddish-yellow	(RY)		0.2 (1)	0.7 (1)	0.0 (0)		0.0 (0)	0.0 (0)	0.0 (0)
	Pink	(P)		0.0 (0)	0.0 (0)	0.0 (0)		2.9 (12)	0.0 (0)	5.3 (12)
	Brown	(Br)		0.7 (3)	0.0 (0)	1.3 (3)		0.0 (0)	0.0 (0)	0.0 (0)
	Red	(R)		26.0 (106)	16.7 (24)	30.3 (69)		11.5 (47)	8.3 (12)	11.0 (25)
	Green	(G)		25.5 (104)	34.0 (49)	19.3 (44)		30.1 (123)	41.0 (59)	25.9 (59)
	Greenish-blue	(GB)		0.2 (1)	0.0 (0)	0.4 (1)		0.0 (0)	0.0 (0)	0.0 (0)
	Bluish-green	(BG)		0.2 (1)	0.0 (0)	0.4 (1)		0.2 (1)	0.0 (0)	0.4 (1)
	Blue	(B)		0.2 (1)	0.7 (1)	0.0 (0)		0.5 (2)	0.0 (0)	0.9 (2)

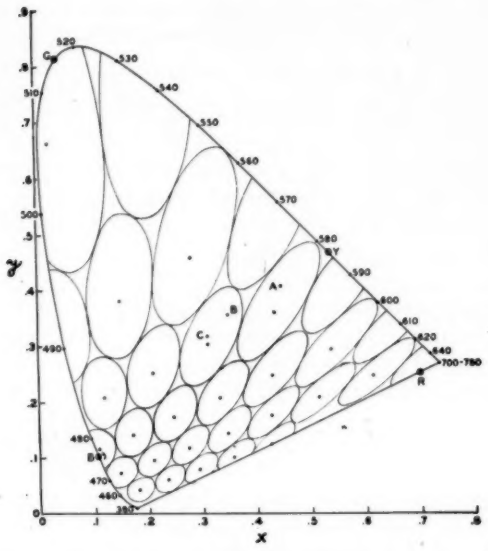

FIG. 1. Equal-chromaticity-difference ellipses for normal color vision. (From Judd, 1936.)

is purposely a little dimmer than the other. As measured with a MacBeth illuminometer, the intensities of the small lights are of the order of 0.0002 candles, of the large lights about 0.015 candles. The light source in the lantern is a 32 candle-power, prefocused, automobile headlight bulb with power provided by an 110 to 8 volt transformer. A Weston No. 594 BB photo-cell is mounted inside the instrument four inches from the light source, to one side and a little to the rear of the bulb. This photo-cell operates a microammeter, and a rheostat permits adjustment of the light source to a constant intensity for all tests.

Procedures

The procedures used in administering this test differ considerably from those suggested in the manual of instructions. The subjects were tested at a distance of twenty feet following a dark adaptation period of five minutes. Thirty-six combinations were tested. The subjects were tested first with the smaller apertures in the following order: GW, GG, RG, WR, WW, RW, RR, GR, WG, GG, WR, RW, GR, GW, RG, WW, RR, and WG. Following this series the subjects were tested with the large lights in the following order: WG, GR, RR, RW, WW, WR, RG, GG, GW, GR, RW, WR, GG, WG, RR, WW, RG, and GW. Instructions to subjects preceding the tests were: "You will be shown pairs of colored lights. These are all simple colors. Name the colors in your own words. You may use only one color name for each colored light which you see. You may take all the time you wish. Name the color on your left first, then the one on your right." As in the case with the chart tests, the subjects were given absolutely no help in identifying any of the lights. The standard response to all leading questions by the subjects was: "How does it look to you?" Whenever the subjects gave multiple responses they were always required to select the one "best" color name for each light. Only these "best choice" responses are tabulated in the following data.

Results

Color Names Used

Table II is a tabulation of the responses made to each colored light on the lantern by the 86 color normal subjects and the 34 color deficient subjects. Of the latter, 12 were classified protano (protanopic or protanomalous) and 19 deuterano (deuteranopic or deuteranomalous). It is evident from an examination of Table II that a large variety of color names was applied to each of the three test colors used on the lantern. This is especially true of the white light which was actually quite yellowish. It is not surprising, therefore, to find a large number of yellow responses made to it.

The variety of color names applied to the test colors is reasonable since there is evidence to show that instability in color naming is the rule, rather than the exception, even among the color normal (21). The difference between the color normal and color deficient lies (a) in the greater variety and (b) in the different kinds of responses the color deficient is apt to make. These characteristics are predictable and the data of Table II can be shown to fit into a consistent pattern by recourse to I.C.I. diagrams.

Equal-Chromaticity-Difference Ellipses for Normal Vision

The standard colorimetric coordinate system adopted in 1931 by the International Commis-

sion on Illumination is now used routinely to portray data of color vision experiments. A minor defect of this system, however, is the fact that equal linear distances in the I.C.I. diagram do not represent equal chromaticity differences for the human eye. In 1935, Judd (18) calculated a uniform chromaticity scale and later transformed this scale into equal-chromaticity-difference ellipses for the I.C.I. system (19). His results are shown in Fig. 1. The distances from the boundaries of any ellipse to the point in the center of the ellipse represent chromaticity differences which are equal to the normal eye. Each such distance in this figure is 100 times the j.n.d. which is obtained under good experimental conditions (careful monocular observation of a 6° circular field divided along a diameter and with retinal illuminations of from 200 to 1000 photons). More recent experimental data (22) yield equal-chromaticity-difference ellipses which agree with the general form of Judd's earlier diagram.

Color Naming and Equal-Chromaticity-Difference Ellipses

For our purposes, it is important to notice the directions of the long axes of the ellipses in Fig. 1.† There is, for example, a large ellipse around green, and the long axis of this ellipse extends toward blue. For the normal individual confusions of green with greenish-blue, bluish-green, or blue should be common, and confusions of green with white rare. The data of Table II show that this is the case. Similarly, the long axes of the ellipses near white extend in the direction of yellow. The data of Table II show that a large number of such confusions were made.

Equal-Chromaticity-Difference Contours in Color Deficient Vision

In dichromatic vision, the equal-chromaticity-difference ellipses are replaced by sets of nearly rectangular zones (28). These have been plotted in the I.C.I. system by Judd (20) and are shown in Figs. 2 and 3 for the protanopic and deuteranopic eye, respectively. Hues falling anywhere within a zone tend to be confused with each other. It is important to notice that the direction of the iso-chromatic lines for dichromatic vision is nearly perpendicular to the major axes of the

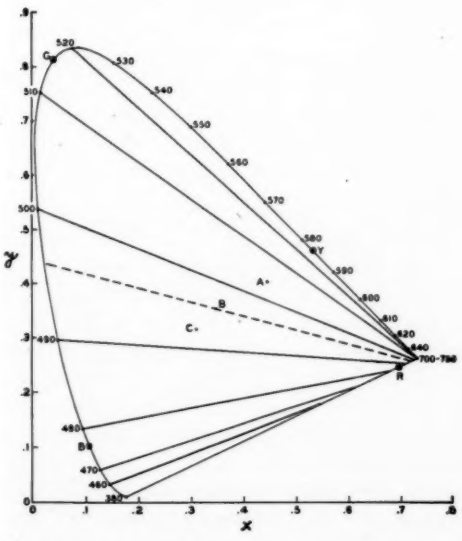

FIG. 2. Equal-chromaticity lines for protanopic vision. (From Judd, 1944.)

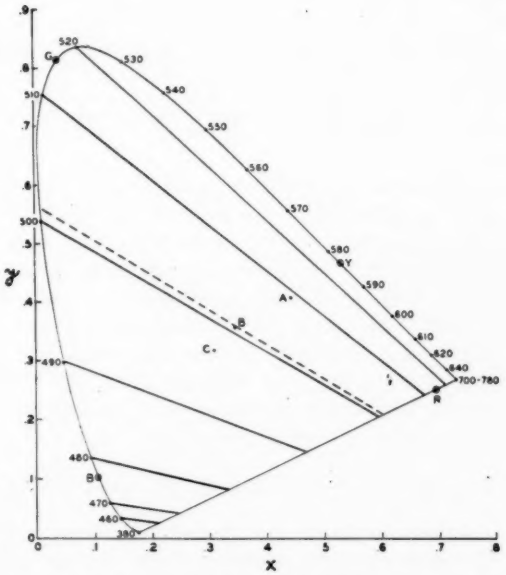

FIG. 3. Equal-chromaticity lines for deuteranopic vision. (From Judd, 1944.)

† For purposes of orientation, the locations of the psychologically unique blue, green, yellow, and red, as determined by Dimmick and Hubbard (4, 5) are also shown on the diagram.

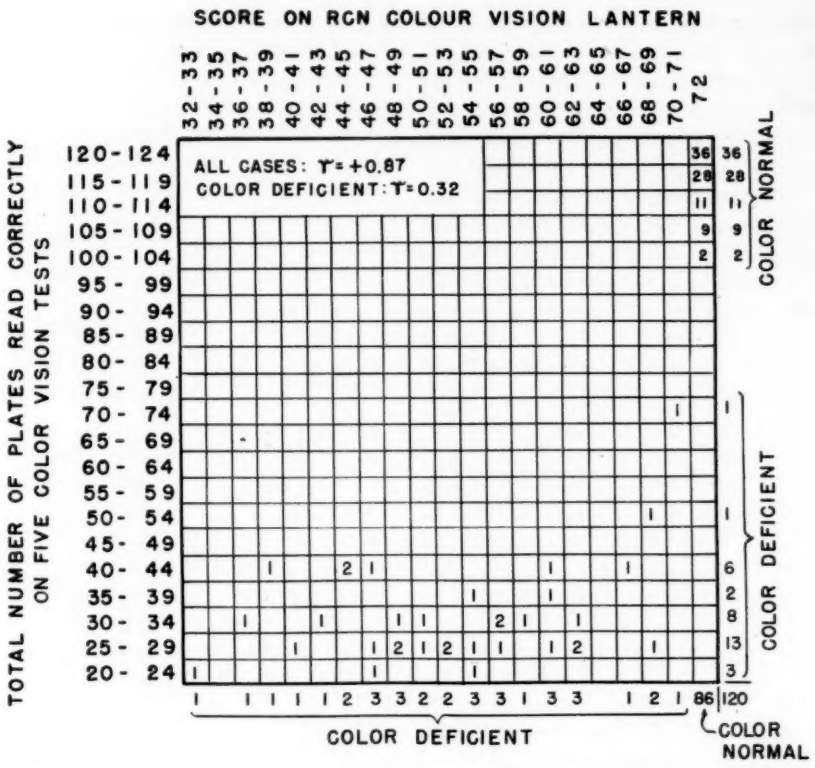

FIG. 4. Relationship between scores on the RCN lantern and the total number of plates read correctly on five pseudo-isochromatic tests by 86 color normal and 34 color deficient individuals.

equal-chromaticity-difference ellipses for the normal eye. Although a large amount of comparable data is not available for anomalous trichromats, it appears that the minor axes of these ellipses for the normal gradually increase with increasing amounts of anomaly (36). The minor axes of the ellipses are stretched, as it were, until, in dichromatic vision, the ellipses burst and are replaced by the large, almost rectangular confusion zones in Figs. 2 and 3.

Color Names Used by the Color Deficient

The iso-chromatic lines in Figs. 2 and 3 account for the numerous confusions of red, green, and white made by the color deficient. Color-naming, as was required of the subjects taking the lantern test, is a crude experimental procedure compared with those which led to the formulation of the curves in Figs. 1, 2, and 3. Even so, the general pattern of responses in Table II conforms to predictions which one might make on the basis of the more careful laboratory work.

Scoring the Lantern Data

These iso-chroma plots emphasize the essentially different character of the color confusions made by the color normal and color deficient and provide a rationale for the system used in scoring the data obtained with the lantern. The uppermost groups of responses in Table II were scored correct for each of the test colors. Those below the space were scored incorrect for each of the test colors. To the normal eye, the latter are fairly serious errors.

Since the results on this test constitute the criterion of color blindness in this study, all of the color-blind individuals, by definition, made at least one error of the type indicated in this

table. Each of the color normal subjects, on the other hand, obtained a perfect score, i.e., 72. Total scores earned by the color deficient ranged from 33 to 71.

Color Naming as a Function of Size of Aperture

In general, performance with the small apertures was slightly poorer than performance with the large apertures. The average score obtained by the color deficient in the former instance was 25.5, and in the latter 27.6. Although this difference is statistically significant at better than the 1 percent level of confidence, it is surprisingly small considering the fact that there is nearly a hundred-fold increase in the intensity of the lights. The correlation between the scores obtained with the large apertures and the small apertures by the 34 color deficient subjects is equal to +0.64. This means that subjects who scored high with the small apertures tended to score high with the large apertures, and vice versa. The relationship is not very high, however, indicating that there are some sizeable exceptions to the trend.

Careful study of Table II also reveals some interesting differences in the character of the responses made to the small and large lights. The color normal, for example, called the W light white more often, and yellow, amber, or orange less often when the stimuli were brighter. The color deficient, on the other hand, confused G with W and W with G more frequently when the lights were bright, G with R and W with R more frequently when the lights were dim. It is obviously impossible to say with certainty whether the size or intensity of the lights accounts for these differences. Intensity is probably more important, however, since at a distance of 20 feet the large lights were still virtually point-sources.

Differences Between the Protano and Deuterano Subjects

The average score obtained by the deuterano subjects was 56.3; by the protano subjects, 48.7. This difference is statistically significant at the 2 percent level of confidence. The overlap is so great between the two groups, however, that the RCN lantern cannot be used for differential diagnosis. This difference may indicate some genuine weighting factor for lantern tests in general, since Neubert (26) also reports that protano subjects have slightly more difficulty with his lantern than do deuteranos.

There are a few interesting differences between the two groups of color deficient subjects in the kinds of responses they made to individual lights on the RCN lantern. Contrary to what one might expect, the deuterano subjects identified the green light correctly more often than did the protanos (cf. Table II). Neubert (31) reports

TABLE III. Tabulation of responses made by 86 color normal and 34 color deficient subjects to "hidden-digit" charts on the Ishihara and AO tests.

Plate Ish.	No. AO	Subjects responses†	Ishihara Color normal	Ishihara Color deficient	AO Color normal	AO Color deficient
18		—*	29			
		4	1			
		5**	56	34		
19		—*	26			
		2**	54	33		
		8	6	1		
20	33	—*	11		38	4
		−5	1			1
		25	1			
		35			1	1
		43	2		2	
		45**	69	34	41	24
		47	1		4	2
		57				1
		65	1			1
21	34	—*	13		39	3
		2—	2			
		3—				1
		7—				1
		21	1			1
		23	28	4	2	4
		25	1		1	
		27	2		3	4
		28	1			
		29			2	
		53	1			
		71			1	
		72			4	
		73**	35	22	20	17
		74			1	
		75	1		7	
		78		8	2	2
		79			4	1
		ZY	1			
30	45	—*	58	2	50	
		Line**	28	32	36	34
31		—*	50	2		
		Line**	36	32		

† These are the actual responses made by the subjects. Responses marked with a single asterisk are "normal" responses according to the test manuals; those marked with a double asterisk are supposed to be read only by the color deficient.

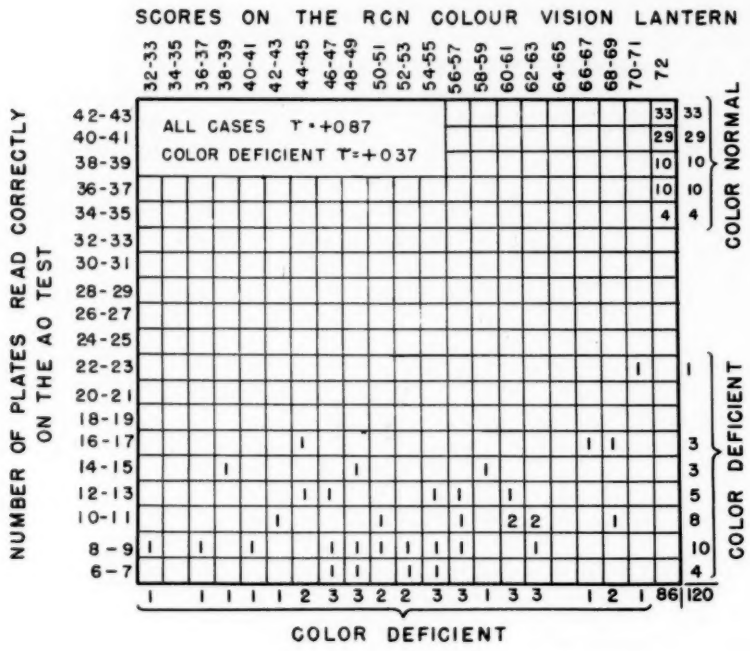
SCORES ON THE RCN COLOUR VISION LANTERN
NUMBER OF PLATES READ CORRECTLY ON THE AO TEST
ALL CASES r=+087
COLOR DEFICIENT r=+037
COLOR NORMAL
COLOR DEFICIENT
COLOR DEFICIENT

FIG. 5. Relationship between scores on the RCN lantern and the number of of plates read correctly on the AO test by 86 color normal and 34 color deficient individuals.

similar findings. The deuteranos confused white with red more commonly, and white with green less frequently, than did the protanos. Finally, the protanos were much more likely to confuse green with white or yellow than were the deuteranos.

IV. THE CRITERIA OF COLOR DEFICIENCY

Although the results obtained on the RCN lantern constitute the primary criterion of color deficiency for this study, it is also important to note that another criterion, that is, the total number of plates read correctly on the five pseudo-isochromatic tests, is equally satisfactory. The extent of the relationship between the scores on the lantern and the total number of plates read correctly is indicated in Fig. 4. All those individuals who were classified color deficient on the lantern obtained scores of 74 or less on the combined color plates. Those individuals who were classified color normal obtained scores of 100 or more. Since each of the individual tests measures color deficiency with some degree of accuracy, the combined score on all of the tests should be a better criterion than the score on any individual test. The data in Fig. 4 show that this is the case.

Although individual tests will be evaluated in later sections of this study by comparison with the lantern scores, it should be remembered that the results are equally applicable to the criterion of the total score obtained on all of the chart tests. As a matter of fact, the latter criterion is better for separating the color normal from the color deficient, since there is a wide separation between the two groups in terms of the total number of plates read. On the lantern, the best color deficient individual missed only 1 of the 72 colors presented. This finding is consistent with earlier studies (26, 29), which show that it is somewhat easier to pass the RCN lantern than the pseudo-isochromatic plates.

V. RESULTS WITH THE PSEUDO-ISOCHROMATIC PLATES

Scoring the Tests

"Hidden-Digit" Plates

Six plates of the Ishihara test and three of the AO test are of the "hidden-digit" type. They, presumably, are seen only by persons

with defective color vision and are rarely seen by individuals with normal color vision. The manual of instructions which accompanies the Ishihara test, for example, states that the majority of the red-green blind read a "5" on plate No. 18 and that the majority of the normal and totally color-blind can hardly read it. It soon became apparent that these charts were of little diagnostic value because the digits were visible to the color normal more often than not. A detailed tabulation of the responses made to these plates is contained in Table III. It is evident from this table that the hidden digits on Ishihara plates 18, 19, and 20 were seen and read by well over half of the color normal subjects. Ishihara plates 30 and 31, which contain a hidden "path," were seen less often by color normal individuals, but enough did see the paths to make the charts of questionable significance. Similar findings have also been reported by Neubert (26).

Charts of the hidden-digit variety are clever, and the designer of these plates exhibited considerable ingenuity in planning them. But, as will be seen later, it is possible to design a good color vision test of the pseudo-isochromatic type without resorting to trick plates. Plates of this sort are also unsatisfactory because they complicate the scoring procedure. The examiner has to remember that a response to these plates must be scored incorrect, and that no response is scored correct. Results on these six charts in the Ishihara and the three in the American Optical Company tests are not included in any of the following data.

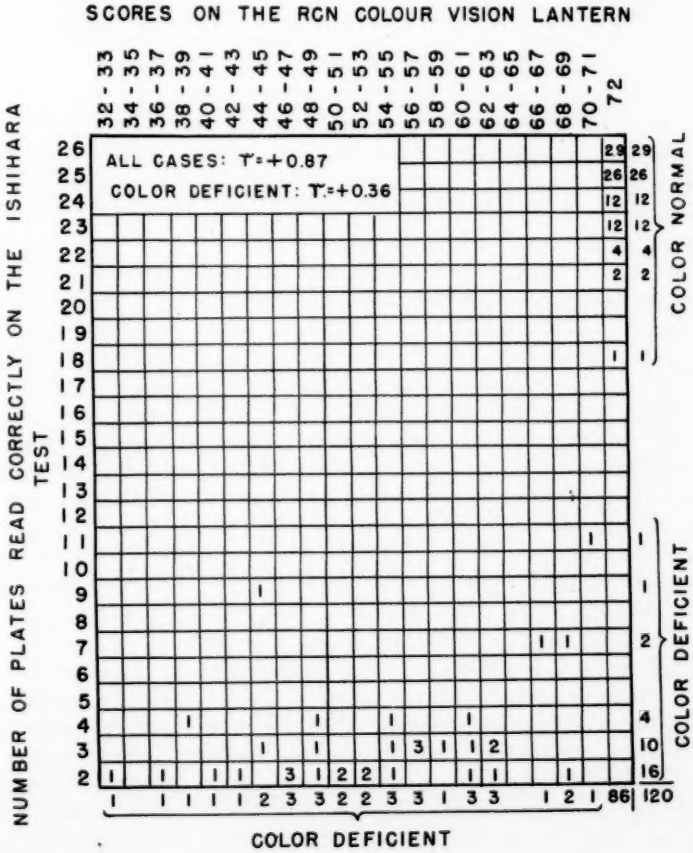
SCORES ON THE RCN COLOUR VISION LANTERN
ALL CASES: T=+0.87
COLOR DEFICIENT: T=+0.36
NUMBER OF PLATES READ CORRECTLY ON THE ISHIHARA TEST
COLOR NORMAL
COLOR DEFICIENT
COLOR DEFICIENT

Fig. 6. Relationship between scores on the RCN lantern and the number of plates read correctly on the Ishihara test by 86 color normal and 34 color deficient individuals.

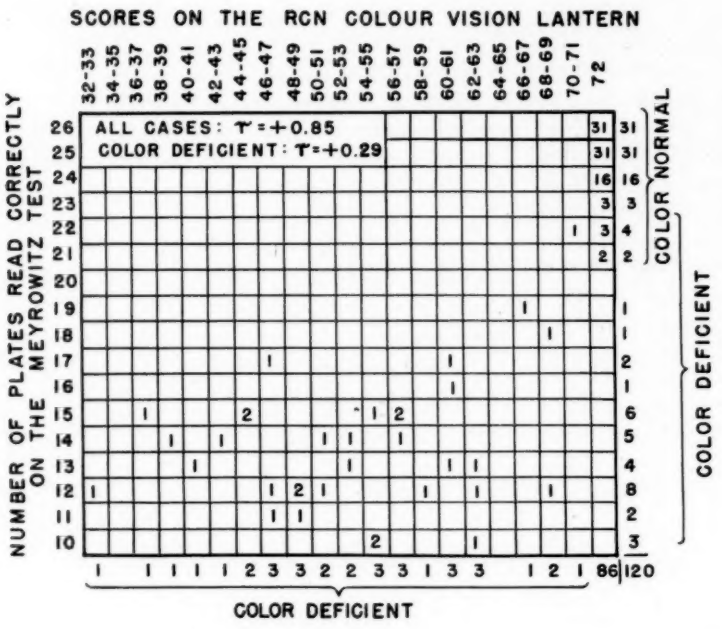

FIG. 7. Relationship between scores on the RCN lantern and the number of plates read correctly on the Meyrowitz test by 86 color normal and 34 color deficient individuals.

Digits vs. Plates Read Correctly

A further difficulty in scoring arose because of the numerous digit-confusion errors. There were many instances, for example, of 3's being confused with 8's, 3's with 9's, etc. Since the charts in these tests contain one, two, or three digits, it might be supposed that the total number of digits read correctly would be a more valid score than the total number of charts read correctly. That this is not the case is shown by product-moment correlations between the total number of digits read correctly and the total number of plates read correctly on the five tests of color vision. For the 34 color deficient subjects, the correlation was +0.98, for the 86 color normal individuals, +0.99, and for all subjects, +0.999. The lowest correlation value for any single test was +0.95. These correlations are so high that results obtained with the one method of scoring are equally applicable to the other. Since it is considerably easier simply to record the total number of plates read correctly, this method of scoring is used throughout this paper. A strictly literal scoring procedure was used. In order for a plate to be scored correct, the examinee must have made the exact response specified in the test manuals. Omissions and misreading errors were all scored incorrect irrespective of their nature.

Gross Results

Scatter Diagrams

Gross analyses of the efficiency of each of the tests were made by comparing the scores obtained on each test against the scores obtained on the RCN lantern. These data are contained in Figs. 5 to 9. It is evident that there of the tests, the AO, Ishihara, and Boström Kugelberg, differentiate clearly between the color normal and the color deficient. Two of the tests, the Meyrowitz and Boström, are not so good in this respect. With both of the latter tests there is overlapping between the scores obtained by the color normal and color deficient.

Correlation Analysis

The correlational technique has also been used to study color vision tests in the past (27, 35) and the results of such an analysis for the data of this study are shown in Table IV. Certain precautions must be observed in interpreting these figures. First, many of the scatter plots are obviously non-linear (cf. Figs. 5 to 9), and the correlation

coefficient is a measure of linear relationship. Second, the pseudo-isochromatic tests (with the exception of the Boström) are dichotomous tests, i.e., they were not intended to yield quantitative estimates of the amount of color defect. This has not actually worked out to be the case, however, since other studies show that the number of plates missed is related, to some extent, to the degree of color defect (13, 14, 17). Finally, several of the correlation coefficients are spuriously high because of overlapping content. For example, identical plates in the Ishihara and AO plates, and the Meyrowitz and AO plates, tend to be failed or passed together. Correlations between (a) the number of plates read on individual tests and (b) the number of plates read on all the tests, are also spuriously high since the former score contributes to the latter.

In view of these difficulties, it is apparent that the correlational technique is not especially helpful. Intercorrelations involving the Boström and Meyrowitz tests are about as high as the other intercorrelations. From these figures alone, there is certainly no basis for deciding which of the tests is satisfactory. As a matter of fact, the Boström-Kugelberg correlates less well with other measures than any of the other tests. Yet this test is the best of the dichotomous tests used in this study. As a general conclusion, therefore, it appears likely that the correlational technique by itself is of little value in evaluating color vision tests.

One point seems to be clear from Table IV, however: the pseudo-isochromatic tests correlate better with each other than they do with the RCN lantern. A similar finding is reported in the study by Thomas (35) who discovered that the AO and Ishihara tests correlated better with each other than they did with two instrument tests, the ISCC (3) and Farnsworth-Munsell 100-hue test (6). His conclusion is that "The pattern of correlations among the tests studied presents a confusing picture." The data of this study do little to clarify the situation since there are several purely statistical artifacts which contaminate the data, e.g., the overlapping of content among the tests and the unknown reliabilities of these tests.

Another finding of Table IV is that the intercorrelations between the number of plates read by the color deficient tend to be higher than comparable intercorrelations for the color normal. The three exceptions to this generalization are correlations involving the Boström-Kugelberg test. A possible interpretation of this finding is that failure to read a plate correctly is a better indication of color deficiency when a color deficient examinee makes the error than when a color normal examinee does. In short, when a color normal fails to read a plate correctly, he

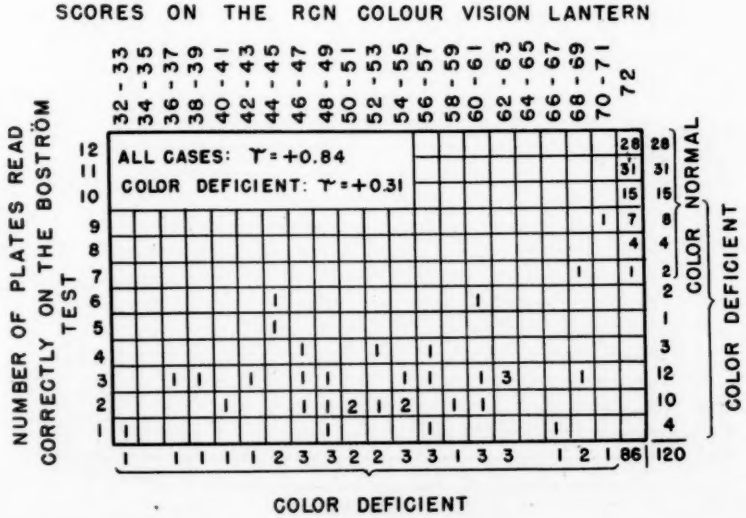

FIG. 8. Relationship between scores on the RCN lantern and the number of plates read correctly on the Boström test by 86 color normal and 34 color deficient individuals.

TABLE IV. Intercorrelations between scores earned on six color vision tests by 34 color deficient (uppermost entry in each block), 86 color normal (middle entry), and and by all subjects (lowest entry).

	Ishihara plates	Meyro-witz plates	Boström plates	B-K plates	All plates	RCN lantern
AO plates	+0.75 +0.54 +0.99	+0.70 +0.21 +0.96	+0.65 +0.56 +0.96	+0.44 +0.47 +0.98	+0.91 +0.86 +0.995	+0.37 — +0.87
Ishihara plates		+0.68 +0.14 +0.96	+0.61 +0.52 +0.95	+0.32 +0.64 +0.98	+0.84 +0.78 +0.99	+0.36 — +0.87
Meyrowitz plates			+0.62 +0.28 +0.94	+0.52 +0.19 +0.95	+0.87 +0.45 +0.97	+0.29 — +0.85
Boström plates				+0.50 +0.43 +0.95	+0.80 +0.76 +0.97	+0.31 — +0.84
B-K plates					+0.64 +0.70 +0.99	−0.14 — +0.84
All plates						+0.32 — +0.87

may do so for some reason other than impaired color sensitivity, e.g., poor numeral design. This problem is discussed more fully in section VI. The findings of that section may be anticipated, however, to point out that the Boström-Kugelberg test had the least ambiguous plate design of any in this study.

Detailed Analysis of Individual Test Plates

Digit-Confusion Errors

Much valuable information can be obtained by examining individual plates in terms of their diagnostic efficiency. There are at least two serious faults apparent in many of these plates. One of them is that they are difficult to score because of the variety of responses made by the testees. In the responses made to plate 38 (cf. Table VII), it is evident that 3's are frequently confused with 8's by the color normal. But there are also a few confusions of 3's with 2's. Section VI will attempt to uphold the thesis that the frequency of these misreading errors can be reduced by proper plate design. But for our present purpose, it is important to notice the sorts of difficulties this produces. Knowing that such misreading errors occur, the conscientious tester is faced with a problem in scoring the color deficient responses. On plate 38 (Table VII), is a confusion of 3 with 6 also a misreading error? What about 0's which are read as 7's, 8's, and 9's on Plate 37? Are these simple misreading errors, or are they indicative of color deficiency or low color discrimination? The ideal test would be made up of plates to

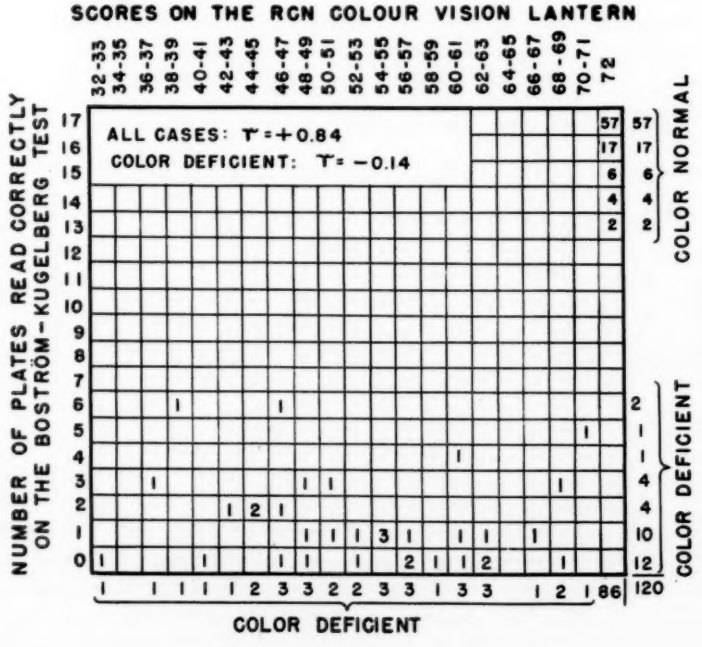

FIG. 9. Relationship between scores on the RCN lantern and the number of plates read correctly on the Boström-Kugelberg test by 86 color normal and 34 deficient individuals.

which all examinees respond with either the correct number or no number (or with an incorrect number, in the case of "transformation figure" plates). Intermediate, ambiguous, or "possibly correct" answers should be reduced to a minimum.

Diagnostic Efficiency of Plates

The other fault of many of these plates is that they do not appear to differentiate between the color normal and color deficient. A plate is diagnostic if most color normal individuals pass it and most color deficient fail it.

A Criterion for Evaluating Plates

These two considerations have been combined into a single criterion as follows: A good plate is one to which 50 percent or more of the color normal make one kind of response *and* to which 50 percent or more of the color deficient make another kind of response. This criterion is not a valid one for all types of test data since it theoretically might accept a plate which gave no differentiation whatsoever. Assume that 50 percent of the normal gave response *A* and the remainder gave response *B*. If, in addition, 50 percent of the color deficient gave response *A*, and the remainder gave response *B*, the plate would satisfy the criterion but would not differentiate the two groups. Since none of the data approached this limiting condition, the criterion is satisfactory as a simple working rule for this experiment. It is obviously a completely arbitrary criterion, but the data are presented in sufficient detail so that they may be re-evaluated in terms of any other criterion.††

Plates Common to the AO and Ishihara Tests

Table V shows the responses made to those plates which are common to the AO and Ishihara tests. All of these plates are of the "transformation figure" variety, i.e., the color normal are supposed to see one number, the color deficient another. In general, this group of plates tends to be fairly diagnostic. The color normal usually see the expected number and the color deficient usually see another number. Only one plate, AO plate 12 (Ishihara plate 5), fails to meet the criterion because of the large number of ambiguous responses made by the color deficient. There are some slight differences between plates on the two tests but they are difficult to evaluate because of the small numbers of cases involved.

TABLE V. Responses made by 86 color normal and 34 color deficient subjects to plates which are common to the AO and Ishihara tests.

Plate No. AO	Plate No. Ish.	Subjects' responses	AO plates Color normal	AO plates Color deficient	Ishihara plates Color normal	Ishihara plates Color deficient
5	2	3		21		29
		8	86	13	86	4
		9				1
6	3	5		24		29
		6	86	10	86	5
11	4	20	9	5	2	3
		28			1	
		29	75		82	
		30				1
		59	2			
		70		29		30
		79			1	
12	5	5—				1
		27	2			
		33				1
		35		14		7
		37				1
		53		2		1
		55		12		16
		57	84	6	86	6
		85				1
19	6	2		34		34
		5	86		86	
20	7	3	85		82	1
		5		34		29
		6				4
		8	1		4	
35	26	—		32	1	27
		Line	86	2	85	7
36	29	—	9	32	16	34
		Line	77	2	70	
41	8	15	86	1	86	
		17		32		34
		□		1		
42	9	21		29	2	33
		24		1	1	1
		71	9	4	27	
		74	77		56	

† Green and Sloan (12), for example, have suggested rigorous statistical criteria for evaluating test plates, but their techniques require certain arbitrary decisions about the importance of misclassifications. These decisions usually depend on the policy and aim of the organization doing the testing. For this reason, it seemed appropriate to use a more general and detailed form of presentation of the data in this paper.

TABLE VI. Responses made by 86 color normal and 34 color deficient subjects to plates which are common to the AO and Meyrowitz tests.

Plate No. AO	Plate No. M	Subjects' responses	AO plates Color normal	AO plates Color deficient	Meyrowitz plates Color normal	Meyrowitz plates Color deficient
2	8	—		1		
		−3		1		
		43	80	27	75	30
		46		2		
		48	6	3	11	4
13	4	—		17		22
		8−		2		
		9−				1
		36		2		1
		86	86	11	85	3
		88		1		
		96		1	1	7
18	3	—		25		22
		−2				1
		−8				1
		2−				1
		15				1
		25				1
		28				1
		36				1
		56		1		
		63		1		
		66		1		1
		68	86	6	86	3
		86				1
28	5	—		33		3
		−3				1
		42			1	
		43	68	1	66	19
		45				1
		48	18		19	10
31	7	—		10		12
		5−		3		
		6−				1
		32		1		
		37				1
		52	77	13	61	8
		55		1		
		57		3		2
		58	1		1	
		59	3	1	1	
		62	5	1	22	3
		65				1
		67				6
		69			1	
		82		1		
44	6	—	1	33		32
		68	3			
		74				1
		88			1	
		92	1	1		
		93	3		1	
		98	78		84	1

Thus, Ishihara plates 2, 3, and 4 appear to be slightly better than their AO equivalents, plates 5, 6, and 11. AO plates 20 and 42, on the other hand, appear to have a slight superiority over their Ishihara equivalents, plates 7 and 9.

Plates Common to the AO and Meyrowitz Tests

A similar tabulation for plates common to the AO and Meyrowitz is contained in Table VI. In general, the subjects responded with an astonishing variety of numbers to each of the plates in this series. For this reason, this group of plates tends to be considerably more difficult to score than those in Table V. It is also evident that certain plates are not diagnostic, AO plate 2 (Meyrowitz plate 8) being a good example. Nearly 80 percent of the color deficient subjects gave the correct response on the AO plate. Eighty-eight percent of the color deficient and 87 percent of the color normal saw the correct figure on the equivalent Meyrowitz plate, number 8. This plate, therefore, appears to be completely worthless for differentiating the two groups. Other plates which fail to meet the criterion are AO plate 31 (Meyrowitz plate 7) and Meyrowitz plate 5, but not its equivalent AO plate 28. This is the only outstanding difference between comparable plates on the two tests.

Table VII is a compilation of responses to those AO plates which do not appear in the Ishihara or Meyrowitz tests.

Evaluation of AO Test

To sum up the status of the AO test, plates 1, 2, 3, 4, 9, 12, 15, 16, 31, 32, 37, and 38 fail to meet the acceptance criterion established earlier. To this list must be added the three "hidden-digit" plates, numbers 33, 34, and 45. Thus, of the 43 usable plates in this test (plates 25, 26, and 46 are not included since they are read by all but the totally color blind) 15, or 44 percent, are unsatisfactory.

Related Studies on the AO Test

This analysis of individual AO plates agrees fairly well, but not completely, with the findings of other experimenters. Hardy, Rand, and Rittler (16), for example, recommended an abridged version of the AO test consisting of 18 plates. Their series, however, includes plates 3, 4, 9, 12, and 16.

Since they do not present their data in detail, it is not possible to compare their data with those presented here. Gallagher *et al.* (9) first recommended a series of 29 plates which includes plates 1, 2, 3, 4, 9, 15, and 16 and later (10) a series of 10 plates which includes 3, 4, 9, 15, and 16. Examination of the data of their first study, however, indicates essential agreement with those of this study. Using a modified scoring technique to obviate misreading errors, they find that none of their color normal subjects made errors on these plates. But only 15.2 percent of their color deficient subjects failed plates 15 and 16. Comparable figures for plates 1, 2, 3, 4, and 9 are 45.5, 39.4, 51.5, 54.6, and 60.6 percent. Thus, their own data show that these 7 plates

TABLE VII. Responses made by 86 color normal and 34 color deficient subjects to AO plates not listed in Tables III, V, and VI.

Plate No.	Subjects' responses	Color normal	Color deficient
1	—		6
	−0		1
	3−		1
	30		2
	39		4
	69		1
	80		8
	86		1
	88		1
	89	86	9
3	−6		3
	36		5
	56	86	21
	66		2
	86		2
	96		1
4	—		6
	2−		1
	26		1
	27	86	23
	86		1
	87		1
	91		1
7	—		19
	25		1
	28		1
	29		2
	32		1
	36		1
	39	44	1
	89	42	7
	90		1
8	—		22
	−2		1
	−9		1
	22		1
	28		1
	42	85	6
	62	1	
	72		1
	78		1
	—		16
	−6		6
	36		1
	56	85	9
	58	1	
	66		1
	96		1
10	—		30
	27	86	4
14	—		31
	25		2
	75	81	1
	76	5	
15	—		8
	7	86	26
16	—		8
	9	86	26
17	—		26
	25	86	4
	26		3
	29		1
21	—		26
	96		4
	97	86	4
22	—		28
	3−		1
	24		1
	34	82	4
	36	1	
	84	3	
23	—		28
	−6		3
	36		3
	56	85	
	86	1	
24	—		30
	−7		1
	22	2	
	27	83	1
	29	1	
	41		1
	85		1
27	—		32
	54		1
	85		1
	86	1	
	89	85	
29	—		29
	−6		1
	8−		1
	38		1
	86	85	2
	96	1	
30	—	1	33
	15		1
	25	4	
	75	79	
	76	2	
32	—		3
	96	86	31
37	—		9
	−−2		1
	−52		4
	−62		2
	−92		1
	002	1	
	052	79	2
	062	2	
	752		2
	762		1
	852		1
	952	3	9
	962	1	2
38	—		7
	−9−		1
	−94		11
	294	2	3
	394	48	4
	694		1
	894	36	7
39	—	2	33
	23	57	
	25		1
	28	26	
	98	1	
40	—	3	34
	6−	1	
	65	81	
	66	1	
43	—	1	31
	−6		1
	17		1
	27	1	
	44	1	
	46	1	1
	47	81	
	49	1	

TABLE VIII. Responses made by 86 color normal and 34 color deficient subjects to Ishihara plates not listed in Tables III and V.

Plate No.	Subjects' responses	Color normal	Color deficient
10	—		33
	2	86	1
11	—		33
	6	85	1
	8	1	
12	—		21
	13		1
	15		6
	27		2
	31		1
	37	3	1
	57	2	1
	87	15	
	91	1	
	97	65	1
13	—		25
	10		1
	15		3
	19		1
	28		1
	29		1
	45	84	
	46	2	2
14	—		31
	5	86	3
15	—		32
	7	85	2
	9	1	
16	—		31
	15	1	
	16	82	
	18	2	
	35		3
	46	1	
17	—		34
	19	1	
	23	8	
	29	1	
	73	63	
	75	2	
	78	6	
	79	5	
22	—		1
	−6		2
	−8		6
	2−		18
	8−		1
	9−		1
	26	84	4
	28	2	
	66		1
23	—		1
	−2		7
	−9		1
	4−		20
	42	86	5
24	—		2
	−3		1
	−5		8
	3−		6
	5−		5
	8−		4
	9−		3
	33		1
	35	86	1
	39		1
	45		1
	85		1
25	—		3
	−5		2
	−6		8
	3−		3
	8−		3
	9−		12
	36		1
	96	86	2
27	—	10	33
	Line	76	1
28	—	1	34
	Line	85	

are among the 12 worst plates in terms of the percentage of color deficient subjects who could pass them.

Sloan (31) has also recommended an abridged AO test consisting of 17 charts. Only one of the 15 defective plates, according to the present study, plate No. 12, appears in her abridged test. This is also true of the 12-plate test selected for the RCAF. Farnsworth and Reed (7) make no specific recommendations concerning individual plates, but their data show plates 15, 16, and 32 to be the least diagnostic and plates 1, 2, 3, 31, 33, 34, 37, 38, and 45 to be generally poor.

In summary, then, the results of this study agree with most others in finding that AO plates 1, 2, 3, 4, 9, 12, 15, 16, 31, 32, 33, 34, 37, 38, and 45 are unsatisfactory for testing purposes.

Ishihara Test

Table VIII is a compilation of responses to those Ishihara plates which do not appear in the AO test. All of these plates differentiate clearly between the color normal and color deficient. The only Ishihara plates which fail to meet the acceptance criterion are the "hidden-digit" plates in Table III, and plate 5 (Table V). Plates 22 through 25 are diagnostic plates and cannot be analyzed according to our criterion since different kinds of color deviant individuals are supposed to give different responses. These plates will be analyzed separately in a later paper. Thus, of the 30 usable plates in this test (Plates 1 and 32, which are seen by all the totally color blind, are omitted) 7, or 23 percent, are unsatisfactory. Taken as a whole, however, the Ishihara still ranks high since it is second-best only to the Boström-Kugelberg in this study. This conclusion is shared by several other writers (13, 14, 17, 27, 35) who report that the Ishihara is still among the best of the pseudo-isochromatic tests which they have studied.

Meyrowitz Test

Table IX summarizes the data on Meyrowitz plates which are not common to the AO test. In the Meyrowitz test, plates 5 (but not its equivalent AO plate 28), 7 (AO plate 31), 8 (AO plate 2), 9, 10, 19, and 20 fail to meet the criterion. Although plates 13, 15, and 16 are diagnostic plates, they also fall into this category because they are read by so many of the color deviant individuals. A plate cannot be used for diagnosing the type of color deficiency if most color deviants give the same response as the color normal. Since there are 19 usable plates in this test (plates 1, 2, and 29 are read by all but the totally color blind, and plates 30 through 33 are presumably failed only by tritanopic individuals), 10, or 53 percent, are unsatisfactory. This is the worst test of the series in this respect, a finding which is confirmed by the comparison of total scores made by the two groups of subjects (cf. Fig. 8).

Boström Test

Table X shows the responses made to each plate of the Boström test. Plates 1 and 2 are for the detection of malingerers, so that there are only 10 usable plates in this test. Of these, only 1, plate 10, fails to meet the criterion of acceptance. In spite of this low ratio of unsatisfactory plates (10 percent), the test as a whole loses in diagnostic efficiency because there are only nine items which can be used for differentiating the normal from the color deficient. It is generally known that the reliability and validity of any test increases as the number of test items increases, and there is no reason to doubt that the rule should apply equally well to color vision

TABLE IX. Responses made by 86 color normal and 34 color deficient subjects to Meyrowitz plates not listed in Table VI.

Plate No.	Subjects' responses	Color normal	Color deficient
9	6	86	30
	8		4
10	—	3	15
	7	83	18
	9		1
11	—		29
	L	86	3
	22		1
	32		1
12	—		27
	B		1
	L	86	5
	6		1
13	8	86	34
14	—		34
	65	81	
	66	5	
15	—		9
	3		1
	5	86	23
	6		1
16	—		4
	6	86	29
	16		1
17	—		4
	−4		1
	3−		8
	8−		2
	24		1
	33		1
	34	86	11
	36		1
	84		5
18	—		2
	−2		1
	−Z		11
	B−		1
	32		1
	57		1
	82		2
	87		1
	92		2
	97		1
	2Z		2
	B2		1
	BZ	1	2
	RZ	85	5
	SZ		1
19	34		1
	64		1
	014		4
	314		2
	614		10
	OH		3
	6H		1
	CH	81	8
	GH	1	1
	C14	3	3
	CL4	1	
20	—		15
	3	86	6
	8		13
21	2		32
	8	86	2
29	5	86	33
	6		1
30	53	1	
	58	85	33
	168		1
31	45	84	32
	46		2
	65	2	
32	92	86	34
33	—	5	
	2		1
	42	10	1
	43	3	
	48		1
	49	68	31

TABLE X. Responses made by 86 color normal and 34 color deficient subjects to the Boström plates. (Responses of another group of 34 color normal and 5 color deficient are shown in parentheses.)

Plate No.	Subjects' responses	Color normal	Color deficient
1	3	78 (33)	26 (5)
	8	8 (1)	8
2	6	86 (34)	34 (5)
3	—	1 (1)	24 (4)
	2	84 (33)	7 (1)
	8		2
	9	1	1
4	—	(3)	25 (5)
	3		1
	5	86 (31)	8
5	—		22 (3)
	3	80 (29)	3 (2)
	8	6 (5)	9
6	—		24 (3)
	6	86 (34)	9 (2)
	8		1
7	—	2 (5)	24 (5)
	6—		2
	32		1
	62	81 (28)	6
	66		1
	68	1	
	69	1	
	82	1 (1)	
8	—	1 (5)	28(5)
	25	(1)	
	45	1	
	58		1
	65	1	
	85	1	
	93	2 (1)	3
	95	79 (27)	
	98	1	
	99		1
	3—		1
9	—	1 (3)	31 (5)
	9—		1
	00	1	
	06	(1)	
	08	2 (1)	
	62	2	
	66	1	
	68	57 (18)	2
	80	1	
	88	21 (11)	
10	—	8 (12)	33 (5)
	—9	1	
	3		1
	34	1	
	38	1	
	39	40 (14)	
	60	1	
	69	2 (1)	
	80	2 (2)	
	84	1	
	89	28 (5)	
	99	1	
11	—	(2)	30 (3)
	2	86 (32)	2
	8		1 (2)
	29		1
12	—	(1)	28 (4)
	5	86 (33)	5 (1)
	6		1

tests. It would be inefficient, of course, to multiply items indefinitely since the gains drop off after a certain optimum number of items is reached. But it is also apparent that a test must contain a reasonable sample of items to be satisfactory for testing purposes. Additional confirmation on this point comes from the study by Foster (8) who found the Jensen test to be unsatisfactory as compared with the Ishihara and AO test. She concludes that "apparently a 3 or 4 plate test is too unreliable for individual diagnosis," and that "the results of this study suggest, but do not prove, that a color blindness test consisting of a small number of plates may not be valid."

Boström-Kugelberg Test

The Boström-Kugelberg plates (Table XI) are exceptionally good. Only one plate, number 10, of the 17 in this test fails to meet our criterion. This test has a much lower percentage (6 percent) of unsatisfactory plates than any of the others used in this experiment.

Tables X and XI also contain data (in parentheses) obtained on another group of 39 subjects who had been tested about six months prior to this experiment. Five of these subjects were color deficient and 6 of the 34 color normal were women. These data are reported only because they contribute additional observations on the two tests which appear to be new to this country. This inclusion seemed worth while especially since the Boström-Kugelberg turned out to be the best of those evaluated in this study.

VI. THE PROBLEM OF PATTERN DESIGN

Legibility of Numerals

As has already been indicated, a common objection to pseudo-isochromatic tests is that the scoring is not objective. The ideal test would be made of charts which are either read correctly or not at all. Examination of Tables V through XI shows that the subjects responded with a variety of numbers and symbols to most of the plates. Psychologists working with the design of numerals for dials and visual displays have long

known that certain kinds of numeral designs are more easily seen and perceived by the normal individual, and that certain other kinds of numerals and digits are very frequently misread. Often, a considerable increase in the legibility of a number can be achieved by a simple change in its configuration—widening a gap, lengthening a stroke, or replacing a curved segment by a straight one (1, 23). This experience appears to have been lost to the designers of color vision tests, although Murray (25) has pointed out that many of the numerals on pseudo-isochromatic tests, especially the Germanic styles borrowed from the Stilling test, are very confusing. Since the numerals and symbols on the pseudo-isochromatic tests are not solid patterns but are made up of discrete dots, it might be anticipated that the perceptual problem in reading these numbers is even more difficult by virtue of this fact alone.

Scoring Several Responses Correct

One solution, adopted by Gallagher *et al.* (9), is to set up alternative correct responses for each plate. This is not a completely satisfactory solution, since it destroys one of the principal advantages of the pseudo-isochromatic test—its ease of administration and interpretation. Thus, these authors find it necessary to score correct six alternative responses on plate 24 of the AO test; four responses on plates 7, 22, and 29; etc.

Legibility of Numerals on the Various Tests

A measure of the comparative legibility of different numeral designs was obtained by computing the percentage of digit-confusion errors made by the color normal individuals in reading these charts. Only the simple plates, that is, those which do not contain hidden figures or transformation figures, were analyzed. For each test the total number of digits which were read as some other symbol was divided by the total number of digits read. This quotient is the percentage of the numbers which were misread by the 86 color normal subjects.

The Boström test was the worst in this respect; 6.9 percent of the numbers were misread by the color normal. The digits 2, 3, 5, 6, 8, and 9 are used in this test and every one of these was incorrectly named at one time or another. The AO test had the next highest percentage (3.7) of

TABLE XI. Responses made by 86 color normal and 34 color deficient subjects to the Boström-Kugelberg plates. (Responses of another group of 34 color normal and 5 color deficient are shown in parentheses.)

Plate No.	Subjects' responses	Color normal	Color deficient
1	—		28 (5)
	2	86 (34)	4
	3		1
	9		1
2	—		28 (3)
	8	86 (34)	6 (2)
3	—	(1)	32 (5)
	3	1	
	5	85 (33)	1
	X		1
4	—		29 (4)
	2		(1)
	7	86 (34)	3
	23		1
	35		1
5	—		31 (4)
	4	86 (34)	3
	6		(1)
6	—		29 (3)
	3	86 (34)	1 (1)
	8		4 (1)
9	—	2 (1)	33 (4)
	0	82 (33)	
	6		(1)
	25		1
	◇	2	
10	—		15 (2)
	2	1	
	3	81 (34)	10 (1)
	5		1
	8	4	5 (2)
	9		2
	S		1
11	—		25 (3)
	2		(1)
	4	86 (34)	8 (1)
	6		1
12	—	3 (1)	22 (3)
	3		5
	6		1
	8	5 (3)	2 (2)
	9	78 (30)	3
	23		1
13	—		29 (4)
	5	86 (34)	4 (1)
	7		1
14	—	(1)	32 (4)
	0		1
	5		1
	8	2	
	9	84 (33)	(1)
16	—		25 (3)
	5	(1)	
	6	80 (30)	5
	8	6 (3)	4 (1)
	9		(1)
17	—		32 (5)
	2	86 (34)	2
18	—		32 (3)
	0		1
	6	85 (34)	1 (2)
	8	1	
19	—	9	34
	Line	77	
20	—	13	34
	Line	73	

digit-confusion errors. The digits 0, 2, 3, 4, 5, 6, 7, 8, and 9 are used in these plates and every one was misread at least once. The Ishihara test was slightly more legible; 3.0 percent of the digits were misread. Of the digits 1, 2, 3, 4, 5, 6, 7, and 9 used on the Ishihara plates, the 2 and 4 were always read correctly. The Meyrowitz test ranks next with 2.8 percent misreading errors. The digits 2, 3, 4, 5, 6, 7, 8, and 9 are used in these plates; the 4, 6, and 7 were never misread by the color normal. By far the best test in this respect is the Boström-Kugelberg; only 1.5 percent of the errors were due to a digit being called some other digit. Of the digits 0, 2, 3, 4, 5, 6, 7, 8, and 9 in this test, the 2, 4, 7, and 8 were never misread.

No sophisticated analysis is necessary to account for these differences in legibility. The AO test, for example, makes use of flowing, rounded numerals which are often differentiated from each other by only a few dots, e.g., the 3 and 8. The numerals in the Boström-Kugelberg test, on the other hand, are characterized by their large, block design. It is also evident from Table XI that the B-K test as a whole is easy to score. There are very few instances in which the examiner is left in any doubt as to the correctness or incorrectness of the subject's response.

Tracing vs. Reading Numerals

The solution to the problem of digit confusions cannot be solved entirely by having the examinee trace out the digits. Observations on this point are, unfortunately, not complete, but the last 20 color normals tested in this program were subjected to an additional routine. After the plates on all tests had been read once, each examinee was required to read those plates which he had read incorrectly the first time. On the second reading, he was instructed to study the plate very carefully and to trace the digits or symbols which he saw. Digit-confusion errors still persisted in many cases. It appears that the perceptual "set" of the subject influenced even his tracing of the digits.

Summary

The chief value of this analysis has been to show that the design of the plates in these tests is far from perfect. Many designs result in misreading errors which appear to have nothing to do with color vision. It would be a mistake to infer that these errors are due solely to the shapes of the numerals, since Farnsworth and Reed have shown that alteration of the chromas of certain critical dots may reduce some misreading errors (7). But this analysis does show that it is possible to design numerals which will be read correctly or not at all by the great majority of all examinees. The Boström-Kugelberg plates are excellent in this respect. Further careful work by test designers could probably improve even this design.

The Role of Visual Acuity and Age

The digit-confusion errors noted above may provide the basis for a common belief that pseudo-isochromatic tests do not measure color vision at all, but measure visual acuity. Although she does not subscribe to this extreme belief, Murray (25), for example, has pointed out the possible role of visual defects in influencing results obtained with these tests. As has already been indicated, binocular visual acuities for the subjects in this study ranged from 20/10 to 20/50 (corrected visual acuity is measured in the case of those subjects who wore correction). Product-moment correlations between visual acuity and the total score of the five tests of color vision were -0.001 for the color normal subjects, -0.16 for the color deficient subjects, and -0.065 for all subjects together. Correlations between visual acuity and total scores on the RCN lantern were -0.026 for the color deficient subjects and -0.044 for all subjects. The 22 color normal subjects who wore correction received an average score of 117.2 on all of the plates of the five color vision tests. The comparable figure for the 64 color normal subjects who did not wear correction was 117.1. It is quite evident, therefore, that visual acuity cannot be regarded as a significant factor in the test results obtained here.

It might be argued that the problem is not settled, since visual acuity in this study was measured at 20 feet whereas the tests were actually administered at about 30 inches. Correlations between visual acuity tested at far and at near distances tend to be rather low. Sulzman

et al. (34), for example, report a correlation of +0.56 (for 256 subjects) between visual acuity measured at 20 feet and at 14 inches. Another set of data by Giese (11) shows a correlation of +0.53 between visual acuity tested at 1 meter and at 5 meters (distances most comparable to those used in this study). In spite of this fairly low correlation between visual acuity at near and at far distances, it might be anticipated that somewhat higher correlations with test results would have been obtained if acuity is a factor to be reckoned with.

An interesting parallel to this problem comes from a study by Mackworth (23). He found that visual acuity was related to the number of mistakes observers made in reading symbols used for designating air raids on sector maps. More important, however, was his finding that the numbers of mistakes could be significantly reduced for observers with all grades of visual acuity by redesigning the letters and numbers. In many cases only very slight changes—a wider gap for certain letters, a heavier stroke, replacing a curved segment by a straight line—increased legibility markedly. The point of this research is one which should be clear to designers of pseudo-isochromatic tests.

Age and Test Performance

Although it has been suspected that age might also be a significant variable in performance on color tests, there were no significant correlations between age and scores on the tests used in this study. Product-moment correlations between age and performance on the RCN lantern were +0.001 for the color deficient and +0.06 for all subjects; between age and the total number of plates read correctly on the five chart tests, +0.13 for the color deficient, +0.01 for the color normal, and +0.08 for all subjects.

VIII. SUMMARY AND CONCLUSIONS

One hundred and twenty men were tested with 5 pseudo-isochromatic tests of color vision, the American Optical Company, Ishihara, Meyrowitz, Boström, and Boström-Kugelberg tests. In addition, each of the men was examined with the Royal Canadian Navy color vision test lantern. The results obtained on the lantern were used to classify the subjects into two groups: color normal (86 men) and color deficient (34 men). The criterion of color deficiency used in this study, that is, one or more errors on the RCN lantern, was found to correlate very highly with the total number of plates read correctly on the five pseudo-isochromatic tests.

Each of the pseudo-isochromatic tests was evaluated as a whole, and plate-by-plate, in terms of its efficiency for separating the color normal from the color deficient. The tests were also evaluated in terms of the legibility of the numeral design used in the plates. The purpose of this analysis was to discover what kind of numeral design yielded the fewest misreading or digit-confusion errors among the color normal.

The results of this study show:

1. The Boström-Kugelberg test is by far the best all-around test of color deficiency evaluated in this experiment. Scores on the test as a whole differentiate clearly between the color normal and color deficient groups as defined in this study. Individual plates are all highly diagnostic, and the numeral design is excellent. Digits are very seldom misread by color normal subjects.

2. The Ishihara test also tends to be exceptionally good. It differentiates clearly between the color normal and color deficient groups and, with the exception of the "hidden-digit" plates, the plates tend to be individually diagnostic. The numerals are fairly legible.

3. The American Optical Company test differentiates clearly between the color normal and the color deficient subjects, although many of the plates are not diagnostic. The numeral design tends to be very poor. The test as a whole appears to differentiate only because of the large number of plates, about half of which are probably worth keeping.

4. The Boström and the Meyrowitz plates are, in general, unsatisfactory. They do not clearly separate the color deficient from the color normal. Many of the plates are individually non-diagnostic. The numeral design tends to be poor.

5. Visual acuity does not appear to be related to performance on any of the color vision tests.

6. Age is unrelated to performance on any of the tests used in this experiment.

7. When subjects are allowed to make unrestricted responses to the test lights on the Royal

Canadian Navy Lantern, the patterns of responses obtained to each light conform closely to predictions which can be made on the basis of experimental data showing iso-chromatic contours in the I.C.I. diagram.

BIBLIOGRAPHY

(1) C. Berger, "Stroke-width, form and horizontal spacing of numerals as determinants of the threshold of recognition," J. App. Psychol. **28**, 208–231, 336–346 (1944).

(2) C. G. Boström and I. Kugelberg, "Official color sense control in Sweden," Arch. Ophth. **38**, 378–379 (1947).

(3) F. L. Dimmick, "A color aptitude test, 1940 experimental edition," J. App. Psychol. **30**, 10–22 (1946).

(4) F. L. Dimmick and M. R. Hubbard, "An experimental determination of the spectral location of the psychologically unique yellow, green and blue," Am. J. Psychol. **52**, 242–254 (1939).

(5) F. L. Dimmick and M. R. Hubbard, "The spectral components of psychologically unique red," Am. J. Psychol. **52**, 348–353 (1939).

(6) D. Farnsworth, "Farnsworth-Munsell 100-hue and dichotomous tests," J. Opt. Soc. Am. **33**, 568–578 (1943).

(7) D. Farnsworth and J. D. Reed, "Comparison and evaluation of American Optical Company pseudo-isochromatic plates, first and second editions," (Med. Res. Dept., U. S. Submarine Base, New London, Connecticut, March 19, 1945), Color Vision Report No. 8, Project N. L. Sub.-1-CV-16, BuMed X-480 (Av-255-p), 32 pp.

(8) H. Foster, "A comparative study of three tests for color vision," J. App. Psychol. **30**, 135–143 (1946).

(9) J. R. Gallagher, C. D. Gallagher, and A. E. Sloane, "A critical evaluation of pseudo-isochromatic plates and suggestions for testing color vision," Yale J. Biol. Med. **15**, 79–98 (1942).

(10) J. R. Gallagher, C. D. Gallagher, and A. E. Sloane, "A brief method of testing color vision with pseudo-isochromatic plates," Am. J. Ophth. **26**, 178–181 (1943).

(11) W. J. Giese, "The interrelationship of visual acuity at different distances," J. App. Psychol. **30**, 91–106 (1946).

(12) E. L. Green, and L. L. Sloan, "Two criteria for the selection of color vision test plates," J. Opt. Soc. Am. **35**, 723–730 (1945).

(13) LeG. H. Hardy, G. Rand, and M. C. Rittler, "Tests for the detection and analysis of color-blindness. I. The Ishihara test: an evaluation," J. Opt. Soc. Am. **35**, 268–275 (1945); also Arch. Ophth. **34**, 295–302 (1945).

(14) LeG. H. Hardy, G. Rand, and M. C. Rittler, "Tests for the detection and analysis of color-blindness. II. The Ishihara test: comparison of editions," J. Opt. Soc. Am. **35**, 350–356 (1945); also Arch. Ophth. **35**, 109–119 (1946).

(15) LeG. H. Hardy, G. Rand, and M. C. Rittler, "Tests for the detection and analysis of color-blindness. III. The Rabkin test," J. Opt. Soc. Am. **35**, 481–491 (1945); also Arch. Ophth. **35**, 251–270 (1946).

(16) LeG. H. Hardy, G. Rand, and M. C. Rittler, "A screening test for defective red-green vision," J. Opt. Soc. Am. **36**, 610–614 (1946).

(17) LeG. H. Hardy, G. Rand, and M. C. Rittler, "The Ishihara test as a means of detecting and analyzing defective color vision," J. Gen. Psychol. **36**, 79–106 (1947).

(18) D. B. Judd, "A Maxwell triangle yielding uniform chromaticity scales," J. Opt. Soc. Am. **25**, 24–35 (1935).

(19) D. B. Judd, "Estimation of chromaticity differences and nearest color temperature on the standard 1931 ICI Colorimetric Coordinate System," J. Opt. Soc. Am. **26**, 421–426 (1936).

(20) D. B. Judd, "Standard response functions for protanopic and deuteranopic vision," J. Research Nat. Bur. Stand. **33**, 407–437 (1944); also J. Opt. Soc. Am. **35**, 199–221 (1945).

(21) D. Katzin and E. Murray, "Instability in color-naming in normal and anomalous observers," Am. J. Psychol. **46**, 611–620 (1934).

(22) D. L. MacAdam, "Visual sensitivities to color differences in daylight," J. Opt. Soc. Am. **32**, 247–274 (1942).

(23) N. H. Mackworth, "Legibility of raid block letters and numbers," (Flying Personnel Res. Com., Psychol. Lab., Univ. Cambridge, April, 1944), Report No. FPRC 423(s), Vol. 4242, 18 pp.

(24) E. Murray, "Evolution of color vision tests," J. Opt. Soc. Am. **33**, 316–334 (1943).

(25) E. Murray, "Color vision tests," in Glasser, O. (Ed.) *Medical Physics* (Year Book Publishers, Chicago, 1944), pp. 275–282.

(26) F. R. Neubert, "Colour vision in the consulting room," Brit. J. Ophth. **31**, 275–288 (1947).

(27) B. R. Philip, "A comparison of color-blind tests," Am. J. Psychol. **51**, 482–488 (1938).

(28) F. H. G. Pitt, "Characteristics of dichromatic vision," Spec. Rep. Ser. Med. Res. Coun. Lond., No. 200 (1935).

(29) J. D. Reed, "An evaluation of the Royal Canadian Navy color vision lantern for use in routine testing of color vision in a large organization," (M. S. Thesis, Brown University, 1944), pp. 52+xvi.

(30) S. Ross and C. G. Mueller, "Comparison and evaluation of the 'pseudo-isochromatic plates for testing of color perception,' American Optical Company, second edition with the first edition now in general use by the United States Navy" (Med. Field. Res. Lab., Camp Lejeune, No. Carolina, August 13, 1945), M and S Research Project No. X-480 (Av-255-p).

(31) L. L. Sloan, "An improved screening test for red-green color deficiency composed of available pseudo-

isochromatic plates," J. Opt. Soc. Am. **35**, 761–766 (1945).
(32) L. L. Sloan, "Selection of color vision tests for the Army Air Forces: A summary of studies made at the Army Air Forces School of Aviation Medicine," Arch. Ophth. **36**, 263–283 (1946).
(33) J. H. Sulzman, "Comparison and evaluation of American Optical Company pseudo-isochromatic plates, first and second editions" (Med. Res. Dept., U. S. Submarine Base, New London, Connecticut, July 16, 1945), Project X-480 (Av-255-p), 16 pp.
(34) J. H. Sulzman, E. B. Cook, and N. R. Bartlett, "The reliability of visual acuity scores yielded by three commercial devices," J. App. Psychol. **31**, 236–240 (1947).
(35) G. J. Thomas, "Visual sensitivity to color: a comparative study of four tests," Am. J. Psychol. **56**, 583–591 (1943).
(36) J. A. Van den Akker, J. E. Todd, P. Nolan, and W. A. Wink, "Use of a monochromatic colorimeter for the study of color blindness," J. Opt. Soc. Am. **37**, 363–387 (1947).

Erratum: The Relation between Efficiency and Exciting Intensity for Zinc-Sulfide Phosphors

[J. Opt. Soc. Am. **38**, 60 (1948)]

H. A. KLASENS, W. RAMSDEN AND CHOW QUANTIE
Material Research Laboratory, Philips Lamps, Ltd., London, England

WE omitted to mention that for each curve in Figs. 3, 4 and 6 the values of I at $J=1$ have been reduced to unity. Thus by calculating line D of Fig. 7 from the slopes of Fig. 6 the relative values of I at the highest exciting intensity $J=1$ have to be taken into account in the same way as has been done in deriving Fig. 5 from Fig. 3. For the phosphor with 4.10^{-4} percent Co these relative values were:

T	−186°	0°	20°	40°C
$I_{J=1}$	1	0.92	0.70	0.16

For the phosphor with 10^{-4} percent Co the relative values of I at the highest exciting intensity were:

T	−186°	20	57	100
$I_{J=1}$	0.97	0.87	0.425	0.100

Letters to the Editor

The Applicability of Judd's Color Tolerance Formula in the Case of Titanium Pigments

ARTHUR C. HARDY
Massachusetts Institute of Technology, Cambridge, Massachusetts
(May 24, 1948)

JACOBSEN'S paper[1] in the May issue of this journal attempts to prove the inapplicability of the I.C.I. system of color specification to the special case of certain white pigments. As evidence, the author computes the standard I.C.I. specification for a sample of anatase and a sample of rutile. Then, using Judd's empirical color tolerance formula for textiles,[2] he calculates that there should be only two perceptible color steps between anatase and rutile, whereas the visual grading of mixtures of the two pigments reveals seven perceptible steps.

It would seem that this paper might have been more appropriately titled, "The applicability of Judd's color tolerance formula in the case of titanium pigments." Such a title would have suggested an immediate explanation for the apparent disparity. In evolving this color tolerance formula, Judd introduced an arbitrary constant to make the unit color difference "of such size that smaller differences can be neglected in the average commercial transaction." The drawdown test commonly used in the comparison of pigment colors undoubtedly provides the observer with a better photometric field than when comparing two textile swatches. As a consequence, color differences that are commercially acceptable in the textile industry should be easily perceived in a comparison of two pigments.

There is a further possibility that the visual gradings to which the author refers were carried out under an illuminant containing a proportionately greater amount of violet light than does Illuminant *C*. The author's spectrophotometric curves show that, at 390 mμ, the spectral reflectances of rutile and anatase are 15 percent and 63 percent, respectively. On the other hand, their spectral reflectances are substantially the same from 430 mμ to 700 mμ. It follows that these pigments should be indistinguishable under a violet-deficient source, but should be conspicuously different under violet light.

[1] A. E. Jacobsen, J. Opt. Soc. Am. **38**, 442 (1948).
[2] D. B. Judd, Textile Research **9**, 253 (1939).

Visual Performance and the Surround

PARRY MOON
Massachusetts Institute of Technology, Cambridge, Massachusetts
AND
DOMINA EBERLE SPENCER
Brown University, Providence, Rhode Island
(May 13, 1948)

IN a recent paper,[1] Simonson and Brozek have reported their experimental results on "optimum illumination." This subject bothered lighting experts in the early part of the century but may now be considered dead. There are two reasons for the change in attitude:

(1) A realization that, in the pharosage range commonly used, *quality* of lighting is more important than quantity.
(2) A knowledge that, with proper quality, *there is no optimum quantity*: the more light, the better the vision.

Simonson and Brozek employed the visual task of recognition of small letters presented on a moving belt behind a slit.[2] The test objects were lighted by means of concentrated sources shielded from direct view of the subject, and the incident pharosage was varied from approximately 20 to 3000 lumen m^{-2}. The results shown an increase in performance up to 1000 lumen m^{-2} and a small but significant drop above 1000 lumen m^{-2}.

This is exactly the effect to be expected if the visual surround is darker than the immediate background of the test object or if there is any reflected glare. Strangely enough, Simonson and Brozek seem to have made no attempt to produce a uniform visual field or to determine the actual helios distribution employed in their research.[1,2] In ignoring this important factor, they make their whole investigation of very questionable value.

König[3] made a similar mistake in 1888, as did Carmichael and Dearborn[4] in 1947. But as a pioneer in the subject, König had an excuse. Since then, the able investigations of Lythgoe,[5] Stiles, Crawford,[6] Hecht, Shlaer,[7] and others[8] have proved, as definitely as anything can be proved, that in a uniform field there is no such thing as an "optimum illumination." Simonson and Brozek[1] refer to none of these investigations.

Psychologists and physiologists are less prone than engineers to neglect human idiosyncracies as factors in visual performance, but they are more likely to ignore important physical details. There is great need for further visual research, but if this research is to be of value it must be performed with *all* independent variables under control. One of the most important of these variables is the helios distribution in the surround.

[1] E. Simonson and J. Brozek, J. Opt. Soc. Am. **38**, 384 (1948).
[2] J. Brozek, E. Simonson, and A. Keys, J. App. Psychol. **31**, 519 (1947).
[3] A. König and E. Brodhun, Akad. Wissen, Sitzungsber., Berlin, 1888, 917; 1889, 641.
[4] L. Carmichael and W. F. Dearborn, *Reading and visual fatigue* (Houghton Mifflin Company, Boston, 1947).
[5] R. J. Lythgoe, *The measurement of visual acuity* (Med. Res. Council Report of Committee upon Physiology of Vision, London, 1932).
[6] W. S. Stiles and B. H. Crawford, Roy. Soc. Proc. **116B**, 55 (1934); *ibid.* Roy. Soc. Proc. **113B**, 496 (1933); W. S. Stiles, Roy. Soc. Proc. **104B**, 322 (1929); W. S. Stiles and C. Dunbar, Illum. Res. Tech. Paper No. 16 (London, 1935).
[7] S. Shlaer, J. Gen. Physiol. **22**, 165 (1937); S. Hecht and E. U. Mintz, J. Gen. Physiol. **22**, 593 (1939); Shlaer, Smith, and Chase, J. Gen. Physiol. **25**, 533 (1942).
[8] P. W. Cobb, J. Exper. Psychol. **1**, 540 (1916); P. W. Cobb and F. K. Moss, J. Franklin Inst. **199**, 507 (1925); *ibid.*, J. Exper. Psychol. **10**, 350 (1927); M. Luckiesh and F. K. Moss, I. E. S. Trans. **34**, 571 (1939).

Minutes of the Thirty-First Meeting of the Board of Directors of the Optical Society of America, Incorporated

HOTEL PENNSYLVANIA, NEW YORK, NEW YORK, MARCH 3, 1948

IN addition to the transaction of routine business, the following items of general interest to members of the Society were considered.

Announcements by Secretary

Under authority conferred by a previous Board, the President and Secretary had appointed Herbert E. Ives and George W. Moffitt proxies for the Optical Society of America at the annual meeting of the American Institute of Physics, held on February 28, 1948.

Results of letter ballots:

1. Approval of resolution to appoint the U. S. National Committee of the International Commission on Optics (I. C. O.).

2. Approval of appointment of Rudolf Kingslake, Chairman, I. C. Gardner, Max Herzberger, H. E. Ives, and Mary Warga as members of the U.S.N.C. of the I.C.O.

3. Approval of appointment of Ralph A. Sawyer, Chairman, G. M. Rassweiler, Vice Chairman, George Nahstoll, Dorothy Nickerson, A. F. Turner, Mary Warga, and Norman Wright as members of the Program Committee for the 1948 Annual Meeting.

4. Approval of appointment of the following committees:

Adolph Lomb Memorial Fund Committee

A. G. Worthing, *Chairman*	L. O. Grondahl
Stanley S. Ballard	Elmer Hutchisson
Walter W. Graeper	Dorothy Nickerson

Adolph Lomb Medal Committee

G. H. Dieke, *Chairman*	H. K. Hartline
I. R. Bowen	L. R. Ingersoll
Bruce Billings	Brian O'Brien

5. Approval of resolution to hold 1948 annual meeting at the Fort Shelby Hotel, Detroit, Michigan, on October 21, 22, and 23.

6. Approval of resolution to authorize Treasurer to withdraw funds deposited with Security Trust Company of Rochester, New York.

7. Approval of appointment of B. H. Carroll and E. H. Greppin as Auditors for the accounts of the Optical Society of America, Inc.

Appointments

L. T. Steadman was appointed alternate to B. H. Carroll and E. H. Greppin, Auditors for the accounts of the Optical Society of America, Inc.

E. O. Hulburt was appointed to succeed himself as O.S.A. Representative to the American Association for the Advancement of Science for a term to expire in February, 1950.

Future Meetings of the Society

The next winter meeting of the Optical Society will be held at the Hotel Pennsylvania, New York, New York, on March 10, 11, and 12, 1949. The Secretary was instructed to investigate open schedules at the Hotel Statler in Buffalo (with Pittsburgh as an alternate) and to make tentative reservations for the annual meeting in 1949.

ARTHUR C. HARDY, *Secretary*

Annual Report of the Editor of Publications

STATEMENT OF OPERATIONS OF THE JOURNAL OF THE OPTICAL SOCIETY OF AMERICA FOR THE YEAR ENDING DECEMBER 31, 1947

Income		
Non-member subscriptions	$10,925.26	
Net income from published articles	2,692.16	
Net income from sale of back numbers	4,655.17	
Total Income Exclusive of Member Subscriptions		$18,272.59
Expense		
Printing and mailing	$17,534.67	
Engraving	3,460.01	

Editorial mechanics at A. I. P.:		
Salaries	$1,839.78	
Office expense	388.43	2,228.21
Subscription expense:		
Salaries	$1,712.13	
Office expense	345.81	2,057.94
Other expenses		73.59
Editorial office, Cambridge:		
Salaries	$1,250.00	
Expenses	128.47	1,378.47
Total Cost of Editing and Publishing Journal		$26,732.89
Net Cost of Operating Journal and Furnishing it to Members		8,460.30

(Signed) GEORGE R. HARRISON, *Editor*

Annual Report of the Secretary of the Optical Society of America, Inc., for the Calendar Year 1947

MEMBERSHIP RECORD
JANUARY 1, 1947 TO JANUARY 1, 1948

	Honorary	Regular Emeritus	Associate Emeritus	Regular Life Payment	Associate Life Payment	Regular Annual Payment	Associate Individual Annual Payment	Associate Corporation	Student	Total
Membership as of record in the books of the Secretary 1/1/47	3	18	1	10	1	576	982	30	12	1633
Gains during 1947										
By election as of 1/1/47	0	0	0	0	0	0	106	1	30	137
By election as of 1/1/48	0	0	0	0	0	0	28	0	1	29
By reinstatement	0	4	0	0	0	1	14	0	1	20
By transfer on 10/22/47	0	0	0	0	0	34	0	0	0	34
By transfer to Associate Membership	0	0	0	0	0	0	2	0	0	2
Losses during 1947										
By death	0	0	0	0	0	3	0	0	0	3
By resignation as of 1/1/47	0	0	0	0	0	5	17	0	0	22
By resignation as of 12/31/47	0	0	0	0	0	6	21	0	0	27
By transfer on 10/22/47	0	0	0	0	0	0	34	0	0	34
By transfer to Associate Membership	0	0	0	0	0	0	0	0	2	2
By separation for Non-payment of Dues	0	0	0	0	0	8	32	0	0	40
By failure to renew student membership status	0	0	0	0	0	0	0	0	23	23
Membership as of 1/1/48	3	22	1	10	1	589	1028	31	19	1704

New Members

Elected during 1947 as of January 1, 1947

Abbitt, W. H. (2611 A)
Accardo, Carl A. (2682 S)
Anderson, Karl R. (2683 S)
Bannon, Robert E. (2584 A)
Bartlett, Neil R. (2620 A)
Benson, Nels, C. (2674 A)
Bickford, L. R., Jr. (2649 S)
Birkel, George, Jr. (2702 A)
Blout, Elkan R. (2621 A)
Braden, John (2681 A)
Braun, Ben (2622 A)
Britton, Wm. C. (2578 S)
Brocklehurst, R. E. (2678 A)
Carls, Robert J. (2656 A)
Carpenter, Robert (2709 A)
Cary, Donald S. (2623 S)
Castor, L. N., Jr. (2589 S)
Chandler, Alfred B. (2705 A)
Charles, George W. (2586 A)
Chess, James S. (2612 A)
Clark, Albert, Jr. (2712 A)
Clark, David G. (2613 A)
Clay, Cassius M. (2590 S)
Cooke, Frank (2624 A)
Cutler, Monarch L. (2659 A)
Davis, Faurest (2596 A)
Davis, George E. (2604 A)
Davis, Harry Floyd (2655 S)
Davis, Richard H. (2654 S)
Debenham, Jack K. (2657 A)
Dixon, Leslie G. (2685 A)
Doller, Samuel (2676 A)
Dreyer, John F. (2703 A)
DuBois, William J. (2660 A)
Duran, D. Armando (2713 A)
Edwards, Hiram W. (2675 A)
Elden, Richard E. (2689 A)
Engelson, Howard R. (2673 A)
Enns, J. H. (2701 A)
Fast, Edwin (2618 A)
Feldman, Cyrus (2648 A)
Fowler, Richard C. (2692 A)
Gardner, Edward E. (2591 S)
Gayhart, E. L. (2700 A)
Ghosh, Chandra S. (2582 A)
Gillis, Ronald C. (2598 S)
Goodbar, Isaac (2625 A)
Gramm, Charles F. (2626 A)
Gray, W. M. (2661 A)
Green, Milton (2627 A)
Hallowell, A. Lincoln (2628 A)
Harding, Samuel W. (2614 A)
Harris, Clyde W. (2684 A)
Haskell, Stanley W. (2629 S)
Hawley, Mones E. (2579 S)
Henninger, John H. (2630 A)
Hill, N. D. (2696 A)
Howland, Walter A. (2652 A)
Huxford, W. S. (2605 A)
Hyde, W. Lewis (2691 A)
Jacobson, Woodrow R. (2679 A)
Johnston, Robert W. B. (2631 A)
Jordan, Joseph, Jr. (2594 S)
Josephson, Raydelle (2706 A)
Kanwisher, John (2588 S)
Keuper, Jerome P. (2601 S)
Kinder, John F. (2583 A)
Krasner, Paul R. (2632 S)
Kruegel, Shea LaBonte (2715 A)
Lee, James H. (2662 A)
Leurgans, Paul J. (2600 A)
Lonergan, Ann (2688 A)
Lord, Bradley (2633 A)
Lovoff, Adolph (2663 A)
Loutfallah, Michel (2634 A)
Lucht, Vivian M. (2653 A)
Magill, Lincoln C. (2587 S)
Martin, Alfred E. (2635 A)
Mayne, Robert H. (2610 S)
McCartney, John S. (2732 A)
McGreevy, Joseph M. (2636 A)
Meissner, K. W. (2734 A)
Miley, H. A. (2686 A)
Miller, Charles G. (2717 A)
Monahan, Thomas I. (2637 A)
Mote, F. A. (2698 A)
Murch, Harold L. (2576 A)
National Aniline Div., Allied Chem. & Dye Corporation (2580 AC)
Neuberger, Hans (2664 A)
Nierenberg, Richard N. (2638 A)
Oszy, Alexander J. (2639 A)
Otero, Jose M. (2714 A)
Palmer, M. W. (2665 A)
Perkins, Willis D. (2640 S)
Petersen, Max (2641 A)
Pickett, Edward E. (2707 A)
Policoff, William A. (2617 A)
Putnam, Thomas E. (2592 S)
Rao, C. S. (2651 A)
Rauch, Seymour (2695 A)
Rogers, Harry L., III (2650 S)
Rosenblum, Lewis (2615 A)
Sable, Arthur J. (2642 S)
Sackett, J. Warren (2690 A)
Sampson, Donald K. (2643 S)
Sanderson, J. A. (2606 A)
Sansonetti, S. John (2602 A)
Saxenian, Hrand (2609 S)
Sayre, W. R. (2731 A)
Schaffner, Frederick Q. (2666 A)
Serfass, Earl J. (2694 A)
Sharo, Ernest (2577 A)
Shuck, Lowell M. (2667 A)
Siganowick, John (2668 A)
Smith, Lee (2593 A)
Smuck, Howard J. (2644 S)
Steiger, W. R. (2608 S)
Steingiser, Samuel (2645 A)
Taylor, A. (2687 A)
Taylor, Philip H. (2733 A)
Templin, Herman A. (2599 A)
Thompson, Melville (2585 A)
Thorndon, Vernon (2607 A)
Tolle, Karl (2647 A)
Triller, Wendell (2680 A)
Ullrich, O. A. (2669 A)
Vasicek, Antonin (2670 A)
Verplanck, William (2671 A)
Wehe, H. G. (2646 A)
White, Locke, Jr. (2616 A)
Williams, Philip (2597 S)
Winnek, Douglas F. (2595 A)
Woodman, J. F. (2603 A)
Woodruff, J. F. (2619 A)
Young, F. Mansfield (2581 S)
Zimmerly, Ray A. (2658 A)
Zito, Ralph, Jr. (2721 S)

Elected during 1947 as of January 1, 1948

Best, William G. (2724 A)
Bloem, Harold H. (2735 A)
Bomke, H. A. (2720 A)
Chapanis, Alphonse (2719 A)
Coleman, Madeline F. (2677 A)
Curcio, Joseph (2716 A)
Derksen, Willard (2736 A)
Elmstrom, George P. (2723 A)
Epstein, L. Ivan (2704 A)
Fassel, Velmer A. (2726 A)
Feldman, Sidney (2729 A)
Field, Norman J. (2737 A)
Gatterer, Alois, S. J. (2699 A)
Hayes, John D. (2738 A)
Howerton, H. K. (2710 A)

Keene, Lester F. (2739 A)
Korbel, Harold (2728 A)
Lueck, Irving B. (2718 A)
Minkler, Marcus W. (2697 S)
Nolan, Philip (2725 A)
Pellissier, George (2727 A)
Price, George R. (2740 A)
Price, William P. (2741 A)
Redies, M. F. (2730 A)
Schepler, Herman C. (2708 A)
Shreve, O. Davis (2693 A)
Sitterly, Charlotte (2722 A)
Warsen, W. (2711 A)
Wilke, John H. (2742 A)

Associate Members

Elected to Regular Membership by Action of the Board of Directors October 22, 1947, effective as of January 1, 1948

Anderson, Scott
Ashley, Samuel E. Q.
Bartlett, Neil R.
Beardsley, Niel F.
Brown, Earle B. Brown
Bryan, Ford R.
Bryant, W. M. D.
Clarke, Richard G.
Cook, Ellsworth B.
Davis, George E.
Downing, Joseph R.
Eaton, William W.
Edgar, William J.
Goodbar, Isaac
Hemmendinger, Henry
Howlett, L. E.
Hughes, Harold Kenneth
Ingalls, Arthur L.
Leverenz, H. W.
Liddel, Urner
Lord, Richard C.
Loutfallah, Michel
Nusbaum, R. E.
O'Neil, Frank J.
Petersen, Max
Polster, Harry D.
Riggs, Lorrin A.
Rozsa, J. T.
Sanderson, John A.
Scofield, Francis
Steadman, F. M.
Sziklai, George C.
Whitney, Will A.
Woodruff, J. F.

Student Members

Transferred to Associate Membership as of January 1, 1948

Anderson, Karl R.
Clapper, F. R.

Deaths Reported During 1947

Hecht, Selig (648 R)
Higbie, H. H. (433 R)
Urbach, Charles (1455 R)

Annual Report of the Treasurer of the Optical Society of America

Cash Transactions January 1, 1947 to December 31, 1947

Receipts

Dues	$ 5,557.92	
Dues in Advance	6,145.24	
Income from unallocated securities	1,613.64	
Income from Ives Medal Fund	12.50	
Income from Adolph Lomb Fund	50.00	
Income from Special Interest Account	25.01	
Total Receipts		$13,404.31

Disbursements

Journal Publication Expense	4,141.39
Journal Editorial Expense	1,348.80
Secretary's Expense	1,611.31
Secretary's Travel Expense	59.50

Treasurer's Expense	553.89	
Meetings & Programs	833.56	
Ives Medal	21.07	
Contributions to the support of other organizations		
American Institute of Physics	1,645.05	
Inter-Society Color Council	25.00	
U.S.N.C. of the I.C.I.	100.00	
Total Normal Expenditures		10,339.57
Excess of Receipts over Normal Expenditures		$ 3,064.74
Special Appropriations		
Reprinting Journals	1,770.80	
Past Presidents' Gavels	177.47	
Investments	6,822.98	
		8,771.25
Excess of Total Disbursements over Receipts		$ 5,706.51

Balances December 31, 1946

Unallocated cash	$10,716.74	
Ives Medal Fund	137.50	
Adolph Lomb Memorial Fund	181.13	
		$11,035.37
Cash Balance, December 31, 1947		$ 5,328.86

Ives Medal Fund

Income

Principal	$ 500.00	
Interest balance, January 1, 1947	137.50	
Interest accrued during 1947	12.50	
Total		$ 650.00

Disbursements

Medal for Wm. F. Meggers	21.07	21.07
Balance December 31, 1947		$ 628.93

Note: The principal sum of $500.00 is invested in Series G War Bonds. They are included in the bonds reported in the accompanying Investment Statement.

Adolph Lomb Memorial Fund

Income

Principal	$ 2,000.00	
Interest balance January 1, 1947	181.13	
Interest accrued during 1947	50.00	
Total		$ 2,231.13

Disbursements

None	0.00	0.00
Balance, December 31, 1947		$ 2,231.13

Note: The principal sum of $2,000 is invested in Series G War Bonds. They are included in the bonds reported in the accompanying Investment Statement.

Investments

Investment portfolio with market value of securities as of December 31, 1947.

		Book Value	Market Value	Annual Income
9M	U. S. Treasury Bonds 2¼%	$ 9,088.14	$ 9,090	$ 202.50
11.6M	U. S. War Savings Bonds Series "G" 2½%	11,600.00	11,600*	290.00
5M	Atch. Top. & Santa Fe 4% Gen. Mtge. 1995	5,000.00	5,800	200.00
2M	Interstate Power Co. 1st Mtge. 5%	2,026.50	1,990	100.00
3M	Consolidated Cigar Corp. S. F. Deb. 3¼%	3,137.25	2,970	97.50
15 Shares	El Paso Natural Gas Co. Cum. Pfd. $4.10	1,636.50	1,425	61.50
30 Shares	20th Century Fox Film Corp. Pr. Pref. $4.50	3,077.80	2,820	135.00
20 Shares	Philip Morris & Co., Ltd. Cum. Pfd. 4%	2,173.70	1,780	80.00
75 Shares	Indianapolis Power & Light Co. Common	2,543.81	1,593	105.00
50 Shares	National Lead Co. Common	1,605.79	1,744	75.00
50 Shares	Eastman Kodak Co. Common	1,718.19	2,238	70.00
65 Shares	General Electric Co. Common	2,544.23	2,324	104.00
35 Shares	Kennecott Copper Corp. Capital	1,729.53	1,706	105.00
40 Shares	Standard Oil Co. of N. J. Capital	2,262.72	3,175	160.00
		$50,154.16	$50,255	$1,785.50
	Average yield			3.55%

* Maturity value.

The undersigned, having been duly appointed to audit the books of the Treasurer of the Optical Society of America, Inc., from January 1, 1947 to December 31, 1947, hereby certify that the Treasurer's report of receipts and disbursements is correct as shown by records, vouchers, bank statement, etc., and that his accounts check accurately with vouchers and bank statements.

(Signed) B. H. CARROLL, L. T. STEADMAN, *Auditors*

Proceedings of the Winter Meeting of the Optical Society of America

HOTEL PENNSYLVANIA, NEW YORK, NEW YORK, MARCH 4, 5, AND 6, 1948

THE regular winter meeting of the Optical Society of America was held at the Hotel Pennsylvania in New York City on March 4, 5, and 6. The total registration was 528; all of the eight separate sessions were well attended.

The two sessions on March 4 were devoted to contributed papers on spectrophotometry and colorimetry, following an introductory invited paper on "The Early History of Recording Spectrophotometry," by Arthur C. Hardy. On Friday, March 5, there were two invited symposia and also several contributed papers. The invited papers by H. C. Hottel of the Massachusetts Institute of Technology and G. H. Dieke of Johns Hopkins University dealt with optical and spectroscopic methods for the measurement of flame temperature. Three invited papers described the role of wind tunnel optics and interferometry, and the Schlieren method of shock wave analysis; the speakers were R. Ladenburg of Princeton University, F. J. Weyl of the Office of Naval Research, and R. B. Kennard of the Naval Ordnance Laboratory. On Saturday, there were simultaneous sessions, morning and afternoon, of contributed papers on infra-red and spectroscopy and on geometrical and general optics. The program included a total of 56 papers.

The dinner on Firday night was attended by 260 members and guests. The principal speaker was Dr. L. R. Hafstad, Executive Secretary of the Research and Development Board of the National Military Establishment, who gave a succinct description of the aims, purposes, and activities of his organization. This was followed by "a novel unrehearsed program of instruction and/or entertainment," which set a new record for hilarity at these sometimes staid gatherings. This was the "Optical Quiz Program," which was ably administered by Interlocutor George R. Harrison, who elicited from his panel of experts a number of surprising answers to some searching questions on the fact and fantasy of optics. The experts included R. Bowling Barnes, Wallace R. Brode, Deane B. Judd, Edwin H. Land, William F. Meggers, Brian O'Brien, Ralph A. Sawyer, and Mary E. Warga.

PLACEMENT REGISTER

The files of the American Institute of Physics' Placement Service Register were available at the meeting for examination, and this opportunity was taken advantage of by about seventy possible employers and employees.

CONTRIBUTED PAPERS

The abstracts of the contributed papers are appended.

MEETING OF THE BOARD OF DIRECTORS

A meeting of the Board of Directors was held on Wednesday, March 3. The minutes of this meeting appear on page 651 of this issue.

STANLEY S. BALLARD, *Chairman*
Program Committee

Program of Sessions

Titles and Abstracts of Papers

Papers on Spectrophotometry and Colorimetry

1. Invited paper, entitled "The Early History of Recording Spectrophotometry," BY ARTHUR C. HARDY, *Massachusetts Institute of Technology.*

2. Some Techniques and Accessories to Facilitate the Application of a G.E. Recording Spectrophotometer. E. E. RICHARDSON, *Kodak Research Laboratories.*

Fiducial marks for quickly placing the graph paper, a method for checking wave-length, a system for cooling the

light source, a convenient provision for replacing lamps, and an air drying unit attached to the amplifier will be described. A modified integrating sphere and its complete assembly having two hemicylindrical tubes with a portion extending from the split lenses to the sphere wall offer a means of making transmittance (total and specular) and reflectance (total and diffuse) measurements, and reduce stray-light errors in testing the transmittance of interference filters and fluorescent filters and solutions. Aluminum plates for supporting MgO surfaces, plates for the specular ports and specular light traps will be described. A prism system has been constructed for testing small areas in the center of transparent objects 8 inches square and 5 inches in length and the axial area of lenses, especially photographic objectives. With this system reflectance can be measured at 45 degrees, with light polarized in the plane of incidence. Accessories are used for measuring the transmittance at oblique angles for polarization both in and perpendicular to the plane of incidence. A method for testing small areas without and with auxiliary lenses, a means of increasing the wave-length range from 425 to almost 1000 mμ, and its wave-length calibration will be explained.

3. Standards of Reflectance. HARRY J. KEEGAN, *National Bureau of Standards.*

In 1931, the International Commission on Illumination adopted a resolution (3a) which may be translated as follows: "For the colorimetric measurement of opaque materials the luminance of the specimen studied ought to be expressed as a function of the luminance of a surface of the oxide of magnesium considered under the same conditions of illumination and observation."[1] Accordingly, the National Bureau of Standards further developed its technique for the preparation of MgO from freely burning magnesium turnings and published an NBS Letter Circular, present number LC-547, describing the advantages and disadvantages of such a standard.[2] Reference is made to this procedure in three engineering test method specifications: (a) the spectral characteristics and color of objects and materials,[3] (b) a colorimetric test for pulp,[4] and (c) certain spectrophotometric and colorimetric test methods for paint, varnish, lacquer, and related materials.[5] Although magnesium-oxide standards of reflectance are widely accepted in principle, it is understood that relatively few laboratories follow a technique of preparation that will yield the most accurately reproducible standards. The details of the technique developed at the National Bureau of Standards will be shown, together with calibrations of a working standard of reflectance made of machine-ground and polished white glass. These repeated calibrations made over a period of about 10 years show, from the minor random fluctuations, the degree to which the successively prepared magnesium oxide standards are reproducible. The maximum spread in spectral reflectance is about 0.5 percent. The calibrations also show from the lack of a significant regular trend in these fluctuations that the master working standard is permanent to a degree even exceeding the best reproducibility that we have been able to obtain with magnesium oxide; and it is, of course, far more permanent than magnesium oxide, which may yellow by a detectable amount within one day after preparation. The Bureau is now prepared to issue reflectance standards of fire-polished white glass calibrated by comparison with the master standards. These standards of spectral reflectance are available both to public and private agencies for spectrophotometry and colorimetry.

[1] Proceedings, Eighth Session, Commission Internationale de l'Eclairage, Cambridge, England, p. 23, September, 1931.
[2] "The preparation and colorimetric properties of a magnesium-oxide standard of spectral apparent reflectance," Letter Circular NBS. LC-547; March 17, 1939.
[3] American Society for Testing Materials. "Standard method of test for spectral characteristics and color of objects and materials." ASTM D-307-44.
[4] Technical Association of the Pulp and Paper Industry. "Spectral reflectivity and color of pulp." TAPPI T216m-42.
[5] Federal Standard Stock Catalog, Section IV (Part 5), "Federal specification for paint, varnish, lacquer, and related materials; general specification for sampling and test methods." TT-P-141a, pp. 37 and 43, June 16, 1944.

4. A Method for Calculating the Dominant Wave-Length of a Dichroic Amber Glass for any Thickness. J. H. WIDMYER, *Armstrong Cork Company.*

In the spectrophotometric determination of the color of experimental glasses, blanks are cast which may vary in thickness from 3 to 5 mm. Certain carbon-sulfur amber glasses are dichroic[1] and, consequently, changes in thickness affect the dominant wave-length which may vary from 575 to 590 millimicrons. Since the color is desired on standard 2-mm blanks, it has been necessary to do considerable grinding with a large expenditure of labor. By measuring dominant wave-length spectrophotometrically for several glasses and plotting as a function of thickness, linear relationships have been found which intersect at a common point. Knowledge of the coordinates of this point, together with a single spectrophotometric determination on a given blank, allows one to determine the dominant wave-length of this glass at any thickness.

[1] W. D. Wright, *The Measurement of Color* (A. Hilger, London, 1944), p. 199).

5. An Application of Spectrophotometry in the Textile Industry: Testing Dyestuff Shipments. E. P. MERSEREAU AND J. L. BARACH, *Alexander Smith and Sons Carpet Company.*

Traditionally, dyestuff shipments have been tested by visual comparison of yarns or fabrics dyed by standard procedures. The comparison is based on a standard dyestuff mutually accepted by the supplier and user. Since this method is both time-consuming and insensitive, many consumers and suppliers are turning to spectrophotometric measurements of the absorption of dye solutions for standardization and testing.[1,2] The application makes use of the well-known Beer-Bouguer-Lambert law.[3] Allowing for the infrequent occurrence of errors caused by a lack of ability of the method to show differences in substantivity of the dyestuff for the fiber, absorption spectrophotometry has been found to be of great value. In the solution preparation, standard chemical analytical techniques are used with the addition of certain precautions[4] such as control of *p*H, solution preparation temperature, time of standing, dye interaction effects,[5] and concentration. All data and pertinent information are placed on a card for

each dyestuff. The strength values expressed as percent of standard concentration are entered on a control chart, the limits of which are so chosen as to indicate the range of acceptable variation in relation to the observed precision of both the dyeing process and the variation of one shipment to another. The standard deviation for 5 determinations of one sampling is 0.33, expressed in percent of standard, while that for one shipment to another is approximately 2.0. Correlation is obtained between this method and actual dyeing experience. It is of clear-cut value to an operating textile company consuming dyestuffs to use spectrophotometric solution measurements to give not only an increased accuracy and precision over the test dyeings, but also a saving of time of as much as one-half hour per test on the average.

[1] E. I. Stearns, Am. Dyestuff Rep. **33**, 1 (1944).
[2] C. Monego and W. Von Bergen, Am. Dyestuff Rep. **32**, 1 (1943).
[3] T. R. P. Gibb, *Optical Methods of Chemical Analysis* (McGraw-Hill Book Company, Inc., New York, 1942), p. 74.
[4] E. I. Stearns, Thesis, Rutgers University (1945).
[5] H. H. Taylor and F. T. Simon, Am. Dyestuff Rep. **34**, 319 (1945).

6. Applications of Spectrophotometry in a Textile Plant. FREDERICK T. SIMON, *Shelton Looms, Sidney Blumenthal and Company, Inc.*

Certain special methods of spectrophotometric technique have been developed or applied in connection with the problems encountered in a textile mill. These mainly concern the measurement of dyed fabrics and the solutions of the dyes which are used to color them. Since the methods of handling water-soluble dyes in aqueous solution is well known, only the procedures for preparing vat and naphthol dyes[1] will be discussed. Multi-component dye mixtures are the usual case encountered in dyeing and printing of textiles. In order to obtain quantitative data on these mixtures, a polyethylene oxide condensate must be added to the solution to produce additivity.[2] The concentration of each component of the mixture then can be accurately computed by means of a reciprocal matrix when a given combination is analyzed repeatedly.[3] Some of the phenomena of the dyeing process are studied, using the spectrophotometer as a tool for the measurement of dyebaths while the dyeing is proceeding. A miniature dye box was developed for simulation of production dyeing and is connected with a continuous flow cell placed in the spectrophotometer. These will be discussed and demonstrated.

[1] Cropper and Giles, J. Soc. Dyers and Colorists **60**, 279 (1944).
[2] Taylor and Simon, Am. Dyestuff Rep. **34** (August 13, 1945).
[3] Saunderson and Grossman, J. Opt. Soc. Am. **36**, 243 (1946).

7. The Orientation of Insoluble Dyes in Cellulose. HENRY HEMMENDINGER, *General Aniline and Film Corporation.*

Among the factors which may induce the orientation of dye molecules are the growth of crystals and the molecular attachment of the dye to an oriented substrate. The spectral absorption of dyes in cellulose may have dichroic characteristics arising from the simultaneous influence of both these factors. Their relative importance, and ways in which one may increase at the expense of the other, are the subject of the present study. A substantive dye attaches itself to cellulose in such a way that the dichroism of a dyed fiber is determined largely by the degree of orientation of the cellulose. A vat dye, on the other hand, while it originally attaches itself to the cellulose in a manner analogous to that of the substantive dye, is subsequently oxidized to an insoluble non-substantive dye. Morton[1] has reported observations of the oxidized form of vat dyeings which he has found to be free of appreciable dichroism. Studies by the author of the transition from the dichroic leuco-dyeing to the "non-dichroic" oxidized form have revealed additional dichroic characteristics. Immediately subsequent to oxidation, the dyeing is under some circumstances still dichroic. Like the leuco-dyeing, the original form of the oxidized dyeing is positively dichroic, indicating that oxidation has not materially shifted the molecule from its original location parallel to the direction of cellulose orientation. Certain after-treatments, such as moist heat, may, however, induce changes in this molecular orientation. Evidently the growth of relatively large crystals, which in the case of highly elongated crystals are constrained to grow only in one direction within the cellulose fiber, first causes the positive dichroism to disappear; then it may be replaced by a negative dichroism as the continued growth of a negatively dichroic crystal compels the dye molecules to reorient themselves perpendicular to the direction of cellulose elongation. These changes in arrangement of the oxidized dye are accompanied by pronounced changes in color, readily apparent to the unaided eye. The effects described, and other more complex ones arising from the existence of two orthogonal vibrations within a dye molecule, have been observed both in Cellophane and in cellulose fibers. Observed in polarized light with a non-polarizing spectrophotometer, the spectrophotometric measurements throw light on the relation between dye and cellulose. Any observations carried out on such materials with a polarizing spectrophotometer must be interpreted with reference to the possible variations in orientation of the absorbing constituent.

[1] T. H. Morton, J. Soc. Dyers Colourists **62**, 272 (1946).

8. Colorimetric Behaviors of Dye Mixtures. DAVID L. MACADAM, *Kodak Research Laboratories.*

Distributions of chromaticities have been computed for 171 pairs of typical dyes, involving five yellows, nine cyans, and nine magentas. Beer's law was assumed, and the computations were performed on automatic, punched-card computing and tabulating machines. A selected ordinate method was used. The concentrations of the dyes in each mixture were considered to be varied systematically, so that ninety chromaticities were computed for each pair of dyes. Since each dye was used in combinations, singly, with as many as eighteen other dyes, the results show the influence of various characteristics of spectrophotometric curves on chromaticity distribution, gamut, and luminous transmittance. Some computations were made to study the behaviors of neutral mixtures of triads of dyes when the concentrations of all components are changed by a common factor.

9. Photometry and Colorimetry of Railroad Fusees. W. E. KNOWLES MIDDLETON, *National Research Council of Canada.*

In connection with the preparation of a standard specification, it became necessary to investigate the luminous intensity and color of a large number of railroad fusees. The rapid and wide fluctuations in intensity made it necessary to use special methods of colorimetry. The intensity was recorded by a high speed electronic potentiometer and a barrier-layer photo-cell with correcting filter. To the pen carriage of the potentiometer was attached a special diaphragm which, with a lens and slit, acted as a "light valve" to keep the flux into the colorimeter at a constant level over a range of about four to one. The very rapid flickering was, of course, not entirely eliminated. Visual colorimetry was used, the comparison field being produced in the lower half of a divided integrating sphere, the upper half of which received light from the fusee under test. The field, 2° in diameter, could be observed with both eyes. The accuracy of the colorimetry was made adequate by a careful choice of filters, taking advantage of a fortunate circumstance regarding the color of the fusees. The results of testing more than 200 fusees will be summarized.

10. Spectrophotometric Studies of Living Human Skin. SEIBERT Q. DUNTLEY, *Massachusetts Institute of Technology.*

The recording spectrophotometer described by Hardy[1] has been used to study normal living human skin.[2] Scattering of light in the stratum mucosum plays an important role in determining the color of skin, but five colorants (melanin, melanoid, carotene, oxyhemoglobin, and reduced hemoglobin) also affect skin color. The five colorants have been extracted and studied separately; the structural elements of skin have been isolated by dissection and their individual optical properties measured, and the components have been reassembled optically in order to observe their relative importance. Studies of those changes in the color of the skin of the hand which result from arterial and venous compressions of the arm have confirmed the findings of the dissection experiments.

[1] A. C. Hardy, J. Opt. Soc. Am. **25**, 305 (1935).
[2] E. A. Edwards and S. Q. Duntley, "The pigments and color of living human skin," Am. J. Anat. **65**, 1 (1939).

11. Spectrophotometry of Living Human Skin as a Research Tool in Medicine. EDWARD A. EDWARDS, *Harvard Medical School.*

Spectrophotometry has shed light on several medical problems involving changes in skin pigmentation, where previous use of the unaided human eye, or of other methods, has given less valid information. By spectrophotometry the normal pigments of the skin have been redefined, their distribution mapped, and differences in the sexes noted. It has been reaffirmed that skin color difference in the races is due only to quantitative variations in one pigment—*melanin*. By virtue of its ability to detect fleeting blood vessel change, the spectrophotometric method promises to be of particular use in problems involving rapid changes in blood supply to the exterior of the body. In this category fall variations due to arterial and venous obstruction, variations in the normal female incident to menstrual cyclic change, and changes following solar irradiation.[1] Likewise, one can demonstrate abnormalities of blood supply caused by castration of the human male or female, and the reversibility of these changes by the giving of the sex hormones.[2] Detection of abnormal pigments is an obvious use of spectrophotometry, but such studies are not included in this paper.

[1] E. A. Edwards and S. Q. Duntley, "An analysis of skin pigment changes after exposure to sunlight," Science **90**, 235 (1939).
[2] E. A. Edwards, J. B. Hamilton, S. Q. Duntley, and S. Hubert, "Cutaneous vascular and pigmentary changes in castrate and eunichoid men," Endocrin. **28**, 119 (1941).

12. Spectrophotometric Method for Determination of Lead. GEORGE L. REYMANN, KENNETH H. SMITH, AND N. F. BARR, *Stoner-Mudge, Inc.*

The application of a recording spectrophotometer as a useful tool in the development of techniques and methods of quantitative analysis has been demonstrated. In the standardization of a procedure for rapid and precise determination of microquantities of lead in lacquers by the dithiozone method, it was observed in measuring the absorption at 520 millimicrons, that at low *p*H ranges high results and poor reproducibility were obtained. By a study of the transmission curves drawn by a G.E.-Hardy recording spectrophotometer throughout the entire visual range, a second absorption band at 620 millimicrons was observed. As the *p*H was raised the absorption at 620 millimicrons decreased, reproducibility was improved, and values approaching the theoretical were obtained. An optimum *p*H range of 10.5 to 11 was thus quickly and easily established.

13. Spectrophotometric Study of the Color of Rosin. ROBERT H. OSBORN AND WESTCOTT C. KENYON, *Hercules Experiment Station, Hercules Powder Company.*

In industrial uses of rosin, color is usually the deciding factor in grade selection. In fact, color is the basis of the market price. Until the advent of recording spectrophotometry, precise color studies on the effect of various refining processes and other treatments on the color of rosin were difficult and costly. Hence, shortly after the acquisition of a recording spectrophotometer by our laboratory, a number of fundamental investigations of rosin color were undertaken. A few of these are reported here. Analysis of spectral transmittance curves of filtered gum rosin, wood rosin, distilled wood rosin, heat-bleached wood rosin, and hydrogenated wood rosin enables a critical color comparison to be made of these products: (1) Grade for grade, wood rosins have approximately 20 percent higher luminous transmittances, on the average, than gum rosins. Furthermore, chromaticities of wood rosins plotted on the I.C.I. *x*, *y* diagram follow a locus which lies above that representing the chromaticities of gum rosins. The effect of the dirt normally found in gum rosin is to lower its luminous transmittance without appreciably altering its chromaticity. (2) One of the effects of the distillation of rosin is to remove a color body having a characteristic absorption

band in the red portion of the spectrum; this color body is believed to be chlorophyll. (3) Heat-bleaching of rosin results in products whose chromaticities fall on a locus which lies above those representing gum and wood rosins. The amount of normal heat-bleach of wood rosin appears to correlate with its color grade. (4) A good correlation between the color of hydrogenated rosin and the amount of absorbed hydrogen was found. Relative concentrations of color bodies in wood and gum rosins have been computed; from these data a rosin-blending slide rule has been developed. By means of this rule, calculations may quickly be made for a blend having a desired intermediate color grade relative to colors of rosins of known grades.

14. Photoelectric Color-Difference Meter. RICHARD S. HUNTER, *Henry A. Gardner Laboratory, Inc.*

An instrument has been designed for the rapid and precise evaluation of small color differences. The instrument is a photoelectric tristimulus colorimeter, measuring color on three scales closely resembling the *L*, *a*, and *b* scales devised by Scofield.[1] Following the work of Judd[2] and Hunter,[3] Scofield developed these scales to give uniform measures of the perceptibility of differences between colors. In the new apparatus, photo-cell windows and the measuring circuits have been selected so that the three values of color are read directly from 10-turn potentiometer rheostats. These three rheostats may be set to the values of some standard color, and a specimen of somewhat similar color is then placed in exposure position. As a selector switch is turned to each of three positions, deflection of the current-detecting galvanometer shows the magnitude on that scale of the color difference between the specimen and the standard. The apparatus is able to detect small color differences, but it suffers the weakness of other photoelectric tristimulus colorimeters in that the source-filter-photo-cell combinations are not spectral duplicates of those required for accurate color measurements in terms of the standard observer. Thus, the new colorimeter is well adapted to the evaluation of normal or non-metameric color differences, but it is not always reliable for the evaluation of non-metameric color differences.

[1] F. Scofield, "A method for determination of color differences," Scientific Section Circular 664, Nat. Paint, Varnish and Lacquer Assn., Washington, D. C. (1943).
[2] D. B. Judd, "Specification of color tolerances at the National Bureau of Standards," Am. J. Psychol. **52**, 418 (1939).
[3] R. S. Hunter, "Photoelectric tristimulus colorimetry with three filters," J. Opt. Soc. Am. **32**, 509 (1942); see also NBS Circular C429 (1942).

Papers on Flame Temperature Measurement

15. Invited paper, entitled "Optical Methods of the, Temperature Measurement of Flames," BY H. C. HOTTEL *Massachusetts Institute of Technology.*

16. Invited paper, entitled "Spectroscopic Temperature Measurements," BY G. H. DIEKE, *Johns Hopkins University.*

17. The Foundation of Optics. HANS MUELLER, *Massachusetts Institute of Technology, Cambridge 39, Massachusetts.*

In contrast to all other fields of physics, classical optics is not based on empirical laws but on a hypothesis, i.e., the wave theory. Since electric and magnetic fields of a light beam, its frequency and phase are unobservable quantities, the wave theory is not a logical foundation of optics. A new formulation of optics has been developed in which all concepts have an operational definition. A light beam is represented by a color parameter and four Stokes parameters. Without using the wave concept, all known facts can be derived from four empirical laws: (a) of spectral decomposition, (b) of polarization, (c) of superposition (coherent, incoherent, and partially coherent), and (d) of reciprocity. The effect of an optical instrument is described by a 4×4 matrix with 16 real coefficients. Many problems, especially those involving natural and partially polarized light, incoherent and partially coherent superposition, can be solved more easily than with wave theory. The relation of this phenomenological theory to wave and photon optics is analogous to that of the theory of gases to statistical mechanics.

18. The Diffraction Theory of Lens Errors. F. ZERNIKE, *Johns Hopkins University.*

The author and his pupils at Groningen University, Netherlands, developed the diffraction theory of small lens errors, finding series in ascending powers of the aberration coefficients (Nijboer, Dissertation 1942). The further problem of the transition of the diffraction patterns into the well-known geometrical figures, such as the coma flare, has now been solved by asymptotically expanding the diffraction integral for large aberrations by the method of stationary phase. This has recently been given a rigorous mathematical foundation by Van der Corput. The first term of the expansion gives the geometrical pattern, supplemented by the interference of overlapping beams. The second term represents the diffraction at the edge of the aperture (N. G. van Kampen). These terms could be checked separately by special experiments (Nienhuis, Dissertation, in press).

19. Gratings Made by Photographing Interference Fringes. ROBERT E. HOPKINS AND FRANKLIN R. CLAPPER,* *University of Rochester.*

Lord Rayleigh in 1875 made numerous photographic copies of gratings. Cornu photographed interference fringes formed in the focal plane of a lens and made zone plates by photographing Newton's rings. Several workers around 1900[1–3] tried to make gratings by photographing standing waves. Today, with the availability of high resolving power films and high intensity narrow line width sources, it is possible to make gratings with interesting characteristics by these methods. In recent experiments, gratings have been made by photographing the interference fringes obtained in Lloyd's mirror experiment. These gratings have approximately 4000 lines at 500 lines per millimeter.

The conditions for obtaining good gratings will be described and some indication of future possibilities will be given.

* Now with General Electric Company, Schenectady, New York.
[1] G. Meslin, "Photographed gratings," J. de Phys. **3**, 750–751 (1901); Sci. Abstracts **5** (1902), No. 453.
[2] A. Cotton, "Photographic gratings," Bull. de la Societe Francaise de Physique **165**, 9–11 (1901); Sci. Abstracts **4** (1901), No. 1882.
[3] A. Cotton, "Gratings made by photography of stationary waves," Bull. de la Societe Francaise de Physique **169**, 4–7 (1901); Sci. Abstracts **4** (1901), No. 1883.

20. Continuously Variable Interference Filters. A. F. TURNER AND O. A. ULLRICH, *Bausch & Lomb Optical Company.*

The potentialities of the Fabry-Perot type interference filter can be extended by making it continuously variable. Three modifications for this purpose will be discussed. In the first a spacer film of graded thickness is provided between the two semi-transparent silver films. With a spacer in the form of a linear wedge an approximately linear wave-length scale is obtained; with a cone-shaped spacer the transmission bands of the filter are circular. Filters for the visible must be first order if no overlapping of spectra can be tolerated. Second-order filters have a higher resolving power, but there is overlapping with third orders above 600 millimicrons. Typical data for a second-order filter are: peak transmission—40 percent, half-width or resolving power—10 millimicrons. Linear wedge filters are convenient for the rapid examination of light sources. For sensitometric work they may be crossed with neutral wedges. The second modification of the variable interference filter employs two spacers of uniform thickness, separated by a thin wedged film of silver. The transmission band in general consists of a doublet, the separation and position of the components being determined by the thickness of the silver wedge, as well as by the thickness of the two spacers. The third modification has three uniform silver films separated, respectively, by one uniformly thick and one wedged spacer film. The transmission band is again a doublet, the position and separation of the components depending on the thicknesses of the spacers. When a monochromatic source is viewed through any of these filters at other than normal incidence, each spectral line is resolved into two components linearly polarized at right angles to each other because of the difference in phase shift of the *p* and *s* components at the silver interfaces. Since this doubling depends on the angle of incidence, the two components appear stereoscopically to lie at different distances from the observer if the angle of incidence is different for the two eyes.

Papers on Wind Tunnel Optics

21. Invited paper, entitled "Wind Tunnel Optics—Especially Interferometry," BY R. LADENBURG, *Princeton University.*

22. Invited paper, entitled "The Task of Wind Tunnel Interferometry," BY F. J. WEYL, *Office of Naval Research.*

23. Invited paper, entitled "The Schlieren Method of Shock Wave Analysis," BY R. B. KENNARD, *Naval Ordnance Laboratory.*

24. Micro-Interferometer Study of Diffraction Gratings. DAVID RICHARDSON AND ROBERT B. TACKABERRY, *Bausch & Lomb Optical Company.*

A micro-interferometer made according to a design proposed by Dr. W. Ewart Williams, using principles first given by Linnik[1,2] will be described. The investigation of the groove contours of a series of gratings is reported to illustrate the usefulness of the instrument. Results obtained from the use of micro-interferometer and electron microscope methods are compared.

[1] W. Linnik, Comptes rendus U.R.S.S. **1**, 21 (1933).
[2] W. Kinder, Zeiss Nachrichten **3**, 91 (1937).

25. The Electrical Response of the Human Retina to Lights of Various Wave-Lengths. LORRIN A. RIGGS AND E. PARKER JOHNSON, *Brown University.*

Flashes of monochromatic light have been used to elicit electrical responses from the human retina. A corneal electrode supported by a contact lens and a neutral electrode located elsewhere on the head were used in recording. The cornea is normally positive with respect to the posterior portion of the eye, and this positivity is increased by the action of light upon the retina. Action-potential waves were recorded photographically by the use of a direct-coupled amplifier and oscillograph. The shape of the wave is partly determined by the wave-length of the stimulating light. Using the magnitude of the potential as an index, it has been possible to obtain data on sensitivity as a function of wave-length. Such data are seen to bear some resemblance to data on scotopic visibility. There are, however, some discrepancies between the two sets of data, particularly at the blue end of the visible spectrum. The electrical response to flashes in this region is larger than would be predicted from the existing data on scotopic sensitivity. There is also evidence that a given increase in intensity of flash will result in a greater increment of response for blue light than for light from other regions of the spectrum. There is no indication that the main component (*b* wave) of the electrical response is aroused by the photopic visual system. The evidence from these experiments is in agreement with other data obtained by the authors in experiments on light and dark adaptation. Even with high intensities of stimulation, red light is relatively ineffective in arousing the principal *b* wave. Blue light of moderate intensity is relatively much more effective. There is some indication of a small electrical effect attributable to photopic mechanisms. It varies independently of the principal *b* wave and effects minor variations in the appearance of the record.

BIBLIOGRAPHY:
(1) L. A. Riggs, "Continuous and reproducible records of the electrical activity of the human retina," Proc. Soc. Exper. Biol. **48**, 204–207 (1941).
(2) E. D. Adrian, "The electrical response in the human eye," J. Physiol. **104**, 84–104 (1945).
(3) E. D. Adrian, "Rod and cone components in the electric response of the eye," J. Physiol. **105**, 24–37 (1946).

26. Pharmacological Properties of Blood Sera and Drugs Treated with Various X-Rays. DAVID I. MACHT AND MARCUS OSTRO, *Departments of Pharmacology and Radiology, Sinai Hospital, Baltimore.*

Normal and pathological human blood sera and a number of drugs in solution were exposed to filtered and unfiltered x-rays in small open glass containers, and their pharmacodynamic properties after irradiation were compared with untreated specimens of the same substances. The biological tests or assays were made in some cases by *phyto*pharmacological methods, in others by *zoo*pharmacological methods, and in still other experiments by biochemical reactions. Among the pathological blood sera studied were those from: pernicious anemia, pemphigus, leprosy, catamenia, trachoma, and various psychoses, all of which are normally very highly toxic for living plant protoplasm. On exposure to certain filtered x-rays in vitro, some of these sera are detoxified while others are not. In at least two diseases, clinical irradiation of patients with small doses of deep therapy rays produces detoxification of the blood corresponding to the results obtained with such bloods in test tube experiments. Hemophiliac blood which clots very slowly can be made to clot more rapidly by exposure to filtered x-rays, both in vitro and in vivo. Among the drugs studied in vitro were: Tincture of digitalis, digitoxin, cobra neurotoxin, crotalus venom, penicillin, and streptomycin. Some drugs are rendered less toxic by irradiation, others more toxic, while still others are apparently unchanged in their pharmacological properties by short exposure to x-rays. A most interesting finding was that even when the Roentgen dosage is the same, divergent pharmacological properties are developed when blood sera and various drugs are exposed to x-rays passed through filters of different thicknesses and composition.

Papers on Infra-Red and Spectroscopy

27. Absorption Spectra with Polarized Infra-Red Radiation. NORMAN WRIGHT, *Dow Chemical Company, Midland, Michigan.*

A transmitting polarizer for infra-red radiation consisting of a pile of silver chloride plates inclined 26° will be described. Slides of a number of spectra of crystalline and oriented plastic material obtained with this device will be presented. Correlation of the spectra with molecular structure will be discussed.

28. Polarization Techniques in the Infra-Red. W. L. HYDE, *Harvard University.*

It has been found that the light passing through an ordinary infra-red spectrometer is partially polarized with the electric vector horizontal. A dichroic sample will give clearly different curves when oriented parallel and perpendicular to this partial polarization. By a simple linear transformation, the observed spectra can be reduced to those which would have been seen in totally polarized light. A double beam system such as that of the Baird Associates spectrometer[1] on which this work was done makes possible additional sensitivity for the detection of weak dichroism such as that found in polymers which are only slightly oriented. Substantially identical samples are placed in both beams but oriented parallel and perpendicular to the polarization of the instrument. Difference due to either thickness differences or dichroism will appear while absorption common to both samples will balance out. The two effects can then be distinguished by rotating each sample 90° and recording a second curve. Thickness differences will be identical while dichroism differences will change sign. By recording three curves with two identical samples in the same beam oriented parallel to each other and vertical, parallel and horizontal, and crossed, the partial polarization of the instrument as well as the dichroism of the samples may be determined. Many of the infra-red bands of crystals are completely polarized. At these wavelengths, a thin crystal can be used as a transmission polarizer. Curves will be shown where the spectrum of oriented polyethylene has been studied with the aid of a calcite polarizer. Curves will be shown for the dichroism from 2 to 16 microns of calcite, polyvinyl alcohol, mica, rubber films under tension, polyethylene, and other materials.

[1] W. S. Baird, H. M. O'Bryan, George Ogden, and Dorothy Lee, J. Opt. Soc. Am. **37**, 754 (1947).

29. The Infra-Red Spectra of Linearly Oriented High Polymers. ELKAN R. BLOUT AND DWIGHT P. MERRILL, *Polaroid Corporation.*

When thin films of high molecular weight polymeric substances such as polyvinyl alcohol, polyvinyl butyral polyethylene, and nylon are stretched to several times their original lengths, substantial orientation of the component chains along the stretch direction results. In the visible and ultraviolet region these oriented polymers show birefringence, but no evidence of appreciable dichroism has been reported. On the other hand, when certain linearly oriented high polymers are dyed or are converted to light-absorbing systems such as $-(CH=CH)_x-$, absorption of light and dichroism may result.[1] In the infra-red region organic high polymers do themselves show absorption bands which correspond to characteristic vibration frequencies of the whole molecule or its component groups.[2] We will report on both the small inherent dichroism of certain linearly oriented high polymers[3] and the dichroism of some polyene systems in the 1 to 15-μ region.

[1] E. H. Land and C. D. West, *Colloid Chemistry* (Reinhold Pub. Corp. 1946), edited by J. Alexander, Vol. VI, p. 160.
[2] H. W. Thompson and P. Torkington, Proc. Roy. Soc. **A184**, 3 (1945), Trans. Faraday Soc. **41**, 246 (1945).
[3] Cf. L. Glatt and J. W. Ellis, J. Chem. Phys. **15**, 884 (1947), who investigated the dichroism of oriented polyethylene and "Parowax" in the 0.6 to 2.7-μ region.

30. Refractive Indices of Two Thallium Bromide-Iodide Crystals for Visible and Infra-Red Radiant Energy.[1] LEROY W. TILTON, EARLE K. PLYLER, AND ROBERT E. STEPHENS, *National Bureau of Standards.*

The refractive indices of two specimens of thallium bromide-iodide (KRS 5) were measured at a constant room

temperature at 27°C from 0.577 to 39μ by use of a minimum-deviation spectrometer and a Perkin and Elmer infra-red spectrometer equipped with a calibrated screw for operation of the Littrow mirror. In order to cover the entire region over which the prism is transparent, many known wave-lengths were used, including lines of mercury, sodium, hydrogen, and helium for the visible region. A cadmium-mercury lamp was the source from 1 to 2μ. From 2 to 39μ various absorption bands of CO_2, H_2O, methylcyclohexane, polystyrene, and polyethylene were used, with a globar as source, for the identification of wave-lengths. A comparison of indices for two crystals grown in different laboratories is made.

[1] The work described in this abstract was carried out in part under Contract S & A 28658 between the Bureau of Ships and the National Bureau of Stanards.

31. Spectrometry with a Thallium Bromide Iodide Prism.* EARLE K. PLYLER, *National Bureau of Standards.*

A thallium bromide iodide (KRS-5) prism has been used for the measurement of spectra from the visible to 38μ. The dispersion of this material is very high through the visible red and as far as 2μ, relatively low between 2μ and 12μ, and again increasing to a high value when 38μ is reached. Reflectors of LiF, CaF_2, and NaF were used to reduce in a great measure the stray radiation in the region from 18 to 38μ. Polystyrene and polyethylene, in thin layers, are more transparent from 25 to 38μ than KRS-5 and these materials have been used for windows of cells. A comparison has been made of the transmission of windows of thallium salts grown in Jena and in different laboratories in this country. The best samples of KRS-5, in 8-mm thicknesses, transmit about 50 percent of the energy at 38μ. One sample was opaque at 26μ and another sample at 32.5μ. TlBr is transparent to about 33μ. TlCl is transparent to about 27μ, and $PbCl_2$, AgCl, and KCl are transparent to about 25μ. Several liquids and vapors have also been measured from 25 to 38μ.

* The work described in this abstract was carried out in part under contract S & A 28658 between the Bureau of Ships and the National Bureau of Standards.

32. Molding Optical Elements of Thallium Bromide Iodide (KRS5).* J. C. EVANS AND M. D. CLARK, *University of Rochester.*

Difficulty in polishing specimens of thallium bromide iodide has prompted an investigation into molding this material. Experiments have shown that this material can be molded plastically at a temperature of approximately 350°F and a pressure of about one ton per square inch. Chromium-plated dies on a high chromium die steel are used. The quality of the surface is limited by evidence of slip bands on the optical surfaces.

* This work was performed for the Engineer Research and Development Laboratories, Contract W-44-009 eng-470.

BIBLIOGRAPHY:
(1) Frank Cooke, "Optical Finishing of KRS Materials," J. Opt. Soc. Am. **37**, 948 (A) (1947).

33. A Rapid Scanning Infra-Red Spectrometer for Emission Spectra.* SHIRLEIGH SILVERMAN, *Applied Physics Laboratory, Johns Hopkins University.*

Some investigations of infra-red emission spectra using a rapid-scanning[1] spectrometer are described. The preliminary instrument is a standard Perkin-Elmer 12-C, with slight modifications including presentation on a long-persistence oscilloscope screen. Present performance permits scanning the intervals 2–7μ, 7–10.5μ, 12–15μ in about 4 seconds each. At this scanning rate signal/noise ratio is somewhat reduced compared to usual performance, but adequate resolving power remains for many purposes. Characteristic emission traces of laboratory flames as well as a typical transient combustion process are shown.

* A portion of this work was supported by the Bureau of Ordnance, U. S. Navy, under Contract NOrd-7386.
[1] Daly and Sutherland, Proc. Phys. Soc. London **59**, 77 (1947).

34. Spectral Response of a Cadmium Sulfide Crystal.* CURTIS J. HUMPHREYS, *National Bureau of Standards.*

The photo-conducting properties of a specimen of artificially grown cadmium sulfide crystal, prepared by Rudolf Frerichs and recently made available to the author by him, have been studied by measuring its spectral response relative to a thermopile, using the most intense lines of zinc, cadmium, and mercury, isolated by means of a quartz spectrometer. This study includes an extension of Frerichs' measurements[1] into the region of wave-lengths shorter than 2537A, down to 2139A. The dark resistance of the specimen was about 3×10^8 ohms. This was reduced to 5×10^5 ohms at the wave-length of maximum response with the largest amount of radiant energy used, amounting to about 300 μw/cm^2. The following properties of the crystal were established: (1) The spectral response diminished gradually from a maximum in the visible violet to about 20 percent of this amount at 2139A. (2) The response was not linear with energy at a given wave-length. Increase of applied voltage from 45 to 180 resulted in no indication of saturation for the radiation intensities employed. (3) The sensitivity depended on immediately previous exposure to radiant energy. (4) An increase in response amounting in some instances to 25 percent was observed on prolonging exposures to 5 minutes. The results point to considerable difficulty in using such an element as a detector for quantitative spectral energy measurements. Its extremely high sensitivity and low dark current will make it useful as a detector for qualitative work even if calibration difficulties cannot be overcome.

* The work described in this abstract was carried out in part under Contract S & A 28658 between the Bureau of Ships and the National Bureau of Standards.
[1] Rudolf Frerichs, "Photo-conductivity of 'Incomplete phosphors'," Phys. Rev. **72**, 594 (1947).

35. An Electronic Apparatus for Determining Phosphorescent Decay. W. S. PLYMALE, JR., *Naval Research Laboratory.*

The measurement of the decay time of phosphors of comparatively low brightness is made for decay periods of 2×10^{-4} sec. to several hours. Irradiation of the phosphor is by ultraviolet light and takes place exterior to the

apparatus. A 1P22 or 1P21 multiplier photo-tube in connection with a direct-coupled amplifier and 5-inch oscilloscope is used to measure the brightness which is recorded on the oscilloscope screen as a vertical deflection. Horizontal deflection is produced by a time-sweep circuit triggered by a 1P28 multiplier tube. Also another 1P28 tube is used to control the intensity of the spot on the screen preventing overexposure at the starting point when a camera is used to photograph the transient decay curve. A time scale is superimposed on the film by setting the vertical gain to zero and introducing a calibrated time pulse into the vertical amplifier during a given sweep. Multirange time scales and convenience of recording transients are features of the apparatus.

Papers on Spectroscopy

36. Double Activation of Zinc Fluoride Phosphors. GORTON R. FONDA AND FRANK J. STUDER, *General Electric Company, Schenectady, New York.*

When activated with manganese alone, zinc fluoride is known to emit an orange fluorescence under excitation by 2537A whose brightness is very weak because its peak excitation lies at 2200A. Other activators, lead, tungsten, cerium, titanium, and germanium, shift the peak excitation to 2500–2600A and produce a higher absorption in the range 2000–2600A than does manganese alone. Their emission lies mainly in the visible with the exception of cerium, whose peak emission is at 3500A. Their combinations with manganese produce greater fluorescence brightness. When manganese is combined with tungsten or titanium, the normal orange emission of manganese is increased four- to sixfold with no change in the spectral distribution nor in the unique exponential decay of its afterglow except that the decay is raised to a higher brightness level. Under double activation by manganese and germanium, the characteristic orange and green bands of each appear in the emission but the peak is shifted to the blue. With manganese and cerium, the individual emission bands of each activator persist, with no particular alteration in intensity. In the enhancement of the orange manganese fluorescence by a secondary activator, some other factor therefore is involved than merely an increase in absorption or a favorable shift in the excitation spectrum. Among other combinations, germanium serves to enhance the fluorescence of titanium.

BIBLIOGRAPHY:
F. E. Williams, J. Opt. Soc. Am. **37**, 302 (1947).

37. The Absorption and Excitation of Luminescent Zinc Silicate. FRANK J. STUDER AND D. A. LARSON, *General Electric Company, Schenectady, New York.*

The absorption and excitation spectra of a number of zinc silicate phosphors of varying manganese content have been studied using automatic recording equipment. The character of the absorption between 2000A and 3000A was determined by using a plaque of the phosphor as a reflector for light from a high intensity hydrogen arc (continuous spectrum). The reflected light was analyzed into its spectrum and the intensity, measured by means of a recording grating spectrometer. The reflection was thus compared with that of a plaque of smoked magnesium oxide. The excitation was studied by painting a coat of the phosphor on a glass slide and placing it in front of the photo-cell receiver of the recording spectrometer, so that as it passed progressively through the spectrum of the hydrogen arc, the intensity of the resulting luminescence was recorded. Results show that there are two excitation bands, one centering between 2500A and 2600A and the other in the neighborhood of 2100A. The relative efficiency of these bands varies widely with the amount of manganese activator, the longer wave-length band becoming relatively stronger as the amount of manganese is increased. Excitation measurements are in the main in agreement with Kroger[1] and Lui.[2] The absorption spectra, as indicated by the reflection data show some discrepancies from those reported by these observers.

BIBLIOGRAPHY:
(1) F. A. Kroger, Physica **6**, 764–778 (1939).
(2) C. K. Lui, J. Opt. Soc. Am. **35**, 492–494 (1945).

38. Wave-lengths Emitted by Mercury 198. WILLIAM F. MEGGERS, *National Bureau of Standards.*

Electrodeless lamps containing five milligrams of Hg^{198} and five millimeters (Hg) of argon excited by 100-megacycle frequency are found to be highly satisfactory sources of exceedingly sharp spectral lines. Employing Fabry-Perot interferometers and prism spectrographs preliminary values of the wave-lengths of thirty-three lines (2537A to 6907A) have been determined relative to the red radiation from cadmium recorded simultaneously by imaging one lamp in the other. Interference patterns of the stronger Hg lines can be photographed in less than one second. Etalons of 5, 25, 40, 50, and 67 millimeters have been used thus far. The probable errors of these preliminary wave-lengths emitted by mercury 198 range from one part in twenty millions to one part in one hundred millions. The relative values of these wave-lengths will be refined by measuring them in vacuum.

39. Evaluation of the Elementary Causes of Deviations in Spectrochemical Analysis. JOSEPH GEFFNER, *Weirton Steel Company.*

The difference between an individual spectrochemical determination and the "true" composition of a sample may be divided into two parts: (1) a constant amount called the *bias*, equal to the difference between the "true" composition and the average of all such spectrochemical determinations made under essentially identical conditions, and (2) a variable amount called the *deviation*, equal to the difference between the individual determination and the average of all such determinations. The frequency distribution of the deviations of all determinations generally approximates the normal, and its sigma (standard deviation) is a measure of the uncertainty of the analytical method. The deviation of an individual determination may be subdivided further into components due to elementary causes such as sample inhomogeneity, photographic response variations, excitation instability, and

others. Using the statistical technique of analysis of variance, the contribution of each of several such elementary causes to the total uncertainty may be estimated, together with fiducial limits within which the "true" value of each estimated contribution may reasonably be expected to lie. The results of a comprehensive experiment for evaluating the total uncertainty, the uncertainty components, and their fiducial limits for the spectrochemical analysis of copper in steel are reported.

40. The Quantitative Spectrographic Analysis of the Rare Earth Elements. VELMER A. FASSEL AND H. A. WILHELM, *Iowa State College.*

The spectrophotometric methods generally used for the quantitative analysis of the rare earths do not permit the determination of low concentrations, i.e., less than 2 percent, of rare earth impurities in another rare earth, and the determination of major amounts of those members of the group which possess no strong absorption bands in the wave-length region 2200–10,000A. Emission spectra methods which are designed to supplement the spectrophotometric methods have been developed. The specific examples described are the determination of (a) samarium in neodymium (0.1 to 2 percent), (b) europium in samarium (0.01 to 4 percent), and (c) yttrium and gadolinium in complex mixtures (10–100 percent). The methods, however, should be readily adaptable to similar determinations involving the other members of the series. For the determination of minor constituents, the procedures involve the high amperage d.c. arc excitation of rare earth oxide-powdered graphite mixtures. Selected lines of the major rare earth constituent serve as almost ideal internal standards. For the determination of major constituents in complex mixtures, similar excitation conditions are used. The selection of cerium as the internal standard for these determinations was based on the relative ease with which any cerium present in a mixture could be preferentially separated from the mixture and then reintroduced in a standard amount. Studies on the variation of the intensity ratios during excitations and the effect of large changes in arc current, percent graphite, and weight of sample charge on the integrated intensity ratios are included. Precision and accuracy data indicate that the experimental error for duplicate determinations is about ±4 percent of the amount present.

* This investigation was performed in part under Contract No. W-7405 eng-82 for the Atomic Energy Commission.

41. Wide Range Analysis for Zinc Using Spectrographic Line Widths. E. JOHN EASTMOND AND BERNICE E. WILLIAMS, *U. S. Department of Agriculture, Albany, California.*

A spectrographic method has been developed for determination of zinc in biological ashes by use of line width as a concentration index. Synthetic standards and analytical samples, in the form of sulfates, are mixed with a potassium sulfate-graphite buffer containing barium and cadmium as internal controls. Samples are excited in a direct-current arc and spectra recorded with a Littrow quartz spectrograph. The contour of Zn 2138A is recorded with a recording microphotometer and the width determined at the maximum density of the control lines Ba 2255A or Cd 2288A. A plot of the logarithm of this width *versus* logarithm of zinc concentration prepared from standard samples containing 0.004 to 10 percent zinc serves as an analytical curve. Results determined by ordinary density measurements have been compared with those from width measurements. Although the two methods show comparable reproducibility of repeated exposures at the lower limit of the analysis range, the width method is more precise at higher ranges and has proven applicable even at concentrations where the line density method is limited by self-reversal and low photographic plate contrast. Concentrations as high as 10 percent have been determined, indicating possible application of such a method to the estimation of major constituents in such biological ashes or inorganic powders.

42. Practical Applications of a Replica Grating Spectrograph Installation. J. T. ROZSA, *National Spectrographic Laboratories, Inc.*

Techniques for analyses by a Wadsworth mounted replica grating* spectrograph with mated accessories have been worked out on a variety of applications, including oil, low alloy steel, lead, aluminum and zinc alloys, siliceous ceramic materials, blood, and general qualitative analysis. Working curves, analytical line pairs, exposure times, and general performance data are given. For applications not involving high spectral line count materials or extreme sensitivity quantitative work a replica grating will be found as satisfactory as an original grating.

* R. W. Wood, O.S.A. December, 1946.

Papers on General Optics

43. The Effect of High Index Glass on the Field Characteristics of Photographic Objectives. GEORGE H. AKLIN, *Eastman Kodak Company.*

Improving field characteristics of photographic objectives has always been the concern of the lens designer. Progress has followed the introduction of glasses with high index and low dispersion. These new glasses have been used in the collective lenses in such a manner as to increase the difference in index between collective and dispersive elements. The high index glasses as given in U. S. Reissue 21,175 (Morey) and in the more recent patents by DePaolis and Eberlin have been used in a number of lens systems. The extent to which Petzval sum is improved and/or covering power is increased will be discussed, and comparative examples will be shown to illustrate the changes in field characteristics.

44. Reduction of Sphero-Chromatic Aberration in Catadioptric Systems. ROBERT E. STEPHENS, *National Bureau of Standards.*

Schmidt and Maksutov catadioptric systems suffer from sphero-chromatic aberrations that are of opposite sign. By the use of a hybrid system, whose corrector is a deep meniscus lens with an aspheric curve on the external

surface, the sphero-chromatic residuals have been reduced and, as a consequence, usable relative apertures have been increased.

45. Aspheric Surfaces in Optical Systems for Television Projection. DAVID S. GREY, *Polaroid Corporation.*

The aberrations of the Schmidt optical system are given, with special attention to the system as commonly used for projection of televised images. The effects of bending the aspheric element and of varying the neutral zone height are discussed. A family of modified Schmidt systems containing more than one aspheric surface is presented, with approximation formulas pertaining to the computation of these systems.

BIBLIOGRAPHY:
J. G. Baker, "The solid glass Schmidt camera and a new type of nebular spectrograph," Proc. Am. Phil. Soc. **82**, 323 (1940).

46. Optical Characteristics of Hyperbolic Paraboloidal Mirrors. ROBERT A. WOODSON, *Consultant Optical Engineer.*

The Gaussian image formation by doubly curved mirrors is examined. Aberrations, particularly axial astigmatism, are discussed. With a relatively small aperture stop, the half-real, half-virtual image of a linear object can be made to rotate by merely translating the object along the optical axis. Uniform rotation of the object does not result in uniform rotation of the image. Combinations of two such mirrors may be free of axial astigmatism. Possible practical applications are indicated.

47. Irradiance Distribution in a Lloyd Mirror Interference Pattern. ROBERT N. WOLFE AND FRED C. EISEN, *Eastman Kodak Company.*

The Lloyd mirror interference pattern reappears and disappears in a periodic manner at distances from the mirror edge greater than the distance to the initial point of disappearance. In certain cases bright lines appear where, according to the text book theory which assumes spectrally homogeneous radiation and a slit source of infinitesimal width, dark lines should appear. A photograph of such a pattern will be shown, measured values of the relative irradiance as a function of distance from the mirror edge will be presented,[1] and a theoretical determination which accounts for certain features of this variation of irradiance with distance will be outlined.

[1] L. A. Jones and R. N. Wolfe, J. Opt. Soc. Am. **35**, 559 (1945).

48. Focal Plane Diffraction Doubling in the Amici Roof Prism. A. I. MAHAN AND E. E. PRICE, *Naval Ordnance Laboratory.*

In an earlier paper[1] a description was given of a focal plane diffraction anomaly occurring in a rather odd-shaped roof prism when unpolarized parallel light passing through the prism is brought to a focus by a lens. The anomaly consisted of a doubling of the diffraction pattern in a direction perpendicular to the roof edge while parallel to the roof edge the image remained single and sharp. If plane polarized light is allowed to enter the prism, the form of the doubling perpendicular to the roof edge could be changed while that parallel to the roof edge was unaffected. Such an image doubling in roof prisms is usually associated with a roof angle error, but the previously mentioned paper clearly established that such a doubling would be expected with a perfect 90° roof angle. The purpose of the present paper is to extend this theory to the case of the more common Amici 90° deviation roof prism. This prism exhibits all the properties of the earlier described prism but to a much smaller degree. The forms of the diffraction patterns for unpolarized and polarized light of different entering azimuths have been computed and are compared with experimentally photographed diffraction patterns. Some simplifications of the former theory have been made which make calculations for all roof prisms more simple. Computations on the form of the diffraction pattern for the case in which the roof surfaces have been silvered will also be presented. The diffraction pattern of the unsilvered roof prism has been photographed on 16-mm film with 90 equispaced settings between 0 and 180 degrees of the azimuth angle of entering polarized light. These successive photographs will be shown as a motion picture.

[1] A. I. Mahan, J. Opt. Soc. Am. **35**, 623 (1945).

49. An Atmospheric Transmissometer: Its Calibration and Applications. C. A. DOUGLAS, *National Bureau of Standards.*

An atmospheric transmissometer has been developed which will provide an automatic continuous measurement of the transmittance between two fixed points over a range of transmittances of 10^5. The instrument comprises a projector source operated at a fixed voltage, a photoelectric receiver giving an indication in the form of pulses, the frequency of which is proportional to the photoelectric current,[1] and a remote indicator which makes it practicable to locate the indicator at some distance from the location at which the measurements are to be made. The circuit details of earlier instruments have been given in previous papers.[2,3] A field calibration of the instrument has been made. The criterion used for determining whether a mark was visible was that the mark could be seen and identified. It was found that for daylight use Koschmieder's law[4] provided a satisfactory calibration curve if a contrast threshold of 0.055 was used. For nighttime use it was found that the use in Allard's law[5] of a fixed value of the threshold illuminance at the eye of the observer did not provide a satisfactory representation of the calibration points. The assumption that the threshold illuminance is not constant but varies inversely with the visual range provides a satisfactory representation. Frequently the sample of the atmosphere between the source and receiver is not representative of the surrounding atmosphere, resulting in large discrepancies between the visual range indicated by the transmissometer and that observed visually, especially when the visual range is large. In view of this limitation there appears at present to be little advantage in the use of a transmissometer to replace visual observations for the determination of general visual range where trained observers and satisfactory marks are available. There are other conditions, however, where the effects of non-representative sampling are greatly reduced or are of little im-

portance. These include (1) the determination of visual range in periods of fog, (2) the determination of fog or haze density over a restricted area remote from an observer, (3) obtaining a measure of visual range when observers or satisfactory marks are not available.

[1] J. B. H. Kuper, F. S. Brackett, and M. Eicher, Rev. Sci. Inst. 12, 87 (1941).
[2] C. A. Douglas and L. L. Young, CAA Tech. Development Report No. 47 (Feb. 1945).
[3] C. A. Douglas, Electronics 20, 106 (1947).
[4] H. Koschmieder, Bectr. z. Phys. D. Freien Atm. 12, 33, 171 (1924).
[5] M. Reynaud, "Illumination and beaconage of the coasts of France," p. 23–28, Govt. Printing Office, Washington, D. C.

50. The Resolving Power of a Coated Objective. HAROLD OSTERBERG AND J. ERNEST WILKINS, JR., *American Optical Company.*

Luneberg has proposed the problem of attempting to increase the resolving power of an objective by applying a coating to the aperture in such a manner that the diffraction pattern produced by the coated objective has a narrower central bright disk than is the case for an uncoated objective. The coating may be described analytically by a function $P(\rho)$ of the numerical aperture ρ which is the complex amplitude transmission of the coating. The shape of the diffraction pattern $|F(r)|^2$ is uniquely determined by the function $P(\rho)$. When $P(\rho)$ is an analytic function of ρ^2 which is expansible in a power series about the point $\rho=\rho_m=$maximum numerical aperture admitted by the objective, it is shown that $F(r)$ is expansible in a series of Bessel functions in which the general term is $a_n r^{-n} J_n(2\pi r\rho_m/\lambda)$. By proper choice of the coefficients a_n, $F(r)$ can be made to vanish at any previously assigned value of r and, in particular, at a value of r less than that defining the Airy limit of resolution. A numerical investigation has been carried out for the case in which $F(r)$ can be represented as a sum of only the first two terms in this series, $F(r)=a_1 r^{-1}J_1(w)+a_2 r^{-2}J_2(w)$, where $w=2\pi r\rho_m/\lambda$. In this case the coefficients are uniquely determined by the requirements that $F(r)$ shall vanish at a specified point r_0 and that the coating function $P(\rho)$ (which is a transmission ratio) is nowhere greater than unity in absolute value. Graphs of the corresponding diffraction patterns $|F(r)|^2$ are given for various values of r_0, and it is concluded that one can reduce the Airy limit by about $\frac{1}{3}$ in this straightforward manner. If one employed additional terms of higher order, one could probably reduce the Airy limit even further and at the same time control the important features of the diffraction pattern (e.g., the central maximum $|F(o)|^2$.

BIBLIOGRAPHY:
Luneberg, "Mathematical theory of optics," Brown University lecture notes, 1944.

51. Image Contrast Control with Phase Microscopy. OSCAR W. RICHARDS, *American Optical Company.*

Four types of diffraction plates are possible, depending on whether the absorbing material is on (*A*) the conjugate, or (B) the complementary area, and the retarding medium is on the conjugate (+), or on the complementary area (−). Bright contrast occurs with $A+$ and $B+$ diffraction plates, because regions of longer optical path in the specimen appear brighter than those of lesser path; conversely, dark contrast occurs in the image when $A-$ and $B-$ plates are used. Dark contrast is useful when the image should resemble that from a stained preparation and for measurement. However, the dense contrast from $A-$ plates may obscure some of the underlying detail in the specimen, which would be visible with the more transparent dark contrast $B-$ or bright contrast $A+$ diffraction plates. Bright contrast is useful for counting, motion study, and for stereophotomicrographic analysis. Smaller objects are seen more easily in the image with bright than with dark contrast. Application of the Weber-Fechner law and the periodic principle reduces the many possible combinations of diffraction plates to those needed in practical microscopy. The image of small biological particles, as virus and certain cancer cells, has best contrast with 0.1λ retardation. Many specimens show best with $\lambda/4$, but other highly refractile materials like glass require greater retardations. At low magnifications ($\pm 100X$) a retardation of $\lambda/3$ is often better than $\lambda/4$. While different retardations could be obtained with one plate and light of different wave-length, the differential sensitivity of the eye to different colors precludes generally satisfactory application. Absorbing material on the diffraction plate increases the contrast in the image of both unstained specimens containing optical path differences and of weakly absorbing, poorly pigmented specimens. Increased visibility is often possible from the use of a diffraction plate which increases the contrast in the image from the principal object and decreases the image contrast of interferring material. Further increased contrast is attained by combining color contrast and phase contrast in the image of specimens with selective wave-length absorption. Photomicrographs will illustrate these principles.

BIBLIOGRAPHY:
Bennett, Jupnik, Osterberg, and Richards, Trans. Am. Micro. Soc. 65, 99 (1946).
O. W. Richards, J. Biol. Photogr. Assoc. 16, 29 (1947).

52. The Multipupil In Phase Microscopy. HAROLD OSTERBERG, *American Optical Company.*

In the conventional phase microscope the diffraction plate is located at or inside the microscope objective and at the plane conjugate to the condenser diaphragm. Condenser diaphragm and diffraction plate act as entrance and exit pupils, respectively. Additional real images of the condenser diaphragm may be formed by means of auxiliary lens systems. These images are called *multipupils*. Diffraction plates may be placed at one or all of these multipupils. The increase in the length of a bi-pupil system can be moderate and can afford ample space at the second pupil for the more complex elements of variable phase systems. As expected, multipupil systems do function as effective phase contrast systems. It will be shown on general theoretical grounds that the multipupil system is equivalent to a single system of phase microscopy whose over-all magnification is equal to the product of the magnifications of the multipupil system and whose pupil function is the product of the complex pupil functions associated with each of the multipupils. The physical interpretation of the composite pupil function as a product is that the optical

paths through corresponding areas of the multipupils are additive, while the corresponding amplitude transmissions are multiplied. This is another expected result. The theory will illustrate the usefulness of Fourier transformations in considering problems of phase microscopy.

53. Method of Calculating the Allowable Number of Newton Rings for Telescope Optics. D. C. HARPER AND J. H. MCLEOD, *Eastman Kodak Company.*

A method is developed for calculating the allowable number of Newtons rings in testing telescope optics with a test glass or with an interferometer. This method considers the position of the surface in question relative to the entire optical system. For each surface, the permissible number of rings is proportional to the square of the ratio of polished surface diameter to axial beam diameter. The two conditions considered in calculating the allowable number of rings are (1) parallax between the target and the reticle images and (2) axial astigmatism of the target image. This system has been used successfully with several telescopes in large production.

54. Method of Calculating the Permissible Size of Appearance Defects for Visual Instruments. D. C. HARPER AND W. T. SHERWOOD, *Eastman Kodak Company.*

A method is developed for calculating the allowable size of appearance defects such as scratches, bubbles, digs, etc., for visual instruments. This method considers the position of the optic in question relative to the entire optical system. The permissible defect size is worked out as a percentage of the diameter of the axial beam which can pass through both the instrument and a 3.5-mm eye pupil. For optics near an image, the allowable defect size is based upon the resolution of the viewing system. In the more critical cases, a larger defect size is permitted in the outer zone. Data from several optical instruments in large production was used in the development of the system.

BIBLIOGRAPHY:
J. H. McLeod and W. T. Sherwood, "A proposed method of specifying appearanec defects of optical parts," J. Opt. Soc. Am. **35**, 136 (1945).

55. An Investigation of the Visibility of Physical Defects in Optical Instruments. HAROLD H. BLOEM, *Bausch & Lomb Optical Company.*

Small physical defects have little or no effect upon the quality of the image seen when looking through an optical instrument. Defects that are present in optical elements located in or near a focal plane of an instrument may be seen or may cause a disturbance which may be objectionable. A study was made to help determine what quality to specify on such elements. McLeod and Sherwood* give a method of specifying appearance defects of optical parts but do not indicate how they arrive at the amount of defect they specify. Graded samples representing pits and scratches were observed under varying conditions of focus, power, beam speed, and field size. Data were taken to give the position at which a defect would cease to be objectionable. From the data taken curves were drawn and formulae were developed to determine the size defect permissible in an optical element near a focal plane in any specific instrument.

* J. H. McLeod and W. T. Sherwood, J. Opt. Soc. Am. **35**, 136 (1945).

56. Computation of Distortion of an "Out-of-Focus" Image. K. PESTRECOV, *Bausch & Lomb Optical Company.*

The usual procedure of computing the distortion of a plane image produced by a centered optical system is based on the assumption that the image is formed in the Gaussian image plane. Generally this assumption is well justified. Cases occur, however, when the balance of aberrations is such that the actual plane of the best average imagery significantly departs from the Gaussian plane. The so formed image should be considered being "out-of-focus" from the point of view of the first-order theory. In order to compute the distortion of an "out-of-focus" image, the paraxial metric constant of the system should be found for the actual image plane. It is shown that the constant is:

$$M_0 = p_0'/m_e p_0 \text{ (for an object at a finite distance),}$$

or

$$F_0 = p_0'/m_e \text{ (for an object at infinity),}$$

where p_0' = image distance from the paraxial exit pupil, p_0 = object distance from the paraxial entrance pupil, m_e = paraxial lateral magnification between the pupils. While the expressions for M_0 and F_0 are similar to the generally known magnification formulas,[1] their validity is not restricted by the requirement that the actual image plane should be a Gaussian conjugate of the object plane.

[1] Arthur C. Hardy and Fred H. Perrin, *The Principles of Optics* (McGraw-Hill Book Company, Inc., 1932), pp. 71–73.

Author Index of Papers

Aklin, George H.—No. 43
Barach, J. L.—see Mersereau, E. P.
Barr, N. F.—see Reymann, George L. and Kenneth H. Smith
Bloem, Harold H.—No. 55
Blout, Elkan R. and Dwight P. Merrill—No. 29
Clapper, Franklin R.—see Hopkins, Robert E.
Clark, M. D.—see Evans, J. C.
Dieke, G. H.—No. 16
Douglas, C. A.—No. 49
Duntley, Seibert Q.—No. 10
Eastmond, E. John and Bernice E. Williams—No. 41
Edwards, Edward A.—No. 11
Eisen, Fred C.—see Wolfe, Robert N.
Evans, J. C. and M. D. Clark—No. 32
Fassel, Velmer A. and H. A. Wilhelm—No. 40

Fonda, Gorton R. and Frank J. Studer—No. 36
Geffner, Joseph—No. 39
Grey, David S.—No. 45
Hardy, Arthur C.—No. 1
Harper, D. C. and J. H. McLeod—No. 53
—— **and W. T. Sherwood**—No. 54
Hemmendinger, Henry—No. 7
Hopkins, Robert E. and Franklin R. Clapper—No. 19
Hottel, H. C.—No. 15
Humphreys, Curtis J.—No. 34
Hunter, Richard S.—No. 14
Hyde, W. L.—No. 28
Johnson, E. Parker—see Riggs, Lorrin A.
Keegan, Harry J.—No. 3
Kennard, R. B.—No. 23
Kenyon, Westcott C.—see Osborn, Robert H.
Ladenburg, R.—No. 21
MacAdam, David L.—No. 8
Macht, David I. and Marcus Ostro—No. 26
Mahan, A. I. and E. E. Price—No. 48
McLeod, J. H.—see Harper, D. C.
Meggers, William F.—No. 38
Merrill, Dwight P.—see Blout, Elkan R.
Mersereau, E. P. and J. L. Barach—No. 5
Middleton, W. E. K.—No. 9
Mueller, Hans—No. 17
Osborn, Robert H. and Westcott C. Kenyon—No. 13
Osterberg, Harold—No. 52
—— **and J. Ernest Wilkins, Jr.**—No. 50
Ostro, Marcus—see Macht, David I.
Pestrecov, K.—No. 56
Plyler, Earle K.—No. 31
—— **see Tilton, Leroy W. and Robert E. Stephens**
Plymale, W. S., Jr.—No. 35
Price, E. E.—see Mahan, A. I.
Reymann, George L., Kenneth H. Smith, and N. F. Barr—No. 12
Richards, Oscar W.—No. 51
Richardson, David and Robert B. Tackaberry—No. 24
Richardson, E. E.—No. 2
Riggs, Lorrin A. and E. Parker Johnson—No. 25
Rozsa, J. T.—No. 42
Sherwood, W. T.—see Harper, D. C.
Silverman, Shirleigh—No. 33
Simon, Frederick T.—No. 6
Smith, Kenneth H.—see Reymann, George L. and N. F. Barr
Stephens, Robert E.—No. 44
—— **see Tilton, Leroy W. and Earle K. Plyler**
Studer, Frank J.—No. 37
—— **see Fonda, Gorton R.**
Tackaberry, Robert B.—see Richardson, David
Tilton, Leroy W., Earle K. Plyler, and Robert E. Stephens—No. 30
Turner, A. F. and O. A. Ullrich—No. 20
Ullrich, O. A.—see Turner, A. F.
Weyl, F. J.—No. 22
Widmyer, J. H.—No. 4
Wilhelm, H. A.—see Fassel, Velmer A.
Wilkins, J. Ernest, Jr.—see Osterberg, Harold
Williams, Bernice E.—see Eastmond, E. John
Wolfe, Robert N. and Fred C. Eisen—No. 47
Woodson, Robert A.—No. 46
Wright, Norman—No. 27
Zernike, F.—No. 18